The neurofilament triplet protein and other neurochemical markers in rat neocortex

Matthew Kirkcaldie, BSc (Hons.)

Submitted in fulfilment of the requirements for the Degree of Doctor of Philosophy

University of Tasmania, April 2001.

Declaration

This thesis is entirely my own work, and contains no material which has been accepted for a degree or diploma by the University or any other institution. No material previously published or written by another person has been utilised without due reference.

Matthew Kirkcaldie.

Authority of access

Abstract

Evidence for intrinsic modularity in the mammalian neocortex is difficult to reconcile in a single coherent scheme of organisation. Instead, it appears that certain characteristics of neuronal morphology and interconnection produce a cortex with an intrinsic columnar bias, formed and regionally differentiated under the influence of subcortical afferents, and that the cortex as a whole is more homogeneous than may have been expected. Against this background, a growing set of characteristic biochemical markers expressed by individual neurons has emerged as an important prospect for recognising the mix of neuronal subgroups in individual regions, and several studies have made progress in associating these "chemical phenotypes" with the morphologies, connectional preferences, distributions and electrophysiological qualities of the neurons exhibiting them. Most chemical phenotypes are expressed by subgroups of GABAergic neurons.

Immunohistochemical labelling of the neurofilament triplet (NF) intermediate filament proteins allows subpopulations of the largest neuronal group, the pyramidal cells, to be identified throughout the brain. Characterisation of the properties associated with cellular expression of NFs would permit phenotypic groupings of most cortical neurons, enabling the evaluation of neuronal populations in wide regions of the brain using simple techniques. This thesis comprises studies of NF-associated properties in the context of several key chemical phenotypes.

The overall distribution of immunolabelling produced by SMI32, an antibody recognising perikaryal neurofilament, was examined and characterised in the rat cortex. Retrograde tracing studies evaluated the possibility that the presence of NF enables longer projections in corticocortical neurons. Ultrastructural examination of cortical axons was used to examine the relationship between axonal neurofilaments, myelination and axon calibre in the rat cortex. The developmental emergence of SMI32 labelling was examined, and comparisons with the appearance of key GABAergic phenotypes was used to correlate NF expression with the changing environment of developing cortex. Finally, the usefulness of cultured embryonic rat neurons for studying the development and intracellular distribution of NFs and GABAergic phenotypes was examined using several timepoints during a three week development *in vitro*.

SMI32-labelled NFs were found in around 10% of neurons in several regions; characteristic laminar patterns of labelling were observed in the cortex as a whole, consistently appearing in particular cortical areas. SMI32 labelling in retrogradely labelled cells was found not to correlate with estimates of the projection distances involved, although some evidence for regionally specific differences in NF proportions of projection neurons was observed. Presumed NFs in cortical axons of the corpus callosum exhibited a strong correlation with axon calibre and myelination, while differences observed in regional NF distribution were found to correlate with obvious ultrastructural differences in the cortex. The emergence of SMI32 labelling correlated with changes in the expression of other chemical markers *in vivo*, whereas the environmental differences of *in vitro* culture produced significant alterations in the observable chemical phenotypes, notably the early absence of NFs recognised by the SMI32 antibody.

The role played by neurofilaments in the cells which express them remains mysterious, but it is clear that there are major variations in their regional and intracellular expression and modification. They remain a strong prospect for subtyping pyramidal cells, since they are probably expressed by neurons whose axons are myelinated.

Acknowledgments

Many people helped and encouraged me through the long process of studying for a PhD.

I would like to thank my supervisor, Dr James Vickers, for his good faith, good humour, sound advice and diligent supervision in these projects. Thanks also to my other supervisors: Dr Peter Kitchener, friend and mentor, Associate Professor Saxby Pridmore for starting it all, and Professor Norman Saunders for the "welcome to academia."

Particular thanks to Irene Jacobs for her painstaking and superb EM work, and for her friendship and support. Thanks also to my fellow students, particularly Dr Tracey Dickson and Bryony Coleman, and to the staff of the Disciplines of Pathology, and Anatomy and Physiology, for their help and their company.

Love and thanks to my friends and my tireless families: Mum and Dad; James and Sarah; Blake and Lindy; Tor, André and Isabella; and Tash, for all their encouragement and support.

Last and greatest, my love and thanks to Mem for her forbearance, and for being there through all of this.

Matthew Kirkcaldie.

Contents

Chapter 1

Neurofilament and other chemical phenotypes of the rat neocortex

1 Introduction

Since the first microscopic observations of brain tissue, regularities in the arrangement of its cells have been obvious (White, 1989). In the century and a half since the first identification of cortical cells (Jones, 1984a) the local and global organisation of cortex has been one of the principal interests of neuroscience. Identifying functionally significant aspects of the brain's rich anatomical detail has been a difficult task; experience has repeatedly demonstrated the problems of separating local from global elements, and experimental outcomes from the methods used. Expanding knowledge of anatomy, physiology, genetics, ultrastructure, cytochemistry and synaptic transmission has resulted in an explosion of factors for consideration in developmental and organisational models.

Against this background, research into cortical function has focused on three principal levels of organisation: individual neurons, the loosely-defined "local circuit", and cortical regions defined by various schemes of anatomy and chemoarchitectonics. Data from each of these levels have been difficult to reconcile and integrate into convincing functional theories.

One observable regularity at the regional level is the heterogeneous distribution of neurons employing the intermediate filament proteins called the neurofilament triplet, whose function remains mysterious despite decades of research. Among markers of chemical heterogeneity in neuronal subpopulations, neurofilaments are particularly interesting because they are expressed by a significant subpopulation of pyramidal cells, among which such markers are comparatively rare. The experiments reported in this thesis have studied the distribution of neurofilaments in the adult and developing cortex, among populations of projections neurons and their axons, and in cortical neuron cultures to examine several hypotheses about their role.

This review will briefly outline the development and differentiation of the cortex and of its individual elements; patterning in the arrangement and characteristic chemistry of neurons; and the notion of local circuits and modular processing in cortex. It was originally envisaged that examining chemical phenotypes in the context of modular cortical arrangements would provide clues to neurofilament

functions, but the modular hypotheses examined in this review do not converge on a consistent framework which could be used as a basis.

Chemical heterogeneity among neurons is also surveyed in the context of correlating chemical phenotypes with functional properties, the goal of the studies of neurofilament localisation in this thesis. Such correlations enable large-area, rapid procedures like immunohistochemistry to be used for functional study of the cortex, which may bring rapid progress in the understanding of the brain. These broad-area perspectives also complement local, detailed studies of interconnections and cortical architecture.

Many markers have been identified in the cortex, but most attention has been paid to known and putative neurotransmitters, calcium binding proteins (particularly parvalbumin, calretinin and calbindin) and various peptides (e.g. vasoactive intestinal polypeptide and somatostatin). This review will also briefly examine the extent to which the distribution and functional correlates of many of these markers have been characterised. With few exceptions, these markers are expressed by local inhibitory cells which represent only one sixth of cortical neurons (Gabbott et al., 1997); understanding the significance of neurofilament expression may extend functional chemical phenotyping to include pyramidal neurons as well.

2 The rat cortex

While the understanding of human brain function is undoubtedly the primary motivator of neuroscience, practical realities mean that other mammals are used as analogues for study. A common choice is the laboratory rat, which shares many cortical features with humans (White, 1989; Morrison & Hof, 1992). While the basic structure and chemistry of rat cortex may provide useful information about human anatomy and function, it is important not to push the analogy too far; for instance, secondary sensory regions in the rat brain project directly to one another (Miller & Vogt, 1984), which is not the case in monkey or human brain (Morrison & Hof, 1992). This review, intended to accompany a series of studies on rat cortex, will naturally focus on data obtained from, or relevant to, the rat nervous system.

Like all mammal brains, the rat cortex is considered to have six cellular layers numbered in roman numerals from the outermost edge inward, whose cellular composition varies quite widely from region to region and may be subdivided accordingly (Zilles, 1985; White, 1989). The cellular components of these layers are described in §2.2.

2.1 Neuronal development

This account of cortical development is a background for subsequent discussions of the type and organisation of its neurons.

2.1.1 Origin of cortical cells

The thirty-odd million neurons of the rat neocortex are generated over a period of ten days, beginning around the eleventh day of gestation (E11) and finishing shortly after birth (reviewed by Uylings et al., 1990). After a day of cell division in the ventricular zone (a layer of progenitor cells on the inner surface of the telencephalic vesicles) fibres invading from mesencephalic structures begin to grow tangentially across the outer surface of the vesicle, forming a layer known as the plexiform primordium or the preplate. This layer forms at the lateral edge of the telencephalon, taking two days to spread to the midline. The earliest neurons, consisting of layer I Cajal-Retzius cells (§2.2.9) and some polymorphous cells, are generated on days E11 to E15 and move into the preplate. Around E13 a new population of cells begin to arise; around E15 they reach the middle of the preplate, dividing it into the outermost marginal zone (precursor of cortical layer I) and the subplate, which separates the ventricular generation zone from the new arrivals. This new population, developing with the same lateral-medial gradient, forms the cortical plate which eventually becomes layers II–VIa of the adult cortex. At the same time, a subventricular zone becomes distinguishable on the outer edge of the ventricular zone, and an intermediate zone (precursor of cortical layer VIb and subcortical white matter) appears, underlying the subplate (Uylings et al., 1990). Most cortical glial cells are formed postnatally (Götz & Bolz, 1992).

2.1.2 Migration of neurons

Glial scaffolding

During this stage of cell birth, a group of glial cells are born from distinct precursors in the ventricular zone, and extend their processes radially from the ventricular zone outward, initially in fascicular groups but later dissociating individually (Uylings et al., 1990). Newly formed neurons, moving radially along these glial fibres from the ventricular zones at 15–30μm/hour, reach the border with the marginal zone and move back inward, assembling in an inside-out order: that is, the earliest cells form layer VI just outside the subplate, while subsequent arrivals migrate to steadily more distant levels from the subplate to form layers V–II in approximate sequence (Rakic, 1981). Inhibitory interneurons tend to finish migration in layers which strongly

correlate to their time of generation, whereas pyramidal cells exhibit more variation in their final placement (Mione et al., 1994). The latter phenomenon may be the result of the more extensive modifications made to their structure and radial extent during growth (Koester & O'Leary, 1992), or may reflect the early segregation of the properties of cells using either glutamate/aspartate or γ-aminobutyric acid (GABA) for transmission (Götz & Bolz, 1994). The use of these radial glial guides means that neurons born in the same ventricular zone region tend to migrate along the same fibre(s), and often finish up in a narrow radial column extending through the cortical plate; this common migration had been hypothesised to create developmental "cohorts" of neurons, leading to an inherent parcellation of cell groups in the adult cortex. The spacing of glial migratory guides is quite uniform, leading to the formation of orderly ranks of developing neurons in the cortical plate as they follow a variety of adhesion molecules along the surface of the glia (Bar & Goffinet, 1999).

Nissl staining demonstrates that the cells of the adult cortex are also arranged in radial narrow columns spanning the depth of the cortex (Jones, 2000). Mountcastle (1978) assumed that this columnar arrangement results from clonal groups (cells derived from the same stem cell in the ventricular zone) following the same fibres, and that functional columns were derived from "sibling" neurons. However, a counter-argument was provided by retroviral labelling studies by Walsh and Cepko (1988; 1992) which indicated that clonal groups disperse in cortex; subsequent studies by them and other groups revealed that these initial findings were a superposition of two major migratory patterns followed by developing cells (Rakic, 1995). Both radial and tangential migration occur in the developing cortex, but the tangential component takes place in the ventricular zone and the subplate, so that cells entering the cortical plate move almost exclusively radially. Thus, most cells generated in the same region of the ventricular zone retain a tight columnar grouping in the adult cortex (Rakic, 1995). Glial fibres themselves are crucial to migration: Götz and Bolz (1992) correlated normal migration in the developing rat brain with the presence of differentiated radial glial fibres in slice cultures; without radial fibres, neurons migrate toward the MZ for about a week, but do not reach their expected places.

Arriving thalamocortical afferents reach the early-maturing cells of the subplate while their neuronal targets are being born, and their interaction with subplate cells halts their progress temporarily, though this delay is negligible in the rat (review by Shatz, 1992). The birth and migration of layer IV cells prompts the apoptosis of subplate neurons as the corticothalamic axons continue into the

developing cortex; the presence of subplate neurons is vital for these axons to reach their target areas, and it is likely that the timing of their spreading maturation guides incoming thalamocortical axons to specific regions (Shatz, 1992; Ghosh et al., 1990). During development these afferents modulate the differentiation, size and organisation of the cortical regions they innervate (O'Leary & Koester, 1993; Schlaggar & O'Leary, 1991).

Chemical guidance

While most neurons appear to follow radial glial fibres to their destinations, extracellular matrix molecules such as fibronectin, as well as plasma proteins, play an important role in their migration and differentiation (Uylings et al., 1990). Chemical factors thought to halt neuronal migration at the inner border of the marginal zone, and allow cells to detach from radial glial fibres once they have reached their destination, have been identified from genetic studies of cortical malformation mutations in mice (Rakic & Caviness, 1995). Recently, a suite of factors involved in neuronal migration and cortical plate patterning have been tentatively identified (Bar & Goffinet, 1999). The differential migration of various neuronal types is suggestive of an association between a cell's final location and its particular repertoire of expressed genes; differently guided neurons must at least be expressing different surface receptors, which presumably give rise to distinct intracellular events and perhaps transcriptional cues for those cells expressing them.

2.2 Neuronal types in the rat brain

The cortex emerging from these processes contains a variety of neurons with distinctive morphology, distribution, connectional preferences and cytochemistry. These properties form the basis of most hypotheses of cortical function, and the strong association of particular chemical markers with some morphological subtypes derives meaning in the context of the makeup of the entire cortex. The principal types of neurons found in the mammalian cortex are outlined in this section.

The studies and reviews used in this overview are based on a variety of mammal species, principally mouse, rat, cat, monkey and human. Cortical cells are similar across mammals, but instances in which rat cortex is known to differ are indicated. The terms "ascending" and "descending" in this section refer to radial directions toward and away from the pial surface of the cortex respectively. Synapses between neurons are classified as asymmetrical or symmetrical on the basis of ultrastructural features; they are likely to be excitatory (employing glutamate or

aspartate) and inhibitory (employing GABA) respectively (review by White, 1989). Studies of the cortex have an historical bias toward categorising neurons on the basis of morphology, and hence most functional and connectional data are classified in this manner. The following survey is organised morphologically, but wherever possible any characteristic chemical phenotypes of the morphological types have been indicated. Throughout this review, the terms "chemistry" and "chemical" are applied to neurons, and refer to characteristic proteins known to be expressed by neuronal subpopulations, whose actual chemical function within those cells may be unknown.

2.2.1 Pyramidal cells

Areal and laminar distribution: Pyramidal cells are the most common neurons in the cortex of all mammalian species (reviewed by Winfield et al., 1981). They are abundant throughout all cortical regions and layers except layer I, and constitute 62–85% of all cortical neurons (Winfield et al., 1981; DeFelipe & Fariñas, 1992). Their distribution varies according to cortical region, though they are generally prominent in layers III and V except in primary sensory regions, where their cell bodies are relatively small (review by Feldman, 1984). They are almost exclusively the projection cells of the cortex.

Morphology: The form and size of pyramidal cells varies widely throughout cortical regions and layers (Feldman, 1984). However, three characteristics have been used to distinguish these cells from others: a pyramidal or ovoid soma, with a prominent ascending apical dendrite usually reaching layer I, and a number of lateral or descending basal dendrites; an axon arising from the base of the soma or proximally from a basal dendrite, descending through and extending out of the cortex; and the presence of dendritic spines on all parts of the dendritic field except for proximal parts of dendrites. The apical dendrite usually forms a tuft of branches at its distal end, which may extend for considerable tangential distances (Figure 1.1; review by DeFelipe & Fariñas, 1992).

Within these criteria a range of variation is observed across various cortical layers. Pyramidal cells can possess reduced or multiple apical dendrites, typically in layers II and V respectively. Layer VI pyramidal cells exhibit a variety of somatic forms; their apical dendrites may not always ascend, and frequently do not reach layer I (DeFelipe & Fariñas, 1992). Rarely, the axons of some cells appear to be purely intracortical (Feldman, 1984).

Dendritic inputs: The dendritic field has been estimated to represent 90–95% of the receptive surface of pyramidal neurons, and receives inputs from a wide variety of

presynaptic cells. Most (75–95%) synapses onto the dendrites are asymmetric and presumed excitatory (DeFelipe & Fariñas, 1992).

Most of these synapses are received by the spines, short narrow processes arising from the surface of the dendritic shafts, ranging from 1–4μm in length (DeFelipe & Fariñas, 1992). Studies suggest that spines may develop in response to repeated synaptic stimulation and represent established synaptic pathways (Maletic-Savatic, Malinow, & Svoboda, 1999; Müller & Connor, 1991) which rely on continued activity for maintenance (Andersen & Figenschou Soleng, 1999). Virtually all spines receive at least one asymmetric synapse, while 10–20% receive two, or an additional symmetric synapse from a bitufted (double-bouquet) or a basket cell (DeFelipe & Fariñas, 1992). These axospinous synapses typically originate with local or projecting pyramidal cells, spiny stellate cells (§2.2.2) and extrinsic afferents, particularly from the thalamus. Dendritic shafts receive fewer synapses of which many are symmetric, probably from local non-spinous neurons.

The dendritic field of an individual pyramidal neuron generally clusters around its body, with an extended field associated with the apical dendrite in more superficial layers (DeFelipe & Fariñas, 1992).

Somatic inputs: The somata of pyramidal cells are relatively free from synapses. Unlike dendritic inputs, virtually all synapses received by the soma and axon initial segment are inhibitory: 90–95% are formed by terminals containing GABA, as well as a variety of peptides (DeFelipe & Fariñas, 1992). Basket cells (§2.2.3) and other non-spiny neurons provide many of the somatic presynaptic boutons. Chains of inhibitory boutons along the axon initial segments of many pyramidal cells, more in layer III than V, originate almost exclusively with chandelier cells (§2.2.4; Peters, 1984a).

Axonal targets: The axons of pyramidal cells are principally descending, and leave the cortex. However, nearly all give rise to collateral branches which make intrinsic, local-region synapses as well (DeFelipe & Fariñas, 1992). Proximal collaterals recurve and ascend, forming a plexus of processes and terminals around their originating soma and in more superficial layers, and extending tangentially for long distances within the cortex (Feldman, 1984). More distant collaterals may extend for large tangential distances; an example measuring 7mm in cat cortex is described by Gilbert and Weisel (1979). Their primary cortical targets are dendritic spines, usually from other pyramidal cells, though non-pyramidal and non-spiny cells are also innervated (Kisvárday et al., 1986b; White, 1989).

Retrograde and degenerative tracing techniques have allowed a broad variety of cortical projections to be examined in detail, suggesting that layer VI (and V) pyramidal cells project to the thalamus; other subcortical regions receive layer V axons; and corticocortical projections, including callosal projections, originate in layers II and III (Morrison & Hof, 1992). In rats, however, corticocortical efferents also originate in layer V (Miller & Vogt, 1984). Jones (1984b) reviews studies of correlations between the laminar distribution of pyramidal cells and the targets of their corticofugal axons. Degeneration studies identified layer V cells as the source of subcortical motor projections, and layer III and V cells for callosal projections from various regions. These findings were confirmed by antidromic conduction in electrophysiological work during the 1970s, which also demonstrated corticobulbar, corticotectal and corticorubal projections from layer V, and corticogeniculate axons from layer IV. Morrison and Hof (1992) and Johnson and Burkhalter (1997) describe the reciprocity of most corticocortical projections; in sensory regions, "forward" projections originate in layer III and terminating in layers III and IV, and "feedback" projections arise in layers III, V and VI and then terminate primarily in layers I, II and V.

The layer VI thalamic projection is directed to the specific nucleus which sends its afferents to that cortical region, while non-reciprocal thalamic projections come from layer V. Layer VI has also been found to project to adjacent and distant ipsilateral cortical regions. Within the projecting lamina of a region of cortex, labelled cells exhibit a patchy distribution, particularly in the case of callosal projections in which the projecting "clumps" follow the distribution of callosal afferents to that region (Morrison & Hof, 1992). Within rat somatosensory cortex, callosally projecting pyramidal cells are interleaved with the spiny stellate cells receiving the main thalamic projections, in contrast to the arrangement of other projection neurons (DeFelipe & Fariñas, 1992).

Transmitters used: Pyramidal neurons are excitatory to their postsynaptic cells, and a large proportion are known to use the excitatory amino acid neurotransmitters glutamate and aspartate (Hornung & de Tribolet, 1995). These transmitters produce a variety of response qualities in their postsynaptic cells due to receptor heterogeneity (Morrison & Hof, 1992); the proportion of pyramidal neurons employing these transmitters has also been investigated with equivocal results; quite few cells use both transmitters (DeFelipe & Fariñas, 1992; DeFelipe, 1997a).

Characteristic chemistry: Aside from the widespread presence of aspartate, glutamate and its synthetic enzyme glutaminase (Hornung & de Tribolet, 1995), few markers identify subpopulations of pyramidal neurons. Some human and monkey pyramidal cells are immunoreactive (IR) for calcium binding proteins (CBPs) such as calbindin (CB) and calmodulin, particularly the latter, which is also widespread among rat pyramidal cells (Hornung & de Tribolet, 1995; Condé et al., 1994); other CBPs have been infrequently detected in the pyramidal cells of various species (DeFelipe, 1997b). Somatostatin and related peptides were observed in rat pyramidal neurons by Morrison and colleagues (1983) and Hendry, Jones, and Emson (1984). Other markers, such as the proteoglycan Cat-301 (DeYoe et al., cited in Hof et al., 1996) and acetylcholinesterase (AChE, associated with reception rather than transmission; Mesulam & Geula, 1991) have been found. Populations of pyramidal neurons are immunoreactive for neurofilament triplet proteins (§4.4), although they are present in other neurons.

Function: Pyramidal cells provide virtually all projections from the cortex to other cortical or subcortical regions. As such, they are the means by which communication in the form of action potentials occurs between cortical regions, and from the cortex to the rest of the nervous system. Local intrinsic connections between pyramidal cells, and to other cell types, facilitate the spread of excitation throughout a cortical region. Their prominent apical dendrite tufts in layer I suggest a role in propagating the influence of the various fibre plexuses in that layer (Morrison & Hof, 1992); during development, most pyramidal cells begin to sprout their apical dendrites when they reach the marginal zone, and leave them attached there while they descend to their destination laminae (Koester & O'Leary, 1992; Marín-Padilla, 1984).

2.2.2 Spiny stellate cells

Spiny stellate (SS) cells are distinguished among nonpyramidal cells by the profusion of spines on their dendrites, which along with their glutamatergic nature and occasional morphologic similarity can lead to their grouping with pyramidal cells (e.g. DeFelipe & Fariñas, 1992).

Areal and laminar distribution: SS distribution is limited to the primary sensory cortices of vision, audition and somatosensation, and some secondary cortex of these senses. In these regions they pack together in a defined band (layer IV), described as a granular layer because of the profusion of their small nuclei in Nissl stains. SS layers often contain few neurons of other types; however, not all granular layers contain SS cells (review by Lund, 1984).

A striking feature of mystacial somatosensory SS layers in many whiskered animals is their arrangement in "barrels" (Woolsey & van der Loos, 1970), ringlike aggregates of 100 or so cell bodies surrounding relatively cell-free zones, which appear to constitute functional units (e.g. Yang, Hyder, & Shulman, 1996). Their regular arrangement and unitary correspondence with the individual whiskers whose inputs they receive has prompted speculation about the functional organisation of somatosensory cortex; the regularity of their arrangement may be determined even before layer IV cells arrive in the developing brain by the regular patterning of glial fibres (Cooper & Steindler, 1986; in Uylings et al., 1990); however, transplanted embryonic visual cortex forms barrels when supplied with the appropriate thalamocortical afferents (Schlaggar & O'Leary, 1991), implicating exogenous rather than intracortical factors in forming barrel structure (cf. §3.2.3).

Morphology: SS cells are identified by profuse dendritic spines on their radiating non-polar dendritic field (Figure 1.1); they lack the pyramidal cell's apical dendrite. Axons nearly always emerge from the descending side of the soma, but often recurve and ascend (Lund, 1984). The existence of pyramidal cells with vestigial apical dendrites, and SS cells whose axons leave the cortex (Peters, Payne, & Josephson, 1990; Jones, 1984b) suggest they may form a morphological continuum with pyramidal cells.

Dendritic inputs: The spiny stellate cell has been assumed to be the principal target of thalamocortical axons, which terminate predominantly in layer IV when SS neurons are present. However, the actual proportion of thalamocortical axons synapsing with their dendrites may be small compared to those from layer VI pyramidal cells and other SS neurons (Ahmed et al., 1994). The observed pattern of synaptic distribution resembles that for pyramidal cells, excepting that asymmetric synapses are rarely seen on dendritic shafts. Their dendritic fields have a variety of distributions, with some having a tangentially stratified appearance, while others ascend or descend radially for one layer. Kisvárday and coworkers (1985; 1986a) identified GABAergic "clutch" cells, a type of basket cell (§2.2.3), supplying most of the symmetric synapses to the dendrites and somata of SS (Ahmed et al., 1994) and pyramidal cells.

Somatic inputs: SS cells also resemble pyramidal neurons in their paucity of somatic synapses, which are chiefly symmetric (White, 1989) and probably come from clutch cells (Ahmed et al., 1994). The axon initial segment is generally free of synapses (Lund, 1984).

Axonal targets: SS axons form asymmetric synapses with their targets. Their distribution is predominantly intrinsic, and generally limited to laminae III, IV and V, with a tendency to ascend (Lund, 1984). SS cells of the primate and cat primary visual cortex have been demonstrated to project to adjacent and distant cortical regions, including transcallosally (Peters, Payne, & Josephson, 1990). SS axon terminals form synapses with spines and shafts of spiny neurons (mostly SS in the region of the axon plexus) and the shafts of non-spinous dendrites, origin unknown but possibly from clutch cells (White, 1989).

Transmitters used: SS neurons' asymmetric synapses and excitatory effects on postsynaptic cells (DeFelipe, 1997b) indicate glutamate and/or aspartate transmission.

Characteristic chemistry: No markers have been reported as localised to spiny stellate neurons.

Function: As a target of thalamic afferents, the excitatory nature of spiny stellate cells facilitates the relay and distribution of afferent sensory data; their patterns of afferent connections suggest intracortical influences combining to alter the properties of incoming thalamic information, according to context and local activity.

Thalamic projections to SS cells have exhibited marked large-scale organisation in many studies. Ocular dominance columns and receptive field orientation are arranged in highly regular patterns throughout cat and monkey cortex, and the barrels of whiskered animals have already been mentioned. The former phenomena are, however, apparently unrelated to the spatial distribution of SS neurons in layer IV (Lund, 1984). Patterns are also evident in the axonal plexuses of SS neurons, suggesting parcellation of function, albeit one whose relationship to discrete regional processing is complex (§3.2.3).

2.2.3 Basket cells

Areal and laminar distribution: Basket cells are probably ubiquitous in the cortex (e.g. Kawaguchi & Kubota, 1993; Gabbott et al., 1997), with somata found in layers II–VI, concentrating in layers III and V. Small basket cells are also present in layer II of cat cortex (White, 1989).

Morphology: Basket cells are large-bodied cells with a multipolar complex of 4–10 sparsely-spinous and infrequently branching dendrites, which radiate in an elongate field extending radially and rostrocaudally for 1–2mm, which may extend through all cortical layers (Jones & Hendry, 1984). Their ascending or descending myelinated

axons (DeFelipe, Hendry, & Jones, 1986), usually originate on the pial side of the soma and give rise to long horizontal layers of axon collaterals, which in turn sprout small branches ending in dense tufts of terminals; they may also continue to ascend and form further plexuses in superficial layers (Figure 1.1; Kisvárday et al., 1987). These baskets of boutons each envelop a pyramidal cell body with a dense complex of terminations (review by Jones & Hendry, 1984). In rodents and other animals with smaller brains, the axonal baskets of each cell may be incomplete or fragmentary (White, 1989), since in all species the terminals of many basket cells may envelop a single pyramidal cell (Szentágothai, 1975). Smaller cells in layer II give rise to similar terminal patterns, and are recognised as a subclass, the small basket cell (Jones & Hendry, 1984).

Dendritic inputs: Basket cell dendrites receive many asymmetric and symmetric synapses; many of the asymmetric population are of thalamocortical and corticocortical origin (Jones & Hendry, 1984).

Somatic inputs: Many glutamic acid decarboxylase (GAD, the enzyme for GABA synthesis) immunoreactive terminals have been described on the soma of probable basket cells; the density of these terminations is comparable to that of pyramidal cells (Jones & Hendry, 1984). Ahmed and colleagues (1997) surveyed synaptic inputs to basket somata in cat cortex; their statistical analysis indicated that the great majority of somatic symmetric synapses were from other basket cells, while asymmetric synapses probably originate with layer VI pyramids, SS neurons and thalamic afferents.

Axonal targets: The targets of basket cells include the soma, dendrites and spines of pyramidal cells (Somogyi et al., 1983). They supply a dense plexus of GAD-IR symmetrical synapses to the cell body (Kisvárday et al., 1987). "Clutch" cells, targeting SS and pyramidal neurons, are probably a variant of basket cells (Kisvárday et al., 1985).

Transmitters used: Tritiated GABA and GAD immunohistochemical studies indicate that basket cells are GABAergic (Jones & Hendry, 1984; Kawaguchi & Kubota, 1997).

Characteristic chemistry: The CBP parvalbumin (PV) has been identified in GABAergic basket cells of the rat frontal cortex (Kawaguchi & Kubota, 1993; Gabbott et al., 1997) and in the monkey (Akil & Lewis, 1992). Calretinin (CR)-IR terminal baskets have also been observed in rat cortex (Gabbott et al., 1997) and may

arise from CR-IR small basket cells, although other studies have not reported CR in basket cells (DeFelipe, 1997a).

Function: Basket cells' function is unusually well characterised, perhaps due to their readily recognisable chemical phenotype and synaptic targets. Their pericellular terminals and fast-spiking behaviour (Kawaguchi & Kubota, 1993) suggest a powerful inhibitory influence on pyramidal neurons (Maier & McCasland, 1997), particularly in depressing the excitation from axospinous synapses (Galarreta & Hestrin, 1998). Inhibitory synapses from other basket cells on the soma suggest a network of complex interaction which modulates basket cell inhibition in response to excitation. Their strong innervation from extrinsic afferents indicates a coactivation with the pyramidal cells receiving these inputs (White & Keller, 1987), providing modulation of incoming excitation as the feedforward circuits deduced in entorhinal cortex by Finch, Tan, and Isokawa-Akesson (1988) may illustrate.

2.2.4 Chandelier cells

Areal and laminar distribution: Chandelier cells are widespread through the cortex in monkeys, cats, rats and other mammals (White, 1989); they are usually found in layers II and III in the rat cortex (review by Peters, 1984a), where corticocortical projection neurons are numerous (§2.2.1).

Morphology: As with basket cells, the form of chandelier cells is extremely distinctive and suggestive of their function. Their cell bodies are generally small and round, and their dendritic arbours vary considerably between multipolar and bitufted morphology, with few spines and an extent which can encompass layers I–IV. Their axons originate on the lower side of the cell body, and may ascend or descend. Collaterals branch off in a generally tangential direction, rebranching repeatedly to form a profuse plexus of varying shape, but generally confined to layers II and III in rat cortex. The hallmark of chandelier cells are their "cartridges", slender radial bundles of boutons which are the main axon terminals of these cells (Figure 1.1). Their candle-like shape gives the cell its name (Peters, 1984a).

Dendritic inputs: Chandelier cell dendrites receive both asymmetric and symmetric synapses; the latter may derive from local populations of smooth or sparsely spinous interneurons (§2.2.7; Peters, 1984a). Transcallosal afferent fibres appear to innervate chandelier cells (Hof et al., 1997).

Somatic inputs: Cell body synapses resemble those on dendrites (Peters, 1984a).

Axonal targets: Chandelier cells' synaptic targets are the axon initial segments of pyramidal neurons in layers II and III, where their cartridge plexuses form multiple symmetrical synapses. Cartridges associate with small corticocortical cells (Akil & Lewis, 1992), specifically callosally projecting cells in the rat and monkey (Hof et al., 1997).

Transmitters used: Chandelier cells have GAD-IR axon terminals (White, 1989).

Characteristic chemistry: Parvalbumin (PV) has also been localised to a large proportion of chandelier cells in monkey (DeFelipe, Hendry, & Jones, 1989a; Hendry et al., 1989; Akil & Lewis, 1992) and rat cortex (Kawaguchi & Kubota, 1997; Gabbott et al., 1997), in layers superficial to PV-IR baskets in most regions (Akil & Lewis, 1992). In human cortex, some layer V and VI chandelier cells are CB-IR (DeFelipe, 1997b).

Function: Clearly, the inhibitory nature of chandelier cells and their specific targets indicate that they are able to powerfully modulate or prevent the firing of the pyramidal cells whose axons they synapse with – termed 'functional amputation' by Szentágothai (1975). Their location suggests the modulation of layer III outputs, which are often corticocortical in nature (Morrison & Hof, 1992). It has been hypothesised that callosal afferents, which synapse with chandelier cells and layer III pyramids, excite chandelier cells to inhibit positive feedback from occurring (Hof et al., 1997).

2.2.5 Bitufted cells

Confusion of bitufted and double-bouquet cells (DeFelipe, 1997b) makes distinction of their properties difficult, although this ambiguity is partially resolved by chemical markers.

Areal and laminar distribution: Bitufted (BT) cells, frequently included as double-bouquet cells along with functionally distinct bipolar cells (§2.2.6) are widespread in the cortex, having their cell bodies in layers II–III in most cases, though the range of BT-like cells in the rat may include layer IV (review by Somogyi & Cowey, 1984).

Morphology: The BT cell has a small body from which usually radiate an ascending and a descending "tuft" of dendrites. Their axons arise usually on the lower side of the cell body and descend for a short distance before giving rise to an intricate, radially elongate plexus of fibres which may ascend and descend throughout the extent of the cortex. In the rat, BT axon plexuses are mostly descending and are more diffuse than in primates (Somogyi & Cowey, 1984).

Dendritic inputs: Asymmetric and, to a lesser extent, symmetric synapses of unknown origin have been described on cat BT dendrites (Somogyi & Cowey, 1984).

Somatic inputs: Sparse, generally symmetrical synapses of unknown origin have been identified on the soma of cat BT cells (Somogyi & Cowey, 1984).

Axonal targets: In the cat, BT axons terminate mostly on dendritic shafts, with a small proportion on spines and on the somata of nonpyramidal cells (Somogyi & Cowey, 1984). Their axon terminals make symmetric synapses on dendritic shafts and spines in monkey and human cortex (DeFelipe, Hendry, & Jones, 1989b; DeFelipe, 1997b).

Transmitters used: CB-IR cells studied by Kawaguchi and Kubota (1993) in rat frontal cortex have a multipolar or BT morphology, and were also GABA-IR. Hornung and de Tribolet (1995) also described human BT cells immunoreactive for tyrosine hydroxylase, an enzyme which synthesises catecholamine neurotransmitters such as dopamine and norepinephrine, which may indicate the use of one of these transmitters by this type of cell. Reduced-NADPH (nicotinamide adenine dinucleotide phosphate) diaphorase activity, associated with nitric oxide synthase (NOS), was found in rat BT cells by Gabbott and colleagues (1997), indicating use of the messenger nitric oxide.

Characteristic chemistry: Calbindin has been detected in BT cells of rat and monkey cortices (Gabbott et al., 1997; Kawaguchi & Kubota, 1993; "double bouquet" cells of DeFelipe, Hendry, & Jones, 1989b), which are the largest subgroup of CB-labelled cells (DeFelipe, 1997b). BT-like cells containing CR and PV have been described in the rat and monkey cortex (Gabbott et al., 1997; Condé et al., 1994), though the latter examples resemble bipolar cells in the figures. The peptide somatostatin (somatotropin release inhibiting factor; SRIF) has been localised to "double-bouquet" cells in the rat (Morrison et al., 1983; Hendry, Jones, & Emson, 1984).

Function: BT cells investigated by Kawaguchi and Kubota (1993) exhibited low-threshold spike activity even when hyperpolarised, preserving their inhibitory role despite external suppression. Symmetric CR-IR synapses have been observed on the soma of human pyramidal cells (del Río & DeFelipe, 1997b) and may arise from BT cells. GABAergic transmission and radial axon plexuses suggest that BT cells perform columnar inhibition.

2.2.6 Bipolar cells

Neurochemical evidence suggests that the bipolar morphological category may include two subgroups with fundamentally different properties.

Areal and laminar distribution: Bipolar (BP) cells, sometimes misidentified as double-bouquet (DeFelipe, 1997b), occur in laminae II–V; they concentrate in layers according to region, e.g. II/III, IV in visual cortex; III, V in cingulate cortex (review by Peters, 1984b).

Morphology: BP cells have two principal dendrites extending radially from the upper and lower poles of the small, ovoid soma, with few spines, and branching in narrow fields spanning up to five layers. Their axons usually originate from a proximal dendrite, generally the lower. They are distinguished from the bitufted cell by a lack of initial ramification in the principal dendrites, and the relative simplicity of the axonal plexus, which ascends and/or descends from its origin (Peters, 1984b).

Dendritic inputs: BP dendrites receive symmetric and asymmetric synapses, which focus onto proximal and distal parts of the dendrite respectively (Peters, 1984b). The former are from multipolar and BT neurons; some of the latter are thalamocortical (White, 1989).

Somatic inputs: BP cells receive few axosomatic synapses, which may be asymmetric or symmetric and probably originate with the same sources as those on dendrites. Abundant symmetric synapses from basket cells have been described in rat cortex (Peters, 1984b).

Axonal targets: BP axons form synapses on the spines of pyramidal and SS cells (DeFelipe & Fariñas, 1992), on pyramidal cell apical dendrites, and the dendrites and bodies of nonpyramidal cells. Axonal branches may run parallel to the apical dendrite of a pyramidal cell, forming a chain of boutons (Peters, 1984b). Myelinated CR-IR axons and asymmetric CR-IR synapses associated with non-spiny dendrites in human cortex (del Río & DeFelipe, 1997b) may originate with an inhibitory subpopulation of bipolar cells.

Transmitters used: Many studies have reported that the synapses made by bipolar cells are asymmetric (Somogyi & Cowey, 1981; Peters & Harriman, 1988, and Peters & Kimerer, 1981, cited in White, 1989), but studies of vasoactive intestinal polypeptide (VIP)-IR neurons, of which bipolar cells are the principal type (see below), indicate that VIP-IR colocalises with GAD and GABA (Peters, 1990; Kubota, Hattori, & Yui, 1994; Kawaguchi & Kubota, 1997; Bayraktar et al., 1997; Staiger, Freund, & Zilles, 1997), despite conflicting reports (Demeulemeester et al.,

1988). Adding to this confusion, the morphologically similar double-bouquet (bitufted) cells form symmetric synapses and are hence probably GABAergic in transmission; evidence for GABAergic bipolar neurons in rat cortex has been contested on morphological grounds (Rogers, 1992).

It seems likely that BP cells are heterogeneous in transmitter use, and that the VIP-IR population are GABAergic, leading to the separation of bipolar cells into glutamatergic and GABAergic subgroups (cf. Peters, 1990; DeFelipe, 1997a); or perhaps, the realisation that peptide expression is a more pertinent criterion for identifying neuronal types in this instance. It is clear that several types of neurons, differing in chemical makeup, transmitters and postsynaptic targets, share a general morphology.

NADPH-diaphorase-positive bipolar cells, which use nitric oxide signalling, were observed in rat frontal cortex by Gabbott and coworkers (1997). Surprisingly, Bayraktar and colleagues (1997) also found choline acetyltransferase (ChAT) colocalisation with VIP-IR and GABA-IR in bipolar cells, indicating that over a third of these cells also use acetyl choline as a transmitter; GABAergic and cholinergic synaptosomes from rat cortex were also found to contain VIP (Foley et al., 1992). Thus the VIP-containing glutamatergic bipolar subgroup joins thalamocortical afferents and basal forebrain fibres in supplying cholinergic terminals to the cortex. The cholinoception revealed by AChE histochemistry in some pyramidal neurons (Mesulam & Geula,1991) may relate to any of these sources.

Characteristic chemistry: The peptides VIP and CCK have been identified in BP cells of rat cortex older than P7 (Kubota, Hattori, & Yui, 1994). VIP largely colocalises with CR labelled in BP neurons of the rat cortex (Gabbott et al., 1997). SRIF was observed in bipolar-like neurons of the rat and monkey cortex (Hendry, Jones, & Emson, 1984).

Function: Most bipolar cells have at least part of their dendritic fields in lamina IV, and hence receive thalamocortical projections (White, 1989). Ascending and descending axonal plexuses, axospinal synapses and multiple synapses with apical dendrites suggest that BP cells spread influence radially, and may be inhibited by basket cells. Glutamatergic, GABAergic and cholinergic subgroups would have fundamentally different actions.

VIP-positive bipolar cells appear to be evenly distributed in cortex, so that no regions larger than 100μm across lack any such neurons (Morrison et al., 1984) and each has its own radial domain an average of 30μm across. VIP function in bipolar

cells is poorly understood, but it may regulate metabolic processes such as glycosylation in the cortex or internal changes by facilitating the formation of cyclic AMP (cAMP; Morrison et al., 1984). The role of cholinergic signalling (Bayraktar et al., 1997) in these neurons may include arousal-related modulation of activity (White, 1989). The electrophysiological burst-spiking associated with VIP labelling in these cells by Kawaguchi and Kubota (1997) was not interpreted in any general functional sense by those authors.

2.2.7 Smooth and sparsely spinous cells

Areal and laminar distribution: This category includes neurons from all cortical layers, with varying distributions; although they all have relatively aspinous dendrites and use GABAergic transmission, their grouping here reflects a lack of type-specific data, rather than implied functional similarities.

Morphology: Most of these neurons have small, local axon plexuses which overlap with their dendritic fields. Naming can derive from the form of the dendritic field: e.g. multipolar, neurogliaform; or from axon plexus morphology: e.g. arcade cells, superficial plexus cells (cf. Figure 1.1; overview by Peters & Saint Marie, 1984).

Dendritic inputs: Smooth and sparsely spinous neurons receive both asymmetric and symmetric axodendritic synapses from various sources; thalamocortical afferents have been observed forming synapses with multipolar cells (White, 1989).

Somatic inputs: These cells typically receive asymmetric and symmetric synapses on their somata, with few on the axon initial segment (Peters & Saint Marie, 1984).

Axonal targets: Smooth / sparsely spinous neurons form synapses with a variety of elements, including somata and dendrite shafts of pyramidal and nonpyramidal cells, and axon initial segments (Peters & Saint Marie, 1984).

Transmitters used: These neurons are GABAergic (Morrison & Hof, 1992; White, 1989). Multipolar cells described by Gabbott and coworkers (1997) displayed NADPH diaphorase activity and hence employ nitric oxide signalling.

Characteristic chemistry: Calretinin has been localised in multipolar cells of the rat frontal cortex (Gabbott et al., 1997). Kawaguchi and Kubota (1997) found no characteristic chemistry for neurogliaform cells, although they have possibly been identified with CB-IR in monkey cortex (Condé et al., 1994). Cells immunopositive for SRIF in rat cortex had multipolar morphology (Hendry, Jones, & Emson, 1984).

Function: GABAergic transmission and variety of postsynaptic targets make these cells locally inhibitory (Peters & Saint Marie, 1984); specific morphology is

presumably tied to specific physiology, chemistry and connectivity (cf. Kawaguchi & Kubota, 1997).

2.2.8 Martinotti cells

A cortically ubiquitous group of non-spinous neurons whose axons ascend without bifurcating and proliferate in layer I were termed Martinotti cells by Ramón y Cajal (in Fairén, DeFelipe, & Regidor, 1984). They are often found in layers V and VI, but may occur in more superficial regions; their dendrites radiate in a multipolar or bitufted pattern, often favouring the descending side. Their axons ascend directly from the superficial side of the soma and form a fan-like plexus or horizontal ramification in layer I. Martinotti cells with SRIF and CB immunoreactivity were described by Kawaguchi and Kubota (1997). Their axon ramifications in layer I are likely to contact the axon tufts of pyramidal cells (§2.2.1) and Cajal-Retzius neurons (§2.2.9).

2.2.9 Cajal-Retzius neurons

The phylogenetically and ontogenetically early Cajal-Retzius (C-R) neurons are restricted to layer I, where their axons descend toward the boundary with layer II and make extensive tangential ramifications with numerous ascending processes (review by Marín-Padilla, 1984). Their distribution is irregular, tending to concentrate in the primary motor and sensory regions (Marín-Padilla, 1984). Axodendritic and axosomatic synapses on C-R neurons have been described at the ultrastructural level, arising from the Martinotti neurons and ascending white matter fibres which terminate in layer I, and from the widespread monoaminergic fibre plexuses on the pial surface of the cortex. Synapses made by C-R axons on the dendrites of layer I have been similarly described. C-R neurons are probably involved more in developmental processes and the early organisation of the cortex, and may die or change phenotype in later development (Mienville, 1999). However, some studies have reported their presence in adult human cortex (Martín et al., 1999) where they displayed immunoreactivity for parvalbumin, calretinin and calbindin, and NADPH-diaphorase reactivity, suggesting an inhibitory role.

2.3 Summary

The principal properties of neurons described in §2 are summarised in Table 1.I, with representative examples of their morphology in Figure 1.1.

Table 1.I: Properties of the major cortical neuron types

Abbreviations: ais, axon initial segment; s, soma; tc, thalamocortical fibre; cc, corticocortical fibre; cell types abbreviated as indicated. Italics indicate inhibition; brackets indicate that a property is not ubiquitous.

Name	Layers	Inputs	Outputs	Chemistry	Transmitter(s)	Function
Pyramidal (P)	II–VI	P, SS, tc, *Bs*, *BT*, *S*, *Cais*	P, S	(CB), (NF), (SRIF), (AChE)	glutamate; aspartate	projection; excitation
Spiny stellate (SS)	IV	SS, P, tc, *S*, *clutch*	SS, P, clutch, S	–	glutamate?	receive, propagate tc input
Basket (B)	II–VI	P, SS, tc, *S?*	*Ps*, *Bs*	PV, (CR)	GABA	lateral inhibition
Chandelier (C)	II–III	cc, *S?*	*Pais*	PV, (CB)	GABA	Inhibit cortico-cortical feedback
Bitufted (BT)	II–III	P, *S?*	*P*, *non-P*	CB, (CR), (PV), (CCK), (SRIF)	GABA, (NO), catecholamines?	Columnar inhibition?
Inhibitory bipolar (BPi)	II–V	P, tc, *B*, *S*, *BT*	*P*, *S*	CR, VIP, CCK?, (SRIF)	GABA, acetyl choline?	Col. inhibition; metabolic?
Excitatory bipolar (BPe) (?)	II–V	P, tc, *B*, *S*, *BT*	P?, S?	CR, not VIP, CCK?	glutamate?	Columnar excitation?
Smooth (S)	I–VI	P, tc, *S?*	*P*, *S?*	(CR), (CB), (SRIF)	GABA, (NO)	local inhibition
Martinotti (M)	II–VI	?	*P*, *C-R*	SRIF, CB	GABA?	wide inhibition?
Cajal-Retzius (C-R)	I	*M*, plexus	*P*	(CB), (CR), (PV)	GABA?, (NO)	wide inhibition?

Figure 1.1

Representative morphology of various categories of cortical neurons. Adapted from DeFelipe (1993), DeFelipe and Fariñas (1992) and Somogyi and coworkers (1983).

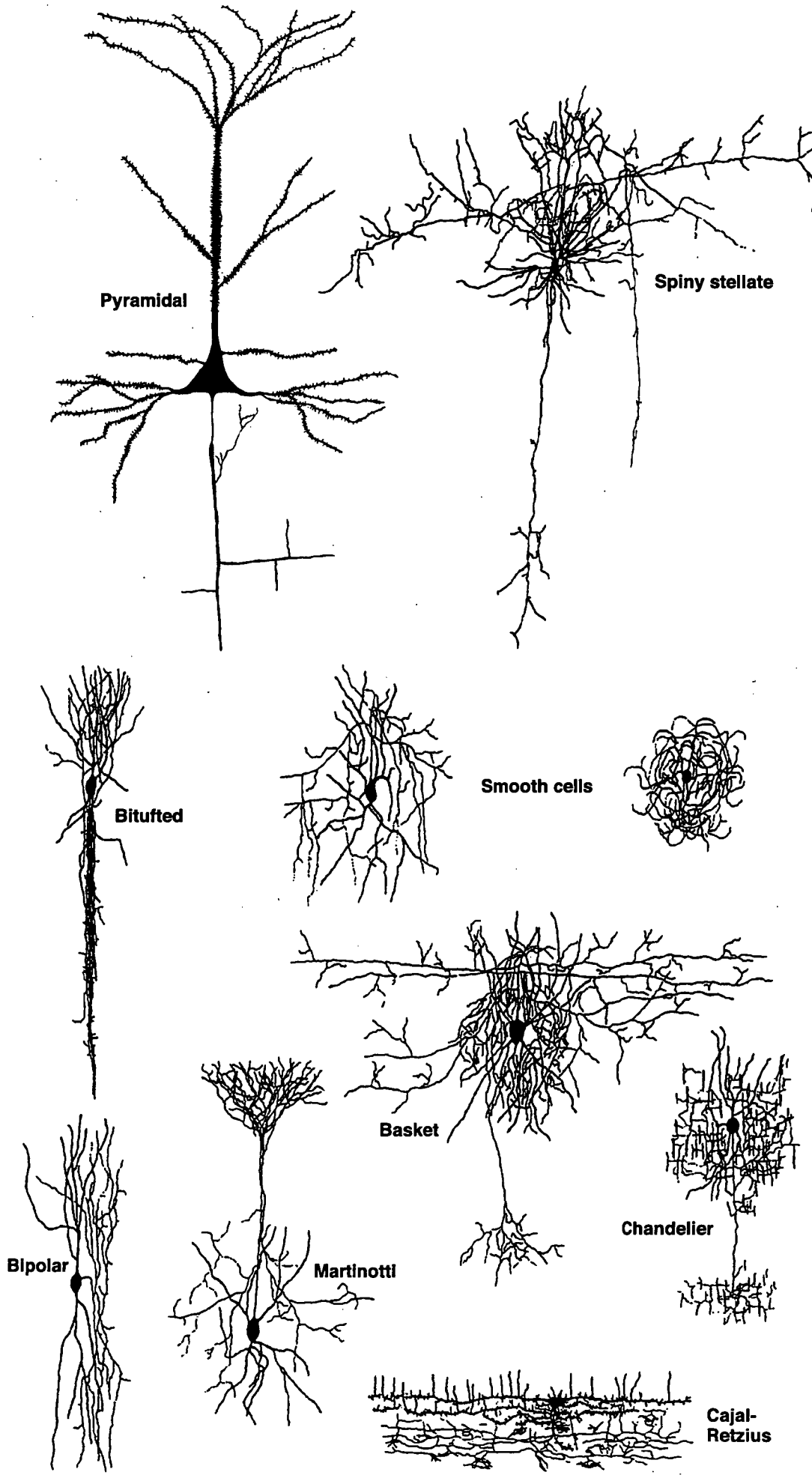
Pyramidal
Spiny stellate
Bitufted
Smooth cells
Basket
Chandelier
Bipolar
Martinotti
Cajal-
Retzius

3 Cortical organisation

Knowledge of the morphology, connections and chemistry of the neuronal types prompts the question of how their diversity can be reconciled in some kind of general organisation. Some clues as to the adult complexity of the cortex can be obtained by observing the development of cortical arrangements in juvenile brains.

3.1 Development of organisation

3.1.1 Local connectivity

Initial cellular growth

After differentiation and migration, the neurons of the cortex begin to assume the adult forms reviewed in section 2.2. For example, Feldman (1984) reviews the development of pyramidal cell morphology: from an initial bipolar form, the apical dendrite thickens while the axon extends toward the white matter. Shortly before birth, the apical dendrite ramifies and basal dendrites become apparent, with spines forming in both regions; most pyramidal cells have similar apical dendrite arrangements early on in development, which may be modified by the subsequent withdrawal of the apical dendrite from superficial layers (Koester & O'Leary, 1992). Dendritic fields of cortical cells develop extensively in the first few weeks after birth, peaking in extent around postnatal day 18 (P18), much of which occurs in the absence of cortical afferents. Similarly, spiny stellate neurons acquire their spines gradually, particularly after the onset of afferent activity; after this period, the number of spines dwindles somewhat (Lund, 1984) in a process that may be activity-dependent (Andersen & Figenschou Soleng, 1999).

The axonal fields of cortical neurons undoubtedly undergo major reorganisation during development, ranging from modification of their synaptic connections through to large-scale reorganisation of their branches, probably including the elimination of some collaterals (e.g. Callaway & Katz, 1990). After birth axon collaterals grow and elaborate throughout postnatal development (O'Leary & Koester, 1993), a sequence which occurs at different times in various regions.

Formation of characteristic connections

Contact guidance and chemoaffinity are the major factors in the guidance of developing axons. For instance, in the developing mouse brain the growing axons of the corpus callosum are guided by an interhemispheric bridge of glial cells known as

the glial sling, and restricted in their rostral extent by another glial structure called the corticoseptal barricade (Uylings et al., 1990). While thalamocortical afferents are important in determining many structural factors of cortex (Schlaggar & O'Leary, 1991), many region-characteristic processes are intrinsic (Miyashita-Lin et al., 1999). For instance, even though visual experience is vital in establishing the ordered pattern of receptive regions in visual cortex (review by Zeki, 1993), it has been shown that thalamic afferents develop the same physical patterning of ocular dominance in the absence of eyes (Crowley & Katz, 1999). Clearly, this anatomical regularity has no functional significance without subsequent developmental synaptic plasticity driven by experience.

At birth, some asymmetrical and symmetrical synapses are detectable between cortical neurons under ultrastructural examination. During the second and third weeks after birth, the number of synapses increases dramatically, coinciding with the development of dendritic spines on cortical neurons; after this period of increase, symmetrical synapses decline around P20, suggesting a process of elimination (Uylings et al., 1990). White (1989) presents data to suggest that synapses are made on any surface which can receive them in the vicinity of a growing axon, which would imply that synaptic formation not as specific or functionally critical as the subsequent modification of synapses. The presence of GABA receptors on cortical neurons prior to the existence of inhibitory synapses (Luhmann & Prince, 1991), for example, is strongly suggestive of synaptic formation guided by the suitability of the postsynaptic membrane. Similarly, studies of dendritic spines suggest that they form connections with active adjacent processes (Barinaga, 1995; Maletic-Savatic, Malinow, & Svoboda, 1999).

From this initial exuberance of projections, axons and axon collaterals are selectively eliminated and establish more specific connectional patterns, in processes which may depend on extracellular afferent-derived factors (O'Leary & Koester, 1993) or incoming activity alone (Killackey, Rhoades, & Bennett-Clarke, 1995; Antonini & Stryker, 1993; Callaway & Katz, 1990). Such disassembly and withdrawal of processes may be achieved by microtubule dynamics and disassembly (§4.3.2; Matus, 1991), again probably driven by afferent stimulation (Aoki & Siekevitz, 1985), and may also be regulated by internal factors such as the action of thyroid hormone on the expression of neurofilaments, another component of the cytoskeleton (§4.4; Gravel & Hawkes, 1990). These changes develop under spatial constraints such as competition between growing processes, crowding, physical barriers and space limitations in the cortex (Katz, 1993).

Synaptic formation or elimination may also be governed by pre and post-synaptic activity in processes analogous to long-term potentiation or depression. For instance, although it is possible for a neuron to form synapses with its own processes (Van der Loos & Glaser, 1972), these synapses may become postsynaptically silent (Gomperts et al., 1998). The relationship between the firing of the presynaptic and postsynaptic neurons also has fundamental bearing on the establishment or strength of any connection formed (Egger, Feldmeyer, & Sakmann, 1999). The implication is that connections formed between growing axons and the postsynaptic elements they encounter will tend toward maximising information as they form complex circuits guided by chemotaxis and firing correlation.

3.1.2 Larger scale organisation

Axons from the subplate are the first constituents of subcortical white matter (review by Shatz, 1992), growing down to reach the thalamus during corticogenesis. However, it is unlikely that they act as pathfinders for later corticofugal axons or thalamocortical fibres (O'Leary & Koester, 1993), and instead interact with them to determine which cortical regions they will innervate (Ghosh et al., 1990). Pyramidal cells of the characteristic projection layers of the adult cortex (transcallosal projections from layers II/III, subthalamic projections from layer V and corticothalamic projections from layer VI) appear to have these characteristics determined by the local environment in which they undergo their final mitotic division before migration, and send generalised projections specifically to their target regions during the last week of embryonic development (O'Leary & Koester, 1993). These connections are later pruned (e.g. subcortical visual cortex efferents lose spinal projections) under the influence of changes induced in their originating regions by invading thalamocortical afferents (O'Leary & Koester, 1993).

3.2 The modular cortex examined

Ever since morphological studies showed radial processes dominating cortical structure, and physiologists discovered columns of similarly responsive cells, the notion that the fundamental structure of the cortex is columnar has dominated neuroscience. While columnar phenomena have been observed by various means, the question of whether they arise from static structural regularities or dynamic groupings is of particular relevance.

3.2.1 Intrinsic modularity

Among models of cortical function, the most successful and enduring have suggested that activity is dominated by regular cellular groupings of a relatively small size, extending through the thickness of the cortex and processing afferents which are qualitatively distinct from those of neighbouring columns. The size and rationale of these columnar units varies according to the evidence considered (Swindale, 1990, 1998); while it is possible that they are hierarchically ordered, the question of whether the various scales can be reconciled with one another is largely unanswered (Swindale, 1990, 1998; Jones, 2000).

Among the most influential models are those based in anatomical regularity by Szentágothai (e.g. 1975) and in physiology by Mountcastle (e.g. 1978; 1997). Szentágothai uses the morphology of various cortical components to propose that activity is characteristically focused on the scale of a 50μm column, while Mountcastle regards the 500μm column and its constituent minicolumns – functionally distinct grouping of around 110 neurons derived from common progenitors – as basic units of cortex. More recently, Buldyrev and co-workers (2000) proposed the microcolumn, containing about eleven neurons, as a fundamental functional unit.

Anatomy, immunohistochemistry, cellular physiology and cortical ontogeny all indicate that columnar organisation exists on various scales, and the coincidence of form is compelling: it seems certain that the cerebral cortex is formed, develops and functions in a columnar fashion. Whether these phenomena reflect a common lower-order structural makeup, or are separate consequences of neuronal development after an initially columnar genesis, remains the subject of debate.

3.2.2 Ontogenesis of the cortex

The relationship between clonal groups (§2.1.2) and functional minicolumns is not explicit in theories which suggest them as an origin (e.g. Mountcastle, 1978, 1997). If common clonal origin produced columnar grouping, a column should consist of a single clone (which would limit them to the size of the microcolumns of Buldyrev, 2000; Walsh & Cepko, 1988), or those of adjacent progenitor cells expressing some common factor which distinguishes them from other neighbours. Rakic (1990) characterises radial groups of neurons as polyclonal in origin, and describes neurons crossing from one radial guide fibre or fascicle to another during migration, so it appears that mini- or microcolumns are likely to be heterogeneous, and that the notion of distinct sets of guidance molecules for adjacent groups is unlikely.

Johnston and van der Kooy (1989) describe heterogeneous expression of protooncogene peptides in radial glial cells of the developing mouse cortex, suggesting that migrational conditions for some groups of neurons would differ depending on location, but the distinct fibres appear in stripes much larger than a minicolumn and relate more to bursts of cell formation in the ventricular zone. No pattern in the stem cell "protomap" (Rakic, 1990) has been suggested to correspond with adult minicolumns.

3.2.3 Spatial and morphological regularity

Neuronal morphology

Purely morphological arguments for cortical modularity have been articulated most successfully by Szentágothai (1975). Since the earliest observations of cortex, it has been apparent that the processes of most neurons are radially elongate (White, 1989). In the 1930s, Lorente de Nó made significant efforts to understand their connections, introducing notions of multiplicity and reciprocity, and abandoning previous notions of sequential chains of activity (Szentágothai, 1975).

Processes in the neocortex exhibit regularity on many scales; for example, the dendritic arbours of many cells form repetitive shapes (e.g. Lund, 1984; summary in Szentágothai, 1975). Thalamocortical afferents from competing inputs tend to ramify in columnar fields 500-2000μm in extent (e.g. Constantine-Paton, 1981). Other cells give rise to highly columnar axonal or dendritic processes of characteristic diameter and extent (e.g. Peters & Saint Marie, 1984). The column is the commonest structural motif in the cortex.

Based on such observations, together with physiological studies, Szentágothai's model has remained influential. It balances the dominance of pyramidal cells and their excitatory influence with a proposed local structure involving radial excitation and lateral inhibition, serving to focus activity in columns of pyramidal neurons.

Szentágothai suggested that the spreading of successive axon collaterals from descending pyramidal axons would, at a fifty micron radius, cause a transition in pyramid-pyramid synaptic arrangements from chains along the apical dendrites of nearby cells to less potent, distributed synapses with the basal dendrites of more distant cells. This sharp drop in influence confines spreading excitation, but activating a column of cells depends on other factors: other transmitters of radial excitation, and the inhibition of neighbouring regions. For these roles he suggested

the bipolar cell and the basket cell, whose physiology and ultrastructure have subsequently been shown to suit. Large inhibitory cells resembling Martinotti cells (Condé et al., 1994), with axonal arbours spreading orthogonally to those of the basket cells, parcellate columns in the other direction.

Szentágothai's model uses observed arrangements to explain the columnar and slab-like patterns of activity observed in physiological experiments. The size of columns derives from cellular anatomy, not static grouping; indeed, confining activity to a consistent column would imply that the described influences apply only to its middle. Otherwise, activity could be sustained in a group made from parts of other columns, and the column would not be invariant. Since the model is based on morphology, invariant columns would be distorted at their edges, which has not been observed except in barrel cortex (see below). In this respect his model differs from that of Mountcastle (1978, 1997) who suggests that his minicolumns are constant groupings.

Barrels

A prominent columnar structure of the rodent cortex is the barrel: Neurons in the somatosensory cortex form clusters in which layer IV cells are pushed into ring-like shapes surrounding cell-sparse regions packed with thalamic afferents (Woolsey & Van der Loos, 1970; Killackey, 1973; Hoeflinger et al., 1995). The cells of each barrel respond to stimuli from a single vibrissa (e.g. Yang, Hyder, & Shulman, 1996). These structural regularities are the result of differential expansion of the neuropil by growing processes (see below); the ability of visual cortex to form these structures when grafted onto the somatosensory subplate (Schlaggar & O'Leary, 1991) indicates that this process is prompted by thalamic innervation, although the region is also neurochemically specialised (Miyashita-Lin et al., 1999).

Dendritic and axonal bundling

Other evidence for physically distinct columns in cortex includes radially bundled processes: studies have reported that the apical dendrites of layer V pyramidal cells form evenly-spaced clusters of thirty or less (Escobar et al., 1986; White & Peters, 1993; Peters & Sethares, 1996), which join similar clusters from layer III cells on their way to the pia.

Peters and Sethares (1996) describe similarly sized clusters of myelinated axons descending through layer IV in the macaque visual cortex, regularly arranged and separated by an average of 23μm like the clusters of apical dendrites. They propose that the cells contributing to these bundles form defined cortical modules

which are an anatomical correlate for Mountcastle's minicolumn (1978), though Mountcastle himself (1997) does not explicitly equate them. The coincidence of scaling is persuasive, although, for example, the termination arbours of thalamocortical fibres in this region extend over about 100–200μm (Blasdel & Lund, 1983; in Lund, 1984). These clusters are similar across species, and begin forming with the earliest cell migration to the cortical plate (Hirst, Asante, & Price, 1991). The notion that they might form basic functional units in the cortex is plausible in terms of size and anatomical arrangement, and of the simple ratios of the various inhibitory neurons which would associate with such a grouping. Gabbott and coworkers (1997) used density measures of GABA-immunoreactive neurons to calculate the number of cells corresponding to these dendrite bundles in rat frontal cortex: they estimated about 16 GABA-labelled and 80 non-GABA-labelled cells per bundle, agreeing with Peters and Sethares' (1996) estimate of 16:64 in macaque visual cortex. Clearly there exists a nearly uniform balance between the proportions of neuronal populations, which is suggestive of specific interrelations between types across all cortical areas. Whether this implies an intrinsic columnar organisation is open to debate (Swindale, 1990), and studies of dendritic bundles have not provided decisive information.

Firstly, no data of the spatial distribution of the somata of dendrite-clustered neurons, or how far the grouping extends, is available. The numbers of axons and dendrites in bundles (7–72, mean 34; 3–18, mean 8) differ greatly from one another, and it is therefore likely that the cells contributing to an axonal bundle in layer IV supply dendrites to different ascending bundles, raising the problem of defining their grouping. The issue of why bundling axons or dendrites implies a functional relationship is not addressed: no gap junctions between the bundled dendrites were observed in the mature cortex (Peters & Sethares, 1996), and myelinated axons are functionally isolated from one another. Early bundles have "intermediate junctions" of unknown significance, but these are not observed in adults (Hirst, Asante, & Price, 1991). Synaptic interconnection or similarity of inputs may be more likely between clumped cells, but these possibilities are not raised. Such questions would depend on whether dendrite-bundled somata are clustered, and how their dendritic and axonal fields compare in extent, for which no data are available.

Evidence linking dendritic or axonal bundles to function is scant. Callosally projecting pyramids do share apical dendrite clusters (Lev & White, 1997; perhaps related to shared guidance molecules, O'Leary & Koester, 1993), but neurons which all project to the opposite hemisphere do not imply a local processing unit.

Conversely, the makeup of descending axonal bundles changes as some leave and ramify in layer V (Peters & Sethares, 1996), so those bundles group neurons with different projection targets. In the barrels of the mouse somatosensory cortex, dendrite clusters are more concentrated around the edges of barrels (White & Peters, 1993). The variation is suggestive, but evaluating reported cell densities below layer IV indicates that the cluster density is distorted to the same extent as the packing of cells contributing to them (29.1% and 24.5%), attributable to physical expansion of the barrel central regions rather than functional similarity.

Speculations about modules in these studies appear to have extrapolated anatomical patterning to functional grouping with little justification. Their spacing could derive from radial structures influencing a field of growing axons and dendrites, or neurophilic adhesion factors mentioned by Rakic (1990) in his description of the differential guidance of growing axons and dendrites from Purkinje cells. Comparisons with numbers of cells per unit area of cortex (Peters & Sethares, 1996) indicate only that the axon bundles contain axons from most cortical pyramidal cells, and that estimates of pyramidal cell density tend to agree whether cell bodies or descending axons are counted. As modules, these bundles are problematic, exhibiting great variation in numbers; if they are functional entities, it would seem that they are far from uniform in size or processing ability. The problems of bundle definition and variations in their size, location and axonal targets make them poor candidates for functional units in the absence of supporting evidence.

3.2.4 Regularities in chemical neuroanatomy

The regularity of patches observed when cortex is histochemically stained to visualise the enzyme cytochrome oxidase has long been used as an argument for intrinsic modularity on the millimetre scale in the cortex (Swindale, 1990; Zeki, 1993; Jones, 2000). This enzymatic concentration has been attributed to GABA-IR neurons which are highly metabolically active (Nie & Wong-Riley, 1995; Maier & McCasland, 1997); the rapid, sustained bursting activity of such cells is a powerful, laterally distributed counterbalance to the excitatory connections of the cortex (Galarreta & Hestrin, 1998); it seems likely that spatial regularities in their arrangement would induce static regularities in cortical activity.

Several studies (Morrison et al., 1984; Jones, 2000) describe the irregular but uniform spatial distribution of bipolar cells expressing the metabolic regulator VIP and CR. When viewed tangentially, the distribution of VIP- or CR-containing cells is

random, and their somata lie at various cortical levels between II and V; however, their tangential distribution is sufficiently dispersed that each cell's axonal arbour occupies a columnar domain 30-60μm in extent; patches wider than 30μm without a VIP/CR neuron are rare.

Such disordered, uniform distributions may be the result of random but equiprobable genesis in the developing cortex (perhaps by the tangential-then-radial migration pattern; Rakic, 1995), uneven cortical growth after initial regularity, or post-migrational differentiation in which developing cells inhibit the development of the same phenotype within their domain of influence.

3.2.5 Physiological patterns

Evidence from physiological recordings in the cortex is the most familiar constituent of theories of cortical modularity, and has been comprehensively reviewed elsewhere (e.g. White, 1989). Briefly, columnar activity in the cortex was first recorded in experiments of the 1950s and 60s, in which the response properties of sensory cortex neurons were observed to cluster in homogeneous, disjoint groups of the order of 500μm in diameter (reviewed by White, 1989; Mountcastle, 1978; 1997; Zeki, 1993) or smaller (e.g. sub-220μm focal areas of fMRI activity after whisker stimulation; Yang, Hyder, & Shulman, 1996). These columns often contain minicolumns of similarly responsive cells (Mountcastle, 1978). Such data is widespread in studies of visual, somatosensory and auditory cortex in cats and primates (reviewed by Mountcastle, 1997), though Swindale (1990, p. 488) states that "So far, the work of Hubel and Weisel is the only evidence for a physiologically discrete representation of any stimulus property on a scale comparable in size to that of the mini-columns." Furthermore, polymaps – in which responses by the same cortical region to various stimulus parameters are simultaneously considered – reveal multiple overlaid scales of activity without any apparent relation to one another, or to some fundamental smaller scale (Swindale, 1990, 1998; Mountcastle, 1997).

3.2.6 Local circuits

If the search for fundamental anatomical units is to shed light on the brain's function, some explanation of the activity of such units must be tackled. Theories of local circuits imply a finite scale of functional organisation, although they do not necessarily require anatomical modularity: cortical activity may be locally confined for one process, without that region remaining invariant for other processes. Conversely, any invariant anatomical unit should exhibit local processing in order to

be functionally significant. Although this sketch does not attempt to review or evaluate local circuit modelling of cortex, such approaches are obviously interlinked with whether the cortex can be described in a modular fashion.

Local-circuit models may attempt to replicate cortical properties at the level of single neurons (e.g. Hahnloser et al., 2000), or may consist of summaries of the known specificity of connections between cell types, with the implication that at the minimum stoichiometric grouping these constitute fundamental processing units (e.g. Peters & Sethares, 1996; Gabbott et al., 1997). The use of the word "circuit" carries implications of closure and modularity, which may be inappropriate for the hugely interconnected cortex, and counterproductive if it hides critical qualities of the brain's organisation (Swindale, 1990).

Connectional patterns between cell types suggest relationships such as those depicted in Figure 1.2, although the implication that all or any groups of these cells in cortex form such grouped connections is misleading. Design principles of human engineering rely on the repetition of simple elements to achieve complexity, but whether this principle applies to the biological domain is unknown. Similarly, the ease of observation of electrical activity in neurons, compared to the difficulty of unravelling chemical interaction, has encouraged an electrical circuit approach which leads in some models to near-neglect of biological properties (e.g. Douglas & Martin, 1991, 1992). These methods would need to be applied to steadily larger groups to approximate cortical processing if no simple unit can be identified. As the scale of modelling expands, progressively more subtle and non-linear effects such as wide scale biasing by catecholaminergic projection systems (Hornung & de Tribolet, 1995) are likely to assert their importance and cannot be ignored.

At minimum, local circuits satisfy observed connectional patterns between cell types and extracortical afferents and efferents. Many studies use the term "local circuit neuron" (e.g. Condé et al., 1994; Gabbott et al., 1997) to impart a functional overtone to anatomical and chemical descriptions, without discussing the "circuits" they may constitute.

3.2.7 Evaluation

Although cortical modularity is a comprehensible way of characterising neuronal activity, it is not necessarily justified; cases can be made for order at various scales from individual cells through clonal groupings, microcolumns, axonal and dendritic clusters, minicolumns, histochemical patches, barrels and cytoarchitectonic regions. Among the hypotheses advanced, the microcolumn of Buldyrev and coworkers

Figure 1.2

Summary diagram of connective relationships between cortical neurons. Outlined cells are inhibitory, while filled cells are excitatory. LP: local plexus neuron; SS: spiny stellate neuron. Adapted from White (1989, p. 81).

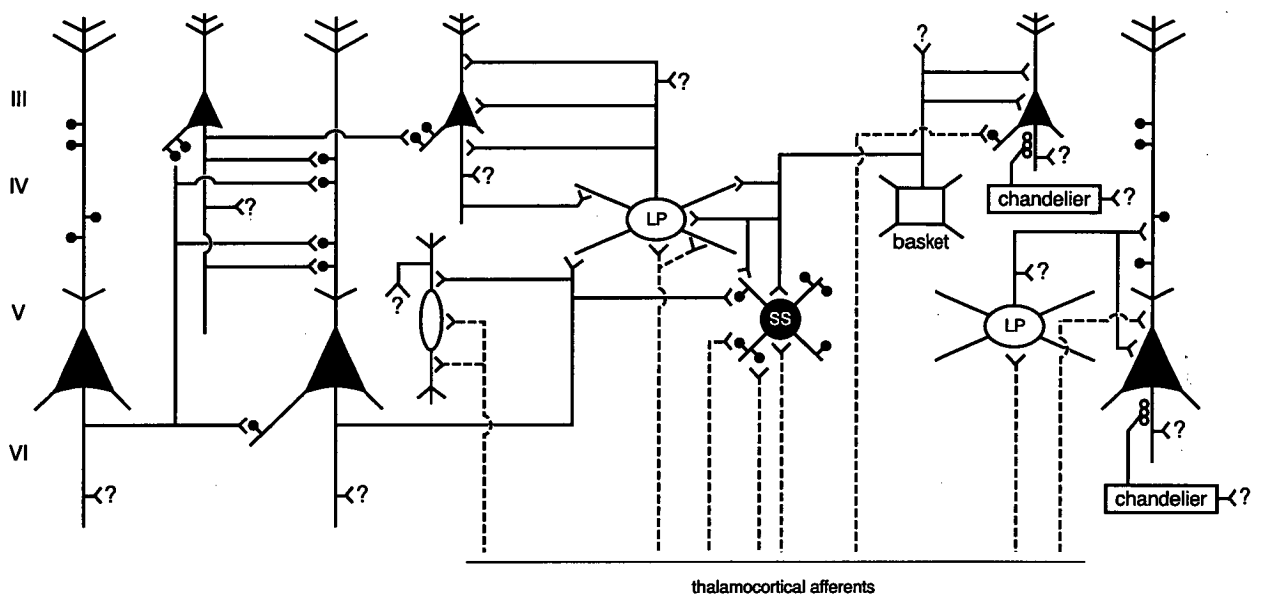
III
IV
V
VI
LP
SS
basket
chandelier
LP
chandelier
thalamocortical afferents

(2000) is statistically distinct and developmentally plausible given the size of clonal groups (Walsh & Cepko, 1988), but seems unlikely to be functionally discrete as they imply.

Swindale (1990) argues that the scales of organisation suggested by physiology, territorial parcellation by terminal fields, cytochrome oxidase staining and bundled processes are incompatible with the discrete larger-scale units they have been used to justify, and bear little relationship to one another: the data fail to converge on any intrinsic scaling or common periodicity. Since cellular genesis and radial migration impose a natural radial "grain" on the cortex (Rakic, 1990, 1995), it is likely that any regularity will be elongated into a columnar shape, leading to the convergence of observed arrangements in the brain. Although they may suggest an underlying modular structure, none seems necessary to explain the data. In fact, as Swindale (1990, p492) concludes: "Not only does it seem wrong to describe the cortex as modular, use of the term obscures the real complexity of cortical organisation and fails to do justice to the diversity of forms of columnar order that are actually present."

The rationale for theories of fundamental units is simplification of cortical function. However, an interconnected group of neurons must behave in ways which are more complicated than single cells; the relevant data are observed at mutually incompatible scales and are highly dependent on observational conditions. Yet another difficulty is posed by the autonomy of group member cells and their interactions with neurons of other groups, so that cortical activity is simplified only if sub-columnar effects are ignored.

From this perspective, the imaginary cylinder drawn by Szentágothai around his local cluster (1975) impedes understanding, since it implies an anatomically specific grouping of cells functioning as a whole, and prompts speculations of canonical subunuits based only on stoichiometry, connectional data and optimism. The grouping of neurons into functional units is at least partially dynamic: even the classical specificity of visual cortex receptive fields depends strongly on lateral inhibition (Crook, Kisvárday, & Eysel, 1998), and the size and response qualities of receptive fields in cortex change markedly with context and under anaesthesia (White, 1989). Examining these phenomena in the context of the minicolumn, as Mountcastle (1997) essays, it is difficult to see how the idea of an ontogenetically discrete columnar unit remains useful.

3.3 Afferent-driven differentiation

In the absence of compelling evidence for intrinsic modules, an explanation is required for the differentiation of function and anatomy in the regions of the adult cortex, despite homogeneous origins and uniform neuronal subpopulations. If the developing cortex does not consist of modules, how do columnar patterns come to dominate its adult form? The obvious possibility is for cortex to be shaped by its inputs, termed afferent-driven differentiation, as distinct from genetic predetermination. The process by which incoming afferents select and innervate regions of cortex is obviously driven by genetic factors, but the distinction is made between direct causation and developmental interaction.

The balance of activity in a given cortical region appears to be driven by extrinsic afferents, which influence the proportions and/or transmitter production of GABAergic neurons (Hendry & Carder, 1992; Kossut et al., 1991; Huntley & Jones, 1991; Hendry & Jones, 1988; Jones, Hendry, & DeFelipe, 1987). Local inhibitory neurons offer a substrate of various influences on activity which are enhanced or repressed according to afferent activity; this regulation may persist in the adult cortex (e.g. Pesold et al., 1999). Corticopetal axons are guided chemotactically, particularly by factors in the thalamus and subcortical white matter (Emerling & Lander, 1994; Ghosh et al., 1990; O'Leary & Koester, 1993), and their incoming activity induces reorganisation (Shatz, 1992). Extrinsic factors exert their influence on a general protocortex, in which the populations and arrangements of neurons are much more similar across regions than they are in the adult cortex (Huntley & Jones, 1991). The fact that the cortical misarrangements of mutant phenotypes such as *reeler* are viable at all (Rakic & Caviness, 1995) is a strong indicator that establishment of cortical function and normal axonal growth rely more on the availability of the appropriate mix of neuronal types than on any predetermination of laminar placement or the shapes of dendritic arbours in relation to surrounding cells.

The distinctive anatomy of barrel cortex is at least partially shaped in this way, as suggested by transplant studies (Schlaggar & O'Leary, 1991; O'Leary & Koester, 1993). The modifications induced by these invading fibres appear to create static groupings (White & Peters, 1993; Zilles et al., 1993), as discussed, but these data simply document the distortion of homogeneous tissue by afferent-induced growth patterns. For instance, the abolition of input from a single vibrissa results in the disappearance of its corresponding barrel, leaving homogeneous cortex rather than a half-formed barrel waiting for afferents (Van der Loos & Woolsey, 1973).

Thalamocortical axons carrying sensation from individual whiskers undoubtedly terminate in discrete regions, but this parcellation is simply one of the observable regularities; it is dominant in the anatomy and physiology of the region, but the distinctiveness of barrel cortex suggests that this is an extreme arrangement concealing other scales of regularity.

The changes wrought on developing cortex by disruptions to its afferents seem to revolve around shifts in GABAergic subpopulations, perhaps due to differential effects of thalamocortical cholinergic transmission (Kawaguchi, 1997). Hence these, and any phenotypes seen to shift in prevalence when afferents change, are likely to illuminate the development and specialisation of cortex. Associations between chemical markers and neuronal function offer insight to the changes induced in cortex by extrinsic signals.

4 Neuronal chemical phenotypes

Chemical phenotypes, differences between the sets of proteins expressed by individual neurons, can be observed using immunocytochemistry. Although neuron activity can be assessed individually and in small groups using electrophysiology, the rapid surveys possible using these markers can suggest function and plasticity on large scales, given correlations between cellular chemistry and functional properties. Of the markers reviewed in this section, only the neurofilament triplet has any appreciable presence in rat spiny neurons; otherwise, the notion of chemical phenotyping applies principally to the nonpyramidal minority of neurons of the cortex (DeFelipe, 1997a).

4.1 Peptides

Although glutamate, aspartate and GABA are the principal neurotransmitters used by cortical neurons (White, 1989), the visualisation of other transmitters, cotransmitters and signal peptides allows more specific subgrouping, and may, in some cases, enable insights to the activity and connections of particular neurons (DeFelipe, 1997a). Although many peptides (e.g. CCK, neuropeptide Y, tachykinins and corticotropin-releasing factor) cotransmitters (NOS, tyrosine hydroxylase-controlled catecholamines and acetyl choline) and surface antigens have been detected in cortical neurons (DeFelipe, 1997a), VIP and SRIF are particularly interesting for their association with specific electrophysiology in the neurons expressing them (Kawaguchi & Kubota, 1997).

It is possible that the small size and rapid transport of signal peptides may make their detection in the neuronal soma difficult, so that the immunoreactive populations mentioned here form only part of the population employing these substances (DeFelipe, 1997a).

4.1.1 Vasoactive intestinal polypeptide

Pattern of expression

Morrison and coworkers (1984) examined the adult distribution of VIP-IR neurons in cortex, and found that they were dispersed in such a way that no areal region of cortex larger than 100μm across lacked a VIP-IR neuron somewhere in its radial extent. Furthermore, the cells were spread so that each was the only VIP-IR neuron in a column of cortex 15-60μm across. Expression in cortical neurons is restricted to inhibitory bipolar cells (Gabbott et al., 1997; Kubota, Hattori, & Yui, 1994; Morrison et al., 1984; Emson & Hunt, 1981).

Functional significance

VIP applied to the cortex has a general excitatory effect, and its release may be modulated by intracellular calcium (Emson & Hunt, 1991). Externally applied VIP also elevates cortical blood flow in the region of application (Emson & Hunt, 1991) via innervation of capillaries on the pial surface; VIP-IR terminals do not innervate the capillaries which penetrate the cortex (Peters, 1990; Chédotal et al., 1994). VIP promotes cAMP formation which may have effects on metabolic regulation, but also may regulate other intracellular cAMP-dependent processes such as kinase-mediated cytoskeletal alterations (Morrison et al., 1984).

4.1.2 Somatostatin

Developmental and adult expression

In the adult rat and monkey cortex, SRIF-IR neurons are distributed throughout the cortex, with particular concentrations in layers II-III and VI, including the underlying white matter (Hendry, Jones, & Emson, 1984). Their axons form dense fibre plexuses in layers I, II and VI (Hendry, Jones, & Emson, 1984). Somatostatin has been identified in rat pyramidal, bitufted, bipolar and multipolar neurons (Morrison et al., 1983; Hendry, Jones, & Emson, 1984), and Martinotti cells (Kawaguchi & Kubota, 1997).

Functional significance

Little is known about the function of somatostatin in the cortex. It has been described as having an excitatory effect when applied extrinsically to hippocampal neurons (Hendry, Jones, & Emson, 1984). SRIF-IR cells, while mostly GABAergic (DeFelipe, 1997a), typically contain low levels of GABA (Gonchar & Burkhalter, 1997). Importantly, SRIF labelling has been associated with specific electrophysiology (regular rather than burst spiking) in rat frontal cortex GABAergic neurons (Kawaguchi & Kubota, 1997), and partially with the secretion of Reelin in adult cortex (Pesold et al., 1999).

4.2 Calcium binding proteins

4.2.1 General properties

The importance of calcium ions in signalling and intracellular transmission is reflected in the numerous proteins used by many cell types to regulate intracellular calcium (review by Baimbridge, Celio, & Rogers, 1992). In addition to general CBPs such as calmodulin, the calpains and protein kinase C, several CBPs such as parvalbumin, calbindin-D28k and calretinin are used by neuronal subpopulations, while S100α and β are restricted to glial cells and may help mediate their effects on neuron growth. The EF-hand domain of this family of CBPs binds one calcium ion (Baimbridge, Celio, & Rogers, 1992).

While some CBPs have a passive role and serve only to absorb free calcium ions when concentrations are high, others undergo a conformational change when absorbing calcium, which may facilitate enzymatic activity; however, the precise role of PV, CB and CR in neurons is unknown (Baimbridge, Celio, & Rogers, 1992), and locating these proteins in individual neurons is not by itself an indication of function (Condé et al., 1994).

Baimbridge, Celio, and Rogers (1992) review hypotheses of CBP function in neurons, which include passive calcium buffering by PV (by analogy with its role in muscle and its effects on previously PV-lacking cells) and effects on the time course and frequency of action potentials by CB; the association of various CBPs with characteristic electrophysiology by Kawaguchi and Kubota (1993; 1997; Kawaguchi, 1995) also suggest a role in modulating the action potential and resultant firing patterns. These effects are probably mediated by the influence of reduced intracellular calcium on transmembrane currents, enabling modification of action potentials or the facilitation of rapid bursts of action potentials to enable more

effective or qualitatively distinct inhibition (Galarreta & Hestrin, 1998). Administration of nimodipine (a "protective" calcium channel antagonist) to pregnant rats accelerates their pups' PV (Buwalda et al., 1994) and CB (Luiten et al., 1994) expression in some cortical regions, which argues against the notion of CBP expression in response to calcium influx, and perhaps supports a role of action potential modulation.

The increased expression may reflect a dependence on calcium regulation in forming organized connections (Lohmann, Ilic, & Friauf, 1998). Calcium management is vital to many connection-forming processes, including spine maintenance (Andersen & Figenschou Soleng, 1999) and cytoskeletal modification (Lohmann, Ilic, & Friauf, 1998); the widespread transient CB expression in the developing cortex (Alcántara et al., 1996; Sánchez et al., 1992; Alcántara, Ferrer, & Soriano, 1993) may indicate a role in regulating the calcium milieu during critical periods of organisation. CBPs appear transiently in many neurons during development, or after differentiation, which suggests that their expression relates to maturational and functional needs rather than intrinsic phenotypes (Liu & Graybiel, 1992; Sánchez et al., 1992; Alcántara, Ferrer, & Soriano, 1993).

CB, CR and PV occur in small cortical populations which represent most of the GABAergic cells (DeFelipe 1993; 1997; Gonchar & Burkhalter, 1997). In rat frontal cortex the proportions of CR, PV and CB-IR neurons are 4.0%, 5.6% and 3.4% respectively, a total comparable to the 16.2% of GABA-IR cells (Gabbott et al., 1997).

4.2.2 Parvalbumin

Patterns of expression

PV-IR has been observed in basket cells (Kawaguchi & Kubota, 1993; 1997), chandelier cells (Kawaguchi & Kubota, 1997), some bitufted cells (Gabbott et al., 1997; Condé et al., 1994) and some Cajal-Retzius neurons (Martín et al., 1999) of the rat cortex. Basket and chandelier cells represent the typical PV-IR neurons of the cortex in many species (DeFelipe, 1997a).

Most PV-expressing neurons express CB during development, prior to the appearance of parvalbumin in the cortex (Alcántara et al., 1996); adult parvalbumin expression is found in similar subgroups of most rat cortical regions (Kawaguchi & Kubota, 1997; Gabbott et al., 1997; Gonchar & Burkhalter, 1997).

Functional significance

The onset of PV-IR (Vogt Weisenhorn, Celio, & Rickmann, 1998) corresponds with the emergence of inhibition (Luhmann & Prince, 1991), and may reflect the establishment of mature inhibitional networks involving the basket and chandelier cells which typically express PV (DeFelipe, 1997a,b).

Studies by Kawaguchi and Kubota (1993; 1997; Kawaguchi, 1995) of rat frontal nonpyramidal neurons shows a clear association between fast spiking behaviour and PV-IR, indicating that PV may enable shorter and more numerous action potentials, whereas CB-IR accompanies low-threshold spiking physiology. Both groups were strongly immunoreactive, and several of the former were identifiable as basket cells and chandelier cells (Kawaguchi & Kubota, 1997; Kawaguchi, 1995). Deoxyglucose uptake has also identified a correlation between PV-IR and high metabolic rates in hamster cortex, while CB-IR neurons were much less active; both were GABA-IR (Maier & McCasland, 1997). More direct functional correlation is suggested by Raussel and colleagues (1992) whose deafferentation studies showed that subcortical and thalamic non-nociceptive somatosensory pathway cells were PV-IR, perhaps for similar physiological reasons.

4.2.3 Calretinin

Patterns of expression

Calretinin is widely expressed in subgroups of most types of cortical neurons, including pyramidal, basket, bitufted, bipolar, smooth and Cajal-Retzius cells (Gabbott et al., 1997; Martín et al., 1999).

Functional significance

CR's direct functions are not known (DeFelipe, 1997a), but its association with burst-spiking electrophysiology in GABAergic cells (Kawaguchi & Kubota, 1997) suggests a specific role in modulating action potentials. DeFelipe (1997) states that most CR-IR synapses described in rat cortex are symmetric and hence GABAergic, but that some (up to one third) are asymmetrical and presumably non-GABAergic. CR in the developing cortex may have a neuroprotective role by buffering intracellular calcium, which may be especially important to migrating and differentiating neurons (Schierle et al., 1997).

4.2.4 Calbindin D28k

Patterns of expression

Calbindin has been localised to primate pyramidal (Horning & de Tribolet, 1995), chandelier (DeFelipe, 1997b), Cajal-Retzius (Martín et al., 1999) and neurogliaform cells (Condé et al., 1994); in the rat cortex, it has been identified in bitufted (Gabbott et al., 1997; Kawaguchi & Kubota, 1993) and Martinotti cells (Kawaguchi & Kubota, 1997). Calbindin shows up in subgroups of many types of neurons, including pyramidal cells, and hence is associated with a variety of functional phenotypes (Gonchar & Burkhalter, 1997).

Strong CB immunoreactivity appears at the earliest stages of cortical development, starting in cells of the VZ around E13, then in the early-maturing cells of the PP and SP, with a dense plexus of CB-IR fibres in the subplate and the marginal zone bracketing the developing cortical plate (Liu & Graybiel, 1992). CB-IR nonpyramidal neurons are widespread throughout all cortical regions and layers before (Sánchez et al., 1992) and at birth, and are increasingly immunoreactive with an inside-out gradient over the next ten days (Alcántara, Ferrer, & Soriano 1993). However, the number of CB positive neurons declines dramatically between P11–P15, due to changing phenotypes (e.g. to PV-IR) rather than cell death (Alcántara et al., 1996; Alcántara, Ferrer, & Soriano 1993). Again, adult patterns are established by P22 (Sánchez et al., 1992). Its transient expression in many cells may indicate separate developmental and adult roles for CB in neurons, which may relate to regulation of local circuit formation (Lohmann, Ilic, & Friauf, 1998).

Functional significance

The deafferentation study by Raussel and coworkers (1992) also found that CB-IR is a hallmark of nociceptive pathway neurons in subcortical structures including the thalamus. Kawaguchi and Kubota (1993; 1997) associate CB-IR with low-threshold spiking in rat frontal GABAergic neurons, again pointing to an influence on action potential dynamics.

4.3 Structural elements

4.3.1 The cytoskeleton

The neuronal cytoskeleton comprises an interconnected network of various elements, some ubiquitous among cells, and some unique to neurons (Lee & Cleveland, 1996). It supports the shape of the neuron and enables growth and movement of neuronal

processes, most notably the axon (Lee & Cleveland, 1994). Skeletal elements common to all cells include microtubules (diameter 22nm) and paired, twined actin strands called microfilaments (6nm diameter; Lee & Cleveland, 1996). Intermediate in size between these are the so-called intermediate filaments, which vary among tissue types. The intermediate filaments of neuronal cytoskeletons are called neurofilaments (NFs), and are strandlike structures consisting of four paired protofilaments, around 10nm in diameter (Lee & Cleveland, 1996). In addition to the three filament types, a variety of specialised proteins serve to link and support the cytoskeleton, and to anchor it to membranes (Klymkowsky, 1999). The microtubules and associated elements form an integrated skeleton in the soma, originating from a structure called the centrosome; in neurons, the axonal cytoskeleton is a separate entity and is not connected to the perikaryal skeleton (Burgoyne, 1991).

4.3.2 Microtubules and associated proteins

Microtubules are the largest cytoskeletal element, consisting of spiral tubular polymers 22μm in diameter made from tubulin subtype heterodimers (review by Mandlekow & Mandlekow, 1995). The microtubule-associated proteins (MAPs) form part of microtubule assembly and transport mechanisms, and bind to microtubules to form side-arms which facilitate interconnections, promoting assembly and stability (Mandlekow & Mandlekow, 1995; Matus, 1991). Neuron-specific MAPs include tau, MAP-1 (various forms), MAP-2 (various forms) and MAP-5 (review by Matus, 1991); MAP-2a, a 280kD protein, is found in dendrites, while tau is largely confined to axons (Mandlekow & Mandlekow, 1995).

Developmental and adult expression

MAP-2 appears to be ubiquitous in adult neurons (Mandlekow & Mandlekow, 1995). During development it is preceded by juvenile forms including MAP-2c, derived from alternate splicing, which appears in axons as well as dendrites in the first postnatal week and is probably involved in plasticity (Tucker, 1990; Aoki & Siekevitz, 1985).

Functional significance

MAP-5 is expressed in growing neurites and is probably involved in the mechanisms of outgrowth and plasticity, after which it is replaced by other MAPs (Matus, 1991). MAP-2 phosphorylation is also implicated in experiential plasticity (Aoki & Siekevitz, 1985). Among many functions, microtubules form the structural basis for

the processes of slow axonal transport and possibly dendritic transport (Kobayashi & Mundel, 1998).

4.4 Neurofilaments

Pyramidal neurons vary widely in their size, distribution density and laminar arrangement, in correlation with their projection targets and morphology. However, in terms of their cellular chemistry, they are largely uniform. Although some primate pyramidal cells selectively express markers like calbindin, somatostatin and acetyl cholinesterase (§2.2.1), there are few consistent pan-specific markers for significant subpopulations of pyramidal cells. However, in many species a subgroup of pyramidal cells express the NF triplet protein, detectable with a range of antibodies specific to its various phosphorylation states. This polymer fills the intermediate filament role for some neurons, whereas others use intermediate filaments such as vimentin and α-internexin (Fuchs & Cleveland, 1998; Lee & Cleveland, 1996; Vickers et al., 1991). This section reviews studies of the distribution, composition and functions of neurofilaments in the central and peripheral nervous systems.

4.4.1 Composition and structure

Structurally, NF triplet polymers consist of groupings of four protofilament dimers, arranged in coiled coils, with multiple side-arms extending perpendicular to the 10nm-wide main filament (Fuchs & Cleveland, 1998). Various bridging proteins tie NFs to each other (at typical distances of about 45nm; Elder et al., 1998b), to other cytoskeletal elements, to the cell membrane and axolemma, and to some organelles (Hirokawa, Glicksman, & Willard, 1984; Pant & Veeranna, 1995; Hirokawa & Takeda, 1998).

The individual protofilaments are heteropolymers composed of three structurally related but distinct subunits, termed light (NFL), medium (NFM) and heavy (NFH) on the basis of molecular weight (66, 95-100 and 110-115 kDa respectively; Lee & Cleveland, 1996). A segment called the rod domain is highly conserved between the three; their different weights and properties arise from the size of the carboxy-terminal "tail domain", which is progressively more extended and structurally complex in the NFM and NFH subunits (Pant & Veeranna, 1995; Elder et al., 1998b). NF lattices undergo dynamic reorganisation on a timescale of hours, with units added and removed at various sites, and move anterogradely through the axon powered by nucleoside triphosphates (Julien, 1999).

Assembly

All three NF subunits participate in the structure of the central "rod" of the filament; NFL is found exclusively in the rod itself, while NFM occurs intermittently along the rod and at the base of inter-filament bridges, which are made from the NFM and NFH tail domains (Hirokawa, Glicksman, & Willard, 1984; Hirokawa & Takeda, 1998; Elder et al., 1998a). The rod domain is not the sole determinant of copolymerisation: the first eighty amino acids of the tail of NFL, and either head or tail integrity of NFM, are also vital for filament formation (Cleveland et al., 1991). Bridged filament structures have characteristic inter-filament spacing (Elder et al., 1998b) although filaments are otherwise distributed randomly (Price et al., 1988) or semi-randomly (Hsieh, Crawford, & Griffin, 1994). Bridging in assemblies of NFs changes their elastic properties, rigidity and shear strength, producing networks with different properties to other intermediate filaments (Leterrier et al., 1996), a process probably governed by manipulation of the phosphorylation states of NFM and NFH (Eyer & Leterrier, 1988; Gotow et al., 1994).

Of the three subunits, NFL alone is capable of independent assembly into filaments *in vitro* (human NFL only; Carter et al., 1998), although this has not been observed *in vivo* (Lee at al., 1993). NFM seems to be the most crucial in inducing normal NF structures (Julien, 1999) and determining filament spacing and regularity (Zhu et al., 1998); NFH knockout mice show similar NFL levels and filament density (Elder et al., 1998b), upregulation and greater phosphorylation of NFM (Hirokawa & Takeda, 1998) and more microtubules in axons (Zhu et al., 1998). Overexpression of NFL in transgenic mice produces denser, disorganised packing of NFs in axons without altering calibre (Monteiro et al., 1990), suggesting that filaments with fewer sidearms occupy less volume.

The stoichiometric relationship between the three subunits is probably important for their normal transport and assembly *in vivo* (Lee et al., 1993; Julien, 1999; Hirokawa & Takeda, 1998; Toyoshima et al., 2000), and may be regulated by NFM levels (Elder et al., 1998a,b). Post-expression transport to the axon exhibits a complex relationship with subunit expression and modification: NFM overexpression appears to accelerate transport (Xu & Tung, 2000), whereas greater NFH phosphorylation slows it down (Jung, Yabe, & Shea, 2000). NF subunits copolymerise with peripherin in peripheral nerve IFs (Parysek et al., 1991) and can copolymerise with α-internexin (Ching et al., 1999) and vimentin (Cleveland et al., 1991; Monteiro et al., 1990).

Phosphorylation

Phosphorylation of the tail domains of the medium and heavy NF subunits alters the spacing and rigidity of the neurofilament lattice, probably by extending the length and spacing of inter-filament bridges due to electrostatic repulsion between phosphate groups (Eyer & Leterrier, 1988; Gotow et al., 1994); these tail domains, particularly NFH, are the most phosphorylated proteins known in the nervous system (review by Pant & Veeranna, 1995). A series of lysine-serine-proline repeats in NFH and NFM tail domains allows for the attachment of multiple phosphate groups to the filaments (Elder et al., 1998b). Phosphorylation processes change the properties of inter-filament bridging (Leterrier et al., 1996; Guadano-Ferraz, Riederer, & Innocenti, 1990) and may also regulate the assembly and disassembly of the triplet polymer, including the prevention of premature assembly before they reach the axon (Nixon, 1993; Lee & Cleveland, 1996). Phosphorylation also alters binding between NFs and microtubules (Hisanaga & Hirokawa, 1990).

Neurofilament phosphorylation occurs predominantly in axons, particularly in proximal regions (Nixon et al., 1994; Schlaepfer & Bruce, 1990); dephosphorylated filaments are present in the perikaryon and dendrites, their less rigid bridging allowing them to form fascicles (Pant & Veeranna, 1995; Hirokawa, Glicksman, & Willard, 1984; Szaro, Whitnall, & Gainer, 1990; Gotow et al., 1994). Phosphorylation may also regulate NF transport from the perikaryon down the axon (Jung, Yabe, & Shea, 2000; Jung & Shea, 1999). Abnormal NF phosphorylation in the perikaryon is observed in Alzheimer's disease, in which NF-containing pyramidal neurons are killed by an unknown process, accompanied by disruption of the cytoskeleton (Hof, Cox, & Morrison, 1990).

The cues regulating NF phosphorylation remain obscure, although studies indicate that glutamate may act via the AMPA receptor to increase the phosphorylation of NFH (Asahara et al., 1999), and that kainic acid administration can reduce it by presumably similar means (Wang et al., 1992; 1994). Schwann cells have also been implicated in the increased phosphorylation of NFs in the axons they envelop (de Waegh, Lee, & Brady, 1992). Maturation in rat cortical neurons (Hornung & Riederer, 1999), in axons of the cat visual cortex (Liu et al., 1994) and in axons of the corpus callosum (Guadano-Ferraz, Riederer, & Innocenti, 1990) have also been correlated to changes in NF phosphorylation.

4.4.2 Patterns of expression

Many studies of cellular NF distribution have been made with the monoclonal antibody SMI32, specific to dephosphorylated NFM and NFH (Sternberger & Sternberger, 1983; Lee et al., 1988; Szaro, Whitnall, & Gainer, 1990). Counts made by Hiscock, MacKenzie, and Willoughby (1996) report that SMI32 labels 7.3%, 10.2%, 1.3% and 0.9% of all neurons in the Fr1, Par1, piriform and entorhinal regions of rat cortex; similar data from Hof, Cox and Morrison (1990) report a prevalence of 6–11% labelled by SMI32 among primate cortical neurons. Campbell and Morrison (1989) observed that human cortex has (qualitatively) markedly greater numbers of SMI32-labelled pyramidal cells than that of the cynomolgus monkey. It is possible, though unlikely, that the variable SMI32-labelled population could even be caused by masking or post-translational modifications of antigen sites in selected cells which *all* contain neurofilaments. A recent immunohistochemical atlas of the rat brain (Paxinos et al., 1998) reveals considerable variation in the distribution of SMI32-labelled perikarya and dendrites throughout the cortex, with some regions almost devoid of labelling, and others heavily immunoreactive in layers II/III and V/VIa.

The three NF proteins are encoded by separate genes (review by Julien, 1999). *In situ* hybridisation assays of NFH expression suggest that "most, but not all, CNS neurons synthesise the NF-H protein" (Roussel et al., 1991, p.102), an observation which is difficult to reconcile with adult distribution. mRNA for the three subunits is upregulated over days P5–P24, and phosphorylation of NFM and NFH occurs (Schlaepfer & Bruce, 1990). Axonal NFH appears during postnatal corpus callosum development in the cat, and may be related to which axons are retained during development (Guadano-Ferraz, Riederer, & Innocenti, 1990). Cues regulating NF production include direct transcriptional regulation of NFH by thyroid hormone (Ghosh, Rahaman, & Sarkar, 1999; Gravel & Hawkes, 1990) and NFL by oestrogen in female rats (Scoville, Bufton, & Liuzzi, 1997). Overall NFL levels may be regulated by post-transcriptional mechanisms in the CNS (Monteiro et al., 1990). NF expression also specifically declines with age, with a concomitant axonal atrophy in the PNS (Parhad et al., 1995).

4.4.3 Function

Surprisingly little is known about the functions of the widely distributed, highly regulated and plentiful neurofilament triplet protein. Their restriction to neurons alone suggests properties which differ from intermediate filaments in general, and

probably from other neuronal IFs. Of particular interest in discussing the function of neurofilament are studies of knockout mice deficient in NFL, NFM, NFH, NFM/NFH, α-internexin, and NFL/α-internexin, which reveal no apparent developmental or behavioural phenotypes, although axon calibre, conduction velocity and nerve regeneration are affected to varying degrees (Zhu et al., 1997; Elder et al., 1998a,b; Julien, 1999).

The appearance of NFs during neuronal maturation suggests they may assist the growth of neurons or their processes; among pyramidal cells, those labelled by SMI32 in monkey and human cortex tend to be larger than non-SMI32-labelled cells, although the latter group does include some large pyramidal neurons (Campbell, Morrison, & Hof, 1990; Hayes & Lewis, 1992). The large corticospinal motor neurons of many mammalian cortices are nearly all labelled by SMI32 (Tsang et al., 2000). A linear relationship between SMI32 labelling fluorescence in 1μm confocal sections, and cross-sectional area of stained cells, was described in human cortex by Campbell and Morrison (1989).

Other observations of properties related to neurons labelled by SMI32 provide few clues. Fewer of them express the early gene c-fos after a picrotoxin-induced seizure; this may reflect a lesser tendency to plasticity (Hiscock, MacKenzie, & Willoughby, 1996) or could reflect plasticity unrelated to gene transcription. Most acetyl-cholinesterase-containing pyramidal cells of the human neocortex are also labelled by SMI32 (Mesulam & Geula, 1991). One of the few papers to link external stimuli to changes in NF expression is the study made by Siegel and coworkers (1993), in which social deprivation of juvenile monkeys greatly increased the SMI32 labelling of dentate gyrus hippocampal neurons, which appeared to constitute a genuine upregulation rather than antigen alterations by dephosphorylation or delayed development.

The numerous binding sites present on NF subunits have been suggested to act as a sink for free calcium, sodium, aluminium and noxious ions and radicals (Lefebvre & Mushynski, 1987, 1988; Julien, 1999). NFs could regulate intracellular calcium, but that is evidently not their primary purpose, since they are found in some human pyramidal cells expressing calbindin (Hayes & Lewis, 1992), and small rat cortical neurons expressing calbindin and parvalbumin (D Grasby, unpublished data, 1996).

Axonal calibre and myelination

Neurofilament content has been correlated with the calibre of myelinated axons in many studies, beginning with the sciatic nerve counts of Friede and Samorajski (1970). Neurofilament immunoreactivity is correlated with cell size, myelination and conduction velocity in the peripheral nervous system (Lawson et al., 1993; Lawson & Waddell, 1991). The correlation is high in some fibre populations but can vary between groups; the degree of phosphorylation of the filaments themselves is not related to axon calibre (Szaro, Whitnall, & Gainer, 1990). A spontaneous NF deficiency mutation in Japanese quail produces a reduction in axonal calibre and conduction velocity accompanying their lack of axonal NFs (Sakaguchi et al., 1993). The causal relationship behind these correlations is ambiguous, with some researchers suggesting that neurofilaments accumulate to fill a given calibre (reviewed by Lee & Cleveland, 1996), whereas later studies indicate that the growing mass of filaments determines calibre (Nixon et al., 1994; Cleveland et al., 1991). NFH expression during development coincides with a slowdown in axonal transport (Hoffman et al., 1983) and knocking it out speeds axonal transport somewhat, perhaps by shifting the assembly equilibrium in favour of less stable filament networks (Zhu et al., 1998). NFM appears to mediate the passage of NF polymers into the axon (Elder et al., 1998a). Following axotomy, reduced NFL expression accompanies a transient reduction in axon calibre (Cleveland et al., 1991), but transgenic overexpression of NFL produces more filaments without increasing calibre (Monteiro et al., 1990). Regional NF aggregations near oligodendroglia in mouse optic nerves produce local expansions (Sánchez et al., 1996), supporting the notion that NFs exert an expanding force on axons.

It is probable that NFs are necessary for axons to widen to normal size during development, since knocking out NFL to prevent NF assembly results in peripheral axons around 30% of their usual diameter (Hirokawa & Takeda, 1998). The relationship is not a simple one, with studies of NFH knockout mice suggesting that axon calibre decreases somewhat in larger peripheral axons (Elder et al., 1998b) or remains similar, compensated for by an increase in NFM expression and in microtubule numbers (Zhu et al., 1998). Knocking out NFM has a far more pronounced effect on calibre, its role in NF transport leading to a reduction in axonal NFL, and hence a lack of neurofilaments (Elder et al., 1998a). Other studies in which NFs were normally expressed but hindered from being transported to the axon produced similarly reduced calibres in peripheral nerves (Hirokawa & Takeda, 1998). In complementary studies, increased expression and phosphorylation of the

NFH subunit resulted in increases of peripheral axonal calibre (Marszalek et al., 1996; Nixon et al., 1994) while increased NFL did not (Monteiro et al., 1990; Cleveland et al., 1991). Confusingly, knockout studies reported by Julien (1999) indicated that axons can grow normally and expand even in the absence of NFL *and* α-internexin.

The factors influencing NF accumulation in expanding axons are also largely unknown. The development of interhemispheric projections is influenced by thyroid hormone (Gravel & Hawkes, 1990), which parallels thyroid regulation of neurofilament expression (Ghosh, Rahaman, & Sarkar, 1999). A visual deprivation study in which optic nerve axon calibres were reduced by 35%, accompanied by a dearth of NFH and a reduction in the spacing of NF lattices, suggest that functional experience is also necessary for normal NF assembly and axon calibre maintenance (Fernández et al., 1993). A proximodistally reducing gradient in neurofilament levels of peripheral axons (Schlaepfer & Bruce, 1990) is not explained by reductions in calibre, but may reflect enzymatic degradation in distal processes.

Neurofilament content has also been tentatively associated with the length of a cell's axonal projection (Campbell & Morrison, 1989) but evidence on this issue remains unclear. However, the longest cortical projection neurons, the corticospinal cells of the motor cortex, ubiquitously express NFs in their perikarya (Tsang et al., 2000).

Conclusion

The widespread CNS distribution of the NF triplet, combined with the high metabolic cost of its production, and its specificity to neurons (Lee & Cleveland, 1996), suggest that it is an important polymer in the cytoskeleton of some neurons. However, aside from an equivocal relationship to axon calibre and myelination, and some correlation with the size of the neurons expressing it, very little is known of its function. Its capacity for extremely high degrees of phosphorylation, and a wide array of cellular mechanisms which can adjust its phosphorylation state (Pant & Veeranna, 1995) indicate that NFs are easily and commonly structurally altered, but whether these processes are restricted to growth and establishment of the cytoskeleton, or to more dynamic ongoing processes, is unknown.

4.5 Relationships between chemical phenotypes

The defining colocalisation phenomenon for the peptides and CBPs mentioned is their near-complete colocalisation with GABA or GAD immunohistochemistry, with

the partial exception of SRIF and CB which are sometimes found in spiny excitatory cells (DeFelipe, 1997a; 1997). The CBPs PV, CB and CR label almost entirely separate populations in the rat, cat and monkey cortex (DeFelipe, 1997a) which together make up around 85% of GABAergic neurons (Gonchar & Burkhalter, 1997). PV-IR and CB-IR neurons also exhibit little colocalisation with peptide markers and other CBPs, excepting the association between CB and SRIF in the rat (Gonchar & Burkhalter, 1997; DeFelipe, 1997b); most GABAergic neurons do not express these peptide markers (DeFelipe, 1997a).

Several studies suggest that there are three distinct subpopulations of GABAergic neurons recognisable by their peptide and CBP expression. Kubota, Hattori, and Yui (1994), examining the rat frontal cortex for colocalisation of various markers, found three groups: PV-IR cells; CR-IR cells also labelled for VIP and CCK; and cells labelled for CB, NOS, SRIF and NPY. Similarly, in the rat visual cortex, Gonchar and Burkhalter (1997) found that the GABAergic PV-IR group had no overlap with CR or SRIF and little overlap with CB; the SRIF-IR, mostly CB-IR neurons expressed no PV or CR; and the CR-IR group showed no PV, CB or SRIF labelling, essentially the same groupings as Kawaguchi and Kubota. Rogers (1992) also found near-complete colocalisation of VIP and CR. In human and monkey cortex, PV-IR neurons are quite frequently surrounded by CR-IR terminals of unknown source (DeFelipe, 1997b).

PV-IR baskets, but not axon initial segment cartridges, appear to preferentially target SMI32-labelled pyramidal cells in the monkey cortex (Akil & Lewis, 1992), though not all of the latter have surrounding baskets. In human tissue, bipolar CR-IR cells frequently form synaptic clusters around the apical dendrites of SMI32-labelled pyramids (del Río & DeFelipe, 1997b). Similarly, in the enteric nervous system of the guinea-pig, VIP-containing terminals preferentially surround NF-IR cell bodies (Vickers et al.,1991). Human pyramidal cells immunoreactive for CB and SMI32 are quite often contacted by CR-IR terminals on the soma and distal dendrites respectively (DeFelipe, 1997b).

4.6 Deducing regional function

The laminar distribution of these markers is remarkably similar across studies of rat, cat, monkey and human cortex, suggesting some functional commonality (DeFelipe, 1997a); the correlation of the three marker groups with well defined electrophysiology in rat neurons (Kawaguchi & Kubota, 1997) suggests that these

populations may provide specific and separate influences on cortical activity which are similar across species.

The close association of PV-IR with the basket and chandelier morphologies, together with their well-characterised postsynaptic associations, suggestive arrangements of terminal fields and boutons, and the clear dependence of PV expression on afferent activity, brings this class of cells close to the kind of characterisation envisaged by Morrison and Hof (1992). Together with the other physiologically significant markers, especially the spatially distinctive arrangement of VIP-IR cells, it seems that the possibility for assessing the characteristic activity of cortical regions based on their populations of chemical phenotypes is increasingly realistic. Further evaluation of the roles of these and other identifiable subpopulations depends on studies building on these foundations.

Indirectly, the activity of a region undergoing a change in the population of a particular phenotype can be examined, such as the emergence of inhibition in a region whose cells are beginning to express PV (Luhmann & Prince, 1991). More directly, further evaluation of individual cellular activity, and its effects on postsynaptic cells, will undoubtedly add to these characterisations. Regional methods such as metabolic evaluation by high resolution cytochrome oxidase (Nie & Wong-Riley, 1995) or 2-deoxyglucose (McCasland, 1996), levels of GABA expression (Hendry & Carder, 1992; Kossut et al., 1991; Huntley & Jones, 1991) or the detection of immediate early genes (e.g. Hiscock, MacKenzie, & Willoughby, 1996) are able to hint at cellular responses to normal and artificial stimulation; less precise methods such as fMRI (Yang, Hyder, & Shulman, 1996) may illuminate cortical regulation of blood flow. The opportunities for rapid growth in knowledge of the gross effects of neuronal subpopulations are apparent.

5 Concluding remarks

In terms of anatomy, development and the range of its morphological subtypes, the rat cortex is representative of the mammalian cortex. Simplicity of tissue processing, coupled with rats' rapid development and ease of experimental manipulation make them an ideal environment in which to study the processes by which the cortex is generated and differentiates. Recent evidence from developmental work in rodents highlights the crucial influence of corticopetal afferents in stimulating the differentiation and specialisation of cortical structure and subpopulations, replacing notions of intrinsic, predetermined connectional patterns and repetitive modular arrangement.

Against this background, it is increasingly evident that the extreme multiplicity and initially unrefined nature of cortical connections make the notion of unravelling "cortical circuits" optimistic at best. Instead, it may be pragmatic to take a population view of cortical regions, in which the contributions of subpopulations are assessed in the light of characteristic physiology, transmitters and connectional preferences. Such an approach requires the concept of "function" to extend across levels ranging from individual neurons to entire cytoarchitectonic divisions. Whereas electrophysiological studies of single neurons may provide a measure of correlation between external events and the timing and type of action and postsynaptic potentials, few would consider that such relations constitute the "function" of the cells involved. Overall responses of neuronal groups whose makeup can be assessed immunohistochemically, may bring us closer to an idea of cortical responses to stimuli and how identifiable subpopulations contribute to them. Such approaches require researchers to determine the level of organisation which needs to be considered before its activity corresponds to something recognisable as a "function".

The greatest potential for understanding cortical specialisation comes from the realisation that this differentiation is driven by thalamocortical afferents (O'Leary & Koester, 1993). Cholinergic fibres, principally originating in the thalamus, have distinct effects on immunohistochemically distinct subgroups of GABAergic neurons (Kawaguchi, 1997), and several studies have illustrated the effects of afferent perturbations on GABAergic populations (§3.3) and on expressions of their characteristic markers (§4.2.1). Taken at face value, these findings indicate that modulation of GABAergic subpopulations, along with regionally specific alterations to generalised projection patterns, are the mediator of this afferent-driven differentiation, and that such regulations of expression may continue into adulthood (Pesold et al., 1999).

The neurochemical phenotypes of 85% of these GABAergic interneurons are well defined, and in two of the three identified subtypes, are also associated with particular morphologies and projection patterns, well-defined postsynaptic elements in the case of PV-IR cells, and a distinctive distribution in the case of VIP-IR neurons (§4.5). Of particular interest are the experiments of Kawaguchi and Kubota (1997; 1993) which associate clearly differentiated electrophysiological qualities with these subtypes.

Although GABAergic subpopulations may be the substrate of cortical differentiation processes, focusing entirely on their heterogeneity excludes the 85% of cortical neurons which are excitatory, particularly the pyramidal cells, whose

activity provides the output of the cortex. One promising marker for pyramidal cell phenotypic differentiation is the subpopulation using the NF triplet (§4.4) as their principal cytoskeletal intermediate filament. The variety of dynamic modulations achievable through NF phosphorylation processes hints at important functions, which may be purely structural, but which nonetheless have important effects on the reception and propagation of activity in these cells. Understanding the development, regional distribution and correlated properties of these neurons may yield insights which differentiate this largest cortical population; the toe-hold offered by increasing characterisation of the GABAergic subtypes can be used in comparisons of distributions and double-labelling to provide further circumstantial evidence about their role in the cortex.

If neurochemical phenotypes can be identified and characterised for all the neuronal types, the possibility emerges for a general-purpose toolkit of preparation methods which can be used to rapidly and inexpensively assess developmental and induced changes. Such an approach would make detailed insight to the development, differentiation and characteristics of cortical regions available to laboratories with relatively basic equipment, and could revolutionise the process of understanding cortical function.

6 Experimental aims

The overall purpose of experiments in this thesis was to study the role of neurofilament triplet proteins in cortical neurons, and hence to extend the notion of functionally significant chemical phenotyping to pyramidal cells. The studies had the following aims:

1. To verify that the antibody SMI32 identifies all of the population of cortical neurons expressing perikaryal neurofilaments in the rat cortex.
2. To characterise the distribution of neurofilament labelling in the neuropil and cell bodies of the rat cortex, and to verify the observed proportion of SMI32 labelling among cortical neurons.
3. To investigate whether neurofilament triplet content is correlated with the length of a cell's axonal projection.
4. To study the relationship between axonal properties and their neurofilament content for corticocortical axons.
5. To characterise the developmental appearance of neurofilament in the rat cortex, and to compare it with the emergence of other chemical phenotypes.
6. To study the expression of neurofilaments and other chemical phenotypes in purely neuronal cultures, so that the influences of glia and extrinsic afferents are removed.

Chapter 2

General methods

1 Ethics

All experimental procedures undertaken in these studies were approved by the University of Tasmania Animal Ethics Committee, and were conducted in accordance with National Health and Medical Research Council guidelines on the treatment and care of animals in experimental studies.

2 Animals

Hooded Wistar rats provided by the Central Animal House of the University of Tasmania were used for all the studies described in this thesis. Male rats in the weight range 200-250g were used for all adult animal studies, and animals of both sexes were used for juvenile developmental series and as source material for neuron cultures. Postnatal age was adjudged on elapsed time since the mother was observed to have given birth, with the first twenty four hour period designated as postnatal day zero (P0).

3 Perfusion and tissue handling

3.1 Frozen sections

Rats were injected intraperitoneally with an overdose of Nembutal (sodium pento-barbitone, 1 ml/kg), and when deeply anaesthetised but still breathing, were injected with an 0.05ml bolus of sodium heparin (1% in 0.9% saline) in the left ventricle, while the right atrium was cut open. A blunt needle was then pushed into the left ventricle and through into the ascending aorta, through which 0.1M phosphate buffered saline (PBS) was perfused under gravity. After two minutes, the perfusate was changed to phosphate buffered 4% paraformaldehyde solution, which continued to perfuse the tissue for a further seven minutes. The brain and any other tissues of interest were immediately removed and placed in the same fixative for six hours.

Neonatal and juvenile animals were perfused using the same procedure except that handheld syringes were used to gently propel the perfusates through the blunted needle. Post-fixation times were shortened for smaller brains, with times of one, two and four hours used for the brains of P0, P7 and P14 rats respectively.

After postfixation, brains were immersed in several changes of PBS, and then placed in a 30% sucrose solution in PBS until they sank. They were then mounted and frozen on the stage of a freezing microtome (Leitz) and sectioned serially at a thickness of 40μm. Sections were collected and stored in ordered well containers of PBS, with 0.1% NaN_3 as an antibacterial agent.

3.2 Vibrating microtome sections

Brain sections cut using a vibrating microtome (Leica VT1000) were used for cytochrome oxidase histochemistry and Gallyas silver staining. They were processed as outlined in §3.1 above, excepting that after overnight washing in PBS, intact brains were embedded in 5% agar (Sigma) dissolved in heated PBS, and cut into coronal sections 100μm thick before further processing.

4 Immunohistochemistry

Most immunohistochemistry was performed on free-floating 40μm sections cut with the freezing microtome. Delicate tissue was occasionally mounted on slides coated with gelatin and chrome alum prior to immunohistochemistry, to prevent tissue damage, but the procedures and solutions used were the same as for the free-floating technique.

4.1 Double labelled fluorescence

Tissue sections were washed three times in ten minute changes of PBS, then immersed in a weak detergent diluent (0.3% Triton-X in PBS) to render their membranes permeable for better antibody penetration. Primary antibodies (rabbit monoclonal and/or mouse monoclonal; see Appendix B for concentrations) were added to this diluent, and left overnight on a shaker table at room temperature. After three ten-minute PBS washes, sections were placed in goat anti-rabbit conjugated to Alexa 594 (red) and/or anti-mouse conjugated to Alexa 488 (green) secondaries (both from Molecular Probes) at 1:1000 in diluent. After one hour's incubation at room temperature in darkness, sections had a further three ten-minute PBS washes and were mounted onto glass slides. After airdrying for an hour, slides were coverslipped with PermaFluor medium (Immunotech) and stored in darkness.

4.2 Immunoperoxidase

Similar procedures were followed for initial treatment and primary antibody incubation as for the previous section. The secondary antibody used was a biotinylated horse anti-mouse-IgG or goat anti-rabbit-IgG as appropriate (both from

Vector labs), diluted 1:1000 in the detergent solution. After three PBS washes, a commercial avidin-biotin mixture was added (Vectastain ABC, each component at 1:100 in PBS) and incubated for thirty minutes followed by three PBS washes. A solution of diaminobenzidine, urea and hydrogen peroxide was prepared from commercial tablets (Sigma Fast DAB), and the sections were placed in the solution to label the secondary antibodies with precipitated DAB. The reaction was stopped using PBS washes once it appeared to have labelled sufficiently, typically after ten minutes of reaction time. Sections were then mounted on slides, air dried, cleared in xylene and coverslipped using DPX.

5 Histochemistry

5.1 Cytochrome oxidase staining

Rats were perfused as described, with the exception that the postfixation time was restricted to one hour to prevent cytochrome oxidase activity from being impaired. After several changes of PBS over twelve hours, brain sections were cut using a vibrating microtome (§3.2 above), and collected in a repeating series in 24 wells of 0.6 ml PBS each. To each well an equal volume of a PBS solution containing 25 $mg.ml^{-1}$ cytochrome C (Sigma; derived from horse heart) and 25 $mg.ml^{-1}$ DAB was added; the wells were then incubated at 37°C for one hour. The reaction was stopped by transferring the sections to PBS, from which they were mounted, air-dried and coverslipped using DPX.

6 Histology

6.1 Silver myelin staining

This myelin stain was adapted from the method published by Zilles (1985), but modified to include the physical developer from the original Gallyas method on which Zilles' was based. Vibrating microtome sections (§3.2 above) were mounted on gelatin/chrome alum subbed slides and air-dried overnight. They were then passed through a series of baths: xylene, 100% ethanol, 90% ethanol, 70% ethanol, and distilled water (dH_2O), for five minutes each. The slides were then immersed in a 2:1 mixture of pyridine and glacial acetic acid for thirty minutes, followed by three five minute washes in distilled water. Slides were immersed in the pretreatment solution (1g NH_4NO_3; 1g $AgNO_3$; 3ml 1M NaOH per litre of distilled water) for thirty minutes, and rinsed three times in 0.5% acetic acid.

The physical developer solution was then made from its stock components: stock A (100g Na_2CO_3 in 1000ml dH_2O); stocks B1 (5g NH_4NO_3; 2g $AgNO_3$ in 500ml dH_2O) and B2 (20g tungstosilicic acid in 500ml dH_2O); combine B1 and B2, and slowly add 5ml 40% formaldehyde. Equal parts of A and the combined B stocks were mixed one minute prior to use, and the slides were immersed to bring out the stain. Frequent inspection allowed the slides to be removed when the stain had reached the appropriate intensity, and after a five minute rinse in dH_2O the slides were fixed in an Agfa AP94 photographic fixer for ten minutes, then dehydrated and coverslipped with DPX.

6.2 Nissl staining

6.2.1 Fluorescent Nissl stain

NeuroTrace fluorescent Nissl stains (Molecular Probes) were combined with fluorescent immunohistochemistry using the following procedure prior to the primary antibody incubation: Sections underwent three ten-minute PBS washes, one ten-minute wash in 0.3% Triton-X in PBS, two ten-minute PBS washes, twenty minutes in diluted NeuroTrace, and ten minutes in 0.3% Triton-X in PBS. NeuroTrace stains were diluted at 1:250 (red) and 1:50 (blue) to achieve good staining in 40μm frozen sections.

6.2.2 Cresyl violet staining

Air-dried sections mounted on gelatine-chrome alum subbed slides were immersed in a series of baths for ten minutes each, passing through xylene, 100% ethanol, 96% ethanol, 70% ethanol and distilled water. Slides were then immersed in a staining solution of 5.44gl^{-1} sodium acetate, 0.1% glacial acetic acid and 20 mgl^{-1} cresyl violet in a sealed container at 60°C for thirty minutes. Slides were then differentiated in 96% ethanol and transferred to xylene when the stain had lightened appropriately, then coverslipped with DPX.

7 Imaging

Fluorescent immunolabelling was imaged using epifluorescence on a Leitz Dialux microscope, using Leica Fluotar air and water-immersion objectives and barrier filters for fluorescein fluorescence (appropriate for the Alexa 488 fluor), Texas Red (for the Alexa 594 fluor) and Fast Blue labelling. Monochromatic fluorescence or brightfield images were obtained by averaging 16 captured video frames from an axially mounted video camera (Ikegami CCD; captured by NIH Image 1.61 software

using the video input of an Apple Power Macintosh 7600AV computer) providing a resolution of 768×576 pixels, or a Nikon Coolpix 950 digital camera with an eyepiece adapter and a resolution of 1200×900 pixels. Contrast enhancement and photomosaic assembly were performed using Adobe Photoshop software (versions 4.0, 5.5 and 6.0); for double labelling, false colour images were made by copying paired video captures into the red, green and/or blue channels of RGB images according to the original fluor colour, and moving them into registration with each other using reference marks. A standard unsharp mask filter (radius 0.5 pixels, weight 75%, threshold 0) was applied to all images to enhance clarity and fine detail for print use.

8 Data analysis

Basic statistics were derived from raw data using Microsoft Excel 2001 and StatView 5.0 software running under Mac OS 9. More sophisticated statistical analyses were performed using StatView 5.0. Graphs were prepared using Microsoft Excel 2001.

Chapter 3

Characterisation and distribution of cortical structures labelled with the monoclonal antibody SMI32

1 Introduction

The three monomers and great variety of phosphorylation states possible for the neurofilament triplet proteins makes their localisation complex. Neurofilament-specific antibodies for immunohistochemistry may recognise epitopes specific to one monomer, or which are shared between several; the phosphorylation state of the larger NFM and NFH subunits can alter epitope availability or change the epitopes themselves, leading to phosphorylation-dependent immunolabelling (Sternberger & Sternberger, 1983; Lee et al., 1988; Szaro, Whitnall, & Gainer, 1990). The variable degree to which the three subunits copolymerise *in vivo* (Elder et al., 1998a,b; Lee et al., 1993) can also lead to ambiguity in assessing which neurons contain the "neurofilament triplet protein" when studying their location or function.

The monoclonal antibody SMI32 (Sternberger & Sternberger, 1983) has been demonstrated to recognise epitopes on dephosphorylated NFM and NFH neurofilament subunits (Lee et al., 1988). This dual subunit, phosphorylation-specific immunoreactivity has been used extensively in human (Campbell & Morrison, 1989; Mesulam & Geula, 1991; Hayes & Lewis, 1992), primate (e.g. Hof & Nimchinsky, 1992; Hof & Morrison, 1995) and rat (Hiscock, Mackenzie, & Willoughby, 1996; Tsang et al., 2000) cortices to label a subpopulation of neurons, where it localises to the cell body and dendrites but not to axonal neurofilaments (Poltorak et al., 1988; Campbell & Morrison, 1989). Its labelling of perikarya and somata, excluding most axons, highlights locally expressed neurofilaments in a given cortical region while excluding those of afferent axons from other regions.

SMI32 labelling has recently been used in a neurochemical atlas of the rat brain (Paxinos et al., 1998) which illustrated its distribution without characterising the patterns of labelling or the cortical regions in which they appeared. Since neurofilament content is one of the few markers which distinguish among pyramidal neuron subpopulations (Hof et al., 1996) it offers the possibility of characterising the neurochemical makeup of specific corticocortical projections. Studies in primates

(Hof, Nimchinsky, & Morrison, 1995; Hof et al., 1996, 1997) have sought to characterise particular regional projections by the proportion of SMI32 labelled neurons contributing to them, although a lack of knowledge of the functions conferred by neurofilament triplet content has made interpretation of the significance of these differences difficult.

Suggestively, marked changes in the pattern of SMI32-labelled neurons have also been observed to coincide with physiologically and cytoarchitectonically defined borders between regions in the monkey cingulate cortex (Hof & Nimchinsky, 1992; Hof, Nimchinsky, & Morrison, 1995; Nimchinsky et al., 1996) and human orbitofrontal cortex (Hof, Mufson, & Morrison, 1995). Similarly, visual regions of the macaque cortex vary in their SMI32-labelled component in a manner which tends to segregate processing streams of the visual system (Hof & Morrison, 1995; Hof et al., 1996).

The reasons for these labelling patterns in cortex are subject to speculation, and at present may only be inferred by correlating neurofilament content with functional properties derived from other types of studies. To this end, a characterisation of basic patterns of SMI32 labelling could allow the joint consideration of similarly patterned areas, in the hope that its functional significance can be derived by considering similarities between functionally heterogeneous regions.

The phosphorylation specificity of SMI32 prompts uncertainty about whether the neurons it labels are a subset of all which contain neurofilaments, or whether they are the entire neurofilament-containing group (Parysek et al., 1991), although such doubts are less relevant when considering the fact that the conformation of neurofilaments in different states of phosphorylation probably alters their functional properties (Eyer & Leterrier, 1988; Gotow et al., 1994).

In this study, the suitability of SMI32 to identify neurofilament triplet containing neurons of the rat cortex was assessed in a two stage process. The degree of colocalisation of the individual triplet proteins was investigated using phosphorylation-independent antibodies to NFL, NFM and NFH for fluorescent double labelling; the ability of SMI32 to label the population(s) so identified was then examined using double labelling with the NFM and NFH antibodies. SMI32 immunoperoxidase/DAB labelling was then used to examine the regional and laminar patterning of SMI32 labelled structures throughout the cortex, with the goal of identifying characteristic patterns and thereby grouping cortical regions according to their neurofilament architecture.

2 Procedures

2.1 Characterisation of neurofilament triplet and SMI32 labelling

For comparison and characterisation of neurofilament labelling, cryostat sections of paraformaldehyde fixed adult rat brain were labelled using either SMI32 or a mouse monoclonal antibody to NF-L (Zymed) and one of the phosphorylation independent rabbit polyclonal NF-M (Serotec) or NF-H (Serotec; both characterised by King et al., 2000) primary antibodies, and fluorescent secondary antibodies (Chapter 2, §5.1). Sections were then mounted and studied using appropriate barrier filters on a Leitz Dialux epifluorescence microscope; images comparing the labelling of each antibody / fluophor combination were captured using a CCD camera (Ikegami) and processed using NIH Image and Adobe Photoshop software. Direct visual comparison was used for the colocalisation surveys, with captured and superimposed false-colour images used to confirm and document the observations. In addition to adult rat brain tissue, twenty-one-day-old cultured neurons (see Chapter 7 for culture procedures) were also stained with the same combinations of antibodies and fluophors, and subjected to similar comparisons.

2.2 Large scale assay of SMI32 immunolabelling in the cortex

For regional distribution surveys, serial cryostat sections of paraformaldehyde fixed adult rat brain were labelled using SMI32 and visualised using immunoperoxidase-DAB staining (Chapter 2, §5.2). Sections were examined using standard Köhler illumination on an Olympus BX50 light microscope. After an initial survey of several brains to assess patterns of SMI32 immunolabelling, broad pattern categories were identified and sections from these and other animals were examined, assigning pattern types to areas delineated on standard atlas section diagrams (Paxinos & Watson, 1998), noting specific variations of labelling. Whole-section micrographs were constructed using a series of captured greyscale CCD images (Galai camera) on an Olympus BH2 light microscope with Köhler illumination and a pale blue filter. Images were then assembled in Adobe Photoshop and compared with standard atlases (Paxinos & Watson, 1998; Paxinos et al., 1999) to identify cortical regions.

2.3 Assay of SMI32-labelled neuron populations

For overall neurofilament prevalence data, fresh sections from five of the ten animals were immunolabelled with SMI32 as described, and counterstained with NeuroTrace fluorescent red Nissl stain (Molecular Probes) according to the manufacturer's instructions. Counts of Nissl-stained nuclei and SMI32-labelled perikarya in the M1,

S1My, S2, V2MM and perirhinal regions (Paxinos & Watson, 1998) were made using three pia-to-white-matter traverses of an eyepiece counting frame (width 140μm at 50×); in-focus cells were counted under red fluorescence filters; the filters were changed to show immunolabelling, and double labelled cells were counted. The field of view was advanced one frame at a time, radially inward until the white matter was reached.

3 Results

3.1 Neurofilament triplet and SMI32 immunolabelling

3.1.1 Neurofilament triplet protein labelling

NFL and NFM/NFH in rat neocortex

Nearly all NFH labelled and NFM labelled somata were labelled by the NFL antibody. These exceptions were observed in less than ten cells each among many thousands surveyed across tissue from three animals. NFL also labels a small (~1%) population of cells very weakly labelled by NFH, and a small, possibly equivalent, population not labelled by NFM. Many small processes throughout the neuropil are labelled by NFL but not NFH, and/or by NFL but not NFM (Figure 3.1).

In vitro *neurofilament labelling on culture day 21*

Although cultured neurons gave a clear indication of the relationship between some neurofilament triplet subunits in various parts of the neuron, it was recognised that they are an imperfect analogy for conditions *in vivo* since SMI32 labelling was absent in all cultures studied for this experiment, mostly taken before it is typically expressed under these conditions (cf. Chapter 7). NFL labelling was clearly restricted to the cell bodies and some processes of cultured neurons, while both NFH and NFM antibodies labelled all NFL-labelled structures in addition to many more processes (Figure 3.2).

3.1.2 Characterisation of SMI32 labelling

SMI32 labelled the cell bodies and usually the dendritic arbours of many neurons throughout the cortex, with labelled perikarya concentrated in layers III, V and VIa; some labelled cells were observed in layers II and IV, but not in layers I or VIb. Most SMI32-labelled cells had a distinctly pyramidal morphology, with prominent apical dendrites occasionally rising through several cortical layers. Generally, only the very proximal portions of axons arising from these neurons were labelled with

Figure 3.1

Comparison of (a) NFL and NFM and (b) NFL and NFH labelling in the retrosplenial granular region of the rat cortex; pairs (a), RSG cortex layer III, and (b), RSG cortex layer III, are double labels of the same section. Note neuron whose cell body is labelled by NFH and not NFL (white arrow), and neuron whose cell body is labelled by NFL and very weakly by NFH (white arrowhead). Scale bar = 20μm for all images.

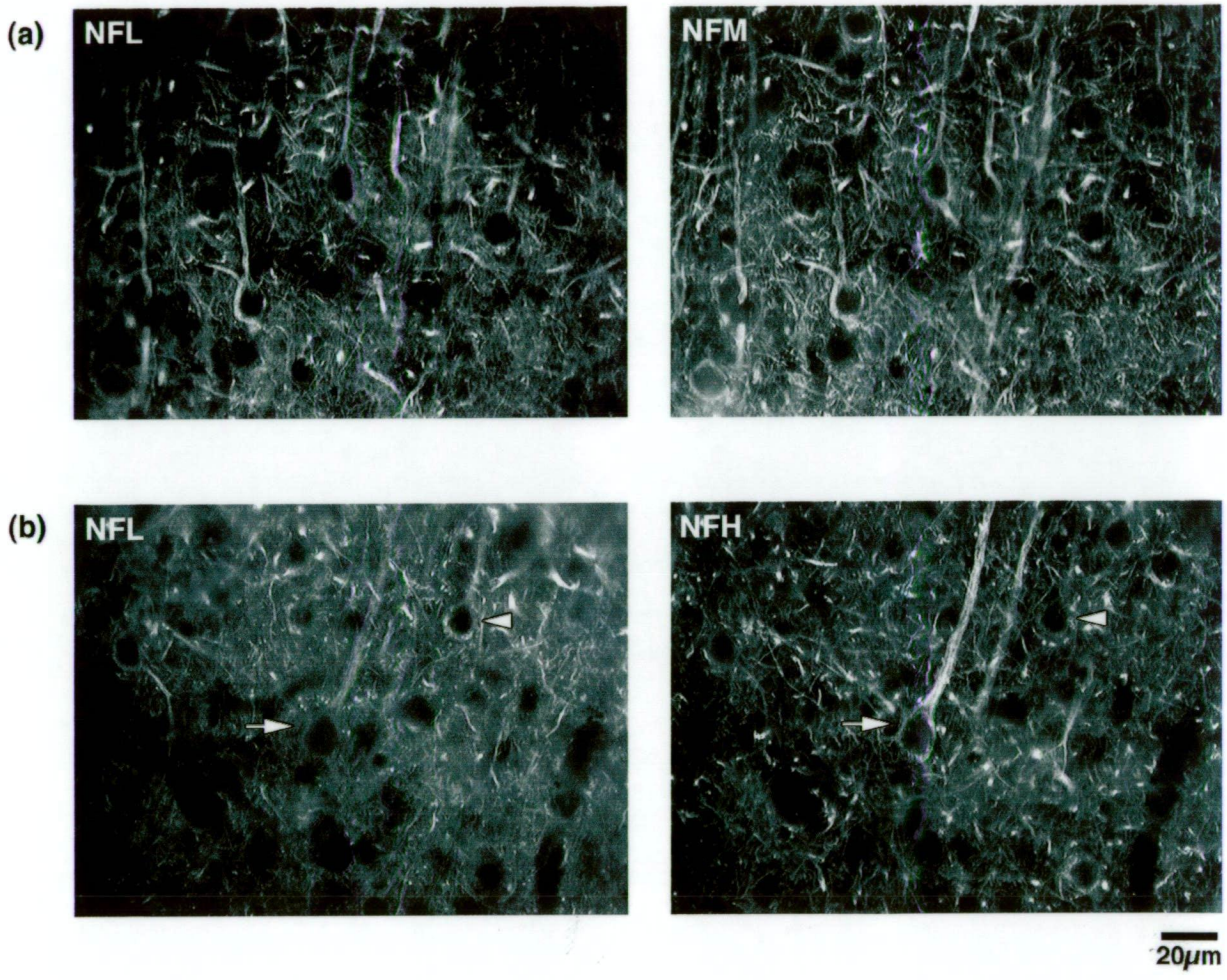
(a)
NFL
NFM
(b)
NFL
NFH
20μm

Figure 3.2

Culture neurons at 21 days *in vitro* labelled for (a) NFL and NFM and (b) NFL and NFH; pairs (a) and (b) are double labels of a single specimen. Cell bodies and some processes are labelled by NFL in both specimens; NFM colocalises with NFL and is additionally present in many more processes, as is the case for NFH labelling. Scale bar = 50μm for all images.

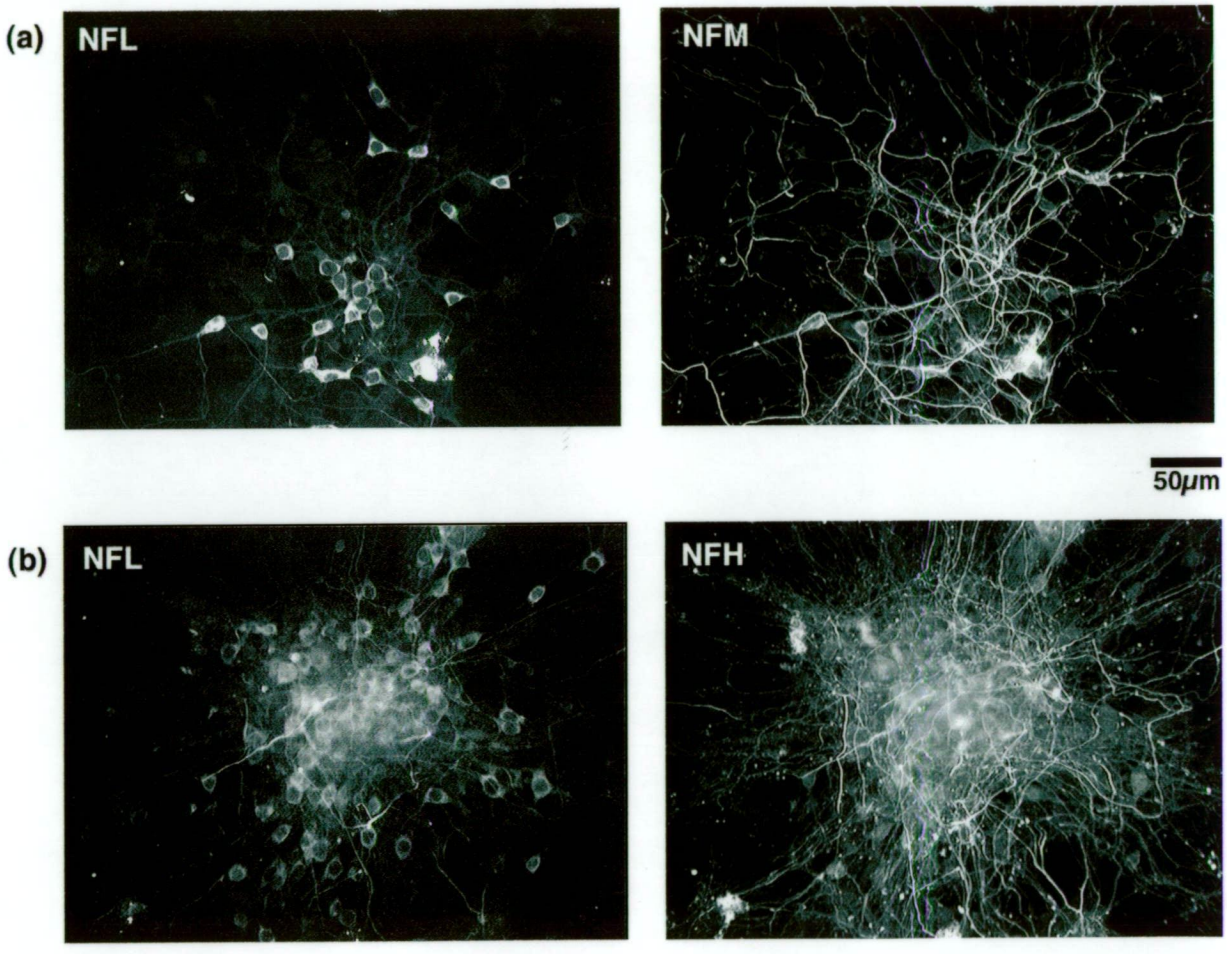
(a)
NFL
NFM
50μm
(b)
NFL
NFH

SMI32; although labelled processes observed in isolation could have been axons, few axons originating from labelled cells were labelled further than ~50μm from their origin. However, a small amount of SMI32 labelling was observed in subcortical white matter, and hence presumably some axons are labelled by the antibody.

Double labelling with rabbit polyclonal phosphorylation-independent antibodies to the NFM and NFH subunits enabled a comparison between SMI32 labelling and the neurofilament triplet combinations described in §3.1.1 above. Figures 3.3a and 3.3b show double-labelled comparison pairs stained with SMI32 and NFM antibodies, and SMI32 and NFH antibodies.

NFH and SMI32 labelling was nearly identical in perikarya and proximal dendrites (Figure 3.3a). Some processes were SMI32 labelled and NFH weak or unlabelled; however, differences in perikaryal labelling were differences only of intensity, not segregation of labelling. There were many more NFH labelled than SMI32 labelled processes in the neuropil, which were presumably axons. NFM and SMI32 exhibited slightly less similar staining (Figure 3.3b), with an appreciable fraction of non-pyramidal neurons being SMI32 labelled but not NFM labelled (~5-10%, informal counts); occasionally some pyramidal neurons were NFM labelled and not SMI32 labelled (Figure 3.3c). As for NFH, there were many more NFM labelled processes than are SMI32 labelled.

3.1.3 Summary of labelling

These observations confirm that the neurofilament triplet subunits in cell bodies are most often colocalised, and that SMI32 clearly labels the perikarya of nearly all neurons in which the triplet is present (i.e. all NFH labelled and virtually all NFM labelled cells), even if the relative intensity of labelling varied from neuron to neuron. It is possible that a subset of neurons may contain NFL alone, in which case they are not detected by SMI32.

3.2 Regional distribution of SMI32 labelling

Characteristic patterns of cortical labelling were evident in the SMI32 immunoperoxidase labelled sections. They are denoted here by the regions in which they are most commonly observed; the four principal patterns are illustrated in Figure 3.4. The extent of regions exhibiting these patterns is evident in the series of section micrographs in Figure 3.5.

Only those regions which consistently exhibited the staining pattern described are indicated in these lists. Frequently, smooth transitions between the labelling

Figure 3.3

Fluorescently labelled immunohistochemistry and Nissl staining.

(a, b, c) Comparison of (a, c) SMI32 and NFM, and (b) SMI32 and NFH labelling in the rat cortex. Pairs (a), S1 cortex layer III, (b), S1b layer V, and (c), occipital layer V, are double labels of the same section. Note unusual neuron whose cell body is labelled by NFM and not SMI32 (white arrow).

(d) Nissl and SMI32 labelling at the RSA/V2MM border. Perinuclear SMI32 labelling is visible in one V2MM neuron (arrow) whose dendrites are unlabelled; a nearby neuron of similar size and Nissl density is not labelled (arrowhead). The contrast in neuropil SMI32 label density between RSA (lower left) and V2MM is also evident.

Scale bars for each pair are indicated at left.

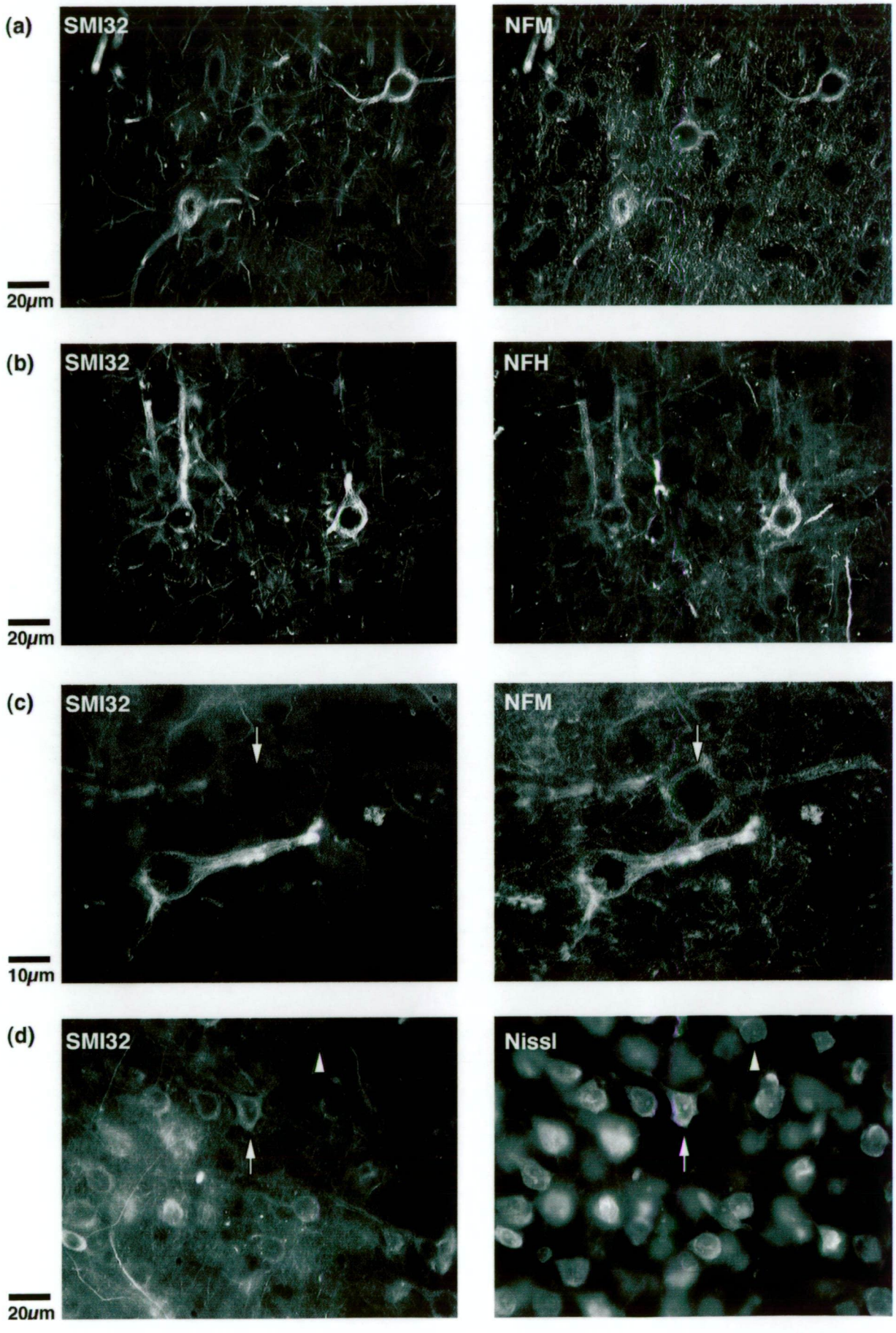
(a)
SMI32
NFM
20μm
(b)
SMI32
NFH
20μm
(c)
SMI32
NFM
10μm
(d)
SMI32
Nissl
20μm

Figure 3.4

Examples of the four patterns of SMI32 immunolabelling in adult rat neocortex, identified by regions in which they occur. Cortical layers are indicated to the left of each image. Note bundled apical dendrites ascending to layer I in the RSG (black arrowhead) and the dense plexus of SMI32-labelled processes in layer II of the RSA (white arrow).

Scale bar = 100μm for all images.

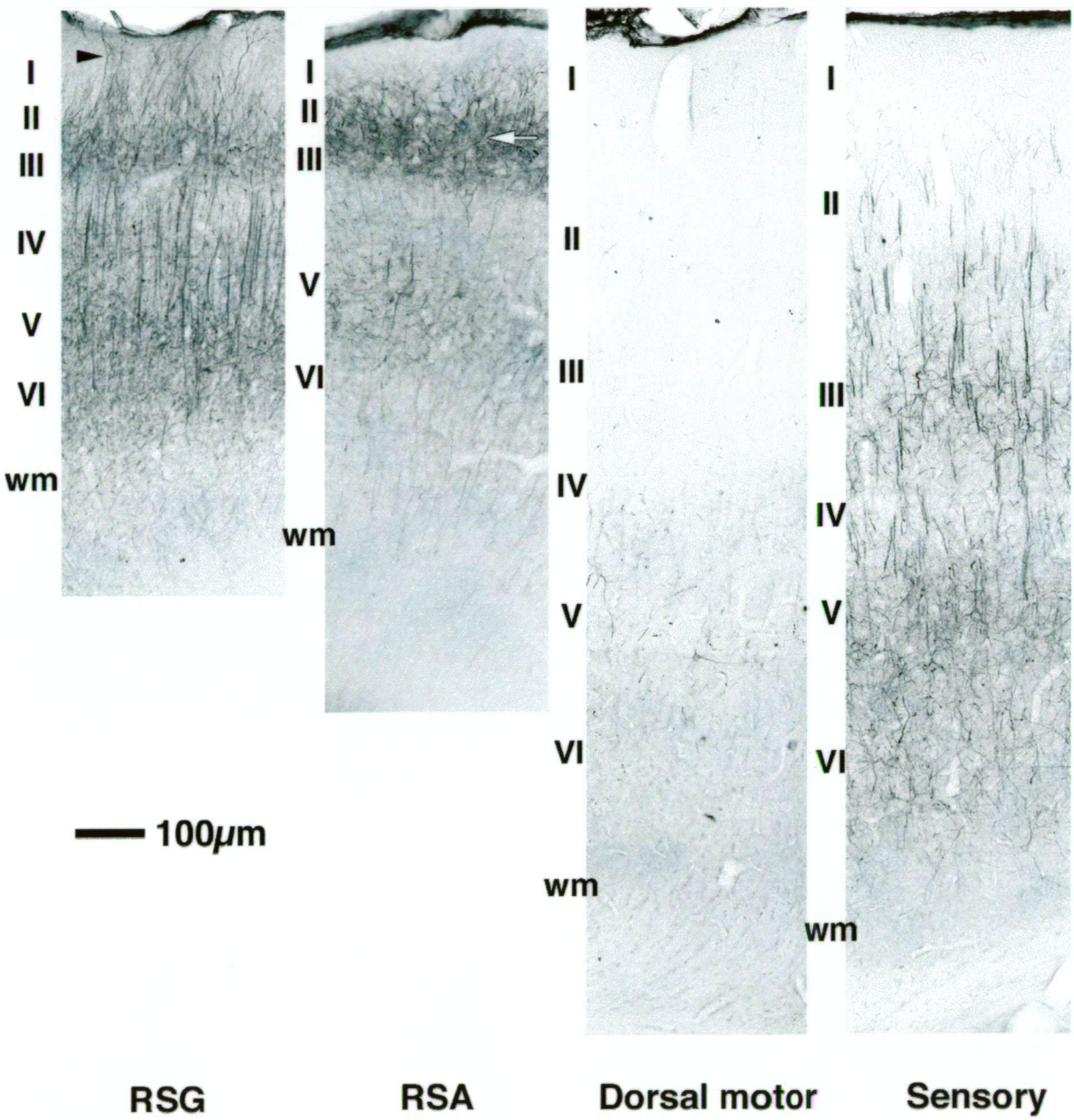
I
II
III
IV
V
VI
wm
100μm
RSG
RSA
Dorsal motor
Sensory

Figure 3.5

Series of sections of the adult rat cortex immunolabelled with SMI32. The distribution of characteristic patterns is evident; most noticeable is the strip of reduced immunolabelling extending back from region M2 in the second section to the occipital pole. Cortical region labels are derived from standard atlases (Paxinos & Watson, 1998; Paxinos et al., 1998); abbreviations are listed in Appendix C. Scale bar = 1mm for all images.

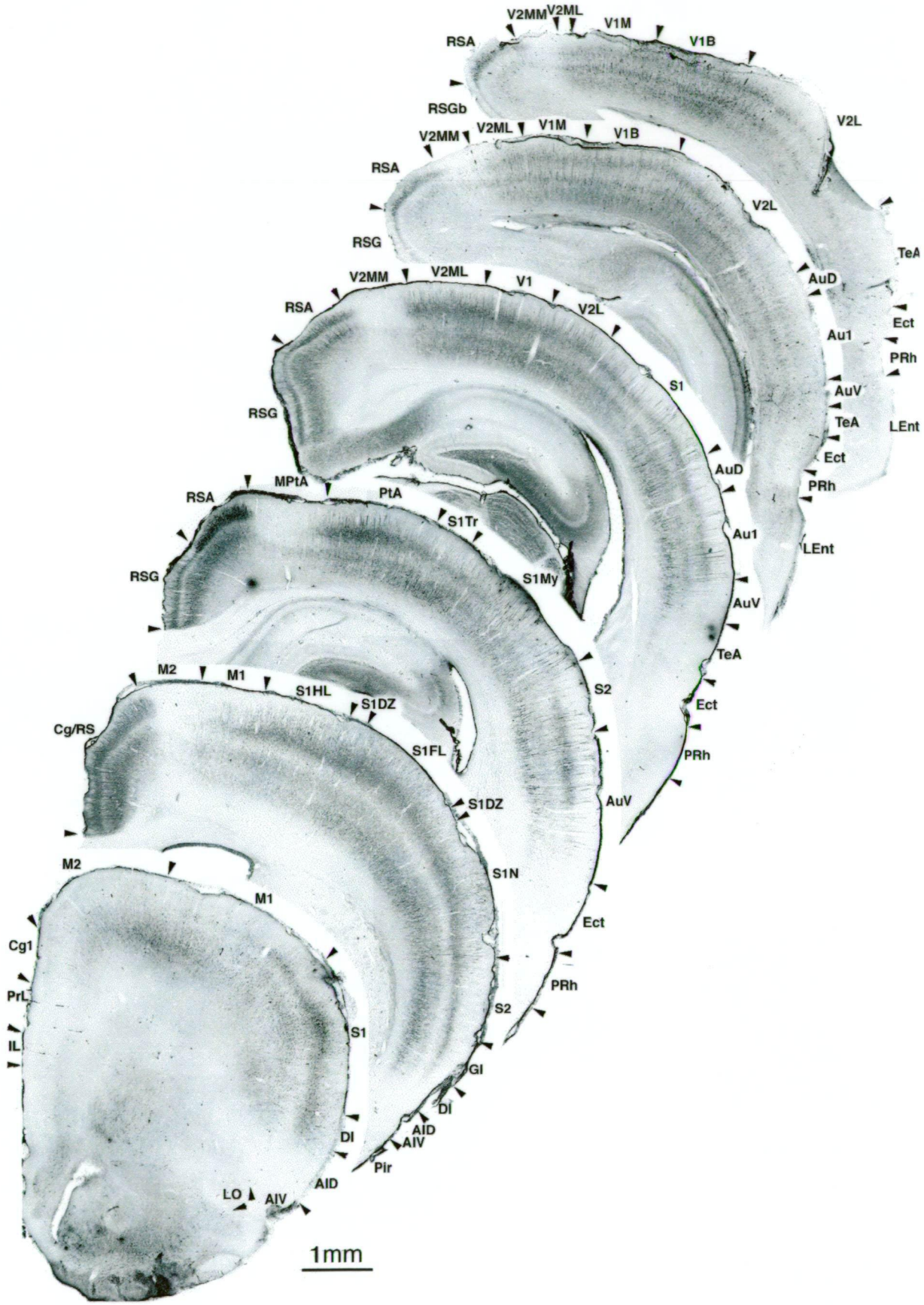
V2MM
V2ML
V1M
V1B
RSA
RSGb
V2L
V2MM
V2ML
V1M
V1B
RSA
V2L
RSG
TeA
V2MM
V2ML
V1
RSA
V2L
AuD
Ect
Au1
PRh
S1
AuV
RSG
TeA
LEnt
Ect
AuD
MPtA
PRh
RSA
PtA
S1Tr
Au1
LEnt
RSG
S1My
AuV
TeA
M2
M1
S1HL
S2
S1DZ
Ect
Cg/RS
PRh
S1FL
S1DZ
AuV
M2
S1N
M1
Ect
Cg1
PRh
PrL
S2
S1
IL
GI
DI
AID
DI
AIV
Pir
AID
LO
AIV
1mm

patterns of adjacent regions made grouping ambiguous; furthermore, the patterns in some regions could not satisfactorily be assigned to one of the described types, or varied between animals. All regional labels derive from the atlas of Paxinos and Watson (1998).

3.2.1 RSG, cingulate

Areas observed

RSG (retrosplenial cortex, granular), Cg1 (cingulate region 1; caudal parts), Cg2 (cingulate region 2; caudal parts).

Description

Thin cortex with labelled somata and light neuropil label in layers III and V; very prominent labelled apical dendrites from layer V (and occasionally layer III) form bundles and extend radially to layer I, where they branch tangentially. Regions with this pattern of labelling run in a band along the medial surfaces of the hemispheres where they overlie the corpus callosum, but extending past its caudal edge. Rostral to the genu of the corpus callosum, anterior cingulate regions exhibited little labelling.

3.2.2 RSA

Areas observed

RSA (retrosplenial cortex, agranular).

Description

Light layer V labelling, moderate layer III soma / neuropil labelling, very heavily labelled layer III apical dendrites and neuropil in a dense field throughout layer II. This labelling pattern consistently lies between the RSG on the medial side and the motor strip to the lateral side (§3.2.3 below) with an abrupt transition to each, in the caudal half of the cortex.

3.2.3 Dorsal strip

Areas observed

M2 (secondary motor cortex), MPtA (medial parietal association cortex), S1Tr (primary somatosensory cortex, transitional), V2MM (mediomedial secondary visual cortex).

Description

Sparse to absent SMI32 labelling in neuropil, though slightly evident in layer V; few somata obviously labelled, mostly in layer V. Extends across regions in a rostrocaudal strip on the dorsal edge of the cortex for most of the brain, from the septum back to the occipital regions. Rostral of the septum, SMI32 labelling in the same band remained light, but the layer V neuropil label was denser.

3.2.4 Sensory regions

Areas observed

S1 (primary somatosensory cortex), S1FL (forelimb primary somatosensory cortex), S1HL (hindlimb primary somatosensory cortex), S1My (mystacial primary somatosensory cortex), PtA (parietal association cortex), S1Tr (primary somatosensory cortex, transitional), S2 (secondary somatosensory cortex), Au1 (primary auditory cortex), AuD (dorsal auditory cortex), AuV (ventral auditory cortex), M1 (primary motor cortex), M2 (secondary motor cortex), V2ML (mediolateral secondary visual cortex).

Description

SMI32 labels somata and the neuropil in layers III, V and VIa; the apical dendrites extending from neurons in layers III and V are more labelled than their somata. The neuropil labelling in layers III, V and VIa is separated by lighter laminae, giving a triple-layered appearance.

While this pattern is widespread and is the most common SMI32 labelling observed, it varies between regions. Table 3.I summarises those variations from the basic pattern observed consistently across all animals studied. Figure 3.5 illustrates these variations on the trilaminar label pattern.

Table 3.I: Regional variations on the trilaminar SMI32 labelling pattern predominant in sensory cortical regions.

Region(s)	*Variation*
S1, S2, AuD/1/V	Trilaminar pattern described.
S1/2, M1/2, V2ML	Less labelled than adjacent trilaminar regions.
S1FL, S1HL, S1Tr	Layer V labelling markedly denser than layer VIa.
M1/2 parts, AuV	Layers V and VIa distinctly denser than layer III.
S1 (bordering S2)	Bands of layers V and VIa merge, giving a double laminar pattern.

Other variations, including a more prominent layer III label or a more prominent layer VIa label, were observed but were inconsistent between animals.

3.3 Overall prevalence of SMI32 labelling among cortical neurons

Table 3.II summarises the observed proportions of SMI32-labelled neurons compared to the total numbers of Nissl-stained nuclei in five regions from five animals. SMI32-labelled percentages were not significantly different between regions (ANOVA; p=0.213), despite the markedly differing overall labelling densities in these regions. Regions V2MM and PRh exhibit very little SMI32 labelling in the neuropil, and the SMI32-labelled neurons observed there had immunoreactivity in a restricted perinuclear ring, with little or no dendritic labelling evident (Figure 3.3d). Such cells formed the bulk of counted neurons in V2MM and PRh, but were a small proportion of counts in other regions. Overall proportions varied significantly between animals (ANOVA, p=0.0003), which may reflect fixation variations (Vickers & Costa, 1992), but the relative proportions of regions remained similar.

Table 3.II: Mean (n=5, ± standard error) percentages of SMI32-labelled neurons among Nissl-stained neurons in five cortical regions. Regional nomenclature from Paxinos and Watson (1998). M1: primary motor cortex; S1My: primary somatosensory cortex, mystacial region; S2: secondary somatosensory cortex; V2MM: secondary visual cortex, mediomedial region; PRh: perirhinal cortex.

M1	S1My	S2	V2MM	PRh
12.93 ±2.26	10.38 ±1.47	13.22 ±3.01	13.28 ±2.83	19.66 ±3.55

4 Discussion

From the double labelling studies, it is clear that the neurofilament triplet proteins are almost entirely colocalised in the cell bodies of the rat cortex, although they seem to be differentially distributed in the processes of neurons. The comparisons also suggest that SMI32-labelled cells are the vast majority of neurofilament triplet containing neurons of the cortex; no appreciably larger neurofilament containing population is labelled or suggested by any of the antibodies used, with the possible exception of a small population expressing NFL alone. Studies of neurofilament assembly indicate that only human NFL could assemble into structural units without the presence of NFM (Carter et al., 1998); either NFL is not functioning as a cytoskeletal protein in these cells, or it is coassembling with other IFs, or other triplet subunits are present in a form not recognised by any of the antibodies used.

The intensity of labelling with neurofilament subunit antibodies and SMI32 varies from cell to cell in a manner inconsistent with simple differences in fixation, antibody affinity or brightness of fluorescent labelling. The observed differences suggest several possibilities:

- There may be genuine differences in the subunit stoichiometry of filament construction, and/or cross-assembly of NF triplet proteins with other intermediate filaments. Co-assembly of NFM with another type of IF could explain the most anomalous phenomena observed, those of NFM labelled cells without NFL labelling, and NFM labelled cells without SMI32 labelling. In the latter case, the phosphorylation state of NFM would need to be abnormal for cell bodies, which may be due to their participation in such hybrid filaments. Intermediate filaments which have been demonstrated to co-assemble with neurofilaments include α-internexin (Ching et al., 1999) and vimentin (Cleveland et al., 1991; Monteiro et al., 1990).
- The recognition sites specific to these antibodies may be masked by the local environment of the filaments, perhaps hidden by the triplet assembly process. The strongest evidence for this phenomenon comes from the cultured neurons, in which we know NFL must be present in the NFM/NFH labelled processes for them to form filaments (Julien, 1999) despite the fact that they are not labelled by the NFL antibody.

Clearly, SMI32 is a useful marker for determining the neurofilament-containing population of cortical neurons, identifying as it does the overwhelming majority of neurons with the neurofilament triplet present in their perikarya. Its general lack of axon labelling simplifies the labelling patterns observed in the cortex and allows an imperfect distinction between axons and dendrites labelled immunohistochemically, particularly when used in conjunction with a phosphorylation-independent antibody for NFM or NFH. In terms of individual cells, the observed overall SMI32-labelled prevalence was comparable to those reported in rat cortex by Hiscock, MacKenzie, and Willoughby (1996); to counts made in human cortex (6–11%; Hof, Cox, & Morrison, 1990); and neurofilament triplet colocalisation with nerve cell body antigen in guinea pig cortex (19.9%; Vickers & Costa, 1992).

The most obvious characteristic of SMI32 immunolabelling across the cortex is the similarity of staining patterns between functionally different regions, although it is worth considering that the rat cortex is much less functionally segregated than that of primates (Miller & Vogt, 1984). Four principal types of labelling distribution were

immediately apparent on examination of the material; of these, two (RSA and RSG types) appear specific to cortical regions defined by other means, whereas the other two extend across many regions.

One of the most striking patterns was the "gap" in staining, observed in many dorsal motor regions running along the lateral edge of the RSA cortex. The appearance of these regions is not due to a lack of neurons expressing SMI32-recognised neurofilament (Chapter 4, §3.2.3); the deficit in labelling compared to adjacent regions is due to restricted perinuclear labelling in cells labelled by SMI32, and a near-absence of dendritic labelling in these regions. Other neurofilament antibodies used in this study showed a similar deficit of labelling in the same regions. The transition between other labelling patterns and this "gap" is quite abrupt (20-50μm in the tangential direction), and is smaller than dendritic arbour sizes which have been observed for pyramidal neurons in the rat cortex (e.g. the dendritic field radius of 185μm measured in rat sensory cortex by Winkelmann et al., 1973, cited in Feldman, 1984). It is clear that the neurons in this region do not contain neurofilaments recognised by SMI32 in their dendrites; however, we would expect labelled dendrites from adjoining regions to overlap into the gap region. Their absence suggests either that SMI32 immunolabelling is restricted to the proximal portions of dendrites, at least in these adjoining regions, or that some factor in the gap region inhibits neurofilament accumulation in distal structures or alters the epitope recognised by SMI32.

As mentioned by Paxinos and coworkers (1999), the cortical parcellation suggested by SMI32 immunolabelling is quite different to those based on standard Nissl architecture or electrophysiology; this alternative classification may also suggest relationships between seemingly disparate regions such as M1 and V2MM, or the broad regions exhibiting the trilaminar "sensory" pattern. Central to such speculation is the causal relationship between cortical activity and the neurofilament distribution patterns: do regions selectively express neurofilaments based on their activity or specialisation, or is the patterning engendered by factors in the developing brain? In the latter case, patterns of neurofilament architecture might provide a substrate of differences in cortical properties which permits otherwise homogeneous cortex to perform diverse functions. The fact that labelling patterns tend to extend uninterrupted across boundaries determined by functional means suggests that they are developmentally intrinsic rather than functionally determined. On the other hand, the possibility exists that there is a standard expression pattern of neurofilaments throughout the cortex, which is subsequently distorted into apparently distinct types

by developmental changes in the architecture of different regions. This argument may apply to the observed variation in the trilaminar pattern between regions, but is less able to explain the "gap" region or the specific features of the RSA and RSG patterning.

5 Summary

SMI32 labels essentially all of the cortical neurons with perikaryal neurofilaments which are recognised by phosphorylation-independent NF subunit antibodies. Its epitopes are expressed by a reasonably consistent minority (10-19%) of cortical neurons. However, the distribution of this epitope in the cell body and dendrites varies considerably with cortical location, and serves to parcellate cortex in ways which differ from standard cytoarchitectonics.

Chapter 4

Neurofilament prevalence and projection distance in neurons of the rat cortex

1 Introduction

The fact that the neurofilament triplet is found only in some cortical neurons prompts speculation about the role it plays in those cells, and why only some neurons require its presence. A direct approach is to identify neurons performing particular functions and examine whether their incidence of neurofilament triplet proteins differs from the norm, so that correlations between neurofilament expression and specific properties may be made.

The participation of neurofilaments in the cytoskeleton, coupled with their restriction to neurons alone, suggest that they facilitate the structural needs of neurons. The most conspicuous structural characteristic of many neurons is the great length of the axon with respect to the cell body; for example, a corticospinal projection neuron of the rat cortex has a cell body of the order of tens of microns across, whereas its axon may extend up to ten centimetres down the spinal cord of an adult animal, a distance ten thousand times larger (Feldman, 1984). In other mammals even greater discrepancies are commonplace, since cortical neurons are of a comparable size but the spinal cord is much longer (White, 1989; Feldman, 1984). The densely packed arrays of neurofilaments evident in ultrastructural studies of long axons (e.g. Szaro, Whitnall, & Gainer, 1990) suggest their importance to such projections.

Many studies of neurofilament content and axon properties have investigated the relationships between neurofilaments and axon calibre (Cleveland et al., 1991; Sánchez et al., 1996), myelination (Friede & Samorajski, 1970; de Waegh, Lee, & Brady, 1992) and axonal transport (Elder et al., 1998a; Zhu et al., 1998) in mature and developing axons. However, attempts to assign a purely structural or developmental regulation role to neurofilaments are countered by studies of mice with genetic knockouts of one or more triplet subunits; in many cases, axonal growth, calibre and myelination are only moderately altered by the absence or disruption of the neurofilament network (Monteiro et al., 1990; Elder et al., 1998b; Zhu et al., 1998) unless the vital NFL subunit is disabled (Julien, 1999). Other hypotheses of cortical neurofilament function include the consolidation of inputs to

neurons (Hof, Nimchinsky, & Morrison, 1995), or the enabling of rapid cortical feedback by means of neurofilament-strengthened projecting axons (Hof & Morrison, 1995).

Although their role may be difficult to ascertain, the substantial neurofilament triplet lattice found in many axons is clearly important, since their manufacture requires considerable energy expenditure (Lee & Cleveland, 1996). Evidence of neurofilament roles in establishing axonal calibre (Julien, 1999) and the dense arrays of neurofilaments evident in axons suggests that they are involved in the growth and/or maintenance of long projections. In addition to their integration in the cytoskeleton, neurofilaments participate in mechanisms of axonal transport (Zhu et al., 1998); clearly, a robust internal framework and regulation of the transport of nutrients, wastes and chemical messengers are functions whose importance increases for the maintenance of longer axons. This suggests that the neurofilament triplet could be more necessary for neurons with long projections.

When identifying the neurons originating neurofilament-rich axons, the antibody SMI32 (Chapter 3; Sternberger & Sternberger, 1983; Lee et al., 1988) is most commonly used to demonstrate perikaryal filaments, since it is specific to the dephosphorylated forms of NFH and NFM which are largely perikaryal in distribution (Campbell & Morrison, 1989). Data obtained from SMI32-based tracing studies generally demonstrates consistent proportions of labelled cells in specific projection groups, which can sometimes be loosely grouped by various post-hoc criteria (Campbell, Hof, & Morrison, 1991; Hof & Morrison, 1995; Hof, Nimchinsky, & Morrison, 1995; Hof et al., 1996; Nimchinsky et al., 1996; Hof et al., 1997). For example, the macaque prefrontal cortex receives projections from cell groups whose SMI32 labelling proportion varies from 24% in the contralateral principal sulcus, up to 89% in the ipsilateral superior temporal sulcus (Campbell, Hof, & Morrison, 1991); 26.5% of projection neurons in various regions of monkey cortex were SMI32 labelled (Hof, Nimchinsky, & Morrison, 1995). Groups of projection neurons from the same region of primate cortex have been found to differ considerably in their SMI32 labelling proportion depending on the target region (Hof, Nimchinsky, & Morrison, 1995; Hof et al., 1996) or whether the projection was ipsilateral or contralateral (Nimchinsky et al., 1996). Feedback projections between various macaque visual regions are very consistent in their SMI32-IR proportion, in contrast to those of the feedforward proportions (Hof et al., 1996).

Examples of neurofilament-containing cells forming a specific projection group have been found in the macaque visual cortex: 94.4% of neurons projecting

transcallosally at the V1/V2 border (Hof et al., 1997) and 100% of the V1-MT projection (Hof et al., 1996) are SMI32-labelled. Essentially all corticospinal projection neurons of the primary motor cortex in rodents, monkeys and primates contain nonphosphorylated neurofilaments (Tsang et al., 2000).

In addition to examining SMI32 labelling proportions at various projection distances, the cortex of a small animal such as the rat, with its much shorter projection distances, may help to determine whether neurofilament content is related to absolute axon length, length relative to the overall size of the brain, or altogether different factors. To this end, the current study used retrograde tracing to identify neurons projecting from various parts of the cortex to injection sites in motor and sensory cortex; SMI32 labelling was then used to determine which of these projecting cells contained neurofilaments, and counts were made of populations at specific distances from the injection site to investigate whether longer projections originated with populations whose SMI32 labelling differed from typical proportions in the cortex, measured in Chapter 3.

2 Procedures

2.1 Fast Blue tracing

Adult hooded Wistar rats were anaesthetised using an intraperitoneally injected ketamine-xylazine mixture (90:10 $mg.ml^{-1}$; 1 $ml.kg^{-1}$). Once anaesthesia was established, the scalp was shaved and the skull exposed by a midline incision. The rat was mounted in a stereotaxic frame (Stoelting) and a burr hole was made above the target region. A flat-tipped Hamilton syringe was used to inject 1.0µl of 5% Fast Blue (Sigma) in ddH_2O over the course of ten minutes, 1.5mm below the pial surface. In total, five animals were injected in cortical region M1 (Paxinos & Watson, 1998; bregma +0.0mm A–P, +2.0mm lat), and five were injected in S1My (bregma -1.8mm A–P, +4.5mm lat). These regions were chosen on the basis of differing function, minimally invasive access, low risk of rupturing venous sinuses, and because one region, S2, projects to both of them.

After recovery and eight days' survival, animals were then re-anaesthetised and perfused; their brains were removed, cryoprotected and sectioned on a freezing microtome (Chapter 2, §3.1). A set of every tenth section was taken and processed for neurofilament immunohistochemistry as floating sections (Ch 2, §5.1), using a 1:2000 dilution of the mouse antibody SMI32 (Sternberger Monoclonals, Inc.) and

an Alexa 488 conjugated secondary. Sections were mounted, dried and coverslipped using Permafluor (Immunotec) and allowed to dry at 4°C overnight.

The sections were examined using epifluorescence on a Leitz Dialux microscope, using Leica Fluotar objectives and appropriate barrier filters for Alexa 488 and Fast Blue labelling. The distribution of labelled cells in each brain was mapped under low power (10× and 25×) and recorded qualitatively on standard section maps (Paxinos & Watson, 1998).

For counting, the 50× water-immersion objective was used. A focal plane in the appropriate region was chosen by focusing on the upper surface of the section, and travelling slightly downward until SMI32 labelling was sharply focused; the plane of focus was selected in this manner because the SMI32 antibody does not completely penetrate 40μm sections. The edge of an eyepiece counting frame (width 140μm at 50×) was positioned on the pial surface, and in-focus cells were counted under the Fast Blue filters; the filters were changed to show immunolabelling, and double labelled cells were counted. The field of view was advanced one frame at a time, radially inward until the white matter was reached, counting each frame similarly. Three non-overlapping counts of the more densely labelled regions on each side of each section were performed. Sections at the injection site, and 400μm and 1200μm anterior and posterior to the site, were used for data collection. In addition, three counts were made in ipsilateral region S2 at a common site for every animal, since this region sends projections to both M1 and S1My.

3 Results

3.1 Distribution of retrogradely labelled cells

Injections 1.5mm below the pial surface generally penetrated to layer V of the underlying cortex, with some tissue distortion and autofluorescent debris observable around the track of the needle. Extracellular Fast Blue was evident in a region around 500μm in diameter centred on the injection site. In addition to the large neuronal nuclei and perikarya labelled with the tracer, many tiny nuclei scattered throughout the surrounding cortex were also labelled; these nuclei did not stain with the fluorescent Nissl stain and were not treated as neurons. Figure 4.3a illustrates the colocalisation of Fast Blue tracer and SMI32 immunolabelling in one neuron.

For M1 injections, strong local labelling extended medial and particularly lateral to the injection site on the sections which included the needle track. Labelling appeared most prominent in the neurons of layers III and V, with a row of small labelled cells directly overlying the white matter in layer VI (see Figure 4.1). On the

contralateral side, labelling in layers III and V at a location congruent with the injection site was prominent. Away from the injection site, labelling in these same layers was observed in some frontal regions (e.g. rostral parts of M2 and M1, as well as olfactory regions), in the S2 region, and in the somatosensory and motor regions which lie approximately caudal to the injection site. Labelling was also evident in the claustrum and thalamus, including the reticular, ventral posteromedial, ventral posterolateral, and ventral anterior nuclei. Figure 4.1 is an example of the distribution map produced for one M1-injected animal.

The pattern for S1My injections was broadly similar in that labelling concentrated in layers III and V for all cortical regions, with a row of layer VI cells immediately below the injection site. Contralateral sites were much more sparsely labelled than for M1 injections, and the ipsilateral S1 regions exhibited labelling in a noticeably parcellated distribution (Figure 4.2). Some cells in frontal ipsilateral M1 were observed, along with various primary somatosensory regions, S2 and various perirhinal regions in the caudal parts of the brain. Some thalamic labelling was evident in various thalamic regions including the ventral anterior, ventrolateral and reticular nuclei.

3.2 Quantitative data

3.2.1 Factors of injection site and transcallosal projection

All quantitative analysis was performed on percentages, calculated from three traverses, of SMI32-labelled neurons among Fast Blue labelled cells at each site in each animal. Means and standard errors of labelling percentages, grouped by the straight-line distance between the counting site and the injection, are presented in Table 4.I. The wide spread of observed proportions, particularly in S1My-injected animals, is evident. Data were evaluated using StatView 5.1 for Macintosh (SAS Institute, Inc.) with a significance criterion of $p \leq 0.05$.

Table 4.I: Mean SMI32-labelled percentage of traced cells for M1 and S1My injections, grouped by counting site (means ± standard error).
† Includes two sites with n<20 (out of 25); ‡ Includes 17 sites with n<20 (out of 25)

Site	+1200µm	+400µm	At site	-400µm	-1200µm	S2	Contralateral
M1	3.72 ±0.67	4.89 ±0.86	7.40 ±1.07	3.72 ±0.75	2.33 ±0.64	2.58 ±1.10	3.53 ±0.51 †
S1My	5.95 ±5.71	7.47 ±2.89	9.99 ±1.54	7.29 ±2.89	9.88 ±3.02	5.65 ±2.79	12.39 ±2.51 ‡

On the basis of this data, the mean SMI32-labelled proportion of cells projecting to S1My (9.83%) was significantly greater than for those projecting to M1

Figure 4.1

Typical distribution of traced neurons from a Fast Blue injection into M1 cortex, noted on standard atlas sections (Paxinos & Watson, 1998) using a low power objective. Stippling is used to indicate relative density and location of traced cells rather than individual neurons. Not to scale. Abbreviations are listed in Appendix C.

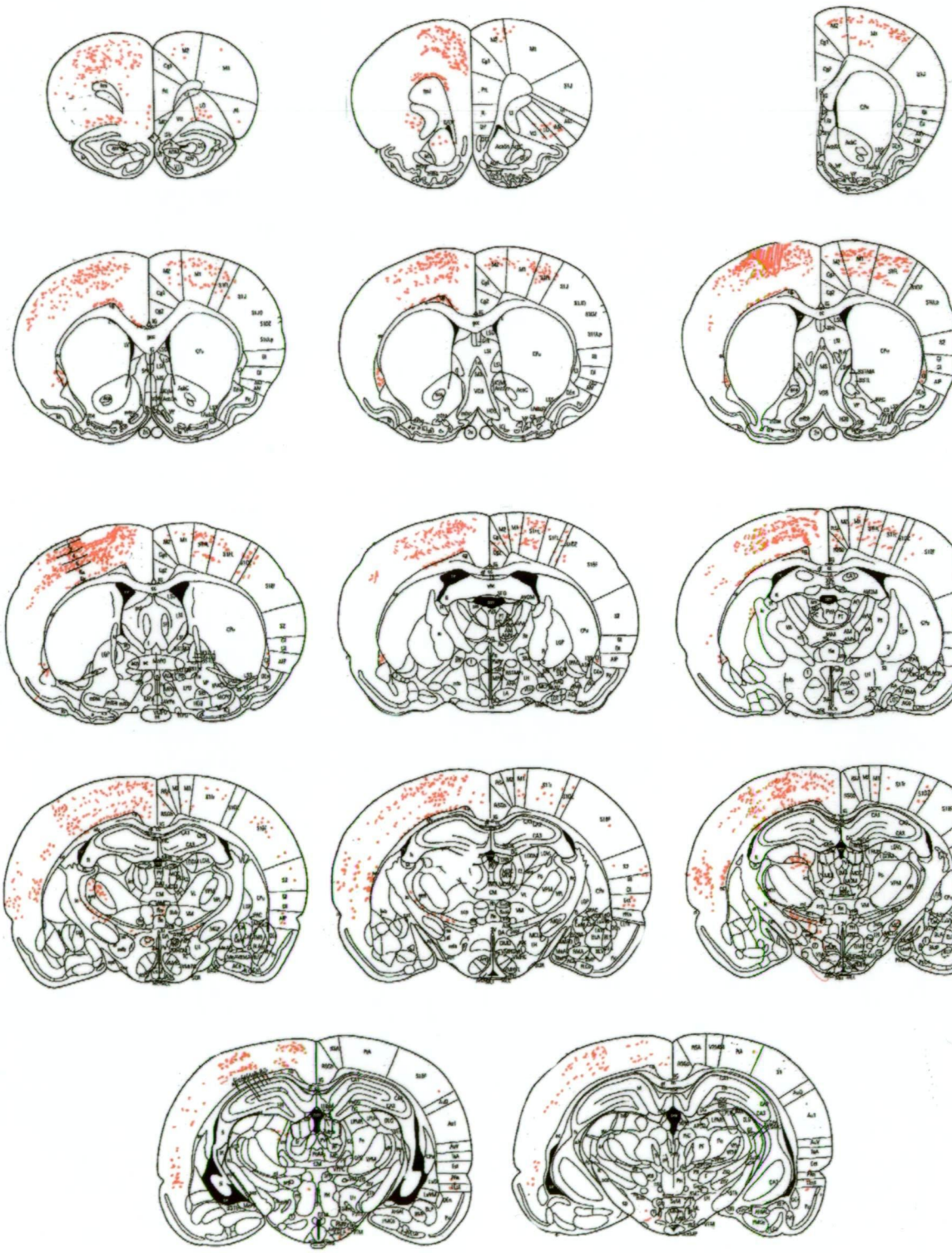

Figure 4.2

Typical distribution of traced neurons from a Fast Blue injection into S1My cortex, noted on standard atlas sections (Paxinos & Watson, 1998) using a low power objective. Stippling is used to indicate relative density and location of traced cells rather than individual neurons. Not to scale. Abbreviations are listed in Appendix C.

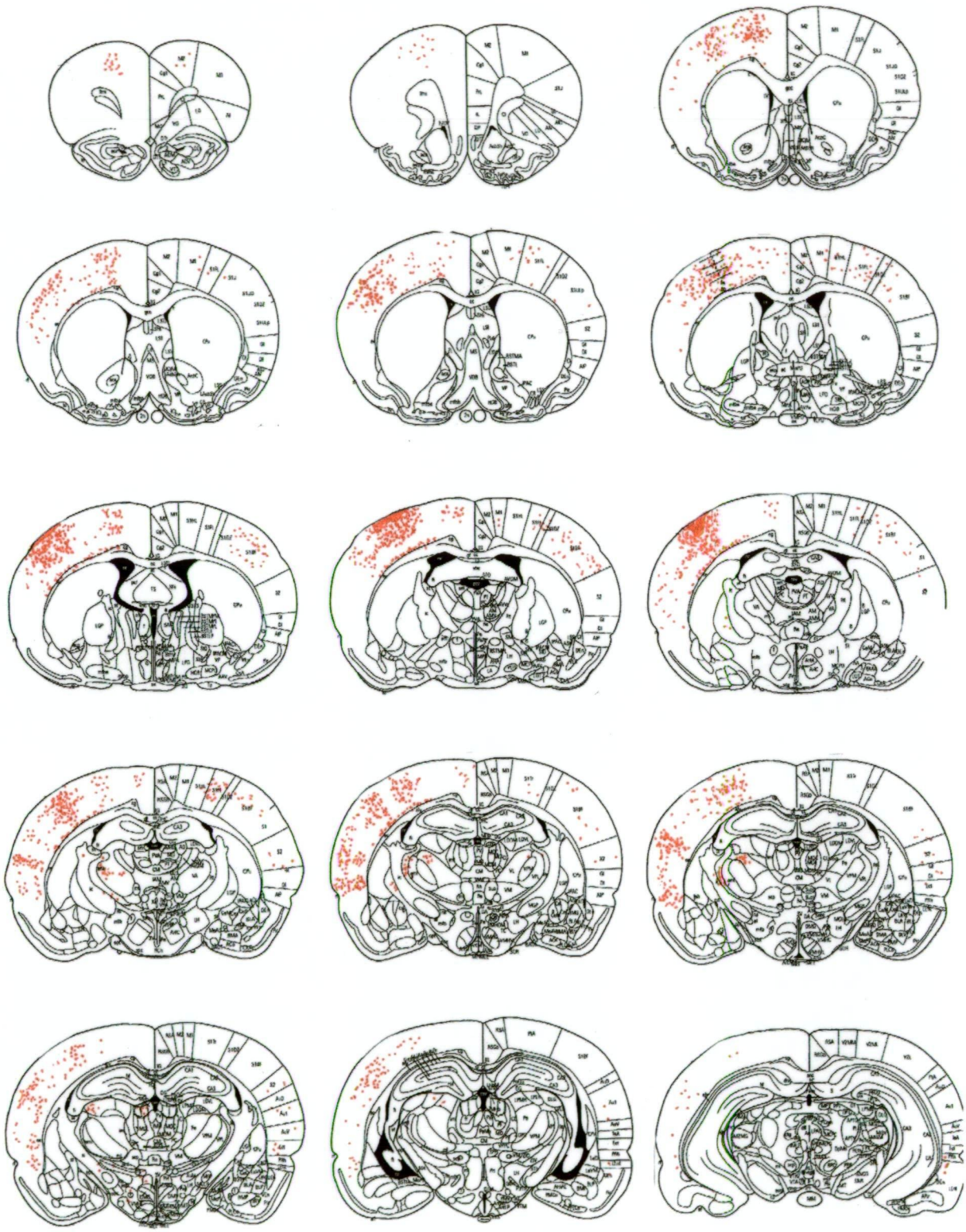

Figure 4.3

Fast Blue tracing and SMI32 immunolabelling in the M1 layer III region of cortex. Note the SMI32-labelled neuron containing Fast Blue (white arrow). Scale bar = 50μm for both images.

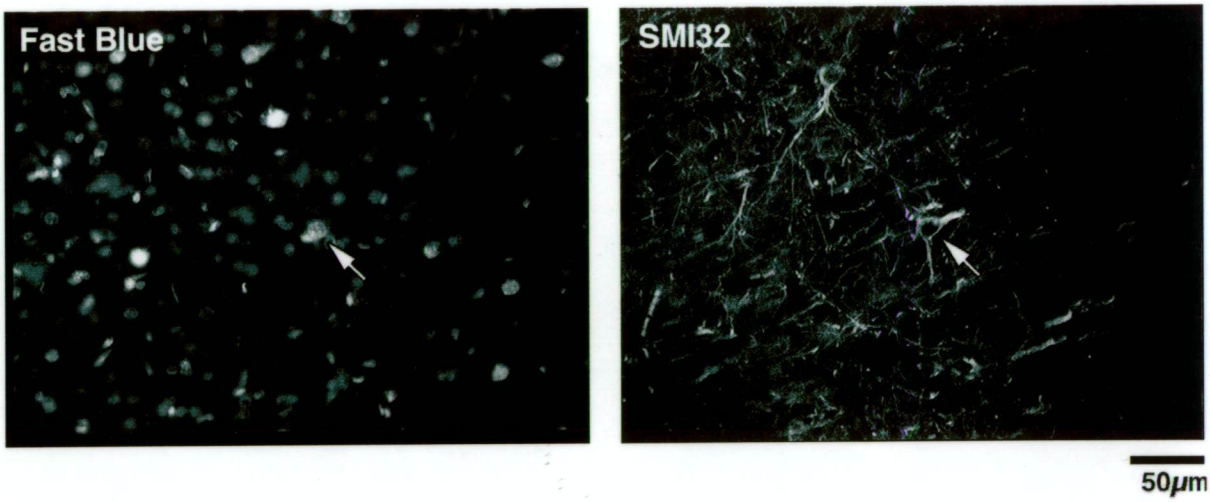
Fast Blue
SMI32
50μm

(3.85%; $p<0.0001$, Fisher's PLSD). SMI32-labelled proportions counted in the S2 region did not differ significantly for projections to M1 and S1My ($p=0.34$, unpaired t-test). ANOVA on data in which contralateral sites were individually considered indicated that the injection site and ipsilateral/contralateral count site factors also interacted moderately significantly ($p=0.042$): S1My projecting neurons from the contralateral hemisphere were more likely to be SMI32-labelled (12.4%) than those ipsilateral to the injection (7.7%), whereas the corresponding means for M1-projecting cells were similar (3.5%, 4.1% respectively).

However, this interaction depends strongly on the inclusion of some counts in which fewer than twenty neurons were observed. Contralateral means were heavily skewed by these counts in several of the S1My-injected animals, in which small numbers of contralateral projection neurons caused extreme variation in the proportions observed (cf. higher counts at the 9000μm distance in Figure 4.4); of the fifteen sites assessed as more than ten percent SMI32-labelled, nine were based on counts of less than twenty cells in total, compared to the more typical range of 100-300 cells; of those nine, seven were from contralateral sites in S1My animals.

3.2.2 SMI32-labelled proportion as a function of projection distance

Linear regression analysis of the regional count data indicated a strong positive correlation between the injection-to-count-site straight-line distance and the proportion of SMI32-labelled cells observed ($R=0.299$; $p=0.0015$). However, two factors confound this finding. Firstly, the highest-proportion distant counts are nearly all from less reliable samples (<20 cells), heavily biasing the determination of correlation. In fact, when sites examining less than twenty neurons are excluded, the value of R drops to 0.137, with a probability of 0.194 – well short of significance – and the slope of the regression line becomes negative. Secondly, when nearby projection neurons are counted, their connections may well be via axon collaterals rather than the primary axon, rendering this data irrelevant to an hypothesis about neurofilaments and overall axon length. When purely transcallosal projections are considered to avoid this ambiguity, the linear regression is similarly non-significant ($p=0.091$) without the less reliable outlier points. Overall, the observed data do not realistically support a correlation between neurofilament content and length of projection.

Figure 4.4

Percentage of SMI32-labelled neurons from counts obtained at seven sites each, in all animals injected in regions M1 (filled circles) and S1My (open circles). The distance measured is the approximate straight-line distance between the injection site and the middle of the counted region, estimated using stereotaxic co-ordinates and section thickness.

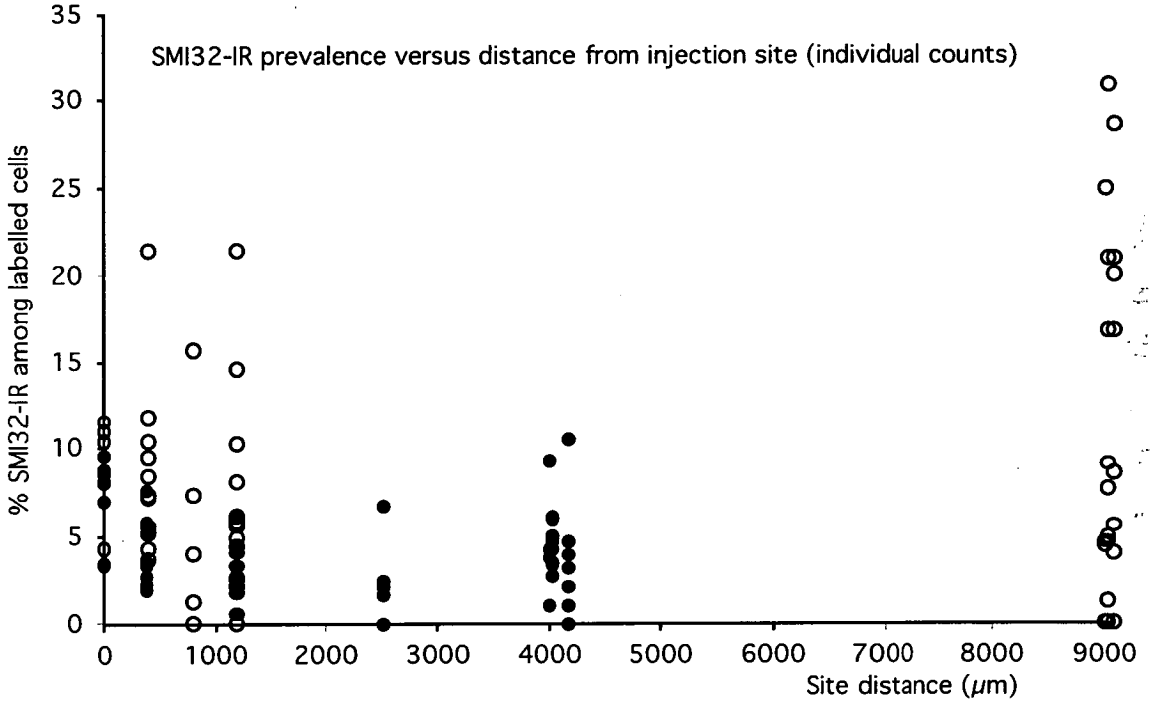
SMI32-IR prevalence versus distance from injection site (individual counts)
% SMI32-IR among labelled cells
35
30
25
20
15
10
5
0
0
1000
2000
3000
4000
5000
6000
7000
8000
9000
Site distance (μm)

4 Discussion

Generally, these studies exhibited similar phenomena to those made of primate cortex: the proportions of SMI32-labelled cells varied consistently according to their source and target regions (so that S1My-projecting groups were consistently richer in SMI32-labelled cells despite their lower overall prevalence). The sparse but more SMI32-labelled transcallosal projections observed in three S1My-injected animals may indicate a sub-regional variation in this projection, so that S1My data includes two separate populations with more specific proportions (cf. transcallosal V1/V2 projection neurons; Hof et al., 1996).

Although the rat brain is similar in these aspects to primate cortical studies, it presents some specific difficulties related to the relative thickness of rat cortex compared to the projection distances measured. Counting traverses were around 1000-2000 μm long, introducing considerable variation to the projection distances of cells on the same section. It is also unclear how far a projection axon may travel before branching or recurving to the injection site, further adding to uncertainty in the distance each traced cell projects. Separate consideration of callosal projections, likely to minimise these difficulties, indicated little or no distance-related increase in SMI32 labelled proportion.

Another complication in the assessment of projection populations for neurofilament content is the finding that mature neurofilament assemblies slow down axonal transport (Zhu et al., 1998). Whether the presence of axonal neurofilaments could impede the passage of Fast Blue on its way to the cell body is not known; however, it is notable that the amount and intracellular distribution of the tracer appeared to be similar for SMI32 labelled and non-immunolabelled neurons in the same regions (refer Figure 4.3a).

A critical point against a relationship between neurofilament and long projections is evident from inter-species comparisons. In the counts reported in Chapter 3, SMI32-labelled cells were roughly as common as for other rat studies, guinea pig cortex, and human tissue. Human corticocortical neurons, on average, need to grow axons for distances an order of magnitude larger than those of the rat or guinea pig cortex; if SMI32-labelling were related to the relative length of a neuron's axonal projection, we would expect that the SMI32-labelled population in human cortex was dramatically higher than for small rodent brains, which is clearly not the case. Other physical dimensions of the neurons such as perikaryon size and axon diameter are similar (Feldman, 1984), and even the smallest inter-gyral projections in

the primate brain involve longer distances than are physically possible for rat corticocortical projections. If neurofilaments were necessary to support some long projections, it is readily apparent that the projection distance relative to cell size or axon diameter in rodents in no way approaches that of primate corticocortical neurons; for it to be necessary for these rat neurons, it would have to be necessary for virtually every non-intrinsically projecting cell in the human or monkey cortex, which it is evidently not. However, Campbell and Morrison (1989) observed that human cortex appeared to have markedly greater numbers of SMI32 labelled pyramidal cells than that of the macaque. Stronger support for the notion that long-projection neurons require neurofilament comes from the observation that nearly all corticospinal pyramidal cells in the cortices of rat, marmoset, rhesus monkey and human brains are immunolabelled for nonphosphorylated neurofilament (Tsang et al., 2000), and the callosally projecting V1/V2 population of Hof and coworkers (1996). Nonetheless, such examples remain isolated among cortical studies which have found no significant correlation between neurofilaments and projection length (Campbell & Morrison, 1989).

Making hypotheses about neurofilament function based on proportions in projections may in itself be unhelpful. For SMI32 to be a useful functional marker, it would need to provide an indication of characteristic cellular activity or the qualities it imparts to a given projection, so that identifying SMI32-labelled neurons could provide clues about the regions in which they are located. Since SMI32 labelling is so widespread in the cortex, it presumably relates to some basic property or requirement in cortical activity, which must be utilised to greater or lesser extents by certain projections. For SMI32 labelling to be meaningful at the level of the individual neuron, the microarchitecture of projections must be assessed using different methods before any realistic conjectures can be made. Any alternative explanation must address the question of how the presence of neurofilaments in some members of an heterogeneous projection group can have functional implications for the group as a whole.

5 Summary

Like primate neurons, the proportion of SMI32 labelling among groups of projection neurons in the rat cortex varies according to their projection target rather than the length of their projections.

Chapter 5

Neurofilament content, calibre and myelination of axons in the mature rat cortex

1 Introduction

The identification of neurofilaments as the principal cytoskeletal component identifiable in axonal ultrastructure has prompted a long series of studies of their organisation and role in mature, developing and degenerating axons of the peripheral nervous system (e.g. Friede & Samorajski, 1970; Hoffman et al., 1985, 1987; Szaro, Whitnall, & Gainer, 1990; Hsieh, Crawford, & Griffin, 1994; Sánchez et al., 1996; Elder et al., 1998b; Zhu et al., 1998). Although strong correlations have been found between the numbers of neurofilaments found in axons and the size and myelination of those axons, the causal underpinnings of these relationships remain open to debate, with some researchers contending that myelination exerts a direct influence on filament spacing by altering their phosphorylation (e.g. de Waegh et al., 1992) and others that the composition and phosphorylation of neurofilaments determines axonal calibre (e.g. Elder et al., 1998b).

Complicating these views are the wide range of observed packing densities of neurofilaments within axons, differing between rodent species and also between separate fibre populations in the CNS of the same species (Price et al., 1988; Szaro, Whitnall, & Gainer, 1990). If neurofilament content *per se* is the major determinant of axon calibre within specific groups of fibres, its influence must be mediated by other factors which differ between these populations.

Despite the widespread presence of neurofilaments in cortical neurons and their axons, no studies have investigated the relationship between neurofilament content and axonal dimensions in cortical tissue in detail. One ultrastructural study of callosal axons described their segregation into large myelinated processes containing large numbers of neurofilaments, microtubules and mitochondria, and smaller unmyelinated processes containing microtubules, mitochondria and few neurofilaments (Gravel, Sasseville, & Hawkes, 1990), but no quantitative analysis of neurofilament numbers was performed. Accordingly, the current study set out to investigate whether neurofilament-axon size relationships, similar to those described

elsewhere, existed in corticocortical axons. The corpus callosum was chosen for study due to its ready identifiability and abundance of myelinated axons (Nuñez et al., 2000; Gravel, Sasseville, & Hawkes, 1990).

Additionally, blocks of cortical tissue from the dorsal strip lacking in neurofilament immunoreactivity (Chapter 3) and the adjacent sensory region with strong neurofilament and myelin staining were compared at the ultrastructural level. Sections from layer I of the sensory cortex, which is also well labelled by some neurofilament antibodies, were examined for comparison with the cortical and callosal samples.

2 Procedures

2.1 Animals

Four adult male Hooded Wistar rats weighing 250-300g were used as specimens in these studies.

2.2 Fixation and tissue collection

The same perfusion procedure detailed in Chapter 2, §3.1, was followed with the exception that the fixative contained an additional 2% glutaraldehyde. Brains were removed and postfixed in the perfusate for an additional six hours. Coronal sections at a level corresponding to bregma –2.8mm (Paxinos & Watson, 1998) were cut using a vibrating microtome at 100μm thickness, and tissue blocks were cut from these sections using spring scissors and/or fine scalpel blades. Four blocks were cut from each slice with the following orientations:

1. a radially oriented block from the pial surface to the white matter, approximately 0.5mm wide, from the strip unlabelled by SMI32 neurofilament staining (Ch 3, Figure 3.5). This strip was easily identifiable by its more translucent appearance compared to the denser cortex on either side.
2. a similar block cut from the S1 cortex approximately 2mm lateral to the first block.
3. the strip of corpus callosum bridging the two hemispheres, around 3mm in extent and 0.5mm wide.
4. a strip of the pial surface and layer I, cut from the outer edge of the cortex lateral to sample 2, around 3mm in extent.

Equivalent blocks were cut from both hemispheres in two consecutive coronal slices (four in the case of the corpus callosum blocks), for a total of four samples per

animal in each category to allow for sample damage during embedding and sectioning.

3.2 Tissue infiltration, staining and embedding

Tissue blocks were washed in PBS and postfixed for up to two hours with 1% osmium tetroxide in 0.1M PIPES (piperazine-1,4-bis(2-ethanesulphonic acid)) buffer. After two five-minute washes in water, tissue was immersed in 5% uranyl acetate in 50% alcohol for an hour. The tissue was dehydrated in a graded alcohol series consisting of ten minute immersion in 70%, 80%, 90%, 95% and 100% ethanol, followed by two washes in 100% ethanol and two in propylene oxide. Tissue was infiltrated overnight in a 1:1 mix of propylene oxide and Epon resin (Araldite), then for four hours in pure Epon resin, followed by two hours in fresh resin. Tissue samples were the flat-embedded in moulds with fresh Epon, vacuum desiccated for an hour, and cured for 48 hours in a 60°C oven.

Embedded tissue blocks were then sectioned using a Leica automated ultratome and a diamond knife at a thickness of 60nm. Cortical blocks (samples 1 and 2) were cut tangentially down to halfway through their length, corresponding to layer IV of the intact cortex. Other samples were similarly cut across their short faces, with the result that cortical blocks were sectioned tangentially, callosal blocks were sectioned sagittally, and layer I blocks were sectioned radially. The aim in each case was to maximise the proportion of axons crossing the plane of section nearly orthogonally.

Sections were collected on 300-mesh grids and stained by Fahmy's method using a solution of 5% uranyl acetate in 50% alcohol for thirty minutes, followed by three minutes in 0.5% lead citrate in 0.3% NaOH. After drying, sections were examined in a Philips 400 transmission electron microscope and photographed using an 88 × 63 mm plate camera. Four low power micrographs of clean areas of sections were taken at 3000× magnification, followed by high power (16 900×) micrographs of individual or groups of axons in the case of corpus callosum samples. Fourteen high power micrographs were made, covering every axon encountered in a series of traverses beginning at one corner of a selected grid. Following development, plates were printed on Ilford multigrade photographic paper with varying filter grades in order to bring out cytoskeletal detail.

2.3 Quantitative analysis

Myelinated axons, easily identified by their electron-dense dark outlines, were counted in all low power micrographs. No attempt was made to distinguish between

axons passing perpendicular to the plane of section and other axons, since the apparent orientation of axons varied continuously from perpendicular to transverse. Crop lines 3mm inside the plate boundaries were used on all plates, and axons either inside or whose centres were judged to lie inside the lines were counted. Minor unusable areas due to plate number markings, section damage, dirt or overlapping micrographs were identified and their areas were subtracted from the overall section area. Approximate actual section areas were calculated using a scaling factor derived from the microscope magnification and the optical enlargement of 2.5× used in making prints, to permit overall axon densities to be evaluated for each sample.

For evaluation of axonal neurofilaments, prints of high power micrographs were used to count intermediate filaments and microtubules. Myelinated axons were assessed whose outlines lay entirely within the print boundaries, and whose filaments were dot-like in appearance (distinct and not running in transverse lines) and were distinguishable from microtubules. The latter were identified on the basis of size and usually an observable lumen within the filament (Friede & Samorajski, 1970). Structures of the appropriate size and spacing were assumed to be neurofilaments because of their presence in axons. Unmyelinated axons were not evaluated because of the difficulty of distinguishing them from other processes such as dendrites (Peters, Palay, & Webster, 1991).

The high power micrographs were also scanned at 100dpi resolution and processed using NIH Image 1.62 software running on Mac OS. Measurements were made of axons whose filaments had been counted; for each axon, the area inside the myelin coat and its maximum and minimum diameters were measured. Myelin thickness was estimated by averaging two straight-line radial measurements at points where the myelin coat was compact and undistorted; where possible the two measures were made orthogonal to one another to allow for differences caused by oblique orientations. These measures were also converted to approximate actual sizes using magnification and optical enlargement factors.

Since disruption in the form of laminar separation of the myelin coating of many axons was evident (cf. the large axon in Figure 5.2a), the area of the outer boundary of the myelin coating was also measured. In cases where this outer boundary had clearly pulled away from the surrounding neuropil, the extent of the resultant cavity was measured instead as the outermost measure of the axon's cross section. To allow for possible tissue shrinkage, the mean of the internal and outer apparent cross sections was used as a measure of the axonal area, since shrinkage of the internal axoplasm and the neuropil shrinking away from the outer myelin sheath

would partially counteract one another. It should be noted that this "compensated" area includes half the area of the myelin sheath as well. Statistical analysis of low-power axon density, high-power filament density and the relationships between neurofilaments, microtubules, compensated axon cross-section and myelin thickness were performed using StatView 5.0 software running on Mac OS.

3 Results

3.1 General observations

Low power micrographs of the four sampled regions were clearly different in their ultrastructure; these differences were consistent across the four animals studied, and corroborated with the appearance of these regions under a Gallyas silver stain for myelin (Figure 5.1). The M1 neurofilament gap region and adjacent sensory cortex (Figures 5.1 a–d) were easily distinguished by the former's paucity of myelinated profiles, although the remainder of the neuropil was essentially similar in terms of its processes and cell bodies. The myelinated axons of sensory cortex samples were also generally larger than those of the gap region. Callosal sections were very different to cortex, being composed largely of variously sized myelinated axons and numerous smaller unmyelinated profiles, with occasional presumed glial cell bodies (Figure 5.1e). Most callosal profiles appeared nearly circular, indicating that axons penetrated the sections orthogonally, although occasional large tracts of oblique, elongated profiles were encountered, with an abrupt transition between areas of different orientations. Layer I samples (Figure 5.1g) consisted of densely packed smaller profiles of a different appearance to those of layer IV, with occasional myelinated profiles of a small calibre. Many synapses were evident in the layer I low power micrographs.

Examination of the high power micrographs of callosal axons revealed minor tissue disruption in the form of a light haze of flocculent material below the limit of resolution, which interfered somewhat with the identification and distinction of neurofilament-sized elements from microtubules. However, this haze was not ubiquitous, raising the question of whether it might be a genuine structural element of some axons, perhaps corresponding to differentially preserved or stained microfilaments (Peters, Palay, & Webster, 1991). Presumed neurofilaments and microtubules formed well-spaced but irregular arrays in most axons studied, with a tendency to cluster separately noticeable in microtubule distribution (Figure 5.2a). Mitochondria were relatively scarce inside axonal profiles. A subpopulation of axons (informally, under 5%) had markedly denser packing of their neurofilaments and

Figure 5.1

Low power electron micrographs of representative tissue samples from the four regions of cortex studied. Comparison light micrographs of the equivalent regions stained with the Gallyas silver method for myelin are shown for each cortical sample, with approximate section planes indicated by lines, and crossbars indicating the approximate width of the electron micrographs.

a) M1 region, which exhibits a lack of labelled cell bodies and processes in neurofilament immunohistochemistry. Note sparsity of myelinated axonal profiles (arrowhead).

b) Coronal section of M1 cortex stained for myelin by the Gallyas silver method. Pial surface at left.

c) Adjacent S1 region which exhibits a different pattern of neurofilament immunoreactivity. Note greater abundance of myelinated axonal profiles.

d) Coronal section of S1 cortex stained for myelin by the Gallyas silver method. Pial surface at left.

e) Corpus callosum sample consisting largely of myelinated axon sections.

f) Coronal section of corpus callosum stained for myelin by the Gallyas silver method. Dorsal is upwards.

g) Layer I sample showing densely packed fine profiles with numerous synapses (arrow). Myelinated axon profiles are infrequent.

h) Coronal section of cortical layer I, overlying M1 and S1 regions, stained for myelin by the Gallyas silver method. Dorsal is upwards.

Scale bars = 2μm for electron micrographs; 200μm for light micrographs.

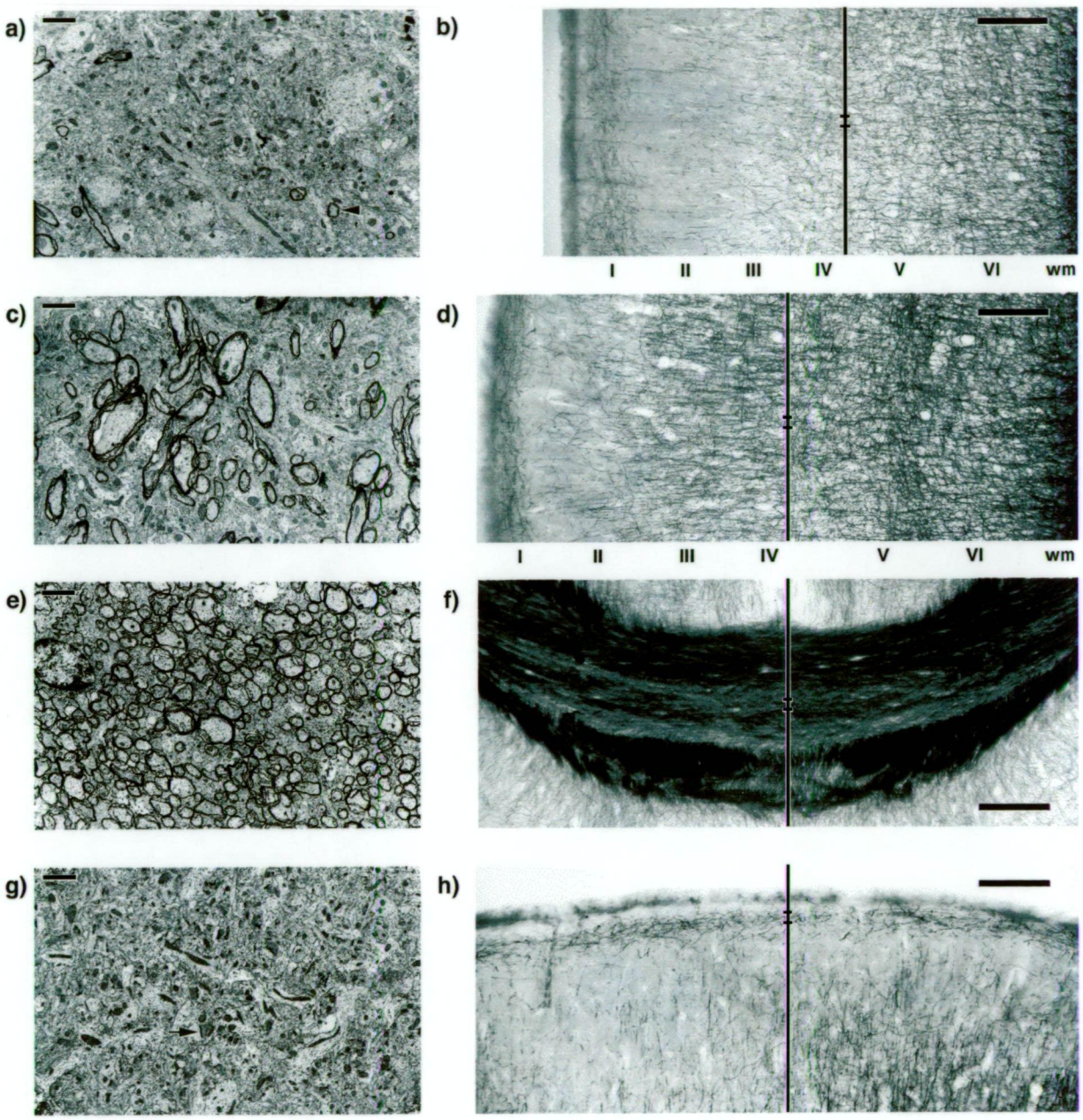
a)
b)
I
II
III
IV
V
VI
wm
c)
d)
I
II
III
IV
V
VI
wm
e)
f)
g)
h)

Figure 5.2

a) Representative high-power electron micrograph from callosal sample showing presumed neurofilaments (arrowhead), microtubules (open arrowhead) and myelin sheath (arrow).

b) Extremes of filament packing density in adjacent axons in a callosal sample. Note also the irregular profile of the axon on the right, without significant distortion of the surrounding neuropil which would be expected for localised shrinkage.

Scale bars = 0.5μm.

a)

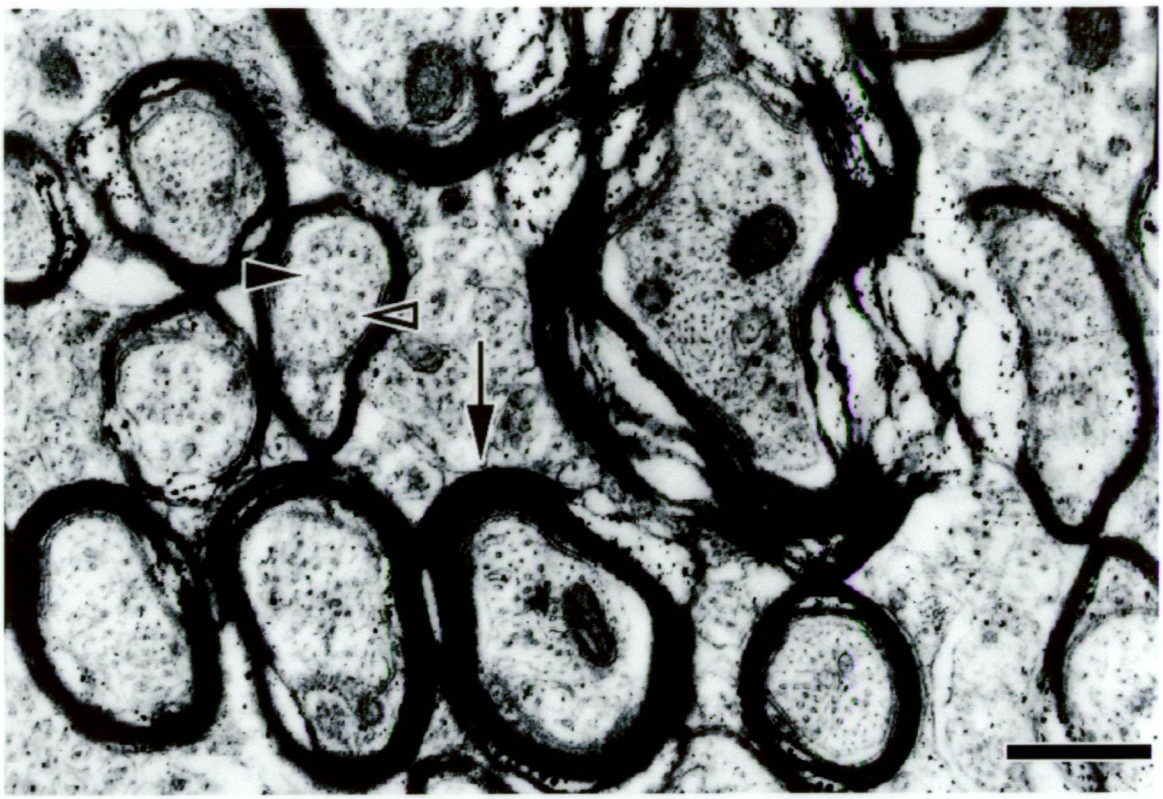

b)

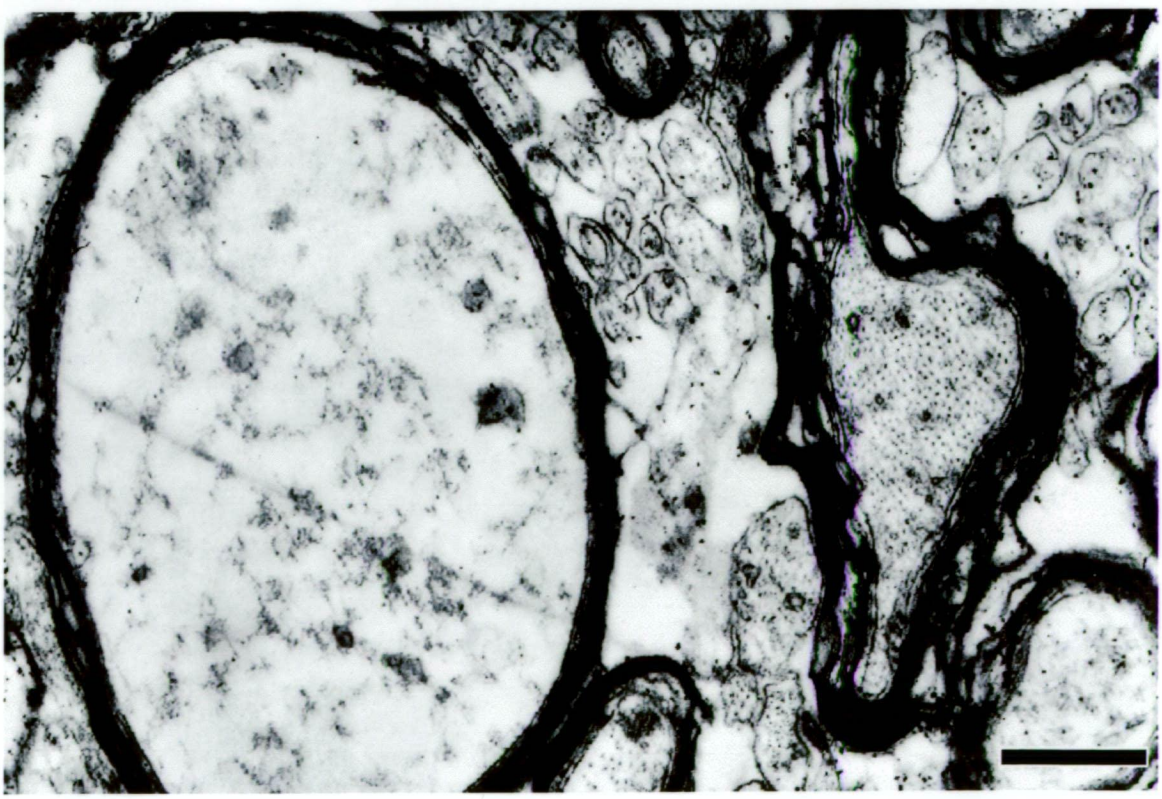

microtubules than that of nearby axons; another subpopulation exhibited markedly dispersed cytoskeletal elements (Figure 5.2b). Although cytoskeletal details were not resolvable in all axons observed, no instance of a myelinated axon with well-defined microtubules and an absence of neurofilament-like structures was ever observed. However, neurofilament-sized structural elements were evident in many smaller, unmyelinated profiles (Figure 5.2).

3.2 Low power analysis

As predicted by their silver-stained appearance, the overall density of myelinated profiles differed markedly between the four cortical regions examined ($p<0.0001$, ANOVA). The mean densities of myelinated axonal profiles in the four cortical regions are listed in Table 5.I. Notably, M1 layer IV density was significantly different from S1 layer IV ($p<0.0001$, Fisher's PLSD) and corpus callosum axon densities were much greater than for all other regions ($p<0.0001$ in all three comparisons, Fisher's PLSD). No significant differences in axonal density between individual animals were evident.

Table 5.I: Mean densities (profiles / μm^2) ± standard errors of counts of myelinated profiles from all animals for the four surveyed regions.

Region	*M1 cortex, IV*	*S1 cortex, IV*	*Corpus callosum*	*Layer I*
Density	0.0174 ±0.0035	0.1292 ±0.0191	0.5905 ±0.0370	0.0015 ±0.0007

3.3 High power analysis

Unlike the low power micrographs, high power ultrastructural analysis revealed significantly different intra-axonal neurofilament densities between the four animals ($p<0.0001$, ANOVA; $n = 162$ except where indicated), although the peaks of density distributions for each animal all occurred close to the mean of 114.5 filaments per μm^2. Mean compensated axonal areas and myelin thickness also differed between animals ($p<0.0001$ for each, separate ANOVAs) with the same animal markedly higher for both measures ($p<0.003$ in all comparisons, Fisher's PLSD), but this was unlikely to explain the density differences given that NF density does not correlate with compensated axonal area or internal area across the samples (Spearman's $R = -0.116; -0.111$).

Despite these differences, several robust correlations were observed between neurofilament and microtubule numbers, and axonal cross section, diameter and myelin thickness. Compensated and intra-axonal area was strongly correlated with NF counts ($R = 0.920; 0.908$), MT counts ($R = 0.701; 0.700$) and the sum of both ($R = 0.930; 0.919$), and approximately linearly related to each of these (Figure 5.3).

Figure 5.3

The relationship between cytoskeletal filaments and compensated axonal cross-sectional area in the corpus callosum of the rat. Numbers of (a) neurofilaments, (b) microtubules, and (c) summed neurofilaments and microtubules counted in axonal profiles in relation to the area of those axons in square microns.

Note that the large axons represented at the upper right of each graph did not unduly skew the observed correlations: data were reanalysed excluding them and showed essentially similar relationships.

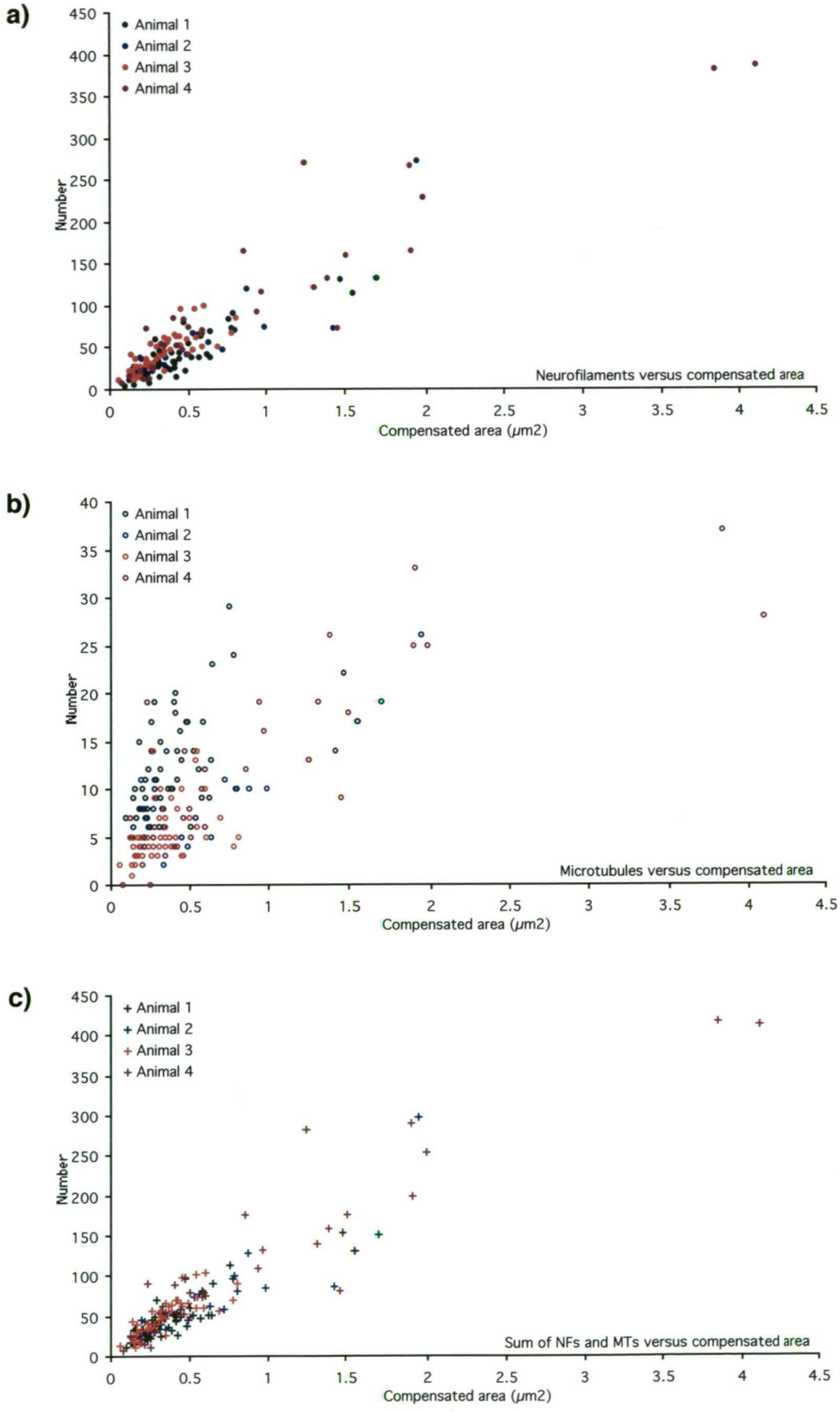
a)
Animal 1
Animal 2
Animal 3
Animal 4
Number
Neurofilaments versus compensated area
Compensated area (μm2)
b)
Animal 1
Animal 2
Animal 3
Animal 4
Number
Microtubules versus compensated area
Compensated area (μm2)
c)
Animal 1
Animal 2
Animal 3
Animal 4
Number
Sum of NFs and MTs versus compensated area
Compensated area (μm2)

Straight-line regression analysis indicated that the number of summed filaments could be derived from the compensated area in square microns by the relationship

$$\text{(summed filaments)} = 10.6 + 106.8 \times \text{(compensated area)}$$

Myelin thickness was moderately correlated with NFs, MTs and summed filaments (R = 0.777, 0.581, 0.784 respectively) and maximum and minimum diameters (R = 0.716, 0.722 respectively). External area was most strongly correlated with myelin thickness (R = 0.863) although compensated area had a similar relationship (R = 0.836). In contrast with studies of myelin-compromised mice (de Waegh, Lee, and Brady, 1992; Cole et al., 1994), variations in the thickness of surrounding myelin were not correlated with NF density, whether calculated by compensated or internal area (R = -0.052 and 0.031 respectively).

4 Discussion

4.1 Regional differences in myelinated fibre density

The differences between low-power counts of myelinated axons in the four regional samples were similar to their appearance in myelin-stained material. The existence of similar populations of Nissl-stained nuclei (each presumably belonging to a neuron with an axon) in the neurofilament-poor region and the adjacent neurofilament-rich region suggests in turn that the axons of these cells are significantly less likely to be myelinated, and the strong correlation between neurofilament content of axons and myelination suggests that axonal neurofilaments would be lacking in this region as well. A clue to the causal relationship between these phenomena is provided by the paucity of SMI32 immunolabelling in this region, indicating that dendritic and somatic neurofilaments, presumably not directly regulated by myelination, are also lacking. It is plausible that the neurons of this region generally express less neurofilaments which makes their axons less likely to receive myelination.

However, this reasoning applies only to axons originating in this area. The relatively sparse group of myelinated axons observed in sections from this region may represent afferents from other regions, indicating that the suitability of glial cells in this region to provide myelin to neurofilament-containing axons remains. Examination of the distribution of cells labelled by a tracer injection made into this region during studies for Chapter 4 suggests that the number of afferents should be comparable to those of the sensory cortex region targeted in that study; therefore, the labelled axons may approximate the typical myelinated proportion of afferent axons for these regions, in which case they are far outnumbered by efferent myelinated

axons in the sensory cortex sample. It may also be that the afferents of this motor region are, like its efferents, unlikely to be myelinated for reasons unknown.

The source of the sparse myelinated axons observed in layer I samples is also intriguing. Cajal-Retzius neurons of layer I have axons which are prenatally myelinated (Marin-Padilla, 1984) and it is possible that these axons are those. However, cell bodies of C-R neurons were not observed in the surveys of Chapters 3 and 6 using neurofilament antibodies, and this explanation would require that axonal neurofilaments are not associated with somatic neurofilaments for this cell type, or that they also lack axonal neurofilaments but nonetheless attract myelination, in contrast to findings in other cortical regions. Alternatively, the myelinated axons of this layer may originate with unknown neurons of deeper layers.

Low power callosal sections resembled the examples illustrated by Gravel, Sasseville, and Hawkes (1990), although small unmyelinated profiles were less common than in their samples, which were approximately 81% unmyelinated axons by number; estimates of proportion in the current study were hampered by tissue damage, particularly in unmyelinated profiles. The predominance by area of myelinated axons in the corpus callosum samples of this study (Figure 5.1e) is also similar to the 75% of total area observed by Nuñez and coworkers (2000) in adult male rats. The restriction of significant neurofilament content to larger, myelinated axons focussed the qualitative aspects of this study on this type, similar to the other studies cited in this chapter.

4.2 Axonal properties and neurofilaments

The primary conclusion supported by the data in this study is that the relationships between neurofilaments and axonal properties found in peripheral and spinal axons, also hold for corticocortical axons in the corpus callosum. Moreover, the characteristic packing densities of neurofilaments found in these fibres are similar to those observed in other regions of rodent nervous systems, indicating that the neurofilament complements of corticocortical fibres are similar to those of peripheral and spinal axons.

The observed correlations between summed filaments and axonal dimensions were somewhat lower than those derived by Friede and Samorajski (1970), perhaps due to the tissue distortion evident in some samples assessed in this study. The slope of the regression line, equivalent to the filament density, was 79.9 filaments/μm^2 in their study of rat sciatic nerves, compared to 106.8 filaments/μm^2 in data from this study. The fact that summed NFs and MTs provided the best correlation with axonal

area and diameter in both studies is a strong indication that cytoskeletal filaments tend to be distributed with a characteristic density in populations of mature axons; the strength and linearity of these correlations indicate that these packing densities tend not to vary across populations which range considerably in size, suggesting that they depend on filament-filament interactions rather than axonal properties.

The significant differences in filament density observed between animals in this study are difficult to reconcile with the lack of overall differences in axon distribution densities from the low-power micrographs, since overall shrinkage or expansion of tissue would influence both analyses similarly. Similarly, it is possible that the unusual packing densities observed in some axons were due to differential shrinkage or expansion of tissue, but unlikely given that the myelin coats of these axons appeared similar to one another. Any shrinkage or expansion of axonal contents would need to have occurred in the short time when the myelin coating remained unfixed and able to accommodate expansion or contraction. However, these phenomena were mostly evident in the sample from one of the four animals. Another possible explanation is a difference in the optical enlargement of high power micrographs printed at different times, since this factor is controlled by a mechanical analogue device.

The overall mean NF densities of callosal axons, calculated by compensated area (114±46 filaments per μm^2) and internal area (202±91), are greater than figures reported for rat corticospinal tract (93±10; Szaro, Whitnall, & Gainer, 1990) and sciatic nerve (78.4 implied; Friede & Samorajski, 1970) and mouse sciatic nerve (90±2; Cole et al., 1994); they bracket those reported for rat sciatic nerve (163±28; de Waegh, Lee, & Brady, 1992) and mouse dorsal root (157±63; Elder et al., 1998b) and optic nerve (117±2; Brady et al., 1999), but are less than figures for the rat cuneate tract (238±24; Szaro, Whitnall, & Gainer, 1990) and dorsal roots (355; Hsieh, Crawford, & Griffin, 1994). Aside from intrinsic differences in filament density for different fibre populations (Szaro, Whitnall, & Gainer, 1990), several factors influence these comparisons: the compensated area used to calculate some neurofilament densities in this study includes half the myelin surrounding the axon, and secondly, membrane-bound organelles were excluded from the intra-axonal sampling used in several of the other studies cited, whereas they were included in areas measured in the present study. Such organelles were relatively uncommon in the axons studied, and while their net effect is to lower estimates of neurofilament density, they are unlikely to have a large effect when spread over the pooled measurements. Area compensation by averaging external and internal areas, on the

other hand, adds approximately 30% to an estimated true internal area (estimated using overall means of external area and myelin thickness) by including half the cross-section of the myelin sheath. Correcting for this factor suggests that true neurofilament density in the processed samples would be approximately 148 neurofilaments per square micron, still well within the range of measures made by other studies. Estimates of tissue shrinkage during processing were not made for this study, and are not quoted in the others mentioned, rendering detailed comparisons pointless.

With these considerations in mind, the range of these figures nonetheless indicates that the density of axonal neurofilaments probably varies between species and CNS regions to an extent which exceeds differences in methodology or tissue processing. If neurofilaments are indeed major determinants of axonal calibre (Chapter 1, §4.4.3), their method of action is obviously modulated by extra- and intra-axonal conditions, perhaps through the modulation of the phosphorylation states of the larger subunits (de Waegh, Lee, & Brady, 1992; Brady et al., 1999). Local variations in filament density point to other factors operating at the level of individual neurons. In light of the filament density differences between fibres in different parts of the nervous system, it is conceivable that the trophic or chemotactic factors leading growing fibres to seek different targets may also influence their cytoskeletal structures, or even that such influence may be one of the methods by which these factors guide growth.

The correlation between neurofilaments and axonal dimensions, while consistent across rodent species and between the CNS and the periphery, does not provide many clues about neurofilament function. Zhu and coworkers (1998) illustrate that knocking out NFH has little effect on axonal calibre (~10%), so that it might be argued that the correlation is the result of axonal size being filled by neurofilaments until they reach a certain packing density. The existence of axons with markedly different filament densities suggests that calibre must be determined by factors other than, or working in concert with, the sheer quantity of neurofilament expressed and transported to the axon. Other roles may be performed by neurofilaments in large axons; for example, Kriz˘ and coworkers (2000) found that the minor changes in axon calibre caused by NFH knockout were accompanied by significantly larger decreases in conduction velocity than would be expected from the physical changes alone. The highly charged, phosphorylated tail domains of the NFH subunit may be involved in the ionic conductance changes these authors

suggest are responsible for the reduction, as well as changes in the action potential time-course.

Although the bulk of neurofilaments were found in myelinated fibres, and no myelinated fibres definitively lacking neurofilaments were observed, many of the small unmyelinated profiles visible in high power callosal micrographs exhibited a few neurofilament-sized structural elements in this study and others (Friede & Samorajski, 1970; Gravel, Sasseville, & Hawkes, 1990). However, these were not usually as clearly defined as neurofilaments in myelinated axons, and may be microtubules damaged in processing or even other types of intermediate filaments such as α-internexin or peripherin. The near-complete colocalisation of immunohistochemically labelled myelin basic protein and neurofilament subunits in axons (J. C. Vickers, unpublished data) appears not to identify these fibres as containing neurofilaments, but whether this is due to the sensitivity of the technique or differing intermediate filament types is not clear. It is possible that phosphorylation changes caused by myelin (Starr et al., 1996; de Waegh, Lee, & Brady, 1992) dictates which axons are picked up by the antibodies by altering the epitopes they recognise.

In conclusion, these observations of neurofilaments, calibre and myelination in callosal axons indicate that their relationship in corticocortical axons is essentially similar to that observed in peripheral axons, despite the fact that different types of glial cells provide the myelination. The underlying factors producing this close association are still open to debate, but peripheral nerve studies of neurofilament knockout mice combine with the reduction of callosal myelination observed in hypothyroid, neurofilament-poor development (Gravel, Sasseville, & Hawkes, 1990) to suggest that axonal accumulations of neurofilament induce glial cells to myelinate the axons which contain them. If this is the case, the expression of neurofilaments in subpopulations of cortical projection neurons may dictate whether their axons are myelinated along their course, with obvious implications for axonal conduction. This relationship appears to hold even for basket cells, whose axons are myelinated (DeFelipe, Hendry, & Jones, 1986) and which exhibit colocalised parvalbumin and SMI32 immunolabelling (Chapter 6). In addition, myelin layers subsequently influence the phosphorylation state and arrangement of neurofilaments (Starr et al., 1996) within these axons in a process of mutual interaction, resulting in large-calibre well-myelinated fibres packed with phosphorylated neurofilaments. This maximisation of the volume occupied by the neurofilament lattice suggests that NFs

are costly for neurons to produce, but vital to the normal function of myelinated axons.

5 Summary

Neurofilaments in corticocortical axons exhibit similar relationships with calibre and myelination in the cortex to those observed in the periphery: myelinated neurons are invariably filled with semi-regular NF lattices which fill the axonal lumen, whereas NFs are rare in unmyelinated fibres. It appears likely that axonal neurofilaments attract myelination and are in turn modified by that myelin.

Chapter 6

Neurofilament distribution compared with other chemical phenotypes in the developing rat brain

1 Introduction

Knowledge of the morphological, connectional and electrophysiological correlates of chemical phenotypes among GABAergic neurons (Kawaguchi & Kubota, 1997) provides cortical researchers with the potential for insights into the dynamics which may prevail in different regions of the cortex. Population surveys of these phenotypes can thus imply physiological influences in a given area of the cortex, which despite a lack of specificity act as a useful complement to detailed electrophysiological, morphological and ultrastructural examinations of cortical organisation. Although such broad functional correlative methods are less established in anatomy, neurochemical subpopulations have already been used in the distinction of cortical regions from one another (e.g. Paxinos et al., 1998), and the recording of massed electrical activity has been one of the mainstays of cortical electrophysiology.

Correlations in the developmental emergence of these markers and that of neurofilament labelling could indicate shared regulatory mechanisms and further clues toward neurofilament function. With this objective in mind, this study set out to examine whether the emergence of known chemical markers in the developing rat brain was associated with that of various neurofilament subunit epitopes.

1.1 Neurofilaments

Various studies have demonstrated the appearance of the neurofilament subunits during development, such as the E9 appearance of all three subunits in the mouse (Cochard & Paulin, 1984; Alfonsi et al., 1984), or the E12 appearance of NFL and NFM, then DP-NFH and finally P-NFH in the rat CNS (Pachter & Liem, 1984). Studies of the rat optic nerve (reviewed by Hirokawa, Glicksman, & Willard, 1984) show that few NFs are evident in its axons at birth; over the three weeks they appear and show evidence of crosslinking, which may stabilise or consolidate the forms of growing neurons (Giasson & Mushynski, 1997; Liu, Dyck, & Cynader, 1994) and coincides with functional maturity (Steinschneider et al., 1996). After birth, axonal

transport of NF decreases eightfold (Hoffman et al., 1983; 1985), presumably as cells mature and the transport of building materials reduces; slowing of transport also encourages NFs to accumulate, possibly increasing axon diameter (Hoffman et al., 1985). No global studies of NF distribution during cortical development have been published.

The three subunits appear in axons at different times before or soon after birth (Giasson & Mushynski, 1997), and the appearance and phosphorylation of NFH appears to accompany electrophysiological maturity and synapse formation (Liu, Dyck, & Cynader 1994; Steinschneider et al., 1996). In humans, cortical expression of perikaryal NFs increases slowly to adult levels over the first three postnatal years (Ang et al., 1991).

1.2 Peptides

1.2.1 VIP

VIP is expressed in a distributed population of bipolar cortical neurons, starting in the second week of postnatal development. At P14 the adult pattern of expression is seen, albeit with elevated somatic VIP levels which gradually subside as their processes grow (Emson & Hunt, 1991). Götz and Bolz (1994) found that VIP expression in cortical cultures only occurs if the entire cortical slice is intact rather than dissociated, strongly suggesting that local factors prompt expression, and that their dispersed distribution does not necessarily result from VIP-expressing cells inhibiting expression in their neighbours.

1.2.2 SRIF

Transient populations expressing somatostatin have been observed in the piriform and occipital cortices, and may have may have some bearing on their development (Fitzpatrick-McElligott et al., 1991). In the rat cortex, SRIF-labelled neurons are apparent in layers V and VI at birth, and are augmented by labelled cells in more superficial layers a week later; normal adult distribution is first evident at P14 (McDonald et al., 1982; Fitzpatrick-McElligott et al., 1991).

1.3 Calcium binding proteins

The expression of calcium binding proteins is determined postmitotically: cells from the same progenitor have the potential to express PV, CR or CB independently, and commit to particular phenotypes based on local factors and location (Mione et al., 1994).

1.3.1 PV

Parvalbumin appears in cortical neurons at the same time as inhibition becomes significant in cortical activity (Luhmann & Prince, 1991). Its expression is extrinsically stimulated (Vogt Weisenhorn, Celio, & Rickmann, 1998) in nonpyramidal neurons of cortical layers V, VI, IV and II/III, in that order, appearing at P6 (Sánchez et al., 1994) or P8, initially in the retrosplenial and cingulate cortices, followed by visual, auditory and motor cortex, and finally secondary regions by P21 (Alcántara, Ferrer, & Soriano, 1993). PV labelling may decrease in pericellular baskets of monkey cortex during maturation (Akil & Lewis, 1992).

1.3.2 CR

Calretinin is far more widespread in the developing cortex than in the adult brain; it can be detected immunocytochemically in neurons of the E14 subplate and marginal zones, remaining widespread in these layers until postnatal day 3, when they nearly disappear, probably by cell death (Fonseca et al., 1995; Condé et al., 1994). In layers II to VI, some neurons appear CR-positive before birth and in increasing numbers, transiently including some pyramidal and Cajal-Retzius cells, during the first postnatal week (Fonseca et al., 1995; Schierle et al., 1997), decreasing sharply until the adult patterns of immunoreactivity appear in the third week. Most neurons displaying transient or ongoing CR-IR are also GABA-IR, with the exception of the pyramidal cells (Fonseca et al., 1995).

2 Procedures

Groups of five rats, aged 0, 7, 14 and 21 postnatal days, were anaesthetised and perfused, and their brains removed, cryoprotected and serial sectioned as described in Chapter 2, §3.1. Sets of every tenth section were processed for immuno-histochemical labelling, using single-antibody immunoperoxidase for regional comparisons at low power (Ch 2, §4.2). To physically preserve the fragile slices, tissue from P0 and P7 animals was mounted on subbed glass slides prior to immunohistochemistry, whereas the more robust P14 and P21 sections were processed free-floating and mounted after staining; comparisons using both methods for tissue at each age indicated that labelling was similar for both, although somewhat enhanced for free-floating sections due to greater surface availability. Sections were mounted serially to provide an overview of marker distributions at each age.

3 Results

3.1 General observations

In general, subcortical structures and allocortical regions exhibited adult patterns of neurochemical distribution earliest, along with some transient labelling not observed in adult material, with the perirhinal-entorhinal strip at the ventrolateral edge of sections and the hypothalamus and amygdala regions frequently labelled before appreciable neocortical labelling became apparent.

Identification of subcortical structures at early ages was subject to uncertainty, owing to the changes in relative placement of structures which occur during development. Where such structures were relatively unambiguous, their names have been given. Since these studies focused on the neocortex, and on differences between regions whose SMI32 labelling differs from one another (Chapter 3), most emphasis has been placed on observations in these areas.

3.2 Immunoperoxidase labelling

3.2.1 SMI32 labelling

The emergence of SMI32 labelling in the developing rat cortex is exemplified by the comparison sections in figure 6.1 and the higher power comparison sections in figures 6.2, 6.3, 6.4 and 6.5.

P0: The developmental expression of SMI32-recognisable neurofilament epitopes was first evident in subcortical structures such as the dorsal endopiriform nucleus and the intercollicular nucleus of the midbrain, both of which contained labelled neurons of a multipolar morphology on the day of birth. In addition to these cells, some hippocampal layers and several tracts in the thalamus and hypothalamus were labelled, particularly the habenula (Figure 6.1, P0).

P7: At P7, the perikaryon and proximal dendrites of many pyramidal cells in layer V of many rostral cortical regions were labelled by SMI32 (Figure 6.3a). Nearly all labelling was confined to the rostral parts of regions which later assume the prevailing "sensory" pattern of SMI32 distribution (Chapter 3), although small labelled cells were visible in rostral RSG and RSA. The dorsal strip and perirhinal regions which in adults are lacking in SMI32 labelling were consistently unlabelled in these and older preparations. Occipital cortical regions remained unlabelled at P7, although hippocampal regions of the same sections exhibited labelled cells, and many midbrain structures had strongly labelled neurons. Smaller cells of a less defined morphology in layer III and larger, multipolar cells in layer VIa were also

Figure 6.1

Representative sections showing the emergence of SMI32 labelling in the developing rat cortex. Note increased thalamic and cortical immunoreactivity at stages P14 and P21 compared to adult.

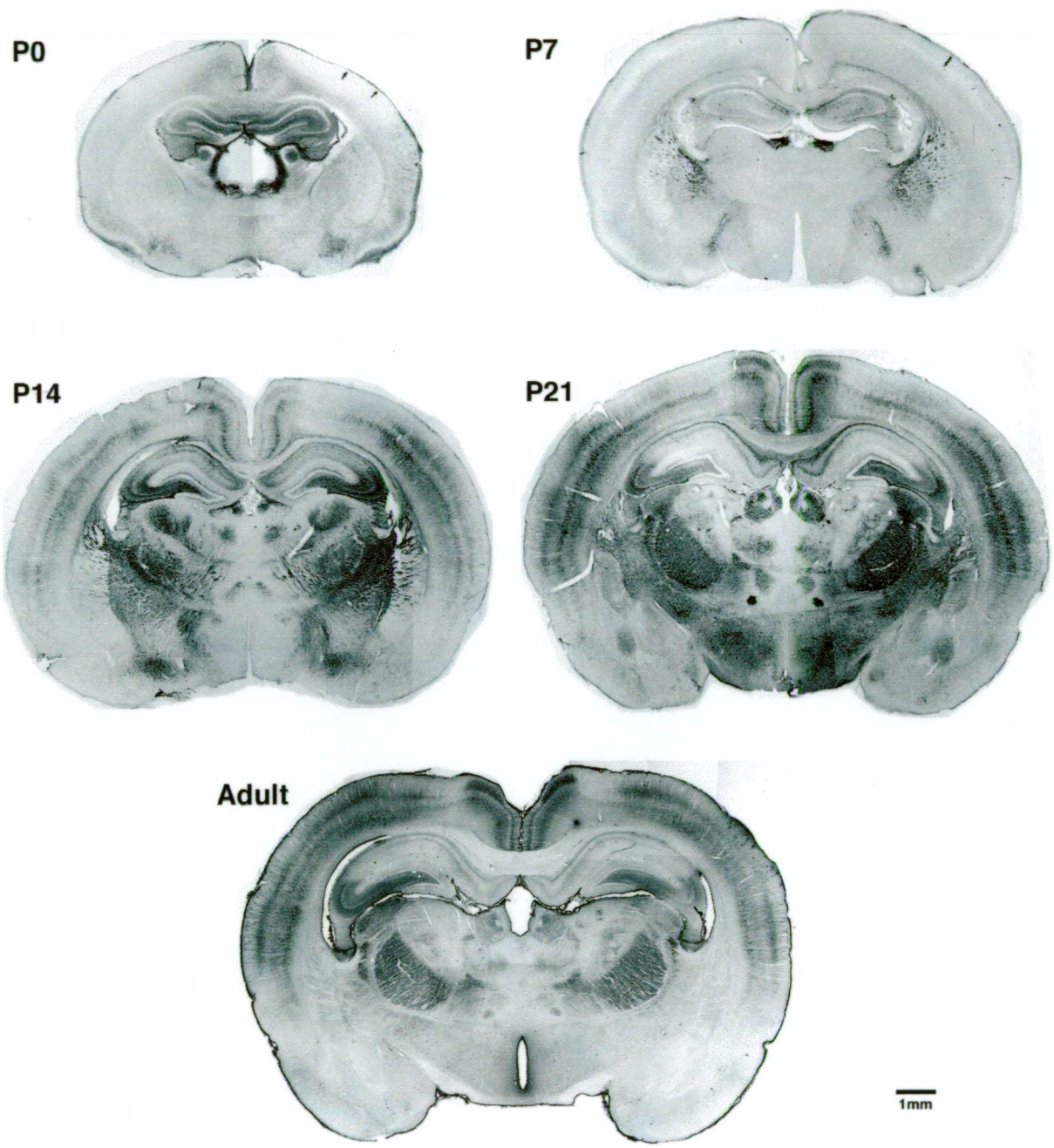
P0
P7
P14
P21
Adult
1mm

Figure 6.2

Comparison of markers in P0 tissue in a region corresponding to bregma – 2.5mm in the adult rat brain; this dorsomedial section of neocortex contains all four of the principal types of SMI32 labelling in the adult cortex.

Scale bar = 1mm for all images.

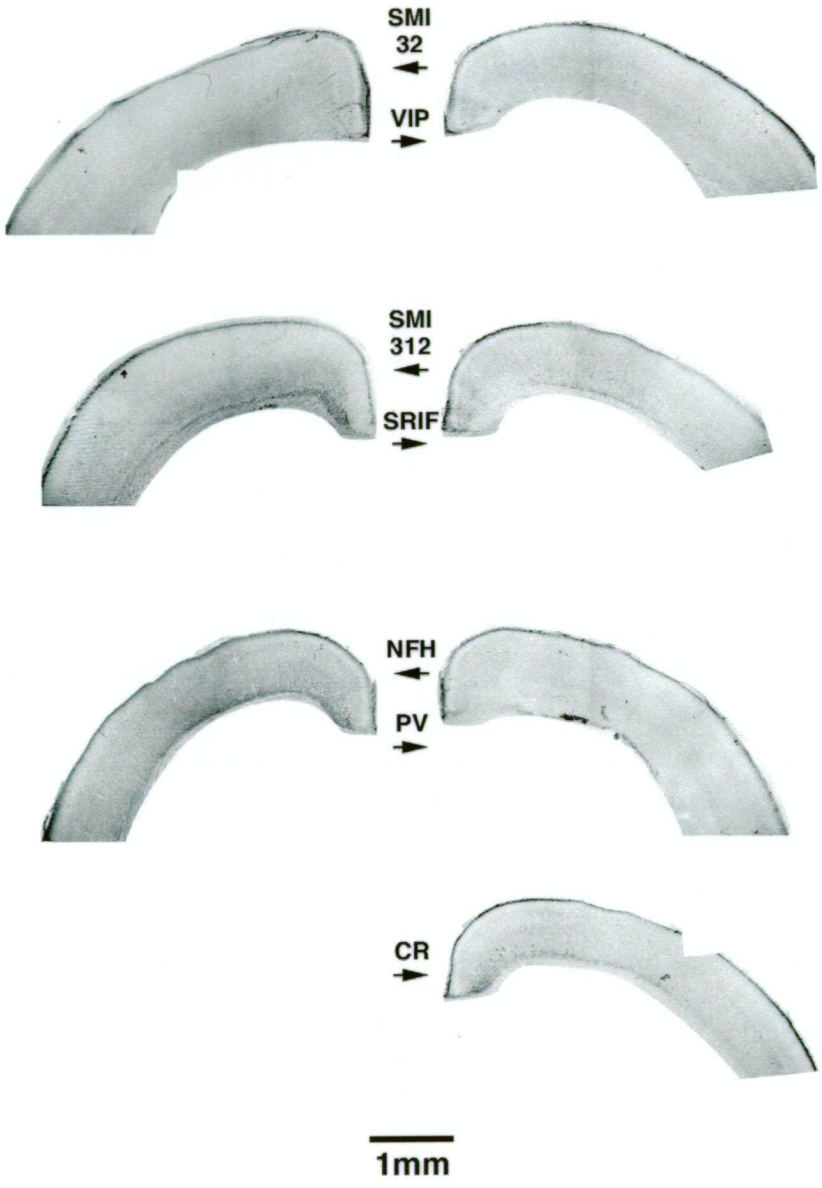
SMI
32
VIP
SMI
312
SRIF
NFH
PV
CR
1mm

Figure 6.3

Comparison of markers in P7 tissue in a region corresponding to bregma – 2.5mm in the adult rat brain; this dorsomedial section of neocortex contains all four of the principal types of SMI32 labelling in the adult cortex.

Scale bar = 1mm for all images.

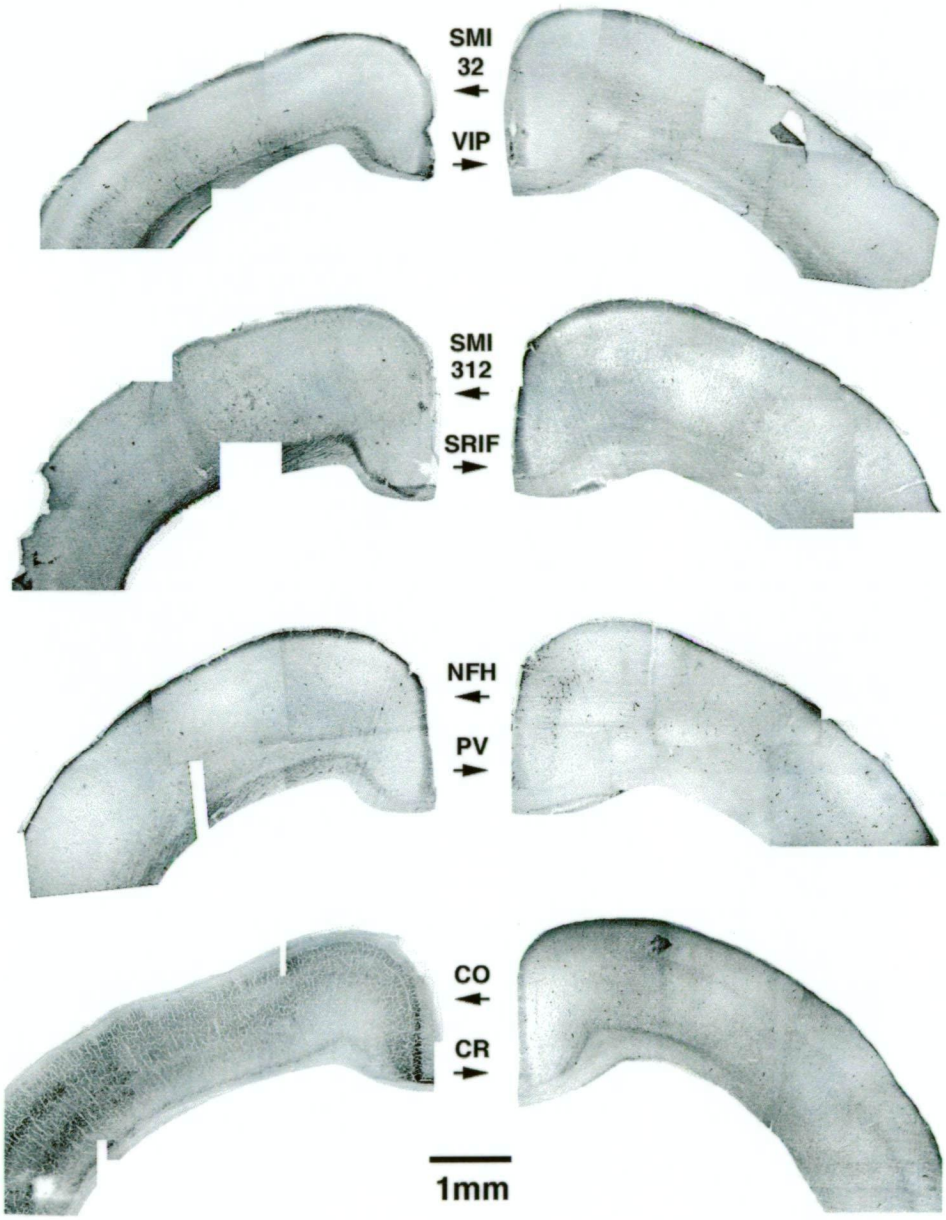
SMI
32
VIP
SMI
312
SRIF
NFH
PV
CO
CR
1mm

Figure 6.4

Comparison of markers in P14 tissue in a region corresponding to bregma – 2.5mm in the adult rat brain; this dorsomedial section of neocortex contains all four of the principal types of SMI32 labelling in the adult cortex.

Scale bar = 1mm for all images.

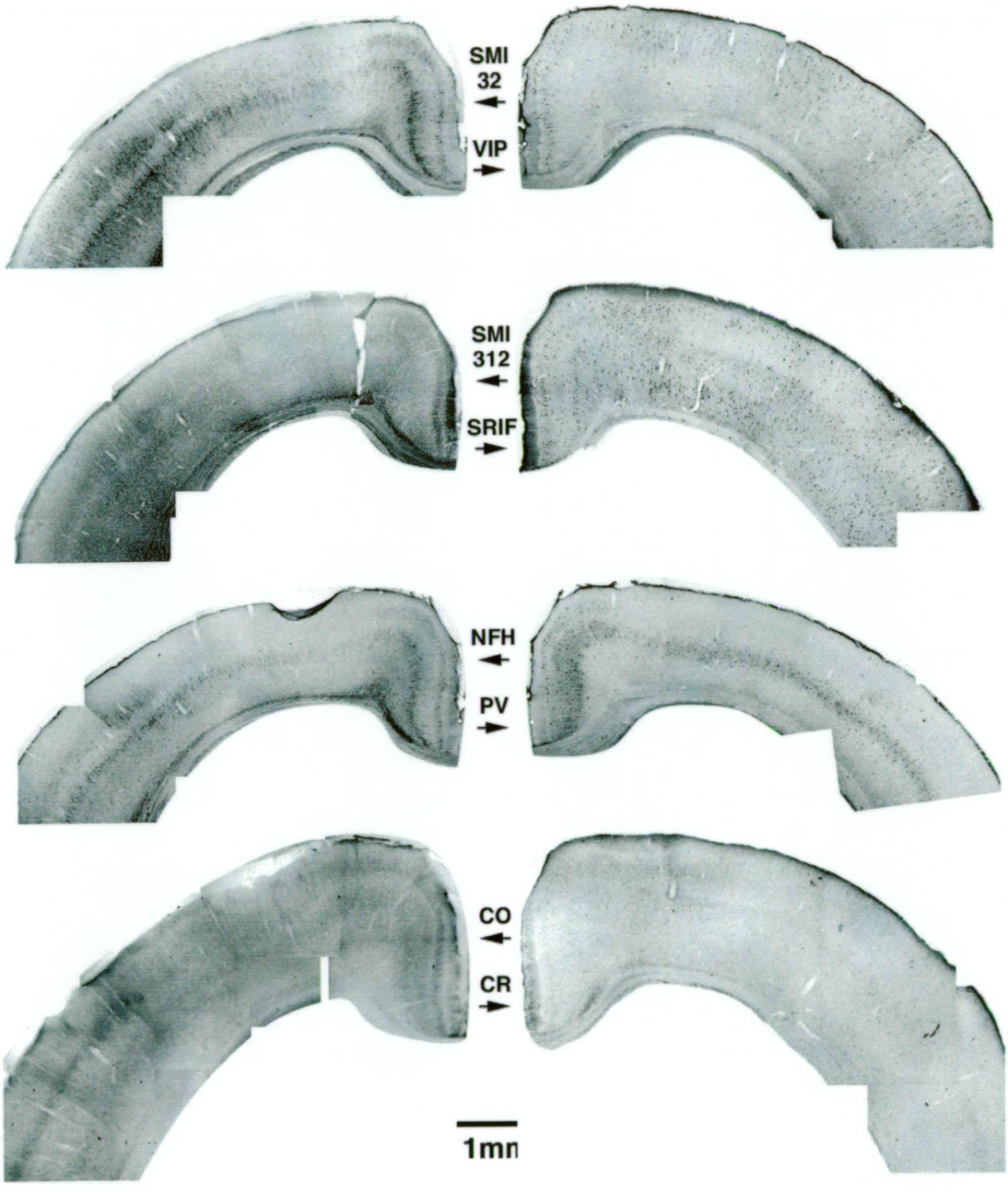
SMI
32
VIP
SMI
312
SRIF
NFH
PV
CO
CR
1mm

Figure 6.5

Comparison of markers in P21 tissue in a region corresponding to bregma – 2.5mm in the adult rat brain; this dorsomedial section of neocortex contains all four of the principal types of SMI32 labelling in the adult cortex.

Scale bar = 1mm for all images.

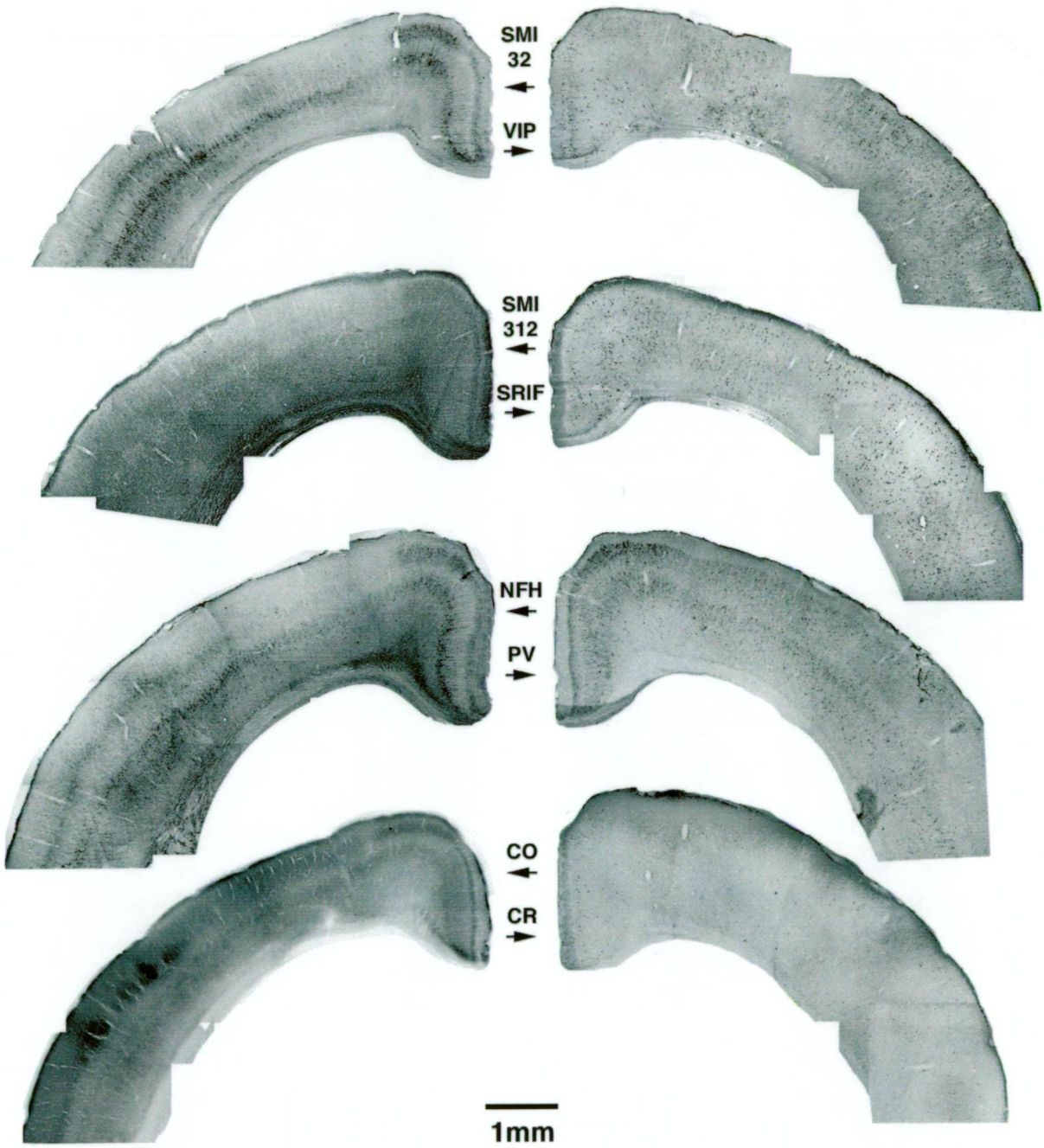
SMI
32
VIP
SMI
312
SRIF
NFH
PV
CO
CR
1mm

usually labelled faintly in regions where the layer V cells were evident. In rostral, dorsal cortical regions, rows of faintly labelled neurons were observed at the transition between cortex and the underlying white matter.

In addition to the labelled tracts seen in the P0 brains, fibres in the lateral olfactory tract and those parts of the external capsule which underlie the labelled cortical regions, together with some of the fibres in bundles passing through the internal capsule, are labelled. Many fine, labelled fibres could be seen descending radially from labelled cortical neurons, and entering the subcortical white matter of the external capsule (Figure 6.1, P7). The dorsal endopiriform nucleus and adjacent nuclei are more extensively labelled. Labelling in processes at this age has a characteristic crenulated appearance at high magnification, with the appearance of flexible filaments or processes pushed and folded into the available space.

P14: At P14 a population of labelled cortical neurons largely absent in adult SMI32 preparations were observed. Small multipolar neurons appeared in layer II of all regions of cortex whose deeper layers contained labelled cells. While lesser in overall density than the labelled cells of layers III, V and VIa, the soma and small dendritic arbours of these cells were stained with a similar intensity. Overall cortical labelling at this age was the most intense of all specimens examined (Figure 6.1, P14).

Although rostral regions were again more labelled than caudal, the layer II, III, V and VIa pyramidal cells of occipital regions were stained at this age. Regions differently labelled in adult cortex (Chapter 3) also differed at this age: the neurofilament-free dorsal strip contrasted with labelling in adjoining regions, and the trilaminar appearance of the "sensory" pattern was evident (Figure 6.4a). The RSA and RSG regions were also distinct, with numerous layer II multipolar cells present at higher density in the RSA region, and at lower density but greater individual size in RSG.

In addition to the cortical labelling described, fibre tracts labelled at P7 were also labelled in P14 material, with the addition of many tracts in the thalamus and midbrain (Figure 6.1, P14). Many subcortical nuclei also exhibited populations of labelled neurons, particularly in the midbrain.

P21: Patterns of SMI32 labelling in P21 brains resembled those at P14, with neuropil labelling less prominent but composed of a greater density of individual processes than at earlier stages. Dendritic labelling, though less intense, was observed to extend considerably further from cell bodies than in P14 specimens, in accordance with the

considerable growth of dendrites during this period (Uylings et al., 1990; Figure 6.5a). In sensory trilaminar regions, the cell bodies and neuropil of layers III and VIa were more strongly labelled, with an overall density similar to that of layer V (Figure 6.5a). The cell bodies of larger pyramidal cells in layer V of trilaminar labelled regions remained the most strongly labelled cortical structures. The distinctive layer II multipolar cells were also still abundant, and the dense layer II neuropil label which characterises the adult RSA region was evident. In the adjoining RSG region, the characteristic elongation of labelled layer V apical dendrites was also evident due to an increase in the thickness of the overlying layer IV; layer V in this region was noticeably deeper than that of the adjoining RSA, which being agranular lacks a large layer IV population (Figure 6.5a). The neurofilament lacking dorsal strip remained free of labelling, except for a few of the layer II multipolar cells.

Descending cortical fibres and tracts such as the external capsule and internal capsule bundles were relatively less labelled than they had been at earlier ages, as were the tracts labelled in the thalamus. Prominent labelling of cell bodies in midbrain nuclei remained, accompanied by a similar growth and reduction of labelling intensity in their proximal processes.

3.2.2 SMI312 labelling

P0: Strong SMI312 labelling of radial cortical fibres and white matter tracts was observed in inner layers of P0 brains at locations corresponding to the SMI32 labelling observed at this age (Figure 6.2c). Cortical labelling was restricted to these fibres, with little differentiation between regions excepting that perirhinal cortex was noticeably more labelled than other regions on the same sections. No labelled cell bodies in cortical or subcortical structures were observed.

P7: SMI312 labelling in P7 specimens resembled that of P0 specimens excepting that the labelled fibres were more numerous in the various tracts, with layers III to VI of most regions filled with labelled fibres contiguous with the underlying white matter of the external capsule (Figure 6.3c). Perirhinal cortex again appeared more densely labelled than other regions, in contrast to the lack of SMI32 labelling in this region at any age. A sparse meshwork of labelled fibres was also observed overlying layer I of much of the neocortex, particularly those regions in which SMI32 labelled cells were observed at this age. Rare, sparsely labelled structures resembling cell bodies were observed in the rostral portions of the dorsal endopiriform nucleus. SMI312 labelling in processes had a crenulated appearance like that of SMI32 labelling at this age.

P14: At P14 the distribution of labelled cortical fibres became denser in layers III and V/VIa where SMI32 labelled cells were observed (Figure 6.4c). Few if any SMI312 labelled processes were observed in the regions where the small multipolar cells were visible in SMI32 preparations. Layer I labelled fibres increased in density in those regions observed at P7. Although SMI312 labelling in the dorsal "gap" remained similar to adjacent regions in animals at this age, the previously denser label in perirhinal regions remained static in contrast to increased labelling in adjacent regions, with the effect that its labelling appeared lighter overall. RSG and RSA regions were distinguished by stronger SMI312 labelling in layers III and (IV)/V respectively. No structures resembling cell bodies were labelled at this age.

P21: Labelled sections from P21 animals had a similar appearance to those at P14 with an apparent increase in the number and extent of labelled fibres in regions previously described (Figure 6.5c). The dorsal "gap" labelling appeared diminished in comparison to adjacent M1 and V2ML regions, such that the label in this region remained static while the rest of the cortex increased in intensity, or that labelled processes may have reduced in number or intensity. The meshwork of layer I fibres increased in apparent density. No structures resembling cell bodies were labelled at this age.

3.2.3 NFH labelling

P0: NFH distribution in P0 tissue was extremely restricted, consisting of some fibre tracts underlying the hypothalamus and in the midbrain, and some doubtful labelling in small cells at the transition between layer VIb and white matter in rostral dorsal cortical regions (Figure 6.2e).

P7: At P7, NFH labelling was sparsely evident in fibres of the external capsule and bundles passing through the internal capsule, the habenula and ventral posterolateral thalamus, subhypothalamic tracts, the anterior commissure, the septum and the dorsal endopiriform nucleus. Cell bodies exhibited small labelled patches in the latter structure and in layer V of cortical regions corresponding to the SMI32 labelling seen at this age (Figure 6.3e).

P14: By P14 the intracellular layer V labelling was more evident in similar regions, and apparent in layer III neurons of these areas (Figure 6.4e). This intracellular labelling was more dispersed than at P7, and extended into the dendrites of labelled cells. Other aspects of NFH labelling appeared similar to P7 material; again, occipital

cortical regions were more sparsely labelled than more rostral areas. Intensely labelled cells were observed in several midbrain nuclei near the periaqueductal grey.

P21: At P21, labelled layer V neurons were more intense and markedly more labelled than those of layer III in neurofilament-containing regions (Figure 6.5e). The dorsal "gap" remained devoid of NFH labelling; RSG cortex exhibited densely labelled somata in layer V, which were less dense in the adjoining RSA region. A concentration of NFH labelled processes was evident in layer II of the latter region, which was much more pronounced than anywhere else in the cortex. The small layer II multipolar cells evident in SMI32 labelling were also present, though their labelling was largely restricted to a small perinuclear region.

In general, NFH labelling resembled that made using SMI32, although in the cortex perikaryal labelling was much less defined and dendritic labelling much reduced, and some presumably axonal labelling was observed in addition. At P21, NFH labelling was noticeably less pervasive than for adult material stained using the same antibody.

3.2.4 VIP

P0: Labelling for VIP is very restricted in the P0 rat brain (Figure 6.2b), consisting of lightly immunoreactive cells in the rostral dorsal endopiriform nucleus and the same nuclei adjoining the periaqueductal grey in the midbrain as were labelled using SMI32, and fibres in the medial forebrain bundle and habenula.

P7: P7 sections exhibited essentially the same labelling pattern as those from P0 animals (Figure 6.3b), although individual cells could be discerned in some cortical regions, and possessed the same bipolar morphology as observed in adult brain (Figure 6.6b).

P14: At P14 a widespread labelling of VIP in cortical neurons was evident, with distribution resembling that of adult cortex (Figure 6.4b). Labelled cells appeared bipolar in morphology, and were concentrated particularly in layer II of all cortical regions, with some regional variability to their distribution in other layers; for example, in the dorsal neurofilament-poor regions, VIP labelled cells were confined almost exclusively to layer II, while they were widely distributed in adjacent regions. Few labelled processes were observed from these cells, with the exception of labelled distributions resembling terminal fields in the dorsal endopiriform and several amygdalar nuclei.

P21: P21 labelling resembled that seen at P14 with the addition of many fine, varicose fibres labelled throughout the cortex, often contiguous with the processes of labelled cells (Figure 6.5b). Terminal fields were also observed in the bed nucleus of the stria terminalis.

3.2.5 Somatostatin

P0: SRIF labelling in the P0 material consisted of small granular perinuclear inclusions in a widespread subpopulation of cells throughout the cortex, concentrated around layers IV and V (Figure 6.2d). Again, labelling was widespread and prominent in rostral cortical regions and largely absent occipitally except for the endopiriform cortex; several amygdalar and dorsal endopiriform nuclei also had populations of labelled cells. Labelled cells were more sparsely distributed in the dorsal strip lacking neurofilaments.

P7: Similar labelled populations were observed in the cortex, with labelling extending further into the perikaryon and proximal parts of processes (Figure 6.3d). Fibre patches resembling terminal fields were also observed in hypothalamic nuclei.

P14: Like VIP, labelling for SRIF underwent a dramatic increase in tissue from P14 rats, with clearly greater numbers of cells labelled for SRIF than were labelled for VIP (Figure 6.4d). Labelling remained concentrated in the perikarya of cells, whose morphology ranged from bitufted to multipolar, and which concentrated in layers II, IV and VIa but were also found in all layers from II to VIb, and throughout the cortex. The distribution of these cells appeared homogeneous, without obvious distinction between cortical regions.

P21: The SRIF labelling patterns established by P14 were similar to those observed at P21, with intracellular labelling further filling cortical neurons, and terminal fields appearing denser (Figure 6.5d). SRIF expression in occipital regions resembled that of rostral cortex more closely; SRIF labelling remained most prominent in the perirhinal-entorhinal strip.

3.2.6 Parvalbumin

P0: PV labelling in P0 brains was very restricted (Figure 6.2f), with some cells at the dorsal border of the external capsule weakly labelled, extending somewhat into layer VI of RSG regions, and cell bodies and fibres evident in the ventral posterolateral thalamus.

P7: Weakly labelled cell bodies were observed in layer V of dorsolateral and RSA cortical regions of P7 material (Figure 6.3f), although the latter group abruptly ended

at the border with the M2 "gap" region. Occipital cortical regions exhibited fewer labelled cells than rostral regions, although the hippocampus underlying the former had a population of labelled cells. Few processes were labelled near labelled cells.

P14: PV labelling in P14 cortex produced similar distributions with greater labelling in the adjacent neuropil; lateral cortical regions had greater concentrations of PV labelled cell bodies in layer III (Figure 6.4f), whereas medial regions showed similar concentrations in layer V. In dorsolateral regions these two bands overlapped one another. A strip of cortex along the medial dorsal surface, corresponding to the region lacking SMI32 labelling, exhibited a reduced density of PV-labelled cells and processes (Figure 6.4a,f); PV-IR processes formed a distinct band in layer V of dorsolateral cortex at this age.

P21: Patterns of cortical expression became more even in terms of laminar distribution of cell bodies, though the segregation observed at P14 remained. A band of immunoreactive processes like that seen in layer V at P14 was evident in layer II/III of most neocortex (Figure 6.5f), with some reduction in occipital regions.

3.2.7 Calretinin

P0: At P0, a large subpopulation of CR-labelled cells was evident throughout the cortex (Figure 6.2g). Fibres in various thalamic regions and in bundles passing through the internal capsule were evident. Fewer labelled cells were observed in occipital cortical regions compared to rostral cortex.

P7: At P7, CR labelling appeared to be present in fewer cell bodies, which were predominantly bipolar in morphology and most common in layer II of rostral regions (Figure 6.3g). Some processes extending from these cells were also immunoreactive.

P14: By P14, multipolar neurons resembling Martinotti neurons were labelled, commonly in layer V of cortex. CR-IR cells were evident in layers II-V throughout most of the neocortex (Figure 6.4g); their distribution appeared similar between the various NF regions.

P21: At P21, CR-IR labelled neurons were similarly distributed but apparently more numerous than at P14 (Figure 6.5g).

3.2 Immunofluorescence labelling

Double labelled preparations involving SMI32 and SMI312 combined with the calcium binding protein and peptide antibodies revealed similar distributions of labelled cell bodies and processes at each age. Several observations of the

relationships between these markers were made possible by double labelling comparisons.

VIP and somatostatin were not associated with neurofilament immunoreactivity in cell bodies or processes (Figure 6.6a,b). The transient expression of somatostatin and SMI32 labelled cells in the dorsal endopiriform nucleus involves different populations (Figure 6.6a) and little association between their processes is evident.

The transient SMI32 labelling of layer II small multipolar cells was shown to be accompanied by some degree of PV immunolabelling in nearly all such cells observed at P21 (Figure 6.6c) and at P14. In other cortical layers, PV labelled neurons were predominantly labelled with SMI32 as well; their processes formed pericellular baskets around SMI32 labelled and non-labelled cells alike, indicating no specific relationship between neurofilament content in pyramidal cells and basket cell innervation.

3.3 Histochemistry

3.3.1 Cytochrome oxidase

P0: Sections of P0 animals were not successfully reacted for cytochrome oxidase (CO) histochemistry; the shorter fixation times of this method made the collection of usable sections problematic, and the use of longer fixation to circumvent this difficulty resulted in severe impairment of the cytochrome oxidation reaction.

P7: CO activity observed in P0 brains was concentrated in cortical layers III and V in regions where SMI32 labelling was observed at this age; medial and lateral to these areas, CO activity was less defined except in layers II and III of RSA and RSG (Figure 6.3g).

P14: At P14, increases in the density of reaction product were observed in the middle layers (III and IV) of somatosensory regions of the cortex (Figure 6.4g). Non-SMI32-labelled regions appeared similar in overall staining density to adjacent regions, although RSA and RSG labelling remained distinct from that of other cortex.

P21: By P21 clear differences in CO histochemistry were evident between regions of different neurofilament expression patterns. In trilaminar cortex, layers III and IV were markedly more intense in some restricted patterns corresponding to mystacial barrels (Nie & Wong-Riley, 1995). The neurofilament gap region exhibited noticeably less staining than adjacent regions, and the RSA and RSG cortex also

Figure 6.6

False colour composites of double-labelled immunofluorescence preparations at various stages of development, illustrating the relationships between neurofilament and various chemical markers.

a) SRIF (red) and SMI32 (green) in the rostral dorsal endopiriform nucleus of a P0 rat. Note complete segregation of the two labelled populations.

b) VIP (red) and SMI312 (green) in layer V of the M1 cortex of a P0 rat. Note granular VIP labelling in this typical bipolar cell, and the absence of neurofilament labelling.

c) PV (red) and SMI32 (green) in layer II of the M1 cortex of a P21 rat. Note the small stellate cells of this layer characteristic of cortical labelling at P14 and P21 (arrowheads). All observed were also PV immunolabelled.

d) PV (red) and SMI32 (green) in layer III of the S1 cortex of a P21 rat. PV labelled cells, many also labelled by SMI32 (double arrowheads) give rise to pericellular terminal baskets around SMI32 labelled cells (arrowhead) and non-SMI32-labelled cells (arrows).

Scale bar = 50μm in all images.

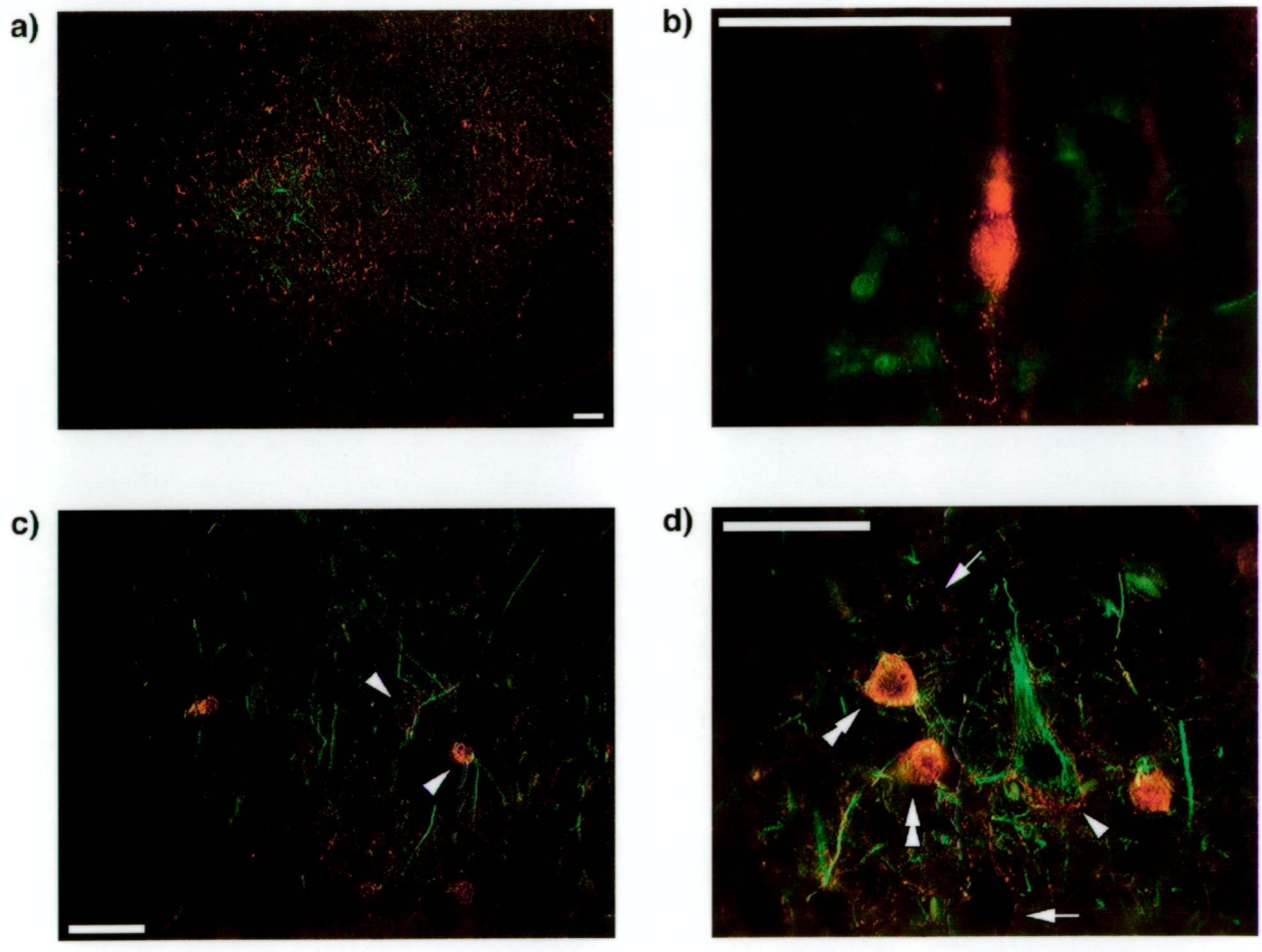
a)
b)
c)
d)

exhibited bands of more intense staining in layers II and V respectively (Figure 6.5g).

4 Discussion

Observations of SMI32 labelling during the first three weeks of postnatal development reveal that the NF makeup of the cells and axons of the brain remains significantly different to adult distribution at P21, unlike any of the other markers used for comparison. Although cortical labelling is essentially like that of adults, with the exception of the small multipolar neurons labelled in layer II, the labelling of subcortical tracts and nuclei remains much more extensive (Figure 6.1). Since myelination is occurring in these structures at the same time (Uylings et al., 1990), this may indicate that axonal accumulations labelled at P21 are later phosphorylated in their interactions with myelin layers (see Chapter 5), after which they would no longer be recognised by SMI32. The significance of the transient population in the dorsal endopiriform nucleus is unknown, but resembles the distinct, transient SRIF labelling observed in the same region.

The changing populations of the various chemical phenotypes surveyed permit some insights to the differences between regions exhibiting different neurofilament distributions. SMI32, SMI312 and NFH labelling followed a consistent pattern in the cortical regions surveyed, with distinct patterns of labelling in RSA, RSG and sensory cortical regions, and a dearth of labelled processes and perikarya in the dorsal NF-poor "gap" strip seen in adult SMI32 labelling (Chapter 3). The dearth of SMI312 labelled processes in this region may reflect an absence of NF-containing efferent axons, leaving a small population of labelled afferents, or may indicate a general inhibition of NF accumulation in this region. These phenomena indicate that perikaryal NF accumulation in cortical neurons is strongly regulated by their environment, which in turn is likely to be determined by thalamocortical innervation (O'Leary & Koester, 1993). The relationship may be as simple as receptor-mediated expression or phosphorylation changes, or may involve other mediators (see below).

The distribution of other markers indicates that phenotypic differences between these cortical types stems from more general influences on cellular differentiation. PV-IR cells, for example, have a restricted distribution in regions where pyramidal cells lack significant SMI32 labelling, despite the lack of an apparent specific relationship between these two phenotypes elsewhere in the cortex (but see Akil & Lewis, 1992). The predominance of SMI32 colocalisation in PV-IR basket cells of layers III and V is good indirect evidence for a link between SMI32 labelling and

axonal myelination, since these cells are unique among GABAergic populations in having myelinated axons (DeFelipe, Hendry, & Jones, 1986), and apparently represent the bulk of non-pyramidal cells labelled by SMI32. Interestingly, the layer II subpopulation of neurons labelled for both markers (Figure 6.6c) remains relatively constant between regions differing in overall SMI32 labelling; the fate of such cells is unclear, although small multipolar cells labelled with SMI32 are occasionally observed in layer II of many adult cortical regions and may be the same population; small basket cells in layer II of cat cortex have been reported (Jones & Hendry, 1984; White, 1989). The restricted, perinuclear extent of labelling in these adult forms suggests that they persist and reduce their NF content, similar to the low-label subpopulation among cells of the "gap" region (Chapter 3).

The factors reducing NF expression in the gap region appear to have different effects on other phenotypic populations. The early proliferation of somatostatin labelled cells appears ubiquitous, for example, whereas the distribution of VIP-IR cell bodies is restricted to layer II of this dorsal strip (Figure 6.4 exhibits these phenomena most clearly). The activity of cytochrome oxidase is also reduced where NF content is reduced, which may reflect the high metabolic cost of NF production (Lee & Cleveland, 1996) or simply a lower overall rate of energy production in these areas. The emergence of this differentiation over the same timescale as NF differentiation, and the congruence of SMI32 labelling bands in RSA and RSG with dense cytochrome oxidase activity, indicates an association between NF accumulation and mitochondrial activity. Since the activity of cytochrome oxidase rich regions is largely confined to GABAergic neurons (Nie & Wong-Riley, 1995), which (with the possible exception of basket cells) are not the principal NF producing cells of the cortex, it is likely that this association is the product of an underlying factor influencing several neuronal types.

An interesting possibility of this type is presented by the study of Pesold and coworkers (1999), who examined the continued expression of the developmental guidance factor Reelin in adult rat brains. Reelin, secreted by Cajal-Retzius neurons of layer I during embryonic development, is a major factor in the guidance of migrating neurons from the ventricular zone to their cortical destinations (Rakic & Caviness, 1995). However, Reelin is also secreted into the extracellular matrix by a population of GABAergic neurons in adult cortex, and may act as a regulator of gene transcription in nearby cells by means of a pathway employing the signalling protein Dab1 (Pesold et al., 1999). Although Reelin has not been associated with the expression of neurofilaments, it is interesting to note that neurons containing Dab1

are nearly all pyramidal, (though not all pyramidal cells contain it; Impagnatiello et al., 1998; Pesold et al., 1999) and that pyramidal cells exhibit few known chemical phenotypic differences other than NF content. In the cerebellum, the cells expressing Dab1 are the neurofilament-rich Purkinje cells (Pesold et al., 1999). Many of the cells which secrete Reelin in the post-embryonic brain are labelled by antibodies to somatostatin (Pesold et al., 1999), the only marker in this study whose distribution remains essentially similar between the different cortical types.

No direct evidence linking Reelin pathways to the expression of the chemical markers surveyed in this study has been published. However, the covariance of differences in their distributions does suggest the possibility of regional differences in the cortical environment which may trigger changes in the differentiation of cortical neurons during development, leading to the observed variations. The connectional, morphological and electrophysiological properties associated with these phenotypes would lead to distinct differences in the activity of these regions, and combined with different expressions of extracellular guidance factors, these different population compositions would perhaps be sufficient for most cortical differentiation and specialisation. Such hypotheses also require the identification of the driving forces behind such changes, which developmental neurobiology has demonstrated must lie in a balance between the intrinsic properties of the developing cortex and the properties of subcortical afferents which seek it out (Chapter 1, §3.3).

5 Summary

The expression of SMI32-labelled NF epitopes (and cellular NFH) in the developing rat cortex shares regionally heterogeneous regulatory factors with the PV-IR and perhaps VIP-IR phenotypes, but not the SRIF-IR phenotype. This suggests that extrinsic factors may regulate the expression of SMI32-recognised NF epitopes. Significant colocalisation of PV and SMI32 in cortical basket cells is strong indirect evidence that SMI32 labelling identifies the cortical population whose axons are myelinated.

Chapter 7

Neurochemical phenotypes *in vitro*

1 Introduction

Primary cultures of embryonic rat cortical neurons permit the investigation of neuronal morphology and the distribution of cellular markers under specific conditions, in which cortical afferents and often glial cells are absent. At sufficient dispersal, the morphology of entire neurons can be examined in ways which are impractical in the dense neuropil of the cortex. In addition to these simplifications, differences between phenomena observed *in vitro* and *in vivo* permit evaluation of endogenous and exogenous factors in neuronal differentiation, and assess the suitability of generalising culture-based studies to *in vivo* conditions.

The developmental regional correlations observed between SMI32 labelling and PV-IR phenotype expression, and to a lesser extent VIP localisation, suggest shared regulatory factors which presumably derive from thalamocortical afferents (Chapter 1, §3.3). Observation of these phenotypes during the development of isolated cortical cultures can indicate whether this relationship is one of regulated or induced expression. The close relationship between myelination and axonal neurofilaments discussed in Chapter 5 may also be illuminated by studying NF expression in the absence of glia.

For this study, the peptide markers VIP and SRIF, and the calcium binding protein markers PV and CR characterised by Kawaguchi and Kubota (1997) were chosen for investigation. In rat cortex, VIP and CR are nearly always found in the same GABAergic neurons, while SRIF and PV identify two further groups of GABAergic cells (Gonchar & Burkhalter, 1997; Gabbott et al., 1997), all with distinct morphologies and electrophysiological properties (Kubota, Hattori, & Yui, 1994; Kawaguchi & Kubota, 1997). Antibodies for phosphorylated (SMI312) and nonphosphorylated (SMI32) large NF subunits, along with MAP-2, were used as a second label to examine their relationship to the peptide and CBP markers.

Most of these markers have been described in primary cortical or hippocampal cultures raised under various conditions. VIP in cultured neurons has been observed to increase over a similar time course to that seen in cortical development, peaking at 15-20 days *in vitro* (DIV) compared to P14 in the juvenile rat cortex (Lorenzo et al., 1989; Emson & Hunt, 1991); however, Götz and Bolz (1994) found that VIP

expression in their dissociated cultures was exceedingly rare, and postulated that the more intact cortical environment of slice culture was necessary for its expression. SRIF appears in subpopulations of cultured cortical GABAergic neurons with small somata, and usually bipolar or multipolar neurite fields (Dichter & Delfs, 1981; Jordan & Thomas, 1987; Alho et al., 1988). Within these cells, differing post-translational products of SRIF are observed around the nucleus and in the cell body and neurites (Naus & Durand, 1990). Studies blocking endogenous VIP secretion (de los Frailes et al., 1991) and adding VIP to the culture medium (Tapia-Arancibia & Reichlin, 1985) suggest that the SRIF accumulation and secretion of cultured cells is probably stimulated by VIP.

PV-IR labelling has been studied in cortical cell cultures (Hartley et al., 1996; Weiss et al., 1990), and CR and its regulation by growth factors have been described in cortical culture (Lavdas et al., 1997; Pappas & Parnavelas, 1998; Fiumelli et al., 2000). CR has been suggested to exert a protective role in cultured cortical neurons exposed to calcium overloads and toxic levels of glutamate (Lukas & Jones, 1994).

MAP-2 localises to the soma and dendrites of all neurons (Mandlekow & Mandlekow, 1995; de Lima, Merten, & Voight, 1997), and is used to differentiate neurons from other cell types in culture (e.g. de Lima & Voight, 1997; Benson et al., 1996; Steinschneider et al., 1996). Neurofilaments have also been examined in cultures derived from rat hippocampus (Shaw, Banker, & Weber, 1985; Benson et al., 1996), superior cervical ganglion (Wang et al., 2000), cerebellum (Asahara et al., 1999) and neocortex (Riederer, Monnet-Tschudi, & Honegger, 1992; Steinschneider et al., 1996; de Lima, Merten, & Voight, 1997; Ha, Robertson, & Weiss, 1998). In hippocampal neurons, NFL and NFM appear soon after axonal outgrowth, and are joined by NFH some days later; all are found throughout the cell body and processes, though the phosphorylated forms of NFM and NFH are much more concentrated in the axon (Shaw, Banker, & Weber, 1985; Benson et al., 1996), as they are in cortical neurons (de Lima, Merten, & Voight, 1997). Neurofilament proteins are similarly detectable in cortical neurons at a timepoint corresponding to E19, with subunits following a similar sequence in conjunction with electrophysiological maturation (Steinschneider et al., 1996) and dependent on medium or glial factors (Riederer, Monnet-Tschudi, & Honegger, 1992). A subpopulation of cortical cultured neurons labelled with SMI32 (Ch 3) has also been described, whose survival may depend on cholinergic innervation (Ha, Robertson, & Weiss, 1998).

The study described in this chapter set out to examine the expression of these chemical phenotypes under culture conditions, and to characterise the relationships

between SMI32-labelled cells and well-characterised chemical subpopulations. Neuronal cultures of E18 rat cortical cells grown in serum-free media were used; four time points for fixing and labelling neurons were chosen to coincide with the developmental stages examined *in vivo* in Chapter 6. Since cultures were prepared from E18 cortex, the postnatal stages P0, P7, P14 and P21 correspond to 3, 10, 17 and 24 DIV.

2 Procedures

2.1 Cultures

2.1.1 Source

Pregnant rats were killed on the eighteenth day of gestation by placing them in a chamber of CO_2 gas. Rat foetuses were removed and dissected in a sterile environment; the outer cortical layers were removed and placed in 10mM HEPES (N-2-hydroxyethyl piperazine-N-2-ethane sulphonic acid; BDH Chemicals, Kilsyth 3137, Australia) buffer at 37°C.

2.1.2 Dissociation

Cortical tissue was placed in 4.5ml of 10mM filter-sterilised HEPES at 37°C, to which 0.5ml of 0.25% trypsin (BDH Chemicals) was added. After 20 minutes incubation, the HEPES-trypsin liquid was drawn off and replaced with 5ml of fresh 10mM HEPES and allowed to stand for five minutes. Two more such washes were performed, and the tissue was then sucked back and forth in a pipette to further dissociate cells. The proportion of viable cells was then assessed using trypan blue (Sigma) exclusion and counting in a haemocytometer.

Neurons were grown on nitric acid-etched glass coverslips (Fisherbrand Microscope Cover Glasses; Fisher Scientific, Pittsburgh PA; one hour immersion in 69% nitric acid), previously coated by immersion in poly-l-lysine ($10mg.ml^{-1}$ in borate buffer).

2.1.3 Plating, media and maintenance

The initial medium for dissociated cells comprised Neurobasal™ (Life Technologies, Gibco BRL, Grand Island NY 14072, USA) to which was added 10% foetal calf serum (Commonwealth Serum Laboratories), 2% supplement B-27 (Life Technologies; Brewer 1995;1997), 1% gentamicin (David Bull Laboratories, Faulding) and L-glutamine (Life Technologies) and glutamate (Life Technologies) to make 0.5 mM and 25μm concentrations respectively. This initial medium was filter

sterilised and 2ml was added to a lysine-coated coverslip in each well of a 12-well sterile tray. Enough cell suspension to ensure 4.5×10^5 cells per coverslip was then added to each well and the trays were then placed in an incubation cabinet (Imbros) at 37°C in an atmosphere with 5% CO_2 added.

Subsequent changes of medium (replacing half the volume of each well with fresh medium every 3-4 days) used Neurobasal™ supplemented with 2% supplement B-27 (Brewer, 1995; 1997), 0.5 mM glutamine and 3% gentamicin.

2.1.4 Fixation

Cells were fixed using 4% paraformaldehyde in phosphate buffer, previously warmed to 37°C. Growth medium was replaced with the fixation solution and incubated for 30 minutes at 37°C, followed by three ten-minute washes in PBS.

2.2 Immunocytochemical series

Five sets of twelve coverslips were obtained at each of three, ten, seventeen and twenty-four days in culture; each set at a given age was derived from a separate animal. The fixed coverslips were processed for fluorescent immunocytochemistry using all combinations of the three mouse monoclonal antibodies (SMI32, SMI312 and MAP-2) and the four rabbit polyclonal antibodies (VIP, SRIF, PV and CR; Ch 2, §4.1). Some sets of coverslips at each age were processed for single-antibody immunoperoxidase labelling (Ch 2, §4.2), and some were labelled using other combinations of neurofilament and MAP-2 antibodies.

3 Results

3.1 General observations

Most cultures survived and developed for the twenty-four day examination period, though a buildup of irregular flocculent material which stained non-specifically was apparent in several cultures. Cells adhered to the etched, lysine-coated glass and drew together into clumps ranging in population between three and several hundred (estimated) neurons; at seventeen and twenty-four days, larger ball-like cellular aggregates measuring 200-300μm in diameter were observed. Isolated cells were also observed, but only one culture exhibited a large proportion of non-aggregated in its early stages.

The Neurobasal™-B27 medium is formulated to promote the survival of neurons alone (Brewer et al., 1993; Brewer, 1995; 1997), and the presumed lack of glial cells in these circumstances makes them fundamentally different to conditions

Figure 7.1

Appearance of primary cortical cultures at (a) 3, (b) 10, (c) 17 and (d) 24 days *in vitro*. Brightfield light micrographs using Nomarski optics.

Scale bar = 100μm in all images.

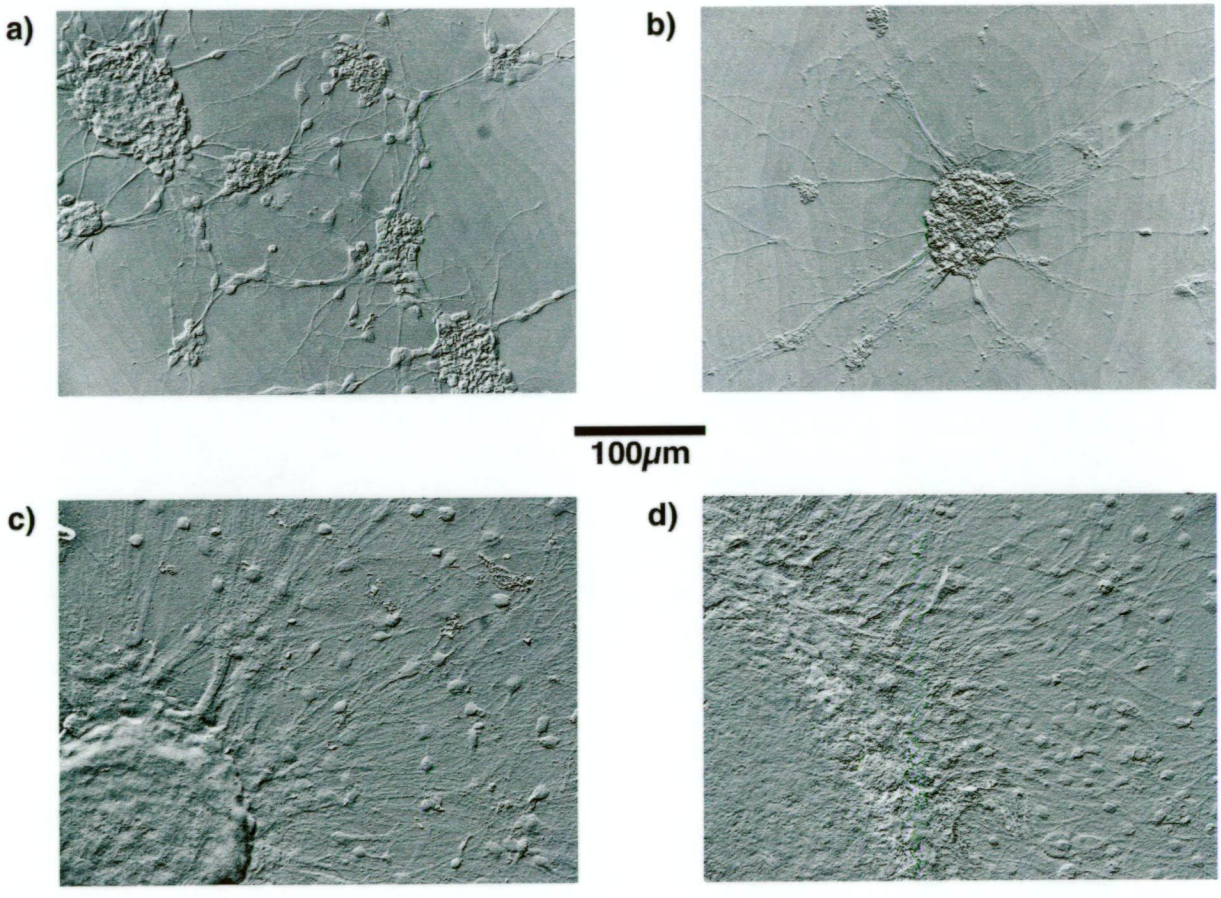
a)
b)
100μm
c)
d)

in the developing cortex. However, several cultures exhibited another cell type with a markedly different appearance to neurons, being flattened and irregular in outline with no neurite-like thin processes. Other, large cells with long processes were occasionally visible in older preparations, and were not labelled by any of the antibodies used.

3.2 Structural proteins

3.2.1 Neurofilaments: SMI32 labelling

SMI32, a monoclonal antibody directed against dephosphorylated epitopes of the NF-M and NF-H subunits of the neurofilament triplet (Chapter 3; King et al., 2000), did not label any structures or cells in all the 3, 10 and 17 DIV cultures (Figure 7.2a). Identical dilutions from the same aliquots labelled many structures in juvenile rat brain sections of comparable developmental stages to the cultures (Ch 6, §3.2.1).

In 24 DIV cultures, single SMI32-labelled neurons were observed in clusters of unlabelled cells, usually with a pyramid-like morphology (Figure 7.2a, 24 DIV), often on the surface of cellular clusters but occasionally in isolation. Although most neurites were dendritic in appearance, many SMI32 labelled neurons exhibited one or two clearly labelled, smooth, non-branching and curving processes extending to adjacent cellular groupings. SMI32 labelling was also observed to colocalise with PV labelling in most of these cells (Figure 7.5e).

3.2.2 Neurofilaments: SMI312 labelling

As in the developing cortex, SMI312 labelling of neurites is widespread by culture day three (equivalent to the day of birth) and thereafter (Figure 7.2b). Occasionally the nuclei of all cells were quite strongly labelled by the SMI312 antibody, but this phenomenon was only observed in two cultures at days three and ten. Although isolated neurons were rarely observed, most but not all exhibited one process more strongly labelled by SMI312 than the others; some isolated cells lacked SMI312 labelling altogether. As the cultures developed and neurites grew, the overall proportion of neurites labelled by SMI312 was visibly reduced (cf. labelling for NFH in Figure 7.5b). SMI312-labelled processes were typically smoothly curved and were torturous in form, excepting those connecting cellular aggregates, which were more linear. SMI312-labelled structures were threadlike in appearance, of a uniform width and smoothly curving; at higher powers, short processes could be observed extending perpendicularly from SMI312-labelled neurites, which were weakly labelled by SMI312 but more strongly labelled by other antibodies (e.g. VIP and SRIF). Aside

Figure 7.2

Cultured neurons at four timepoints, labelled using antibodies for (a) non-phosphorylated NFs (SMI32), (b) phosphorylated NFs (SMI312) and (c) MAP-2, with fluorescent secondary antibodies.

Scale bar = 50μm in all images.

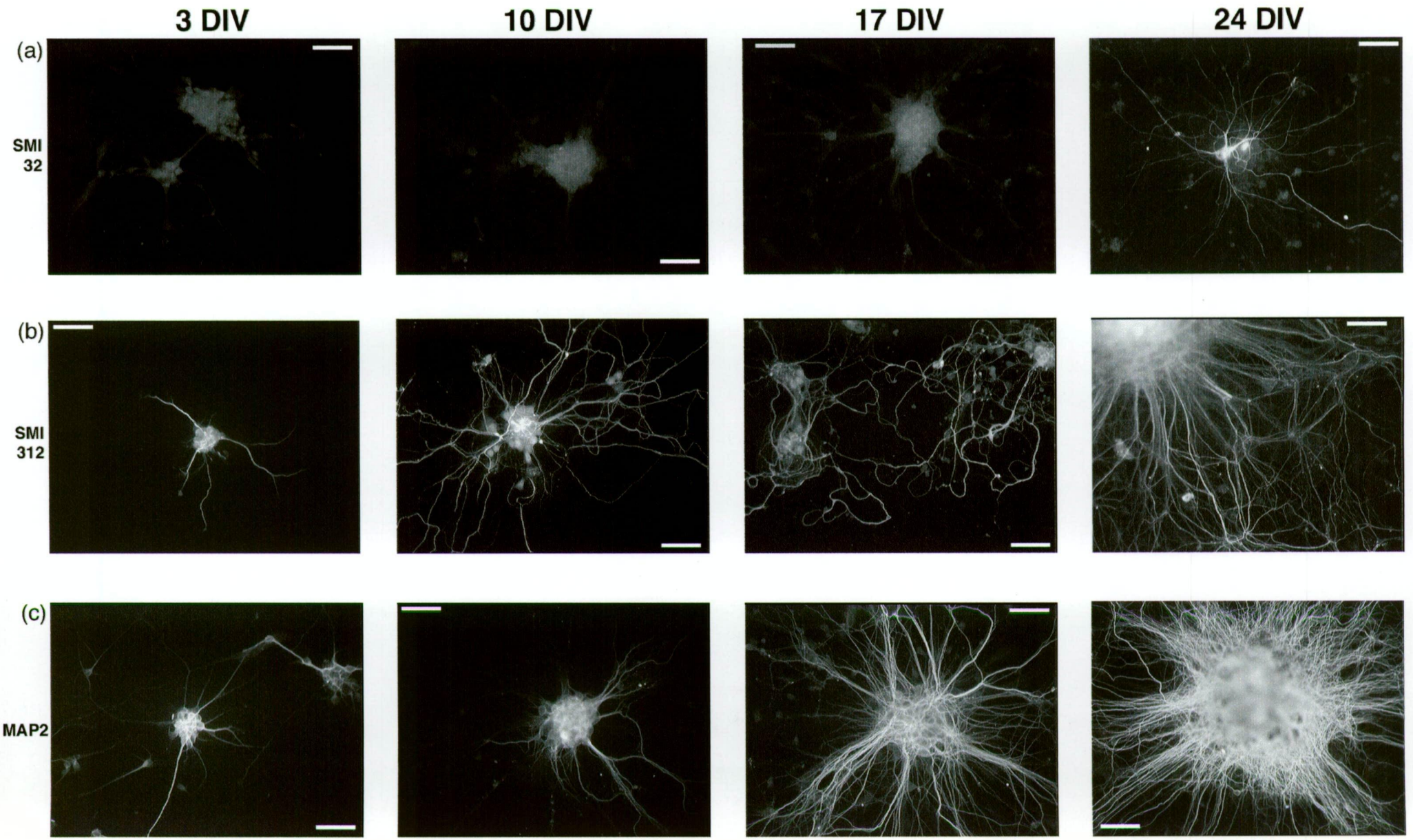
3 DIV
10 DIV
17 DIV
24 DIV
(a)
SMI
32
(b)
SMI
312
(c)
MAP2

from the nuclear label mentioned, no perikaryal SMI312 labelling could be unambiguously identified, although some cells in aggregates appeared to have SMI312-labelled processes running across their perikaryal surfaces. Double labelling with various markers indicated that the SMI312-labelled structures within a given process reached near but not into the distal tip of the process, whose tip was frequently wider and irregular in outline in three and ten day cultures; older cultures had few processes terminating outside cellular aggregates.

Thin linear structures sharply labelled with SMI312 were observed to run within structures whose visible outlines were wider; in some cases, double labelling indicated processes lacking SMI312 labelling intertwined with labelled ones. This was interpreted as a tendency for heterogeneous processes to bundle together along common physical paths, and makes the interpretation of double labelling problematic. For the same reasons it is difficult to judge whether individual labelled processes are branched, or if two closely intertwined processes are divergent; the latter seems to be prevalent among SMI312 labelled processes. In double labelling with peptide markers, SMI312 labelled structures were observed not to run right to the sides of labelled processes, including the short irregular projections from their sides, and fell short of the splayed end structures on extending neurites, which were presumed to be growth cones (Figure 7.5c).

3.2.3 MAP-2

As for SMI312 labelling, the MAP-2 antibody produced widespread labelling in most or all neuron-like cells from culture day three onward (Figure 7.2c). Unlike SMI312 labelling, isolated neurons were labelled in many neurites and the soma, exhibiting a granular texture in the cell bodies of earlier timepoints. At 10, 17 and 24 DIV, MAP-2 labelling remained predominant in the neurites radiating from cellular aggregations, and labelled neurites were more linear and angular than those observed with SMI312 labelling, occasionally exhibiting a "jointed" appearance. The structures actually labelled by the antibody were threadlike as in the case of SMI312, but generally thinner in appearance, although their width varies more than does that of SMI312 labelled structures. Similar embedded and intertwined labelling were observed as for SMI312. At high magnification some MAP2-labelled neurites of ten day and older cultured cells exhibited spike-like perpendicular protrusions at intervals along their length; limitations of resolution meant that it was not possible to determine if they were protrusions from the MAP2-labelled structures of a single

neurite (perhaps dendritic spines), or bundled structures branching repeatedly, although the former is more sensible given the number of protrusions.

3.3 Peptides

3.3.1 VIP

The antibody to VIP labelled a large proportion of cultured neurons from the earliest timepoint onward (Figure 7.3a); proportions within aggregates were difficult to estimate because cells were labelled on their surfaces rather than throughout their volume. In aggregates of cell bodies, diffuse label coated the surfaces of many or most neurons (30–100%, informal estimate), and may have represented extracellular accumulations (Figure 7.5d). This soluble peptide appeared to be uniformly distributed across the soma and some processes of the neurons in which it was detected; even in fine processes, VIP labelling appeared to be restricted to the surface of the process. Small but strongly VIP labelled "knots" were occasionally observed on the surface of labelled neurites, smaller in extent than the nuclei visible in nearby cells.

VIP labelling was not observed to colocalise with SMI32 labelling. VIP labelling in neurites was largely but not exclusively colocalised with SMI312 labelling, and variably associated with MAP2 labelling: short VIP labelled processes were occasionally MAP2 labelled, whereas long ones were not. In general, VIP labelled processes which extended outside aggregates often appeared branched or diverging, and were labelled by SMI312; indeed, most (~80%) SMI312 labelled processes leaving clusters were VIP labelled at 10 DIV. Within clusters, fine, tortuous VIP-labelled processes lacking SMI312 label were observed within the VIP labelling coating cell surfaces. Such observations are probably indicative of cytoskeletal differences between processes with different destinations, rather than differences in antibody penetration, since fine SMI312-labelled processes lacking a VIP label were observed within the aggregates adjacent to VIP-labelled, non-SMI312-labelled neurites. VIP labelling often outlined irregularities of processes which appeared smooth with SMI312 and MAP2 labelling, again possibly due to extracellular accumulations.

Labelling for VIP remained widespread in the plexuses of neurites surrounding cell aggregates in more developed cultures, where small rounded VIP-labelled structures were observed on some VIP-labelled processes. It is possible but unlikely that these structures were the perikarya of a population attached to the

Figure 7.3

Cultured neurons at four timepoints, labelled using antibodies for (a) vasoactive intestinal polypeptide (VIP) and (b) somatostatin (SRIF), with fluorescent secondary antibodies.

Scale bar = 50μm in all images.

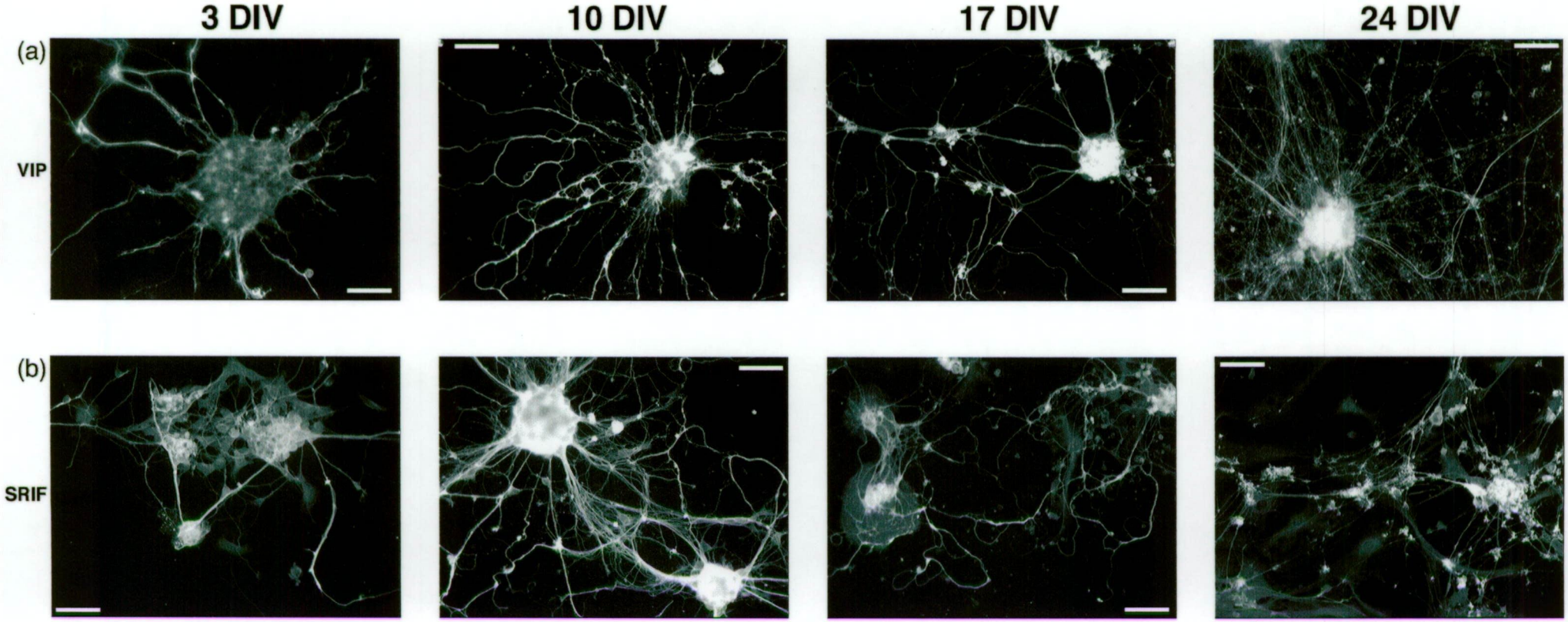
3 DIV
10 DIV
17 DIV
24 DIV
(a)
VIP
(b)
SRIF

Figure 7.4

Cultured neurons at four timepoints, labelled using antibodies for (a) parvalbumin (PV) and (b) calretinin (CR), with fluorescent secondary antibodies.

Scale bar = 50μm in all images.

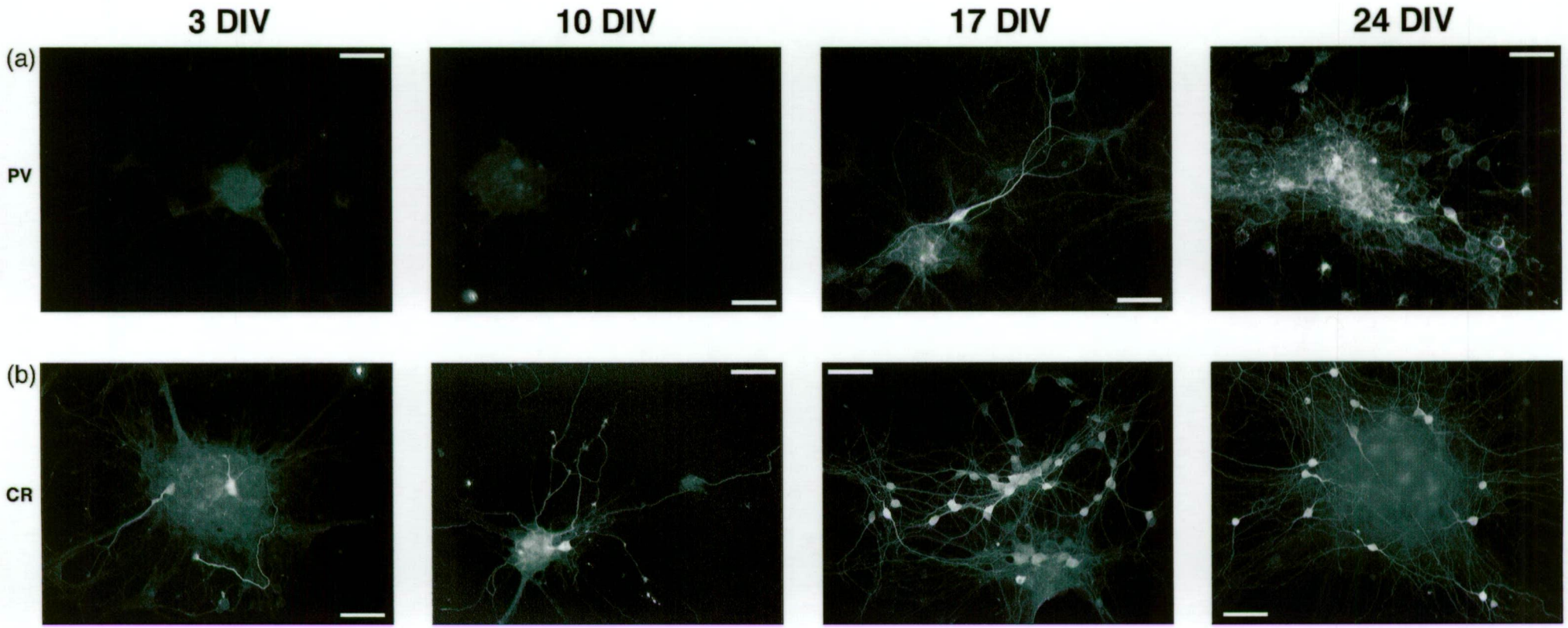
3 DIV
10 DIV
17 DIV
24 DIV
(a)
PV
(b)
CR

Figure 7.5

Examples of double labelling between markers in neuronal cultures. False colour superimposed images, in which red indicates labelling with Alexa 594 conjugated anti-rabbit secondaries recognising rabbit primary antibody binding, and green represents Alexa 488 conjugated secondaries labelling mouse monoclonal antibody binding.

a) NFH (red) and MAP-2 (green) labelling in a cluster of 24 DIV neurons. Note complete segregation of labelling between processes.

b) NFH (red) and MAP-2 (green) labelling in a cluster of 24 DIV neurons. Note relative predominance of MAP-2 labelling in processes radiating from the cluster.

c) SRIF (red) and SMI312 (green) labelling in a 3 DIV neuron. SMI312 does not completely label the area outlined by SRIF labelling.

d) VIP (red) and MAP-2 (green) labelling in a group of 24 DIV neurons. VIP labelling fills the space between cells labelled with MAP-2.

e) Pair of greyscale images showing PV (left) and SMI32 (right) immunolabelling in the same 24 DIV neuron.

f) Pair of greyscale images showing PV (left) and MAP-2 (right) immunolabelling in 17 DIV neurons. PV labels several cells of irregular morphology, which are not labelled by MAP-2.

g) CR (red) and MAP-2 (green) labelling in 17 DIV bipolar-type CR-labelled neurons, at the periphery of a large cellular aggregation.

h) CR (red) and SMI312 (green) labelling showing a 24 DIV multipolar-type CR-labelled neuron, whose processes are in close apposition to SMI312 labelled neurites.

Scale bar = 20μm in all images.

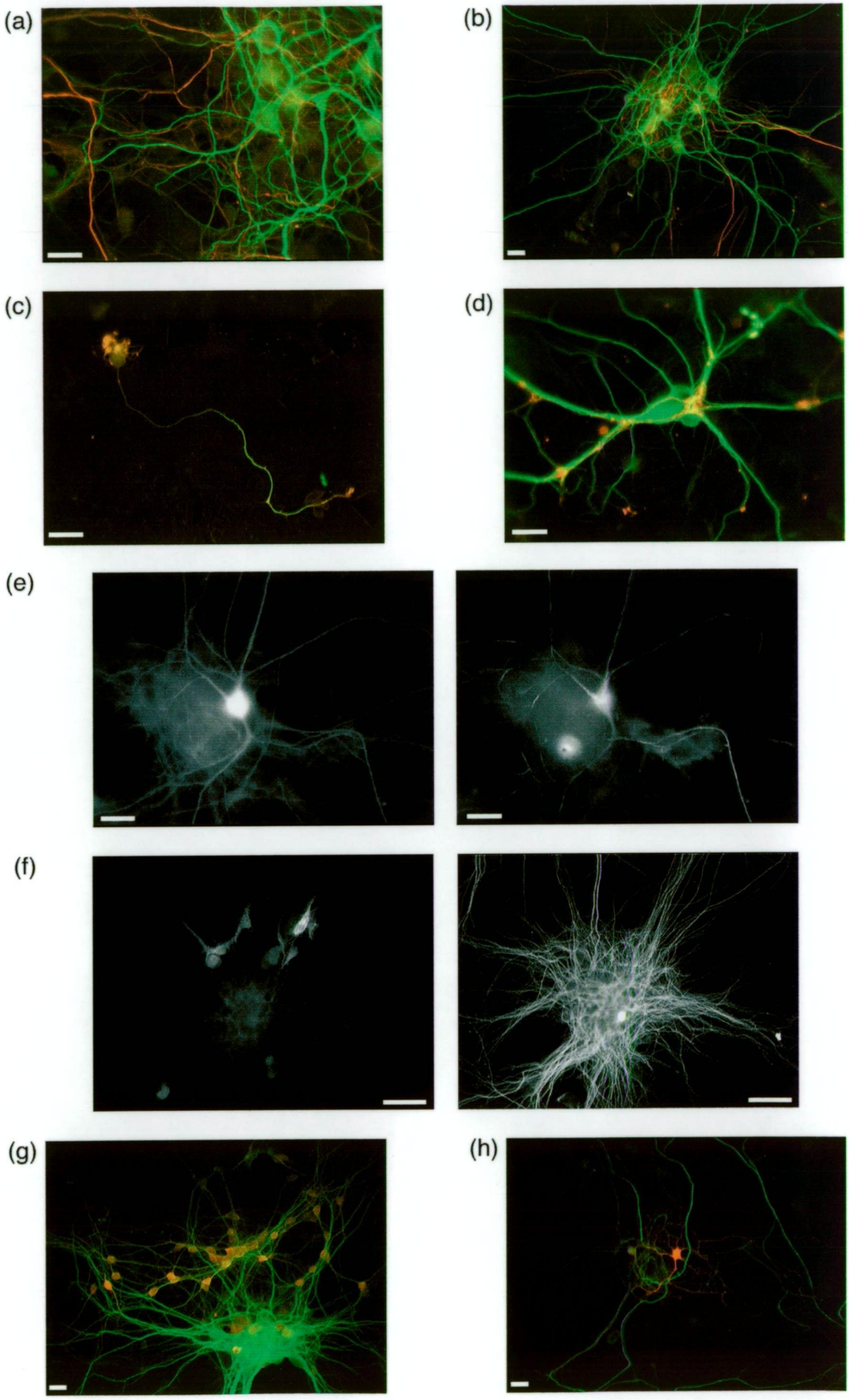
(a)
(b)
(c)
(d)
(e)
(f)
(g)
(h)

periphery of the large aggregates; such structures were seldom observed in or directly on the aggregates, but appear to be too small to contain a typical neuronal nucleus. Occasional isolated neurons were observed both with and without VIP antibody labelling. Aside from these structures, no characteristic morphology of other VIP-labelled neurons was apparent.

3.3.2 Somatostatin

Like VIP, immunocytochemical labelling for SRIF was widespread from culture day three onward (Figure 7.3b); in some three day cultures, faintly labelled cells of a flattened morphology without processes were observed. SRIF labelling was clearest in neurites labelled with SMI312, sometimes with MAP-2, and changed little during development, although labelled processes appeared less predominant in more developed cultures, and SRIF-IR was observed in the fringes around extending processes at early timepoints. Like VIP labelling, SRIF-IR processes had irregular edges, perhaps indicating that these peptides localised to the surfaces of processes more than cytoskeletal elements (Figure 7.5c).

Somatostatin labelling resembled VIP labelling in extent, predominance and colocalisation with structural proteins; however, the same antibodies label different populations in sections from juvenile rat brains, and the other rabbit polyclonal antibodies exhibit different patterns. Although SRIF and VIP antibodies both labelled cell surfaces in accumulations, diffuse internal SRIF labelling of cell somata was also observed. These perikaryally labelled cells comprised between 5 and 30% of the cells in different aggregates (estimated). At 17 and 24 DIV, clearly SRIF labelled processes were common, whereas somatic labelling usually appeared diffuse, with an occasional strongly labelled cell (Figure 7.3b, 24 DIV).

3.4 Calcium binding proteins

3.4.1 Parvalbumin

No neurons were clearly labelled by the PV antibody at 3 and 10 DIV (equivalent to P0 and P7), although diffuse labelling could be observed in a few cell bodies at 10 DIV. On day seventeen, isolated PV-IR neurons were clearly evident in several cultures, with fine granular labelling distributed throughout the soma and neurites. By 24 DIV, many neurons labelled for PV were evident throughout the cultures. Many, though not all, PV-IR neurons exhibited a bipolar or bitufted morphology. Occasional PV-labelled cells were observed which were not labelled by MAP-2 or NF antibodies, and lacked neuron-like processes (Figure 7.5f).

PV labelling was often observed on the surface of cells adjacent to the processes of cells whose entire soma was labelled. These cell bodies appeared to be surrounded by PV-IR terminals rather than labelled within their cytoplasm. PV labelling was often observed in the rare 24 DIV cells labelled with SMI32. PV-IR processes were occasionally labelled by SMI312, or ran in close parallel with SMI312 labelled processes; PV labelling did not extend into the MAP2 defined spiky processes on some cells. Frequently, fine SMI312-labelled processes were observed running over the surface of PV labelled cells.

3.4.2 Calretinin

Calretinin antibodies labelled under five percent of neurons from day three onward. Labelled neurons observed at days three and ten had a bipolar or multipolar appearance and were strongly labelled throughout the soma and processes; at day seventeen, most cultures exhibited a second type of CR-labelled cell, characterised by a small, smooth cell body, MAP2 labelling on processes, and an overall bipolar morphology (Figure 7.5g). This subgroup appeared in concentrations of cells on some culture preparations, in addition to the larger multipolar labelled neurons, and added to the overall proportion of CR-labelled cells in the culture. These groups differed in the appearance of their neurites, with multipolar cells exhibiting large fields of jointed and knotted processes (Figure 7.5h), whereas bipolar cell neurites were less branched and more uniform in thickness. Bipolar cells were also commonly observed on the fringes of large clusters, whereas the multipolar cells were usually isolated or had few neighbours.

CR labelling was not observed to colocalise with SMI32 labelling. Labelled processes extending from aggregates were sometimes labelled by SMI312 or bundled with such processes, and were distinct from those labelled by MAP2. Isolated CR-labelled cells were occasionally observed with numerous MAP2-labelled processes and a single, thin and torturous CR-labelled process not labelled by MAP2. CR-labelled knots, like those observed in VIP labelling, were observed on the plexus of processes radiating from cellular aggregates.

4 Discussion

Purely neuronal cultures of cortical neurons are a relatively recent technique (Brewer, 1995; 1997) and are likely to exhibit significant differences from cultures in which glia survive. For instance, the interaction between axonal neurofilaments and glia (Riederer, Monnet-Tschudi, & Honegger, 1992; Ch 1, §4.4.3) is disrupted, and

Neurobasal™ has only 5mM of the 30mM K^+ concentration (Brewer et al., 1993) which Riederer and colleagues used to restore NFM and NFH levels to those expressed by cells cocultured with glia. However, neurofilament expression in these cultures was much greater than is found in the cortex, with essentially all neurons observed having axons labelled by SMI312 (Fig 7.2b) and other neurofilament antibodies (Figures 7.5a, 7.5b, 3.2).

The larger aggregates observed in later cultures (Figure 7.1) may be the result of increased volumes of neuronal processes; however, their markedly greater numbers of cell bodies suggest that smaller aggregates coalesce under elastic forces which must be mediated by the processes joining them; processes running between aggregates are more linear which may be the result of tension (Figure 7.2). These elastic forces also shape the developing cortex *in vivo* (Katz, 1993).

The important role played by glia in maintaining the extracellular milieu and regulating growth (de Lima, Merten, & Voight, 1997) is only partially replaced by regular changes of medium. Within the cellular agglomerations, local environments are free to take on characteristics which would never occur *in vivo*; concomitant effects on the growth, development and connections of nearby neurons remain to be characterised. For example, as many as 40% of cells from E19 embryos have not committed to glutamatergic or GABAergic phenotypes (Götz & Bolz, 1994) and thus differentiate in the absence of glia and extrinsic afferents in these cultures.

Much of the labelling observed in these cultures reflects phenomena already well characterised in cortical and hippocampal cultures with and without glia, such as the somatodendritic localisation of MAP-2 (de Lima, Merten, & Voight, 1997; Benson et al., 1996) and the axonal localisation of phosphorylated medium and heavy neurofilament (Shaw, Banker, & Weber, 1985; Benson et al., 1996; de Lima, Merten, & Voight, 1997). The complete segregation of MAP-2 and NFH in dendrites and axons respectively (Shaw, Banker, & Weber, 1985) and the predominance of dendrites among processes extending from large aggregations are apparent in Figures 7.5a and 7.5b.

However, many differences from *in vivo* development are readily apparent. VIP and CR are nearly completely colocalised in cortical neurons *in vivo* (Gabbott et al., 1997; Kubota, Hattori, & Yui, 1994; Gonchar & Burkhalter, 1997) but the groups of cells labelled by CR and VIP antibodies in these cultures are clearly different in morphology and distribution. Since these VIP/CR neurons have distinct electrophysiological properties *in vivo*, it would be interesting to determine whether such properties are associated with one marker rather than the other, or whether the

two groups seen in culture differ from those in intact cortex. The morphologies of *in vitro* CR-labelled neurons (resembling the large and small GABAergic groups of de Lima & Voight, 1997) are much more similar to the VIP/CR group *in vivo* than those of the VIP-labelled group, suggesting that CR is more closely tied to morphology than VIP. The use of rabbit polyclonal antibodies to label both markers prevented colocalisation studies.

Indeed, the contrast between the near-complete absence of VIP labelling in dispersed cortical cultures described by Götz and Bolz (1994) and the widespread labelling observed in 3 and 10 DIV cultures in this study suggests that VIP expression is highly dependent on culture conditions. The observed shift from intracellular labelling to diffuse surface labelling with some strongly labelled processes suggests that VIP is expressed in response to conditions encountered by neurons early in the culture process (perhaps in the initial medium) but that expression is downregulated as cultures age. Much of the later VIP labelling appears on the interfaces between cells, suggesting a surface distribution or extracellular accumulations (Figure 7.5d). VIP in later cultures is also extensively labelled in what appears to be detritus throughout the processes radiating from cellular agglomerations (Figure 7.3a, 17 and 24 DIV) and in small bulbs attached to the fibre plexus, reminiscent of those observed by Rothman and Cowan (1981). The monolayer of astrocytes supporting the cultures made by Götz and Bolz (1994) may have maintained the culture environment in such a way that VIP expression was not triggered.

SRIF immunolabelling resembled the populations of cells observed *in vivo* (Ch 6) but was more prevalent at 3 and 10 DIV than for P0 and P7. If VIP does indeed promote SRIF secretion in cultured cells (de los Frailes et al., 1991; Tapia-Arancibia & Reichlin, 1985), the unusually high level of VIP expression in the cultures may well have contributed to this increase.

Of the peptide and CBP markers, PV labelling most closely followed the pattern of developmental expression observed *in vivo*, appearing at 17 DIV (corresponding to P14) in neurons whose prevalence and morphology was similar to those in the developing cortex (Ch 6). PV labelled neurons also gave rise to processes which enveloped the somata of non-PV-labelled neurons, in a manner similar to the basket cells of the intact cortex (Figure 7.4a, 24 DIV).

In contrast to the expected patterns observed with SMI312 labelling, the early absence of SMI32 labelling in these resembles the reduction observed by Ha, Robertson and Weiss (1998) when basal forebrain cholinergic neurons were removed

from their co-cultures, and is difficult to reconcile with descriptions of perikaryal NF distributions observed in Chapter 3 and by others (Steinschneider et al., 1996; Benson et al., 1996). Since antibodies to phosphorylated neurofilaments (§3.2.2) and neurofilament subunits NF-M and NF-H (Ch 3, §3.1.1) labelled structures in cultures from the same sources, it must be concluded that the epitopes recognised by SMI32 are not formed in purely neuronal cultures at these stages. In terms of the studies of Chapters 3 and 4, the absence of SMI32-labelled perikarya in cultures whose axons clearly contain neurofilaments suggest that this antibody does not always label neurons whose axons have neurofilaments, as was suggested in Chapter 4. It is instead possible that SMI32 labels neurons which process neurofilaments differently, and that axonal neurofilaments are more ubiquitous than is suggested by the subset of perikarya labelled by SMI32 and the subunit antibodies.

Two other unusual phenomena were observed in the SMI32-labelled cells which eventually appeared at 24 DIV (Figure 7.2a, 24 DIV). The long SMI32-labelled processes extending between cellular aggregates had the appearance of axons (Figure 7.2a, 24 DIV, lower right), perhaps corresponding to SMI32 labelling in cortical white matter observed *in vivo* (Vickers et al., 1994). The lack of myelinating glial cells may have caused a reduction of neurofilament phosphorylation in these axons (see de Waegh, Lee, & Brady, 1992). Alternatively, these cells may represent a very small subpopulation of axonally SMI32-labelled cells normally present in cortex, whose neurofilament expression remained undisturbed in culture conditions, while the normal SMI32-labelled population were absent or changed their cytoskeletal makeup in response to the culture environment. A large proportion of these unusual neurons were also PV-IR (Figure 7.5e) in a similar association to that observed in cortical basket cells *in vivo* (Chapter 6).

A recent study of glutamate-induced NF phosphorylation in cultured P7 cerebellar granule cells (Asahara et al., 1999) goes some way toward explaining these anomalies. These researchers found that the addition of 10μM glutamate to glutamate-free culture medium had a profound effect on the phosphorylation of neurofilaments, such that immunoblotting with SMI32 showed a 70% decrease in labelling by the third day in culture. Although the cultures in this study derived from embryonic neocortex, it is plausible that the 25μM glutamate component of the medium had a similar effect, altering the SMI32-detectable dephosphorylated NFH and NFM filament expression to a more phosphorylated form. Indeed, 25μM glutamate is near neurotoxic levels according to the dose-response curve derived by Asahara and coworkers (1999) for cerebellar granule cells. Furthermore, their

investigation of the glutamate receptors involved suggested that this excessive phosphorylation was mediated by intracellular calcium release, which may also explain why PV-labelled cells were predominant among the SMI32 labelled cells eventually detected. If so, the subsequent regulation of calcium by this calcium binding protein may have enabled the maintenance of an SMI32-detectable dephosphorylated state in these neurons' neurofilaments, although PV expression actually enhances excitotoxic vulnerability in some culture conditions (Hartley et al., 1996; Weiss et al., 1990).

From these observations, it is clear that the normal early proliferation and later smaller population of SRIF-labelled interneurons is not sufficient for the expression of SMI32-recognisable neurofilament epitopes in most pyramidal cells. The fact that SMI32 immunoreactivity can be induced in a much larger population by co-culture with basal forebrain cholinergic neurons (Ha, Robertson, & Weiss,1998) suggests that cholinergic afferents, which include thalamocortical fibres, are necessary for the expression of the SMI32 phenotype. It is conceivable that direct cholinoceptive pathways, or an indirect mechanism such as Reelin secretion by a partially SRIF-immunoreactive GABAergic subpopulation, described by Pesold and coworkers (1999), may enable cholinergic afferents to induce the neurochemical phenotype specialisation observed in populations of cortical neurons during normal development.

This development of phenotypes in the absence of thalamocortical afferents suggests that SMI32 labelling is probably an induced phenotype whereas neurofilament expression per se is not; PV labelling is a regulated phenotype because it is regionally specific in development *in vivo,* but labels similar cells in the absence of extrinsic differentiating factors. By the same reasoning, CR and SRIF are probably intrinsically regulated by the cells expressing them, with similarities in the cells exhibiting them *in vivo* and *in vitro*, and in the time course of their expression (CR strongly evident throughout; SRIF plentiful early on but throttled back later). VIP appears to follow a different course in culture to the intact cortex, and different from the dissociated cultures of Götz and Bolz (1994), and may be regulated by factors which are actually present in the culture medium.

5 Summary

Neuronal culture development in the absence of extrinsic regulators and glia indicates that NFs are overexpressed in the absence of glia, but that the epitope recognised by SMI32 is induced in cortical neurons by extrinsic factors, with the

exception a population observed at 24 DIV. Other studies indicate that cholinergic afferents are required for SMI32-recognised epitopes to be expressed in purely neuronal cultures (Ha, Robertson, & Weiss, 1998). This suggests that the phenotype is induced either by direct cholinergic signalling (AChE histochemistry is commonly accompanied by SMI32 labelling in human pyramidal cells; Mesulam & Geula, 1991) or by cholinergic activity on an effector population of neurons which survive in neuronal cultures.

Chapter 8

Concluding discussion

1 Principal findings

The aims set out in Chapter 1 were as follows:

1. To verify that the antibody SMI32 identifies all of the population of cortical neurons expressing perikaryal neurofilaments in the rat cortex.
2. To characterise the distribution of neurofilament labelling in the neuropil and cell bodies of the rat cortex, and to verify the observed proportion of SMI32 labelling among cortical neurons.
3. To investigate whether neurofilament triplet content is correlated with the length of a cell's axonal projection.
4. To study the relationship between axonal properties and their neurofilament content for corticocortical axons.
5. To characterise the developmental appearance of neurofilament in the rat cortex, and to compare it with the emergence of other chemical phenotypes.
6. To study the expression of neurofilaments and other chemical phenotypes in purely neuronal cultures, so that the influences of glia and extrinsic afferents are removed.

These aims were met in the following ways:

1. SMI32 was found to label essentially all cortical neurons whose perikarya were labelled with phosphorylation-independent NF subunit antibodies (Chapter 3). Its epitopes are expressed by a consistent but small subpopulation (10-19%) of cortical neurons, most of which are pyramidal in appearance.
2. Perikaryal and dendritic neurofilament labelling was found in four principal patterns throughout the rat neocortex, which were found in (a) the RSG strip overlying the corpus callosum, which exhibited prominent, long bundled apical dendrites and a dense layer I plexus; (b) the RSA strip adjoining RSG, which exhibited layer V cellular labelling and a dense plexus of labelled processes in layer II; (c) a strip nearly devoid of labelling adjoining the RSA strip along the dorsal surface of the cortex, including the regions M2, MPtA, S1Tr and V2MM, and a similar deficiency in perirhinal regions; and (d) most dorsolateral sensory and motor cortical regions, in which prominently labelled cell bodies and processes were evident in three major bands (layers III, V and VIa) whose relative intensity varied (Chapter 3). This segregation of labelling patterns offers

a different cortical parcellation to those of standard cytoarchitectonics (e.g. Zilles, 1985; Paxinos & Watson, 1998; Paxinos et al., 1998).

3. The proportion of projection neurons containing the neurofilament triplet was not significantly correlated with the length of their projection; instead, it varied more significantly with the target of that projection (Chapter 4). This finding is similar to proportions observed in monkey and primate cortical projections (e.g. Campbell & Morrison, 1990; Campbell, Hof, & Morrison, 1991; Hof, Nimchinsky, & Morrison, 1995; Hof et al., 1996).
4. Axonal neurofilaments examined ultrastructurally exhibited similar correlations with myelination and axon cross-section to those observed in peripheral nerves (e.g. Szaro, Whitnall, & Gainer, 1990). Myelinated axons alone exhibited semi-regularly spaced NFs packed throughout their internal area; numbers of neurofilaments were strongly linearly correlated with axonal cross-sectional area, and moderately well correlated with myelin thickness (Chapter 5). It appears likely that axon bearing neurofilaments attract myelination and that the neurofilaments may be modified by that myelin (Starr et al., 1996).
5. The developmental emergence of the neurofilament triplet followed the patterns observed in Chapter 3 from the outset, with the addition of a population of small multipolar neurons in layer II labelled strongly at P14 and P21, but not in adult material. Among other neurochemical phenotypes, PV labelling most clearly exhibited similar developmental regulation to the SMI32 phenotype, and the two markers were extensively colocalised in basket cells of layers III, V and possibly II (Chapter 6), offering strong indirect evidence that SMI32 labelling identifies the cortical population whose axons are myelinated. The VIP-IR phenotype appeared to vary somewhat between regions with different neurofilament architecture, but SRIF-IR phenotype did not. This suggests that extrinsic factors may regulate the expression of SMI32-recognised NF epitopes.
6. Axonal neurofilaments were abundant in cultures without glia, but the SMI32 phenotype was observed only in isolated and morphologically unusual neurons after 24 DIV; the latter cells frequently contained PV. SRIF, PV and CR phenotypes appeared little affected by the lack of extrinsic afferents and glia (Chapter 7). The absence of perikaryal dephosphorylated neurofilaments in almost all neurons expressing neurofilaments suggests that the epitope recognised by SMI32 is induced in cortical neurons by extrinsic factors. Other studies indicate that cholinergic afferents are required for SMI32-recognised epitopes to be expressed in purely neuronal cultures (Ha, Robertson, & Weiss,

1998). This suggests that the phenotype is induced either by direct cholinergic signalling (AChE histochemistry is commonly accompanied by SMI32 labelling in human pyramidal cells; Mesulam & Geula, 1991) or by cholinergic activity on an effector population of neurons which survive in neuronal cultures.

2 Summary of implications

The neurofilament triplet protein occurs at immunohistochemically detectable levels in only 10-19% of neurons in the rat cortex, and a similar proportion in other mammal species; other neurons are likely to use α-internexin or other neuronal intermediate filaments (Lee & Cleveland, 1996). This differential use of triplet proteins, whose core filament part is largely homologous with other neuronal intermediate filaments (Lee & Cleveland, 1996) but whose C-terminal regions are far larger and capable of extreme phosphorylation (Pant & Veeranna, 1995), is highly suggestive of specific functional properties required only by a subpopulation of neurons. In Chapter 3, the distribution and specific proportions of these cells using the neurofilament triplet in the rat cortex was characterised on a regional basis. Its differential distribution patterns imply differing needs for these functions, with sensory and motor regions exhibiting either extensive dendritic neurofilaments or none at all.

The strong ultrastructural associations between axons' neurofilament content and their calibre and myelination, extended by this thesis to corticocortical axons for the first time, suggest that one role of the neurofilament triplet is to chemically interact with myelin in axon formation. The dearth of axonal intermediate filaments in the non-myelinated 80% of callosal axons (Gravel, Sasseville, & Hawkes, 1990), combined with studies of filament and myelin knockout mice reviewed in Chapter 5, suggest that the presence of neurofilaments in the axons of the triplet-containing subpopulation allows them to become myelinated during development. The near-uniform density of neurofilaments observed across a wide range of cross sectional areas in Chapter 5 suggests that filament spacing, which can be altered by a variety of intracellular mechanisms (Leterrier et al., 1996), is carefully regulated by processes which probably involve chemical interaction with the myelin sheath (argued in Chapter 5). Virtually all non-pyramidal cells expressing perikaryal neurofilaments were revealed by double labelling in the developing cortex (Chapter 6) as PV-IR basket cells, whose axonal myelination (DeFelipe, Jones, & Hendry, 1986) is similarly unique among GABAergic neurons, and is further indirect evidence for a link between neurofilament triplet expression and axonal myelination.

Neurons cultured in the absence of glia and extrinsic afferents differ from those in the cortex in that they nearly all express NFs in their axons (Chapters 3 and 7). Whether these elevated proportions of NF expression reflect an absence of glial regulation, expression-promoting factors in the culture medium, or differential survival of neurons expressing the neurofilament triplet remains unanswered, although similar labelling patterns of other neurochemical markers not associated with NF labelling *in vivo* argues against differential survival. This widespread NF expression was also abnormal in that the *in vivo* segregation of phosphorylated NFs in axons from dephosphorylated NFs in the perikaryon and dendrites (Lee et al., 1988) was not observed. The rarity of the latter class of filaments, coupled with the observation that cholinergic afferents can restore the *in vivo* pattern in cultured cells (Ha, Robertson, & Weiss, 1998), suggest that NFs are prevented from phosphorylating by extrinsic cholinergic afferents in the developing cortex, and are then able to fill the cell body and dendrites.

Comparing the onset of neurofilament expression with those of other chemical phenotypes and metabolic indicators in the developing rat cortex suggests that the regional neurofilament patterns are determined from the earliest onset of NF expression, and that these variations are correlated with those of parvalbumin (and VIP to some extent). The strong association between neurofilament labelling and PV immunoreactivity observed in developing cortical neurons may indicate that mechanisms altering cellular neurofilaments also determine the expression of parvalbumin. However, PV-IR neurons in 17 and 24 DIV cultures were frequently observed forming basket-like terminal fields in the absence of perikaryal filament labelling. Of those neurons expressing epitopes recognised by SMI32 at 24 DIV, many were labelled for parvalbumin as well.

Although the findings of this thesis offer no definitive characterisation of the role of cellular neurofilaments, they strongly suggest that the subpopulation of cells which express them have axons which become myelinated due to their NF content, even if they are local inhibitory basket neurons. In corticocortical projections identified ultrastructurally (Chapter 5) and using retrograde tracing (Chapter 4), only a small proportion of axons and cell bodies contain neurofilaments. That proportion varies according to the source and destination of the projection, and the neurofilament-containing neurons are likely to have myelinated axons. Comparison of development *in vitro* and *in vivo* suggest that the proportions of cells expressing the neurofilament triplet, and the post-translational modification of the resultant filaments, are regulated by extrinsic afferents. Regulation of the neurofilament triplet

is probably a principal mechanism in developmental determination of the makeup of cortical connections.

3 Future directions

If neurofilament phosphorylation is regulated by extrinsic afferents, as suggested, then the mechanisms of this modification are worthy of investigation. It has been suggested that GABAergic interneurons secrete differentiating factors like Reelin into the neuropil and alter gene transcription even in adult cortex (Pesold et al., 1999); the population possessing the Disabled-1 receptor has a similar makeup to those with neurofilaments. Such interneurons may be the immediate agent of this kind of differentiation, under the control of cholinergic afferents such as those from the basal forebrain, and those from the thalamus. The fact that the cells thought to be differentiating are mostly pyramidal cells, and that pyramidal cells have few chemically distinguishable phenotypes, makes neurofilament expression a prime candidate for the differentiation being induced in them.

Also relevant in extrinsic regulation of neurofilament configuration is the colocalisation of AChE and neurofilament labelling in human cortical neurons observed by Mesulam and Geula (1991). Receptors for cholinergic extrinsic afferents on neurofilament-containing cells may directly trigger chemical pathways leading to neurofilament dephosphorylation. Labelling and histochemical investigations could distinguish these hypotheses.

The notion that the SMI32 epitope identifies cells whose axons are myelinated could also be directly tested using immunohistochemistry on thick slices followed by intracellular filling of SMI32 labelled cells, followed by further sectioning and immunohistochemistry to test whether those cells' axons are all myelinated. Should it prove to be correct, the ability to identify the proportion of myelinated axons contributing to projections is significant in itself, and may reveal details of cortical projection dynamics (e.g. the proportions observed by Hof et al., 1996, which differ between different visual processing pathways). Plasticity in such proportions (e.g. Siegel et al., 1993) would also gain new significance; sensory deafferentation studies offer a direct model for initial investigation.

Afterthought

Two people sat watching a line of ants travel back and forth. "I wonder where it ends," said one. The other put his hand through the line, saying, "It ends here."

References

Ahmed B, Anderson JC, Douglas RJ, Martin KAC, Nelson JC. Polyneuronal innervation of spiny stellate neurons in cat visual cortex. *Journal of Comparative Neurology* 1994;341(1):39-49.

Ahmed B, Anderson JC, Martin KAC, Nelson JC. Map of the synapses onto layer 4 basket cells of the primary visual cortex of the cat. *Journal of Comparative Neurology* 1997;380(2):230-42.

Akil M, Lewis DA. Differential distribution of parvalbumin-immunoreactive pericellular clusters of terminal boutons in developing and adult monkey neocortex. *Experimental Neurology* 1992;115:239-49.

Alcántara S, de Lecea L, Del Río JA, Ferrer I, Soriano E. Transient colocalisation of parvalbumin and calbindin D28k in the postnatal cerebral cortex: Evidence for a phenotypic shift in developing nonpyramidal neurons. *European Journal of Neuroscience* 1996;8:1329-1339.

Alcántara S, Ferrer I, Soriano E. Postnatal development of parvalbumin and calbindin D28k immunoreactivities in the cerebral cortex of the rat. *Anatomy and Embryology* 1993;188:63-73.

Alfonsi F, Darmon M, Forest N, Paulin D. Intermediate filaments as markers of neuronal differentiation. In Duprat AM, Kato AC, Weber M (eds.) *The Role of Cell Interactions in Early Neurogenesis*. Plenum Publishing Corporation, 1984.

Alho H, Ferrarese C, Vicini S, Vaccarino F. Subsets of GABAergic neurons in dissociated cell cultures of neonatal rat cerebral cortex show co-localization with specific modulator peptides. *Brain Research* 1988;467(2):193-204.

Andersen P, Figenschou Soleng A. A thorny question: How does activity maintain dendritic spines? *Nature Neuroscience* 1999;2(1):5-7.

Ang LC, Munoz DG, Shul D, George DH. SMI-32 immunoreactivity in human striate cortex during postnatal development. *Developmental Brain Research* 1991;61:103-109.

Antonini A, Stryker MP. Rapid remodelling of axonal arbors in the visual cortex. *Science* 1993;260:1819-1821.

Aoki C, Siekevitz P. Ontogenetic changes in the cyclic adenosine 3',5'-monophosphate-stimulatable phosphorylation of cat visual cortex proteins, particularly of microtubule-associated protein 2 (MAP-2): effects of normal and dark rearing and of the exposure to light. *Journal of Neuroscience* 1985;5:92465-83.

Asahara H, Taniwaki T, Ohyagi Y, Yamada T, Kira J. Glutamate enhances phosphorylation of neurofilaments in cerebellar granule cell culture. *Journal of the Neurological Sciences* 1999;171:84–87.

Baimbridge KG, Celio MR, Rogers JH. Calcium-binding proteins in the nervous system. *Trends in Neurosciences* 1992;15(8):303-8.

Bar I, Goffinet AM. Decoding the Reelin signal. *Nature* 1999;399:645-646.

Barinaga M. Dendrites shed their dull image. *Science* 1995;268:200-201.

Bayraktar T, Staiger JF, Acsady L, Cozzari C, Freund TF, Zilles K. Co-localization of vasoactive intestinal polypeptide, gamma-aminobutyric acid and choline acetyltransferase in neocortical interneurons of the adult rat. *Brain Research* 1997;757(2):209-17.

Benson DL, Mandell JW, Shaw G, Banker G. Compartmentalization of alpha-internexin and neurofilament triplet proteins in cultured hippocampal neurons. *Journal of Neurocytology* 1996;25:181-196.

Brady ST, Witt AS, Kirkpatrick LL, de Waegh SM, Readhead C, Tu PH, Lee VM. Formation of compact myelin is required for maturation of the axonal cytoskeleton. *Journal of Neuroscience* 1999;19(17):7278-7288.

Brewer GJ. Isolation and culture of adult rat hippocampal neurons. *Journal of Neuroscience Methods* 1997;71:143-155.

Brewer GJ. Serum-free B27 Neurobasal™ medium supports differentiated growth of neurons from the striatum, substantia nigra, septum, cerebral cortex and dentate gyrus. *Journal of Neuroscience Research* 1995;42:674-683.

Buldyrev SV, Cruz L, Gomez-Isla T, Gomez-Tortosa E, Havlin S, Le R, Stanley HE, Urbanc B, Hyman BT. Description of microcolumnar ensembles in association cortex and their disruption in Alzheimer and Lewy body dementias. *Proceedings of the National Academy of Sciences of the USA* 2000;97(10):5039-5043.

Burgoyne R. Cytoskeleton is a major neuronal organelle. In Burgoyne R (ed), *The Neuronal Cytoskeleton* pp. 1-3. Wiley-Liss, New York 1991.

Buwalda B, Naber R, Nyakas C, Luiten PGM. Nimodipine accelerates the postnatal development of parvalbumin and S-100β immunoreactivity in the rat brain. *Developmental Brain Research* 1994;78:210-6.

Callaway EM, Katz LC. Emergence and refinement of clustered horizontal connections in cat striate cortex. *Journal of Neuroscience* 1990;10(4):1134-1153.

Campbell MJ, Hof PR, Morrison JH. A subpopulation of primate corticocortical neurons is distinguished by somatodendritic distribution of neurofilament protein. *Brain Research* 1991;539:133-136.

Campbell MJ, Morrison JH. Monoclonal antibody to neurofilament protein (SMI-32) labels a subpopulation of pyramidal neurons in the human and monkey neocortex. *Journal of Comparative Neurology* 1989;282:191-205.

Carter J, Gragerov A, Konvicka K, Elder G, Weinstein H, Lazzarini RA. Neurofilament assembly; divergent characteristics of human and rodent NF-L subunits. *Journal of Biological Chemistry* 1998;273(9):5101-8.

Chédotal A, Umbriaco D, Descarries L, Hartman BK, Hamel E. Light and electron microscopic immunocytochemical analysis of the neurovascular relationships of choline acetyltransferase and vasoactive intestinal polypeptide nerve terminals in the rat cerebral cortex. *Journal of Comparative Neurology* 1994;343(1):57-71.

Ching GY, Chien C-L, Flores R, Liem RKH. Overexpression of α-internexin causes abnormal neurofilamentous accumulations and motor coordination deficits in transgenic mice. *Journal of Neuroscience* 1999;19(8):2974-2986.

Cleveland DW, Monteiro MJ, Wong PC, Gill SR, Gearhart JD, Hoffman PN. Involvement of neurofilaments in the radial growth of axons. *Journal of Cell Science Supplement* 1991;15:85-95.

Cochard P, Paulin D. Initial expression of neurofilaments and vimentin in the central and peripheral nervous system of the mouse embryo *in vivo*. *Journal of Neuroscience* 1984;4(8):2080-2094.

Condé F, Lund JS, Jacobowitz DM, Baimbridge KG, Lewis DA. Local circuit neurons immunoreactive for calretinin, calbindin-D28k or parvalbumin in monkey prefrontal cortex: Distribution and morphology. *Journal of Comparative Neurology* 1994;341:95-116.

Constantine-Paton M. Induced ocular-dominance zones in tectal cortex. In Schmitt FO, Worden FG, Adelman A, Dennis SG (eds.) *The Organization of the Cerebral Cortex: Proceedings of a Neurosciences Research Program Colloquium*. Cambridge, MA: MIT Press, 1981.

Crook JM, Kisvárday ZF, Eysel UT. Evidence for a contribution of lateral inhibition to orientation tuning and direction selectivity in cat visual cortex: reversible inactivation of functionally characterized sites combined with neuroanatomical tracing techniques. *European Journal of Neuroscience* 1998;10(6):2056-2075.

Crowley JC, Katz LC. Development of ocular dominance columns in the absence of retinal input. *Nature Neuroscience* 1999;2(12):1125-30.

de Lima AD, Merten MDP, Voight T. Neuritic differentiation and synaptogenesis in serum-free neuronal cultures of the rat cerebral cortex. *Journal of Comparative Neurology* 1997;382:230-246.

de Lima AD, Voight T. Identification of two distinct populations of γ-aminobutyric acidergic neurons in cultures of the rat cerebral cortex. *Journal of Comparative Neurology* 1997;388:526-540.

De los Frailes MT, Sanchez Franco F, Lorenzo MJ, Tolón RM, Lara JI, Cacicedo L. Endogenous vasoactive intestinal peptide (VIP) regulates somatostatin secretion by cultured fetal rat cerebral cortical and hypothalamic cells. *Regulatory Peptides* 1991;34(3):261-74.

de Waegh SM, Lee VMY, Brady ST. Local modulation of neurofilament phosphorylation, axonal caliber, and slow axonal transport by myelinating Schwann cells. *Cell* 1992;68:451-463.

DeFelipe J, Fariñas I. The pyramidal neuron of the cerebral cortex: morphological and chemical characteristic of the synaptic inputs. *Progress in Neurobiology* 1992;39:563-607.

DeFelipe J, Hendry SH, Jones EG. A correlative electron microscopic study of basket cells and large GABAergic neurons in the monkey sensory-motor cortex. *Neuroscience* 1986;17(4):991-1009.

DeFelipe J, Hendry SHC, Jones EG. Synapses of double bouquet cells in monkey cerebral cortex visualised by calbindin immunoreactivity. *Brain Research* 1989b;503:49-54.

DeFelipe J, Hendry SHC, Jones EG. Visualisation of chandelier cell axons by parvalbumin immunoreactivity in monkey cerebral cortex. *Proceeding of the National Academy of Sciences of the USA* 1989a;86:2093-2097.

DeFelipe J, Hendry SHC, Jones EG. Visualization of chandelier cell axons by parvalbumin immunoreactivity in monkey cerebral cortex. *Proceedings of the National Academy of Sciences of the USA* 1989;86:2093-2097.

DeFelipe J. Neocortical neurochemical diversity: Chemical heterogeneity revealed by colocalisation studies of classic neurotransmitters, neuropeptides, calcium-binding proteins, and cell-surface molecules. *Cerebral Cortex* 1997a;3:273-289.

DeFelipe J. Types of neurons, synaptic connections and chemical characteristics of cells immunoreactive for calbindin-D28k, parvalbumin and calretinin in the neocortex. *Journal of Chemical Neuroanatomy* 1997b;14:1-19.

del Río MR, DeFelipe J. A study of SMI 32-stained pyramidal cells, parvalbumin-immunoreactive chandelier cells, and presumptive thalamocortical axons in the human temporal neocortex. *Journal of Comparative Neurology* 1994;342(3):389-408.

del Río MR, DeFelipe J. Synaptic connections of calretinin-immunoreactive neurons in the human neocortex. *Journal of Neuroscience* 1997;17(13):5143-54.

Demeulemeester H, Vandesande F, Orban GA, Brandon C, Vanderhaeghen JJ. Heterogeneity of GABAergic cells in cat visual cortex. *Journal of Neuroscience* 1988;8(3):988-1000.

Dichter MA, Delfs JR. Somatostatin and cortical neurons in cell culture. *Advances in Biochemistry and Psychopharmacology* 1981;28:145-57.

Douglas RJ, Martin KAC. A functional microcircuit for cat visual cortex. *Journal of Physiology* 1991;440:735-769.

Douglas RJ, Martin KAC. Exploring cortical microcircuits: A combined anatomical, physiological and computational approach. In McKenna, Davies, Zornetzer (eds.), *Single Neuron Computation*. San Diego, CA, USA: Academic Press, 1992.

Egger V, Feldmeyer D, Sakmann B. Coincidence detection and changes of synaptic efficacy in spiny stellate neurons in rat barrel cortex. *Nature Neuroscience* 1999;2(12):1098-105.

Elder GA, Friedrich VL Jr, Bosco P, Kang C, Gourov A, Tu PH, Lee VM-Y, Lazzarini RA. Absence of the mid-sized neurofilament subunit decreases axonal calibers, levels of light neurofilament (NF-L), and neurofilament content. *Journal of Cell Biology* 1998a;141(3):727-739.

Elder GA, Friedrich VL Jr, Kang C, Bosco P, Gourov A, Tu PH, Zhang B, Lee VM-Y, Lazzarini RA. Requirement of heavy neurofilament subunit in the development of axons with large calibers. *Journal of Cell Biology* 1998b;143(1):195-205.

Emerling DE, Lander AD. Laminar specific attachment and neurite outgrowth of thalamic neurons on cultured slices of developing cerebral neocortex. *Development* 1994;120:2811-2822.

Emson PC, Hunt SP. Anatomical chemistry of the cerebral cortex. In Schmitt FO, Worden FG, Adelman A, Dennis SG (eds.), *The Organization of the Cerebral Cortex: Proceedings of a Neurosciences Research Program Colloquium*. Cambridge, MA: MIT Press, 1981.

Escobar MI, Pimienta H, Caviness VS Jr, Jacobson M, Crandall JE, Kosik KS. Architecture of apical dendrites in the murine neocortex: dual apical dendritic systems. *Neuroscience* 1986;17(4):975-89.

Escobar MI, Pimienta H, Caviness VS Jr, Jacobson M, Crandall JE, Kosik KS. Architecture of apical dendrites in the murine neocortex: dual apical dendritic systems. *Neuroscience* 1986;17(4):975-989.

Eyer J, Leterrier JF. Influence of the phosphorylation state of neurofilament proteins on the interactions between purified filaments in vitro. *Biochemistry Journal* 1988;252(3):655-60.

Feldman ML. Morphology of the neocortical pyramidal neuron. In Peters A, Jones EG (eds.), *Cerebral Cortex, Volume 1: Cellular Components of the Cerebral Cortex*. New York: Plenum, 1984.

Fernández E, Cuenca N, Cerezo JR, De Juan J. Visual experience during postnatal development determines the size of optic nerve axons. *Neuroreport* 1993;5:365-367.

Finch DM, Tan AM, Isokawa-Akesson M. Feedforward inhibition of the rat entorhinal cortex and subicular complex. *The Journal of Neuroscience* 1988;8(7):2213-26.

Fitzpatrick-McElligott S, Card JP, O'Kane TM, Baldino F Jr. Ontogeny of somatostatin mRNA-containing perikarya in the rat central nervous system. *Synapse* 1991;7(2):123-134.

Fiumelli H, Kiraly M, Ambrus A, Magistretti PJ Martin JL. Opposite regulation of calbindin and calretinin expression by brain-derived neurotrophic factor in cortical neurons. *Journal of Neurochemistry* 2000;74(5):1870-7.

Foley P, Hughes PD, Bradford HF, Ghatei MA, Khandanian N, Bloom SR. The presence of neuropeptides in GABAergic and cholinergic rat cerebrocortical synaptosome sub-populations. *Neuropeptides* 1992;23(2):67-72.

Fonseca M, Del Río JA, Martínez A, Gómez S, Soriano E. Development of calretinin immunoreactivity in the neocortex of the rat. *Journal of Comparative Neurology* 1995;361:177-92.

Friede RL, Samorajski T. Axon caliber related to neurofilaments and microtubules in sciatic nerve fibers of rats and mice. *Anatomical Record* 1970;167:379-388.

Fuchs E, Cleveland DW. A structural scaffolding of intermediate filaments in health and disease. *Science* 1998;279:514-9.

Gabbott PLA, Dickie BGM, Vaid RR, Headlam AJN, Bacon SJ. Local-circuit neurones in the medial prefrontal cortex (areas 25, 32 and 24b) in the rat: Morphology and quantitative distribution. *Journal of Comparative Neurology* 1997;377:465-499.

Galarreta M, Hestrin S. Frequency-dependent synaptic depression and the balance of excitation and inhibition in the neocortex. *Nature Neuroscience* 1998;1(7):587-94.

Ghosh A, Antonini A, McConnell SK, Shatz, CJ. Requirement for subplate neurons in the formation of thalamocortical connections. *Nature* 1990;347:179-81

Ghosh S, Rahaman SO, Sarkar PK. Regulation of neurofilament gene expression by thyroid hormone in the developing rat brain. *Neuroreport* 1999;10(11):2361-5.

Giasson BI, Mushynski WE. Developmentally regulated stabilization of neuronal intermediate filaments in rat cerebral cortex. *Neuroscience Letters* 1997;229(2):77-80.

Gilbert CD, Wiesel TN. Morphology and intracortical projections of functionally identified neurons in the cat visual cortex. *Nature* 1979;280(5718):120-125.

Gomperts SN, Rao A, Craig AM, Malenka RC, Nicoll RA. Postsynaptically silent synapses in single neuron culture. *Neuron* 1998;21:1443-1451.

Gonchar Y, Burkhalter A. Three distinct families of GABAergic neurons in rat visual cortex. *Cerebral Cortex* 1997;7(4):347-358.

Gotow T, Tanaka T, Nakamura Y, Takeda M. Dephosphorylation of the largest neurofilament subunit protein influences the structure of crossbridges in reassembled neurofilaments. *Journal of Cell Science* 1994;107(7):1949-57.

Götz M, Bolz J. Differentiation of transmitter phenotypes in rat cerebral cortex. *European Journal of Neuroscience* 1994;6:18-32.

Götz M, Bolz J. Formation and preservation of cortical layers in slice cultures. *Journal of Neurobiology* 1992;23(7):783-802.

Gravel C, Hawkes R. Maturation of the corpus callosum of the rat: I. Influence of thyroid hormones on the topography of callosal projections. *Journal of Comparative Neurology* 1990;291:128-146.

Gravel C, Sasseville R, Hawkes R. Maturation of the corpus callosum of the rat: II. Influence of thyroid hormones on the number and maturation of axons. *Journal of Comparative Neurology* 1990;291:147-161.

Guadano-Ferraz A, Riederer BM, Innocenti GM. Developmental changes in the heavy subunit of neurofilaments in the corpus callosum of the cat. *Developmental Brain Research* 1990;56(2):244-56.

Guthrie PB, Lee RE, Rehder V, Schmidt MF, Kater SB. Self-recognition: a constraint on the formation of electrical coupling in neurons. *Journal of Neuroscience* 1994;14:1477–1485.

Ha DH, Robertson RT, Weiss JH. Distinctive morphological features of a subset of cortical neurons grown in the presence of basal forebrain neurons *in vitro*. *Journal of Neuroscience* 1998;18(11):4201-15.

Hahnloser RHR, Sarpeshkar R, Mahowald MA, Rodney J. Douglas RJ, Seung HS. Digital selection and analogue amplification coexist in a cortex-inspired silicon circuit. *Nature* 2000;405:947-951.

Hartley DM, Neve RL, Bryan J, Ullrey DB, Bak SY, Lang P, Geller AI. Expression of the calcium-binding protein, parvalbumin, in cultured cortical neurons using a HSV-1 vector system enhances NMDA neurotoxicity. *Brain Research: Molecular Brain Research* 1996;40(2):285-96.

Hayes TL, Lewis DA. Nonphosphorylated neurofilament protein and calbindin immunoreactivity in layer III pyramidal neurons of human neocortex. *Cerebral Cortex* 1992;2:56-67.

Hendry SHC, Carder RK. Organization and plasticity of GABA neurons and receptors in monkey visual cortex. *Progress in Brain Research* 1992;90:477-502.

Hendry SHC, Jones EG, Emson PC, Lawson DEM, Heizmann CW, Streit P. Two classes of cortical GABA neurons defined by differential calcium binding protein immunoreactivities. *Experimental Brain Research* 1989;76:467-72.

Hendry SHC, Jones EG, Emson PC. Morphology, distribution, and synaptic relations of somatostatin- and neuropeptide Y-immunoreactive neurons in rat and monkey neocortex. *Journal of Neuroscience* 1984;4(10):2497-2517.

Hendry SHC, Jones EG. Activity-dependent regulation of GABA expression in the visual cortex of adult monkeys. *Neuron* 1988;1:701-712.

Hirokawa N, Glicksman MA, Willard MB. Organization of mammalian neurofilament polypeptides within the neuronal cytoskeleton. *Journal of Cell Biology* 1984;98(4):1523-36.

Hirokawa N, Takeda S. Gene targeting studies begin to reveal the function of neurofilament proteins. *Journal of Cell Biology* 1998;143(1):1-4.

Hirst E, Asante J, Price J. Clustering of dendrites in the cerebral cortex begins in the embryonic cortical plate. *Journal of Neurocytology* 1991;20(5):431-438.

Hisanaga S, Hirokawa N. Dephosphorylation-induced interactions of neurofilaments with microtubules. *Journal of Biological Chemistry* 1990;265(35):21852-21858.

Hiscock JJ, MacKenzie L, Willoughby JO. Fos induction in subtypes of cerebrocortical neurons following single picrotoxin-induced seizures. *Brain Research* 1996;738:301-312.

Hoeflinger BF, Bennett-Clarke CA, Chiaia NL, Killackey HP, Rhoades RW. Patterning of local intracortical projections within the vibrissae representation of rat primary somatosensory cortex. *Journal of Comparative Neurology* 1995;354:551-563.

Hof PR, Cox K, Morrison JH. Quantitative analysis of a vulnerable subset of pyramidal neurons in Alzheimer's disease: I. Superior frontal and inferior temporal cortex. *Journal of Comparative Neurology* 1990;301:44-54.

Hof PR, Morrison JH. Neurofilament protein defines regional patterns of cortical organization in the macaque monkey visual system: A quantitative immunohistochemical analysis. *Journal of Comparative Neurology* 1995;352:161-186.

Hof PR, Mufson EJ, Morrison JH. Human orbitofrontal cortex: Cytoarchitecture and quantitative immunohistochemical parcellation. *Journal of Comparative Neurology* 1995;359:48-68.

Hof PR, Nimchinsky EA, Morrison JH. Neurochemical phenotype of corticocortical connections in the macaque monkey: Quantitative analysis of a subset of neurofilament protein-immunoreactive projection neurons in frontal, parietal, temporal, and cingulate cortices. *Journal of Comparative Neurology* 1995;362:109-133.

Hof PR, Nimchinsky EA. Regional distribution of neurofilament and calcium-binding proteins in the cingulate cortex of the macaque monkey. *Cerebral Cortex* 1992;2:456-467.

Hof PR, Ungerleider LG, Adams MM, Webster MJ, Gattass R, Blumberg DM, Morrison JH. Callosally projecting neurons in the macaque monkey V1/V2 border are enriched in nonphosphorylated neurofilament protein. *Visual Neuroscience* 1997;14:981-987.

Hof PR, Ungerleider LG, Webster MJ, Gattass R, Adams MM, Sailstad CA, Morrison JH. Neurofilament protein is differentially distributed in subpopulations of corticocortical projection neurons in the macaque monkey visual pathways. *Journal of Comparative Neurology* 1996;376:112-127.

Hoffman PN, Cleveland DW, Griffin JW, Landes PW, Cowan NJ. Neurofilament gene expression: a major determinant of axonal caliber. *Proceedings of the National Academy of Sciences of the USA* 1987;84(10):3472-6.

Hoffman PN, Griffin JW, Gold BG, Price DL. Slowing of neurofilament transport and the radial growth of developing nerve fibers. *Journal of Neuroscience* 1985;5(11):2920-9.

Hoffman PN, Lasek RJ, Griffin JW, Price DL. Slowing of the axonal transport of neurofilament proteins during development. *Journal of Neuroscience* 1983;3(8):1694-700.

Hornung J-P, de Tribolet N. Chemical organisation of the human cerebral cortex. In Tracey DJ, Paxinos G, Stone J (eds.) *Neurotransmitters in the Human Brain.* New York: Plenum, 1995.

Hornung J-P, Riederer BM. Medium-sized neurofilament protein related to maturation of a subset of cortical neurons. *Journal of Comparative Neurology* 1999;414:348-360.

Hsieh S-T, Crawford TO, Griffin JW. Neurofilament distribution and organization in the myelinated axons of the peripheral nervous system. *Brain Research* 1994;642:316-326.

Huntley GW, Jones EG. The emergence of architectonic field structure and areal borders in developing monkey sensorimotor cortex. *Neuroscience* 1991;44(2):287-310.

Impagnatiello F, Guidotti AR, Pesold C, Dwivedi Y, Caruncho H, Pisu MG, Uzunov DP, Smalheiser MR, Davis JM, Pandey GN, Pappas GD, Tueting P, Sharma RP, Costa E. A decrease of Reelin expression as a putative vulnerability factor in schizophrenia. *Proceedings of the National Academy of Sciences of the USA* 1998;95:15718-15723.

Jacomy H, Zhu Q, Couillard-Després S, Beaulieu JM, Julien JP. Disruption of type IV intermediate filament network in mice lacking the neurofilament medium and heavy subunits. *Journal of Neurochemistry* 1999;73(3):972-84.

Johnson RR, Burkhalter A. A polysynaptic feedback circuit in rat visual cortex. *Journal of Neuroscience* 1997;17(18):7129-40.

Johnston JG, van der Kooy D. Protooncogene expression identifies a transient columnar organization of the forebrain within the late embryonic ventricular zone. *Proceedings of the National Academy of Sciences of the USA* 1989;86:1066-1070.

Jones EG, Hendry SHC, DeFelipe J. Regulation of substance P immunoreactivity in GABA neurons of monkey visual cortex by sensory deprivation. In Henry JL, Couture R, Cuello AC, Pelletier G, Quirion R, Regoli R (eds.), *Substance P and Neurokinins.* New York: Springer-Verlag, 1987.

Jones EG, Hendry SHC. Basket cells. In Peters A, Jones EG (eds.), *Cerebral Cortex, Volume 1: Cellular Components of the Cerebral Cortex*. New York: Plenum, 1984.

Jones EG. History of cortical cytology. In Peters A, Jones EG (eds.), *Cerebral Cortex, Volume 1: Cellular Components of the Cerebral Cortex*. New York: Plenum, 1984a.

Jones EG. Laminar distribution of cortical efferent cells. In Peters A, Jones EG (eds.), *Cerebral Cortex, Volume 1: Cellular Components of the Cerebral Cortex*. New York: Plenum, 1984b.

Jones EG. Microcolumns in the cerebral cortex. *Proceedings of the National Academy of Sciences of the USA* 2000;97(10):5019-5021.

Jordan FL, Thomas WE. Identification of somatostatin-containing neurons in primary cultures of rat cerebral cortex. *Neuroscience Letters* 1987;77(3):249-54.

Julien J-P. Neurofilament functions in health and disease. *Current Opinion in Neurobiology* 1999;9:554-560.

Jung C, Shea TB. Regulation of neurofilament axonal transport by phosphorylation in optic axons in situ. *Cell Motility and the Cytoskeleton* 1999;42:230-240.

Jung C, Yabe JT, Shea TB. C-terminal phosphorylation of the high molecular weight neurofilament subunit correlates with decreased neurofilament axonal transport velocity. *Brain Research* 2000;856:12–19.

Katz LC. Cortical space race. *Nature* 1993;364:578-9.

Kawaguchi Y, Kubota Y. Correlation of physiological subgroupings of nonpyramidal cells with parvalbumin- and calbindin-D28k-immunoreactive neurons in layer V of rat frontal cortex. *Journal of Neurophysiology* 1993;70(1):387-96.

Kawaguchi Y, Kubota Y. GABAergic cell subtypes and their synaptic connections in rat frontal cortex. *Cerebral Cortex* 1997;7:476-486.

Kawaguchi Y. Physiological subgroupings of nonpyramidal cells with specific morphological characteristics in layer II/III of rat frontal cortex. *Journal of Neuroscience* 1995; 15(4):2638-2655.

Kawaguchi Y. Selective cholinergic modulation of cortical GABAergic cell subtypes. *Journal of Neurophysiology* 1997;78(3):1743-1747.

Killackey HP. Anatomical evidence for cortical subdivisions based on vertically discrete thalamic projections from the ventral posterior nucleus to cortical barrels in the rat. *Brain Research* 1973;51:326-331.

Killackey HP, Rhoades RW, Bennett-Clarke CA. The formation of a cortical somatotopic map. *Trends in Neurosciences* 1995;18(9):402-407.

King CE, Dickson TC, Jacobs I, McCormack G, Riederer B, Vickers JC. Acute CNS axonal injury models a subtype of dystrophic neurite in Alzheimer's disease. *Alzheimer's Reports* 2000;3:31-40.

Kisvárday ZF, Cowey A, Somogyi P. Synaptic relationships of a type of GABA-immunoreactive neuron (clutch cell), spiny stellate cells and lateral geniculate nucleus afferents in layer IVC of the monkey striate cortex. *Neuroscience* 1986a;19(3):741-761.

Kisvárday ZF, Martin KAC, Freund TF, Maglóczky Zs, Whitteridge D, Somogyi P. Synaptic targets of HRP-filled layer III pyramidal cells in the cat striate cortex. *Experimental Brain Research* 1986b;64(3):541-552.

Kisvárday ZF, Martin KAC, Friedlander MJ, Somogyi P. Evidence for interlaminar inhibitory circuits in the striate cortex of the cat. *Journal of Comparative Neurology* 1987;260(1)1-19.

Kisvárday ZF, Martin KAC, Whitteridge D, Somogyi P. Synaptic connections of intracellularly filled clutch cells: a type of small basket cell in the visual cortex of the cat. *Journal of Comparative Neurology* 1985;241(2):111-37.

Klymkowsky MW. Weaving a tangled web: the interconnected cytoskeleton. *Nature Cell Biology* 1999;1:E121-E123.

Kobayashi N, Mundel P. A role of microtubules during the formation of cell processes in neuronal and non-neuronal cells. *Cell and Tissue Research* 1998;291:163-174.

Koester SE, O'Leary DD. Functional classes of cortical projection neurons develop dendritic distinctions by class-specific sculpting of an early common pattern. *Journal of Neuroscience* 1992;12:1382-93.

Kossut M, Stewart MG, Siucinska E, Bourne RC, Gabbott PLA. Loss of γ-aminobutyric acid (GABA) immunoreactivity from mouse first somatosensory (SI) cortex following neonatal, but not adult, denervation. *Brain Research* 1991;538:165-170.

Kubota Y, Hattori R, Yui Y. Three distinct subpopulations of GABAergic neurons in frontal agranular cortex. *Brain Research* 1994;649:159-173.

Lavdas AA, Blue ME, Lincoln J, Parnavelas JG. Serotonin promotes the differentiation of glutamate neurons in organotypic slice cultures of the developing cerebral cortex. *Journal of Neuroscience* 1997;17(20):872-80.

Lawson SN, Perry MJ, Prabhakar E, McCarthy PW. Primary sensory neurones: Neurofilament, neuropeptides, and conduction velocity. *Brain Research Bulletin*, 1993;30:239-243.

Lawson SN, Waddell PJ. Soma neurofilament immunoreactivity is related to cell size and fibre conduction velocity in rat primary sensory neurons. *Journal of Physiology* (London) 1991;435:41-63.

Lee MK, Cleveland DW. Neuronal intermediate filaments. *Annual Review of Neuroscience* 1996;19:187-217.

Lee MK, Xu Z, Wong PC, Cleveland DW. Neurofilaments are obligate heteropolymers in vivo. *Journal of Cell Biology* 1993;122:1337-1350.

Lee VM-Y, Otvos Jr L, Carden MJ, Hollosi M, Dietzschold B, Lazzarini RA. Identification of the major multiphosphorylation site in mammalian neurofilaments. *Proceedings of the National Academy of Sciences of the USA* 1988;85:1998-2002.

Lefebvre S, Mushynski WE. Calcium binding to untreated and dephosphorylated porcine neurofilaments. *Biochemical and Biophysical Research Communications* 1987;145(3):1006-1011.

Lefebvre S, Mushynski WE. Characterization of the cation-binding properties of porcine neurofilaments. *Biochemistry* 1988;27:8503-8508.

Leterrier JF, Käs J, Hartwig J, Vegners R, Janmey PA. Mechanical effects of neurofilament cross-bridges: Modulation by phosphorylation, lipids, and interactions with F-actin. *Journal of Biological Chemistry* 1996;271(26):15687-94.

Lev DL, White EL. Organization of pyramidal cell apical dendrites and composition of dendritic clusters in the mouse: emphasis on primary motor cortex. *European Journal of Neuroscience* 1997;9(2):280-290.

Liu FC, Graybiel AM. Transient calbindin-D_{28k}-positive systems in the telencephalon: ganglionic eminence, developing striatum and cerebral cortex. *Journal of Neuroscience* 1992;12(2):674-90.

Liu Y, Dyck R, Cynader M. The correlation between cortical neuron maturation and neurofilament phosphorylation: A developmental study of phosphorylated 200 kDa

neurofilament protein in cat visual cortex. *Brain Research: Developmental Brain Research* 1994;81(2):151-61.

Lohmann C, Ilic V, Friauf E. Development of a topographically organized auditory network in slice culture is calcium dependent. *Journal of Neurobiology* 1998;34(2):97-112.

Lorenzo MJ, Sánchez-Franco F, de los Frailes MT, Reichlin S, Férnandez G, Cacicedo L. Synthesis and secretion of vasoactive intestinal peptide by rat fetal cerebral cortical and hypothalamic cells in culture. *Endocrinology* 1989;125(4):1983-90.

Luhmann HJ, Prince DA. Postnatal maturation of the GABAergic system in the rat neocortex. *Journal of Neurophysiology* 1991;65:247-63.

Luiten PGM, Buwalda B, Traber J, Nyakas C. Induction of enhanced postnatal expression of immunoreactive calbindin-D28k in rat forebrain by the calcium antagonist nimodipine. *Developmental Brain Research* 1994;79:10-18.

Lukas W, Jones KA. Cortical neurons containing calretinin are selectively resistant to calcium overload and excitotoxicity in vitro. *Neuroscience* 1994;61(2):307-16.

Lund JS. Spiny stellate neurons. In Peters A, Jones EG (eds.), *Cerebral Cortex, Volume 1: Cellular Components of the Cerebral Cortex*. New York: Plenum, 1984.

Maier DL, McCasland JS. Calcium-binding protein phenotype defines metabolically distinct groups of neurons in barrel cortex of behaving hamsters. *Experimental Neurology* 1997;145:71-80.

Malach R. Patterns of connections in rat visual cortex. *Journal of Neuroscience* 1989;9(11):3741-3752.

Maletic-Savatic M, Malinow R, Svoboda K. Rapid dendritic morphogenesis in CA1 hippocampal dendrites induced by synaptic activity. *Science* 1999;283:1923-7.

Mandlekow E, Mandlekow E-M. Microtubules and microtubule-associated proteins. *Current Opinion in Cell Biology* 1995;7:72-81.

Marín-Padilla M. Neurons of layer I: A developmental analysis. In Peters A, Jones EG (eds.), *Cerebral Cortex, Volume 1: Cellular Components of the Cerebral Cortex*. New York: Plenum, 1984.

Marszalek JR, Williamson TL, Lee MK, Xu Z, Hoffman PN, Becher MW, Crawford TO, Cleveland DW. Neurofilament subunit NF-H modulates axonal diameter by selectively slowing neurofilament transport. *Journal of Cell Biology* 1996;135(3):711-724.

Martín R, Gutiérrez A, Peñafiel A, Marín-Padilla M, de la Calle A. Persistence of Cajal-Retzius cells in the adult human cerebral cortex. An immunohistochemical study. *Histology and Histopathology* 1999;14:2487-90.

Matus A, Microtubule-associated proteins and neuronal morphogenesis. *Journal of Cell Science* 1991;Supplement 15:61-67.

McCasland JL. Metabolic activity in antigenically defined neurons: a double-labeling method for high-resolution 2-deoxyglucose and immunohistochemistry. *Journal of Neuroscience Methods* 1996;68:113-123.

McDonald JK, Parnavelas JG, Karamanlidis AN, Brecha N, Koenig JI. The morphology and distribution of peptide-containing neurons in the adult and developing visual cortex of the rat. I: Somatostatin. *Journal of Neurocytology* 1982;11(5):809-824.

Mesulam M, Geula C. Differential distribution of a neurofilament protein epitope in acetylcholinesterase-rich neurons of human cerebral neocortex. *Brain Research* 1991;544:169-173.

Mienville JM. Cajal-Retzius cell physiology: just in time to bridge the 20th century. *Cerebral Cortex* 1999;1:8776-82.

Miller MW, Vogt BA. Direct connection of rat visual cortex with sensory, motor, and association cortices. *Journal of Comparative Neurology* 1984;226:184-202.

Mione MC, Danevic C, Boardman P, Harris B, Parnavelas JG. Lineage analysis reveals neurotransmitter (GABA or glutamate) but not calcium-binding protein homogeneity in clonally related cortical neurons. *The Journal of Neuroscience* 1994;14(1):107-23.

Miyashita-Lin EM, Hevner R, Montzka Wassarman K, Martinez S, Rubenstein JLR. Early neocortical regionalization in the absence of thalamic innervation. *Science* 1999;285:906.

Monteiro MJ, Hoffman PN, Gearhart JD, Cleveland DW. Expression of NF-L in both neuronal and nonneuronal cells of transgenic mice: Increased neurofilament density in axons without affecting caliber. *Journal of Cell Biology* 1990;111:1543-1557.

Morrison JH, Benoit R, Magistretti PJ, Bloom FE. Immunohistochemical distribution of pro-somatostatin-related peptides in cerebral cortex. *Brain Research* 1983;262:344-51.

Morrison JH, Hof PR. The organisation of the cerebral cortex: From molecules to circuits. *Discussions in Neuroscience* 1992;IX(2):1-80.

Morrison JH, Magistretti PJ, Benoit R, Bloom FE. The distribution and morphological characteristics of the intracortical VIP-positive cell: An immunohistochemical analysis. *Brain Research* 1984;292:269-282.

Mountcastle VB. An organizing principle for cerebral function: The unit module and its distributed system. In Edelman GM, Mountcastle VB. *The Mindful Brain.* Cambridge, MA: MIT Press, 1978.

Mountcastle VB. The columnar organization of the neocortex. *Brain* 1997;120:701-722.

Müller W, Connor JA. Dendritic spines as individual neuronal compartments for synaptic Ca^{2+} responses. *Nature* 1991;354:73-6.

Naus CC, Durand MM. Ontogeny of somatostatin expression in primary cultures of cortical neurons parallels that seen *in vivo*. *Brain Research Bulletin* 1990;25(5):749-54.

Nie F, Wong-Riley MTT. Double labelling of GABA and cytochrome oxidase in the macaque visual cortex: Quantitative EM analysis. *Journal of Comparative Neurology* 1995;356:115-131.

Nimchinsky EA, Hof PR, Young WG, Morrison JH. Neurochemical, morphologic and laminar characterization of cortical projection neurons in the cingulate motor areas of the macaque monkey. *Journal of Comparative Neurology* 1996;374:136-160.

Nixon RA, Paskevich PA, Sihag RK, Thayer CY. Phosphorylation of the carboxy terminus domains of neurofilament proteins in retinal ganglion cells in vivo: Influences on regional neurofilament accumulation, interneurofilament spacing, and axon caliber. *Journal of Cell Biology* 1994;126(4):1031-1046.

Nixon RA. The regulation of neurofilament protein dynamics by phosphorylation: Clues to neurofibrillary pathology. *Brain Pathology* 1993;3:29-38.

Nuñez JL, Nelson J, Pych JC, Kim JH, Juraska JM. Myelination in the splenium of the corpus callosum in adult male and female rats. *Brain Research: Developmental Brain Research* 2000;120(1):87-90.

O'Leary DDM, Koester SE. Development of projection neuron types, axon pathways, and patterned connections of the mammalian cortex. *Neuron* 1993;10:991-1006.

Ohara O, Gahara Y, Miyake T, Teraoka H, Kitamura T. Neurofilament deficiency in quail caused by nonsense mutation in neurofilament-L gene. *Journal of Cell Biology* 1993;121:387-395.

Pachter JS, Liem RK. The differential appearance of neurofilament triplet polypeptides in the developing rat optic nerve. *Developmental Biology* 1984;103(1):200-10.

Pant HC, Veeranna. Neurofilament phosphorylation. *Biochemistry and Cell Biology* 1995;73:575-592.

Pappas IS, Parnavelas JG. Basic fibroblast growth factor promotes the generation and differentiation of calretinin neurons in the rat cerebral cortex *in vitro*. *European Journal of Neuroscience* 1998;10(4):1436-45.

Parhad IM, Scott JN, Cellars LA, Bains JS, Krekoski CA, Clark AW. Axonal atrophy is associated with a decline in neurofilament gene expression. *Journal of Neuroscience Research* 1995;41:355-366.

Parysek LM, McReynolds MA, Goldman RD, Ley CA. Some neural intermediate filaments contain both peripherin and the neurofilament proteins. *Journal of Neuroscience Research* 1991;30:80-91.

Paxinos G, Kus L, Ashwell KWS, Watson C. *Chemoarchitectonic Atlas of the Rat Forebrain*. Academic Press: San Diego 1998.

Paxinos, G, Watson C. *The Rat Brain in Stereotaxic Coordinates*, 4th edition. Academic Press, 1998.

Pesold C, Liu WS, Guidotti A, Costa E, Caruncho HJ. Cortical bitufted, horizontal, and Martinotti cells preferentially express and secrete Reelin into perineuronal nets, nonsynaptically modulating gene expression. *Proceedings of the National Academy of Sciences of the USA* 1999;96:3217-3222.

Peters A, Payne BR, Josephson K. Transcallosal non-pyramidal cell projections from visual cortex in the cat. *Journal of Comparative Neurology* 1990;302:124-42.

Peters A, Saint Marie RL. Smooth and sparsely spinous nonpyramidal cells forming local axonal plexuses. In Peters A, Jones EG (eds.), *Cerebral Cortex, Volume 1: Cellular Components of the Cerebral Cortex*. New York: Plenum, 1984.

Peters A, Sethares C. Myelinated axons and the pyramidal cell modules in monkey primary visual cortex. *Journal of Comparative Neurology* 1996;365:232-55.

Peters A. Bipolar cells. In Peters A, Jones EG (eds.), *Cerebral Cortex, Volume 1: Cellular Components of the Cerebral Cortex*. New York: Plenum, 1984b.

Peters A. Chandelier cells. In Peters A, Jones EG (eds.), *Cerebral Cortex, Volume 1: Cellular Components of the Cerebral Cortex*. New York: Plenum, 1984a.

Peters A. The axon terminals of vasoactive intestinal polypeptide (VIP)-containing bipolar cells in rat visual cortex. *Journal of Neurocytology* 1990;19(5):672-85.

Poltorak M, Stevens JR, Freed WJ, Casanova MF. The expression of phosphorylated neurofilament epitopes in human brains. *Brain Research* 1988;475:328-332.

Price RL, Paggi P, Lasek RJ, Katz MJ. Neurofilaments are spaced randomly in the radial dimension of axons. *Journal of Neurocytology* 1988;17:55-62.

Rakic P, Caviness VS Jr. Cortical development: View from neurological mutants two decades later. *Neuron* 1995;14:1101-4.

Rakic P. Developmental events leading to laminar and areal organization of the neocortex. In Schmitt FO, Worden FG, Adelman A, Dennis SG (eds.) *The Organization of the Cerebral Cortex: Proceedings of a Neurosciences Research Program Colloquium*. Cambridge, MA: MIT Press, 1981.

Rakic P. Principles of neural cell migration. *Experientia* 1990;46:883-891.

Rakic P. Radial versus tangential migration of neuronal clones in the developing cerebral cortex. *Proceedings of the National Academy of Sciences of the USA* 1995;92:11323-11327.

Raussel E, Cusick CG, Taub E, Jones EG. Chronic deafferentation in monkeys differentially affects nociceptive and nonnociceptive pathways distinguished by specific calcium-binding proteins and down-regulates γ-aminobutyric acid type A receptors at thalamic levels. *Proceedings of the National Academy of Sciences of the USA* 1992;89:2571-2575.

Riederer BM, Monnet-Tschudi F, Honegger P. Development and maintenance of the neuronal cytoskeleton in aggregated cell cultures of fetal rat telencephalon and influence of elevated K+ concentrations. *Journal of Neurochemistry* 1992;58(2):649-658.

Rogers JH. Immunohistochemical markers in rat cortex: Co-localization of calretinin and calbindin-D28k with neuropeptides and GABA. *Brain Research* 1992;587:147-57.

Rothman S, Cowan WM. A scanning electron microscopic study of the *in vitro* development of dissociated hippocampal cells. *Journal of Comparative Neurology* 1981;195:141-155.

Roussel G, Felix JM, Dautigny A, Pham-Dinh D, Hindelang C, Jolles P, Nussbaum JL. *In situ* localization of NF-H neurofilament subunit mRNAs in rat brain. *Developmental Neuroscience* 1991;13(2):98-103.

Ruoslahti E, Pierschbacher MD. New perspectives in cell adhesion: RGD and integrins. *Science* 1987;238:491–497.

Sakaguchi T, Okada M, Kitamura T, Kawasaki K. Reduced diameter and conduction velocity of myelinated fibres in the sciatic nerve of a neurofilament-deficient mutant quail. *Neuroscience Letters* 1993;153:65-68.

Sánchez I, Hassinger L, Paskevich PA, Shine HD, Nixon RA. Oligodendroglia regulate the regional expansion of axon caliber and local accumulation of neurofilaments during development independently of myelin formation. *Journal of Neuroscience* 1996;16(16):5095-105.

Sánchez MP, Frassoni C, Álvarez-Bolado G, Spreafico R, Fairén A. Distribution of calbindin and parvalbumin the developing somatosensory cortex and its primordium in the rat: an immunocytochemical study. *Journal of Neurocytology* 1992;21:717-36.

Schierle GS, Gander J-C, D'Orlando C, Celio MR, Vogt Weisenhorn DM. Calretinin-immunoreactivity during postnatal development of the rat isocortex: a qualitative and quantitative study. *Cerebral Cortex* 1997;7:130-142.

Schlaepfer WW, Bruce J. Neurofilament proteins are distributed in a diminishing proximodistal gradient along rat sciatic nerve. *Journal of Neurochemistry* 1990;55:453-460.

Schlaggar BL, O'Leary DDM. Potential of visual cortex to develop an array of functional units unique to somatosensory cortex. *Science* 1991;252:1556-60.

Scoville SA, Bufton SM, Liuzzi FJ. Estrogen regulates neurofilament gene expression in adult female rat dorsal root ganglion neurons. *Experimental Neurology* 1997;146:596-599.

Shatz CJ. How are specific connections formed between thalamus and cortex? *Current Opinion in Neurobiology* 1992;2:78-82.

Shaw G, Banker GA, Weber K. An immunofluorescence study of neurofilament protein expression by developing hippocampal neurons in tissue culture. *European Journal of Cell Biology* 1985;39:206-216.

Siegel SJ, Ginsberg SD, Hof PR, Foote SL, Young WG, Kraemer GW, McKinney WT, Morrison JH. Effects of social deprivation in prepubescent rhesus monkeys: immunohistochemical analysis of the neurofilament protein triplet in the hippocampal formation. *Brain Research* 1993;619:299-305.

Somogyi P, Cowey A. Combined Golgi and electron microscopic study on the synapses formed by double bouquet cells in the visual cortex of the cat and the monkey. *Journal of Comparative Neurology* 1981;195:547-66.

Somogyi P, Cowey A. Double bouquet cells. In Peters A, Jones EG (eds.), *Cerebral Cortex, Volume 1: Cellular Components of the Cerebral Cortex*. New York: Plenum, 1984.

Somogyi P, Kisvárday ZF, Martin KAC, Whitteridge D. Synaptic connections of morphologically identified and physiologically characterized large basket cells in the striate cortex of cat. *Neuroscience* 1983;10(2):261-94.

Staiger JF, Freund TF, Zilles K. Interneurons immunoreactive for vasoactive intestinal polypeptide (VIP) are extensively innervated by parvalbumin-containing boutons in rat primary somatosensory cortex. *European Journal of Neuroscience* 1997;9(11):2259-68.

Starr R Attema B DeVries GH Monteiro MJ. Neurofilament phosphorylation is modulated by myelination. *Journal of Neuroscience Research* 1996;44(4):328-37.

Steinschneider R, Delmas P, Nedelec J, Gola M, Bernard D, Boucraut J. Appearance of neurofilament subunit epitopes correlates with electrophysiological maturation in cortical embryonic neurons cocultured with mature astrocytes. *Brain Research: Developmental Brain Research* 1996;95(1):15-27.

Sternberger LA, Sternberger N. Monoclonal antibodies distinguish phosphorylated and nonphosphorylated forms of neurofilaments in situ. *Proceedings of the National Academy of Sciences of the USA* 1983;80:6126-6130.

Swindale NV. Cortical organization: Modules, polymaps and mosaics. *Current Biology* 1998;8:R270-R273.

Swindale NV. Is cerebral cortex modular? *Trends in Neurosciences* 1990;13(12):487-492.

Szaro BG, Whitnall MH, Gainer H. Phosphorylation-dependent epitopes on neurofilament proteins and neurofilament densities differ in axons in the corticospinal and primary sensory dorsal column tracts in the rat spinal cord. *Journal of Comparative Neurology* 1990;302:220-235.

Szentágothai J. The 'module-concept' in cerebral cortex architecture. *Brain Research* 1975;95:475-96.

Tapia-Arancibia L, Reichlin S. Vasoactive intestinal peptide and PHI stimulate somatostatin release from rat cerebral cortical and diencephalic cells in dispersed cell culture. *Brain Research* 1985;336(1):67-72.

Toyoshima I, Kato K, Sugawara M, Wada C, Okawa S, Kobayashi M, Masamune O, Watanabe S. Massive accumulation of M and H subunits of neurofilament proteins in spinal motor neurons of neurofilament deficient Japanese quail, Quv. *Neuroscience Letters* 2000;287:175-178.

Tsang YM, Chiong F, Kuznetsov D, Kasarskis E, Geula C. Motor neurons are rich in nonphosphorylated neurofilaments: cross-species comparison and alterations in ALS. *Brain Research* 2000;861:45-58.

Tu P-H, Elder G, Lazzarini RA, Nelson D, Trojanowski JQ, Lee VM-Y. Overexpression of the human NFM subunit in transgenic mice modifies the level of endogenous NFL and the phosphorylation state of NFH subunits. *Journal of Cell Biology* 1995;129:1629-1640.

Tucker RP. The roles of microtubule-associated proteins in brain morphogenesis: a review. *Brain Research Reviews* 1990;15:101-120.

Uylings HBM, van Eden CG, Parnavelas JG, Kalsbeek A. The prenatal and postnatal development of the rat cerebral cortex. In Kolb B, Tees RC (eds.). *The Cerebral Cortex of the Rat*. Cambridge, MA: MIT Press, 1990.

Van der Loos H, Glaser EM. Autapses in neocortex cerebri: synapses between a pyramidal cell's axon and its own dendrites. *Brain Research* 1972;48:355-360.

Van der Loos H, Woolsey TA. Somatosensory cortex: structural alterations following early injury to sense organs. *Science* 1973;179:395-398.

Vickers JC, Costa M. The neurofilament triplet is present in distinct subpopulations of neurons in the central nervous system of the guinea-pig. *Neuroscience* 1992;49(1):73-100.

Vickers JC, Vitadello M, Parysek LM, Costa M. Complementary immunohistochemical distribution of the neurofilament triplet and novel intermediate filament proteins in the autonomic and sensory nervous system of the guinea-pig. *Journal of Chemical Neuroanatomy* 1991;4:259-270.

Vogt Weisenhorn DM, Celio MR, Rickmann M. The onset of parvalbumin-expression in interneurons of the rat parietal cortex depends upon extrinsic factor(s). *European Journal of Neuroscience* 1998;10:1027-36.

Walsh C, Cepko CL. Clonally-related cortical cells show several migration patterns. *Science* 1988;241:1342-1345.

Walsh C, Cepko CL. Widespread dispersal of neuronal clones across functional regions of the cerebral cortex. *Science* 1992;255:434-440.

Wang L, Ho C-L, Sun D, Liem RKH, Brown A. Rapid movement of axonal neurofilaments interrupted by prolonged pauses. *Nature Cell Biology* 2000;2:137-141.

Wang S, Hamberger A, Yang Q, Haglid KG. Changes in neurofilament protein NF-L and NF-H immunoreactivity following kainic acid-induced seizures. *Journal of Neurochemistry* 1994;62:739-748.

Wang S, Hamberger A, Yang Q, Haglid KG. In vivo activation of kainate receptors induces dephosphorylation of the heavy neurofilament subunit. *Journal of Neurochemistry* 1992;59:1975-1978.

Weiss JH, Koh J, Baimbridge KG, Choi DW. Cortical neurons containing somatostatin- or parvalbumin-like immunoreactivity are atypically vulnerable to excitotoxic injury in vitro. *Neurology* 1990;40(8):1288-92.

White EL, Keller A. Intrinsic circuitry involving the local axon collaterals of corticothalamic projection cells in mouse SmI cortex. *Journal of Comparative Neurology* 1987;262:13-26.

White EL, Peters A. Cortical modules in the posteromedial barrel subfield (Sml) of the mouse. *Journal of Comparative Neurology* 1993;334(1):86-96.

White EL. *Cortical Circuits: Synaptic Organization of the Cerebral Cortex; Structure, Function and Theory.* Boston: Birkhäuser 1989.

Winfield DA, Brooke RNL, Sloper JJ, Powell TPS. A combined Golgi-electron microscopic study of the synapses made by the proximal axon and recurrent collaterals of a pyramidal cell in the somatic sensory cortex of the monkey. *Neuroscience* 1981;6:1217-30.

Woolsey TA, Van der Loos H. The structural organization of layer IV in the somatosensory region (SI) of mouse cerebral cortex. The description of a cortical field composed of discrete cytoarchitectonic units. *Brain Research* 1970;17:205-242.

Xu Z, Tung VW-Y. Overexpression of neurofilament subunit M accelerates axonal transport of neurofilaments. *Brain Research* 2000;866:326–332.

Yamasaki H, Itakura C, Mizutani M. Hereditary hypotrophic axonopathy with neurofilament deficiency in a mutant strain of the Japanese quail. *Acta Neuropathologica* 1991;82:427-434.

Yang X, Hyder F, Shulman RG. Activation of a single whisker barrel in rat brain localized by functional magnetic resonance imaging. *Proceedings of the National Academy of Sciences of the USA* 1996;93:475-478.

Zeki S. *A Vision of the Brain*. Oxford: Blackwell Scientific, 1993.

Zhu Q, Lindenbaum M, Levavasseur F, Jacomy H, Julien J-P. Disruption of the NF-H gene increases axonal microtubule content and velocity of neurofilament transport: Relief of axonopathy resulting from the toxin β,β'-iminodipropionitrile. *Journal of Cell Biology* 1998;143(1):183-193.

Zilles K, Hajós F, Csillag A, Kálmán M, Sotonyi P, Schleicher A. Vasoactive intestinal polypeptide immunoreactive structures in the mouse barrel field. *Brain Research* 1993;618:149-154.

Zilles K. *The Cortex of the Rat: A Stereotaxic Atlas*. Berlin: Springer-Verlag, 1985.

Appendices

Appendix A: Standard solutions

Phosphate buffered saline (PBS)

0.01M, pH 7.4 (4°C)

100 ml	10x saline stock (90g NaCl; ASTRAL; per litre MilliQ® water)
40 ml	Disodium hydrogen orthophosphate (Na_2HPO_4, BDH) (28.4g.l^{-1} MilliQ® water)
10 ml	Sodium dihydrogen orthophosphate ($NaH_2PO_4.2H_2O$; UNILAB) (31.2g.l^{-1} MilliQ®)
850 ml	MilliQ® water

Paraformaldehyde fixative

40 g	Paraformaldehyde (BDH)
100 ml	Sodium di-hydrogen orthophosphate (UNILAB) (31.2 g.l^{-1} MilliQ® water)
400 ml	Di-sodium hydrogen orthophosphate (BDH) (28.4 g.l^{-1} MilliQ® water)
500 ml	MilliQ®

Solution heated, but not boiled, until dissolved.

Appendix B: Antibody concentrations for immunohistochemistry

Antigen	Host	Concentration	Vendor
SMI32	Mouse	1:2000	Sternberger Monoclonals, Inc
SMI312	Mouse	1:2000	Sternberger Monoclonals, Inc
NFL	Mouse	1:1000	Zymed
NFM	Rabbit	1:500	Serotec
NFH	Rabbit	1:500	Serotec
MAP-2	Mouse	1:1000	Chemicon International
VIP	Rabbit	1:1000	Peninsula Laboratories
SRIF	Rabbit	1:1000	Peninsula Laboratories
PV	Rabbit	1:4000	SWAnt Antibodies
CR	Rabbit	1:4000	SWAnt Antibodies
Mouse IgG (+Alexa 488)	Goat	1:1000	Molecular Probes, Inc
Rabbit IgG (+Alexa 594)	Goat	1:1000	Molecular Probes, Inc
Mouse / Rabbit IgG (+biotin)	Goat	1:1000	Vector, Inc

Appendix C: Abbreviations

CB	calbindin-D28k
CCK	cholecystokinin
CR	calretinin
C-R	Cajal-Retzius
GABA	γ-aminobutyric acid
GAD	glutamic acid decarboxylase
-IR	immunoreactively labelled
MAP-2	microtubule-associated protein 2
NADPH	nicotinamide-adenine-dinucleotide-phosphate
NF	neurofilament triplet protein heteropolymer
NFH	heavy subunit of NF polymer
NFL	light subunit of NF polymer
NFM	medium subunit of NF polymer
NOS	nitric oxide synthase
PV	parvalbumin
SRIF	somatostatin
VIP	vasoactive intestinal polypeptide

Cortical regions

2n	optic nerve
3V	3rd ventricle
A11	A11 dopamine cells
A13	A13 dopamine cells
AA	anterior amygdaloid area
AAD	anterior amygdaloid area, dorsal
AAV	anterior amygdaloid area, ventral
ac	anterior commissure
aca	anterior commissure, anterior
AcbC	accumbens nucleus, core
AcbSh	accumbens nucleus, shell
Acc	accessory neurosecretory nuclei
aci	anterior commissure, intrabulbar
ACo	anterior cortical amygdaloid nucleus
acp	anterior commissure, posterior
AD	anterodorsal thalamic nucleus
ADP	anterodorsal preoptic nucleus
af	amygdaloid fissure
AHA	anterior hypothalamic area, anterior part
AHC	anterior hypothalamic area, central
AHiAL	amygdalohippocampal area, anterolateral
AHiPM	amygdalohippocampal area, posteromedial
AHP	anterior hypothalamic area, posterior
AI	agranular insular cortex
AID	agranular insular cortex, dorsal
AIP	agranular insular cortex, posterior
AIV	agranular insular cortex, ventral
al	ansa lenticularis
alv	alveus of the hippocampus
AM	anteromedial thalamic nucleus
AMV	anteromedial thalamic nucleus, ventral
Ang	angular thalamic nucleus
AOM	anterior olfactory nucleus, medial
AOP	anterior olfactory nucleus, posterior
aopt	accessory optic tract
AOV	anterior olfactory nucleus, ventral
APF	anterior perifornical nucleus
APir	amygdalopiriform transition area
APTD	anterior pretectal nucleus, dorsal
APTV	anterior pretectal nucleus, ventral
Aq	aqueduct (Sylvius)
ar	acoustic radiation
ArcD	arcuate nucleus, dorsal
ArcL	arcuate nucleus, lateral
ArcLP	arcuate hypothalamic nucleus, lateroposterior
ArcM	arcuate nucleus, medial
ArcMP	arcuate hypothalamic nucleus, medial posterior
AStr	amygdalostriatal transition area
Au1	primary auditory cortex
AuD	secondary auditory cortex, dorsal area
AuV	secondary auditory cortex, ventral area
AV	anteroventral thalamic nucleus
AVDM	anteroventral thalamic nucleus, dorsomedial
AVPe	anteroventral periventricular nucleus
AVVL	anteroventral thalamic nucleus, ventrolateral
B	basal nucleus (Meynert)
BAC	bed nucleus of the anterior commissure
BAOT	bed nucleus of the accessory olfactory tr
BLA	basolateral amygdaloid nucleus, anterior
BLP	basolateral amygdaloid nucleus, posterior
BLV	basolateral amygdaloid nucleus, ventral
BMA	basomedial amygdaloid nucleus, anterior
BMP	basomedial amygdaloid nucleus, posterior
bsc	brachium of the superior colliculus
BSTIA	bed nucleus of the stria terminalis, intraamygdaloid division
BSTL	bed nucleus of the stria terminalis, lateral division
BSTLD	bed nucleus of the stria terminalis, lateral division, dorsal
BSTLI	bed nucleus of the stria terminalis, lateral division, intermediate
BSTLJ	bed nucleus of the stria terminalis, lateral division, juxtacapsular
BSTLP	bed nucleus of the stria terminalis, lateral division, posterior
BSTLV	bed nucleus of the stria terminalis,

	lateral division, ventral
BSTMA	bed nucleus of the stria terminalis, medial division, anterior
BSTMPI	bed nucleus of the stria terminalis, medial division, posterointermediate
BSTMPL	bed nucleus of the stria terminalis, medial division, posterolateral
BSTMPM	bed nucleus of the stria terminalis, medial division, posteromedial
BSTMV	bed nucleus of the stria terminalis, medial division, ventral
BSTS	bed nucleus of stria terminalis, supracapsular
CA	field CA of hippocampus
CA	field CA of hippocampus
CA	field CA of hippocampus
CB	cell bridges of the ventral striatum
cc	corpus callosum
CeC	central amygdaloid nucleus, capsular
CeL	central amygdaloid nucleus, lateral division
CeM	central amygdaloid nucleus, medial division
cg	cingulum
Cg	cingulate cortex, area
Cg	cingulate cortex, area
CL	centrolateral thalamic nucleus
Cl	claustrum
CM	central medial thalamic nucleus
cp	cerebral peduncle, basal
CPu	caudate putamen (striatum)
csc	commissure of the superior colliculus
cst	commissural stria terminalis
ctg	central tegmental tract
CxA	cortex-amygdala transition zone
DV	dorsal rd ventricle
DA	dorsal hypothalamic area
df	dorsal fornix
DG	dentate gyrus
DHC	nucleus of the dorsal hippocampal commissure
dhc	dorsal hippocampal commissure
DI	dysgranular insular cortex
Dk	nucleus of Darkschewitsch
dlf	dorsal longitudinal fasciculus
DLG	dorsal lateral geniculate nucleus
DMC	dorsomedial hypothalamic nucleus, compact
DMD	dorsomedial hypothalamic nucleus, dorsal
DMPAG	dorsomedial periaqueductal gray
DMV	dorsomedial hypothalamic nucleus, ventral
DP	dorsal peduncular cortex
DpMe	deep mesencephalic nucleus
dtg	dorsal tegmental bundle
DTM	dorsal tuberomammillary nucleus
DTr	dorsal transition zone
DTT	dorsal tenia tecta
E	ependyma and subependymal layer
ec	external capsule
Ect	ectorhinal cortex
eml	external medullary lamina
Eth	ethmoid thalamic nucleus
EW	Edinger-Westphal nucleus
exc	extreme capsule
F	nucleus of the fields of Forel
f	fornix
FC	fasciola cinereum
fi	fimbria of the hippocampus
fmi	forceps minor of the corpus callosum
fmj	forceps major of the corpus callosum
fr	fasciculus retroflexus
gcc	genu of the corpus callosum
Gem	gemini hypothalamic nucleus
GI	granular insular cortex
GrDG	granular layer of the dentate gyrus
hbc	habenular commissure
HDB	nucleus of the horizontal limb of the diagonal band
hf	hippocampal fissure
Hil	hilus of the dentate gyrus
I	intercalated nuclei of the amygdala
IAD	interanterodorsal thalamic nucleus
IAM	interanteromedial thalamic nucleus
IBl	inner blade of the dentate gyrus
ic	internal capsule
ICj	islands of Calleja
ICjM	islands of Calleja, major island
IF	interfascicular nucleus
IG	indusium griseum
IGL	intergeniculate leaf
IL	infralimbic cortex
IM	intercalated amygdaloid nucleus, main
IMA	intramedullary thalamic area
IMD	intermediodorsal thalamic nucleus
IMG	amygdaloid intramedullary gray
iml	internal medullary lamina
IMLF	interstitial nucleus of the medial longitudinal fasciculus
IMLFG	interstitial nucleus of medial longitudinal fasciculus, greater
imvc	intermedioventral thalamic commissure
InfS	infundibular stem
IPAC	interstitial nucleus of the posterior limb of the anterior commissure
IPACL	interstitial nucleus of the posterior limb of the anterior commissure, lateral part
IPACM	interstitial nucleus of the posterior limb of the anterior commissure, medial part
IPF	interpeduncular fossa
LA	lateroanterior hypothalamic nucleus
lab	longitudinal association bundle
LAcbSh	lateral accumbens shell
LaDL	lateral amygdaloid nucleus, dorsolateral
LaVL	lateral amygdaloid nucleus, ventrolateral
LaVM	lateral amygdaloid nucleus, ventromedial
Ld	lambdoid septal zone
LDDM	laterodorsal thalamic nucleus, dorsomedial
LDVL	laterodorsal thalamic nucleus, ventrolateral
LEnt	lateral entorhinal cortex
LGP	lateral globus pallidus
LH	lateral hypothalamic area
LHb	lateral habenular nucleus
LHbL	lateral habenular nucleus, lateral
LHbM	lateral habenular nucleus, medial
LM	lateral mammillary nucleus
LMol	lacunosum moleculare layer of the hippocampus
LO	lateral orbital cortex
lo	lateral olfactory tract
LOT	nucleus of the lateral olfactory tract
LPAG	lateral periaqueductal gray
LPLC	lateral posterior thalamic nucleus, laterocaudal

LPLR lateral posterior thalamic nucleus, laterorostral
LPMC lateral posterior thalamic nucleus, mediocaudal
LPMR lateral posterior thalamic nucleus, mediorostral
LPO lateral preoptic area
LSD lateral septal nucleus, dorsal
LSI lateral septal nucleus, intermediate
LSS lateral stripe of the striatum
LSV lateral septal nucleus, ventral
LT lateral terminal nucleus of the accessory optic tract
LV lateral ventricle
M1 primary motor cortex
M2 secondary motor cortex
mch medial corticohypothalamic tract
MCLH magnocellular nucleus of the lateral hypothalamus
MCPC magnocellular nucleus of the posterior commissure
MCPO magnocellular preoptic nucleus
MD mediodorsal thalamic nucleus
MDC mediodorsal thalamic nucleus, central
MDL mediodorsal thalamic nucleus, lateral
MDM mediodorsal thalamic nucleus, medial
MeAD medial amygdaloid nucleus, anterodorsal
MeAV medial amygdaloid nucleus, anteroventral
MEE medial eminence, external layer
MEI medial eminence, internal layer
MePD medial amygdaloid nucleus, posterodorsal
MePV medial amygdaloid nucleus, posteroventral
mfb medial forebrain bundle
mfba medial forebrain bundle, 'a' component
mfbb medial forebrain bundle, 'b' component
MGD medial geniculate nucleus, dorsal
MGM medial geniculate nucleus, medial
MGP medial globus pallidus
MGV medial geniculate nucleus, ventral
MHb medial habenular nucleus
ML medial mammillary nucleus, lateral
ml medial lemniscus
MM medial mammillary nucleus, medial
MMn medial mammillary nucleus, median
MnPO median preoptic nucleus
MO medial orbital cortex
Mol molecular layer of the dentate gyrus
mp mammillary peduncle
MPA medial preoptic area
MPO medial preoptic nucleus
MPOC medial preoptic nucleus, central
MPOL medial preoptic nucleus, lateral
MPOM medial preoptic nucleus, medial
MPT medial pretectal nucleus
MRe mammillary recess of the rd ventricle
MS medial septal nucleus
MT medial terminal nucleus of the accessory optic tract
mt mammillothalamic tract
mtg mammillotegmental tract
MTu medial tuberal nucleus
MZMG marginal zone of the medial geniculate
ns nigrostriatal bundle
OBl outer blade of the dentate gyrus
OPC oval paracentral thalamic nucleus
OPT olivary pretectal nucleus
opt optic tract
Or oriens layer of the hippocampus
OT nucleus of the optic tract
OV olfactory ventricle (olfactory of lateral ventricle)
ox optic chiasm
PaAM paraventricular hypothalamic nucleus, anterior magnocellular
PaAP paraventricular hypothalamic nucleus, anterior parvicellular
PaDC paraventricular hypothalamic nucleus, dorsal cap
PAG periaqueductal gray
PaLM paraventricular hypothalamic nucleus, lateral magnocellular
PaMP paraventricular hypothalamic nucleus, medial parvicellular
PaPo paraventricular hypothalamic nucleus, posterior
PaV paraventricular hypothalamic nucleus, ventral
PBP parabrachial pigmented nucleus
PC paracentral thalamic nucleus
pc posterior commissure
pcf precommissural fornix
PCom nucleus of the posterior commissure
PDP posterodorsal preoptic nucleus
Pe periventricular hypothalamic nucleus
PeF perifornical nucleus
PF parafascicular thalamic nucleus
PH posterior hypothalamic area
PIL posterior intralaminar thalamic nucleus
Pir piriform cortex
PiRe pineal recess
PLCo posterolateral cortical amygdaloid nucleus
PLd paralambdoid septal nucleus
PLi posterior limitans thalamic nucleus
pm principal mammillary tract
PMCo posteromedial cortical amygdaloid nucleus
PMD premammillary nucleus, dorsal
PMV premammillary nucleus, ventral
PN paranigral nucleus
Po posterior thalamic nuclear group
PoDG polymorph layer of the dentate gyrus
PoMn posteromedian thalamic nucleus
PoT posterior thalamic nuclear group, triangular
PP peripeduncular nucleus
PPT posterior pretectal nucleus
PR prerubral field
PrC precommissural nucleus
PRh perirhinal cortex
PrL prelimbic cortex
PS parastrial nucleus
PSTh parasubthalamic nucleus
PT paratenial thalamic nucleus
PtA parietal association cortex
PV paraventricular thalamic nucleus
pv periventricular fiber system
PVA paraventricular thalamic nucleus, anterior
PVP paraventricular thalamic nucleus, posterior
Py pyramidal cell layer of the hippocampus
Rad stratum radiatum of the hippocampus
RCh retrochiasmatic area

Re	reuniens thalamic nucleus
REth	retroethmoid nucleus
rf	rhinal fissure
Rh	rhomboid thalamic nucleus
RI	rostral interstitial nucleus of medial longitudinal fasciculus
ri	rhinal incisura
RLi	rostral linear nucleus of the raphe
RMC	red nucleus, magnocellular
RPC	red nucleus, parvicellular
RSA	retrosplenial agranular cortex
RSGb	retrosplenial granular b cortex
Rt	reticular thalamic nucleus
S	subiculum
S1	primary somatosensory cortex
S1BF	1ary somatosensory cortex, barrel field
S1DZ	primary somatosensory cortex, dysgranular region
S1FL	primary somatosensory cortex, forelimb
S1HL	primary somatosensory cortex, hindlimb
S1J	primary somatosensory cortex, jaw
S1JO	primary somatosensory cortex, jaw region, oral surface
S1Tr	primary somatosensory cortex, trunk
S1ULp	primary somatosensory cortex, upper lip
S2	secondary somatosensory cortex
SC	superior colliculus
scc	splenium of the corpus callosum
SCh	suprachiasmatic nucleus
SCO	subcommissural organ
SCom	subcommissural nucleus
scp	superior cerebellar peduncle (brachium conjunctivum)
SFi	septofimbrial nucleus
SFO	subfornical organ
SG	suprageniculate thalamic nucleus
SHi	septohippocampal nucleus
SI	substantia innominata
SIB	substantia innominata, basal
SID	substantia innominata, dorsal
SIV	substantia innominata, ventral
SL	semilunar nucleus
SM	nucleus of the stria medullaris
sm	stria medullaris of the thalamus
SMT	submammillothalamic nucleus
SNCD	substantia nigra, compact part, dorsal tier
SNL	substantia nigra, lateral
SNM	substantia nigra, medial
SNR	substantia nigra, reticular
SO	supraoptic nucleus
SOR	supraoptic nucleus, retrochiasmatic
sox	supraoptic decussation
SPa	subparaventricular zone of the hypothalamus
SPF	subparafascicular thalamic nucleus
SPFPC	subparafascicular thalamic nucleus, parvicellular
st	stria terminalis
StA	strial of the preoptic area
Stg	stigmoid hypothalamic nucleus
STh	subthalamic nucleus
StHy	striohypothalamic nucleus
str	superior thalamic radiation
SubD	submedius thalamic nucleus, dorsal
SubG	subgeniculate nucleus
SubI	subincertal nucleus
SubV	submedius thalamic nucleus, ventral
SuM	supramammillary nucleus
SuML	supramammillary nucleus, lateral
SuMM	supramammillary nucleus, medial
sumx	supramammillary decussation
TC	tuber cinereum area
Te	terete hypothalamic nucleus
TeA	temporal association cortex
TS	triangular septal nucleus
Tu	olfactory tubercle
TuDC	olfactory tubercle densocellular layer
TuPl	olfactory tubercle plexiform layer
TuPo	olfactory tubercle polymorph layer
V1B	primary visual cortex, binocular area
V1M	primary visual cortex, monocular area
V2L	secondary visual cortex, lateral area
V2ML	secondary visual cortex, mediolateral
V2MM	secondary visual cortex, mediomedial
VA	ventral anterior thalamic nucleus
VDB	nucleus of the vertical limb of the diagonal band
VEn	ventral endopiriform nucleus
vhc	ventral hippocampal commissure
VL	ventrolateral thalamic nucleus
VLG	ventral lateral geniculate nucleus
VLGMC	ventral lateral geniculate nucleus, magnocellular
VLGPC	ventral lateral geniculate nucleus, parvicellular
VLH	ventrolateral hypothalamic nucleus
VLPO	ventrolateral preoptic nucleus
VM	ventromedial thalamic nucleus
VMHC	ventromedial hypothalamic nucleus, central
VMHDM	ventromedial hypothalamic nucleus, dorsomedial
VMHVL	ventromedial hypothalamic nucleus, ventrolateral
VMPO	ventromedial preoptic nucleus
VO	ventral orbital cortex
VP	ventral pallidum
VPL	ventral posterolateral thalamic nucleus
VPM	ventral posteromedial thalamic nucleus
VPPC	ventral posterior thalamic nucleus, parvicellular
VRe	ventral reuniens thalamic nucleus
VTA	ventral tegmental area
vtgx	ventral tegmental decussation
VTM	ventral tuberomammillary nucleus
VTRZ	visual tegmental relay zone
VTT	ventral tenia tecta
Xi	xiphoid thalamic nucleus
ZI	zona incerta
ZID	zona incerta, dorsal
ZIV	zona incerta, ventral
ZL	zona limitans